Functional and transcriptional characterisation of synovial fibroblasts in early inflammatory arthritis and established rheumatoid arthritis

By

María Jesús Juárez Pérez

A thesis submitted to

The University of Birmingham

For the degree of

DOCTOR OF PHILOSOPHY

School of Immunity and Infection

College of Medical and Dental Sciences

The University of Birmingham

August 2014

ABSTRACT

A pathogenic role for synovial fibroblasts has been established based on the study of samples originating from patients with longstanding rheumatoid arthritis (RA). To assess whether these cells also have such role in early RA and whether they play a part in the resolution of inflammatory arthritis, functional and transcriptional characterisation was performed on synovial fibroblasts from patients in five distinct outcome groups: normal joints, resolving arthritis, very early RA, early RA and longstanding RA.

Functional characterisation revealed differences in migration rates between groups. Migration rates of very early RA and longstanding RA synovial fibroblasts were significantly slower than those of normal ones. No differences in invasive characteristics were identified.

Transcriptional analysis demonstrated differing transcriptional signatures between very early and longstanding RA synovial fibroblasts in both, unstimulated and TNF stimulated samples. No differences in the transcriptomic profile of resolving and very early RA cells were identified. The study of transcriptional responses to TNF stimulation in each outcome group revealed generic changes in response to pro-inflammatory stimuli as well as outcome group-specific responses.

These data extend previous observations of the pathogenic role of synovial fibroblasts indicating that they may play a role in early RA and providing clues to potential targets differentiating early and late RA.

To my parents

"The three great essentials to achieve anything worthwhile are hard work, stick-to-itiviness and common sense"
Thomas A Eddison

ACKNOWLEDGMENTS

Many people deserve my thanks for their contribution to this thesis. My supervisor, Andrew Filer, has been crucial to the completion of this project. He has challenged me and allowed me to become an independent researcher whilst providing direction and guidance. He also supported me during very difficult personal times and for that I will always be in his debt. The arrival of Andy Clark to Birmingham marked a step change in my project and enabled it to become what it is. I am very grateful to Andy and his team that took me under their wing and helped me navigate the complexities of molecular biology. My thanks to Chris Buckley who gave me the opportunity of doing a basic science PhD, despite not having any lab experience. Chris has always had time, a smile and words of wisdom for me. Many thanks to Karim Raza who has always had an open door and has been the source of support and inspiration.

Past and present members of the Rheumatology Research Group deserve my thanks for their fantastic technical support, stimulating scientific conversations and copious amounts of cake and good humour. In particular, I would like to acknowledge the contributions of Holly Adams, Tim Smallie, Kath Bignal, Tina Tang, Martin Fitzpatrick, Dagmar Scheel-Toellner, Mark Pearson, Lorraine Yeo, Helen McGettrick, Debbie Hardie, Beth Clay, Rachel Bayley, Banesa de Paz, Eva Li and Julia Spengler. My special thanks to Holly, Martin and Beth for filling me with sweets and cups of tea, always answering my questions with a smile and most importantly, making my every day great.

My thanks also to my collaborators in this project Mark Cooper, Rowan Hardy, Paul Badenhorst and Steve Kissane. Thanks to Lyn Williamson, Elizabeth Price, David Collins and Robert Marshall for their career guidance and continued support.

I would like thank my parents who, amongst many other things, have taught me the value of hard work and things well done. They love me more than I will ever be able to express and have given me the most precious gift: my siblings. Thanks to Dev for being a source of happiness, love and support, driving for miles so that we could live together and making me smile every single day.

The patients that contributed to this study deserve special gratitude. I would also like to acknowledge the support of the Wellcome Trust in funding my Clinical Research Training Fellowship.

When I embarked on this project, having worked as a clinician for years, some of my good friends and colleagues warned me I might not like this job. The pace is markedly different to clinical work and the challenges posed of a different nature. They need not have worried. I can honestly say that I have loved my time here and have found my career passion.

TABLE OF CONTENTS

LIST OF FIGURES

LIST OF TABLES

LIST OF IMAGES

ABBREVIATIONS

ACR	American College of Rheumatology
ACPA	Anti citrullinated protein antibodies
ARA	American Rheumatism Association
BSA	Bovine serum albumin
CD	Cluster of differentiation
CIA	Collagen induced arthritis
CRP	C reactive protein
CTLA4	Cytotoxic T lymphocyte antigen 4
DAS28	Disease activity score (28 joints)
DKK1	Dickkopf related protein 1
DMARDs	Disease modifying antirheumatic drugs
DMSO	Dimethyl sulphoxide
DNA	Deoxyribonucleic acid
ECM	Extracellular matrix
EdU	5-ethynyl-2-deosyuridine
ELISA	Enzyme linked immunosorbent assay
ENA-78	Epithelial cell derived neutrophil attractant 78
ERK	Extracellular signal regulated kinases
ESR	Erythrocyte sedimentation rate
FCS	Fetal calf serum
FDR	False discovery rate
FGF	Fibroblast growth factor
GAPDH	Glyceraldehyde 3-phosphate dehydrogenase
HLA	Human leucocyte antigen
HUVEC	Human umbilical vein endothelial cells
IFN	Interferon
IL	Interleukin
JNK	c-jun N terminal kinases
lncRNA	Long non-coding RNA
MAPK	Mitogen-activated protein kinases
MDCK	Madin-Darby canine kidney epithelial cells
mRNA	Messenger RNA
miRNA	MicroRNA
MMPs	Matrix metalloproteases
NET	Neutrophil extracellular trap
NGS	Next generation sequencing
PADI	Peptidylarginine deiminase
PBS	Phosphate buffered saline
PCA	Principal component analysis
PCR	Polymerase chain reaction
PDGF	Platelet derived growth factor
PolyA	Polyadenylated
PsA	Psoriatic arthritis
PTPN22	Phosphatase non-receptor type 22 RA
RANKL	Receptor activator of NF-κβ ligand

RF	Rheumatoid factor
RNA	Ribonucleic acid
SAGE	Serial analysis of gene expression
SCID	Severe combined immunodeficient
TGF	Transforming growth factor
TIMP	Tissue inhibitor of metalloproteinases
TLR	Toll-like receptor
TNF	Tumour necrosis factor
Tris	Tris(hydroxymethyl) aminomethane
VCAM	Vascular cell adhesion molecule
VEGF	Vascular endothelial growth factor
Wnt	Wingless

1 Introduction

1.1 Rheumatoid arthritis

Rheumatoid arthritis (RA) is a chronic multi system disease of unknown aetiology that affects 1% of the population. In RA, the primary pathology localises to synovial joints and is characterised by chronic inflammation that can lead to bone and cartilage destruction, loss of function and long term disability.

1.1.1 Classification of RA

RA is a heterogeneous disease with multiple manifestations. The clinical diagnosis of RA is based on a history of symmetrical polyarthritis affecting the small joints of the hands and feet sometimes in the context of a family history of RA (first degree relative) and often associated with raised inflammatory markers and positive antibody testing to rheumatoid factor (RF) and anti citrullinated protein antibodies (ACPA).

In order to facilitate recruitment of patients into studies and direct comparisons between clinical trials, classification criteria were developed by the American Rheumatism Association in 1956 (Ropes et al 1957). These criteria were revised in 1987 (Arnett et al. 1988) and have since been widely used for this purpose. Under these criteria patients are assessed against 7 items and are said to fulfil classification criteria for RA if 4/7 criteria are satisfied (Table 1.1). In recent years, these criteria have come under criticism as they lack sensitivity in early disease. As a consequence, the American College of Rheumatology and the European League Against Rheumatism developed new criteria

(Aletaha et al. 2010). The major advantage of the 2010 Rheumatoid Arthritis classification criteria is that whilst they can be applied to patients with established disease they also allow identification of patients at high risk of chronicity in early disease (Table 1.2). Also noteworthy, is the inclusion of ACPA in these classification criteria. In clinical practice, their presence or absence in the sera of RA patients is used to further sub-classify RA into ACPA positive and ACPA negative disease. This distinction is based on evidence that these disease subsets are associated with differing environmental and genetic risk factors thus suggesting that they may be caused by different pathophysiological mechanisms (Eyre et al. 2012;Klareskog et al. 2006;Linn-Rasker et al. 2006;Plenge et al. 2005). Furthermore, although both diseases may have very similar clinical features at presentation, disease course is markedly different with ACPA positive patients displaying a less favourable course characterised by increased extra-articular manifestations and excess cardiovascular risk and earlier and more severe joint damage (Willemze et al. 2012).

Table 1.1 The 1987 American Rheumatism Association revised criteria.

Criterion	Definition
1. *Morning stiffness*	Stiffness in and around the joints lasting at least 1 hour before maximal improvement.
2. *Arthritis of ≥3 joints*	At least 3 joint areas simultaneously have had soft tissue swelling or fluid observed by a physician. The 14 possible areas are: MCP, PIP, wrist, elbow, knee, ankle and MTP joints.
3. *Arthritis of hands*	At least 1 area swollen in a wrist, MCP or PIP joint.
4. *Symmetric arthritis*	Simultaneous involvement of the same joint areas on both sides of the body (bilateral involvement of PIPs, MCPs, or MTPs is acceptable without absolute symmetry).
5. *Rheumatoid nodules*	Subcutaneous nodules over bony prominences or extensor surfaces or in juxtaarticular regions observed by a physician.
6. *Rheumatoid factor*	Demonstration of abnormal amounts of serum rheumatoid factor by any method for which the result has been positive in <5% of normal control subjects.
7. *Radiographic changes*	Radiographic changes typical of rheumatoid arthritis on posteroanterior hand and wrist radiographs, which must include erosions or unequivocal bony decalcification localized in or most marked adjacent to the involved joints (osteoarthritis changes alone do not qualify).

For classification purposes a patient shall be said to have rheumatoid arthritis if he/she has satisfied at least 4 of these 7 criteria. Criteria 1 through 4 must have been present for at least 6 weeks. Patients with 2 clinical diagnoses are not excluded.

Table 1.2 The 2010 Rheumatoid Arthritis classification criteria

Criterion	Score
A. Joint involvement	
1 large joint	0
2-10 large joints	1
1-3 small joints (with or without involvement of large joints)	2
4-10 small joints (with or without involvement of large joints)	3
>10 joints (at least 1 small joint)	5
B. Serology (at least 1 test result is needed for the classification)	
Negative RF and negative ACPA	0
Low positive RF or low positive ACPA	2
High positive RF or high positive ACPA	3
C. Acute phase reactants (at least 1 test result is needed for classification)	
Normal CRP and normal ESR	0
Abnormal CRP or abnormal ESR	1
D. Duration of symptoms	
< 6 weeks	0
≥ 6 weeks	1

The score of each section (A-D) is added. A score of ≥ 6/10 is needed for the classification of RA.

1.1.2 Pathophysiology

The pathogenesis of RA is complex and incompletely understood. It is postulated that a combination of genetic, epigenetic and environmental factors coincide in an individual leading to disease. It is generally accepted that exposure of susceptible individuals to certain environmental triggers leads to loss of self-tolerance and over time to development of inflammatory arthritis.

1.1.2.1 Genetic and environmental factors

The importance of genetics in determining disease susceptibility has long been recognised. Disease concordance in monozygotic twins is estimated at 15% with overall heritability estimated at 60% (MacGregor et al. 2000). Genome-wide association studies have identified risk alleles that are associated with increased disease susceptibility. Perhaps the best known of these is the human leucocyte antigen (HLA) system. The HLA system is the most polymorphic genetic system in humans and a number of alleles have been associated with increased RA susceptibility. Amongst these, alleles that contain a common amino acid substitution (QKRAA) at positions 70-74 in the third hypervariable region of the DRβ1 chain within the peptide binding groove (known as the shared epitope) confer increased susceptibility to RA (Gregersen et al. 1987). This and other risk alleles of genes coding for proteins including protein thyrosine phosphatase non-receptor type 22 (PTPN22) and cytotoxic T lymphocyte antigen 4

(CTLA4) have been associated with increased susceptibility to ACPA positive disease. PTPN22 encodes a tyrosine phosphatase involved in T and B cell activation (Kallberg et al. 2007) whilst CTLA4 is involved in down-regulation of T cell activation and maintenance of peripheral tolerance (McCoy et al. 1999). Genetic associations to ACPA negative disease also exist although they are less well established. An example is the proved association between HLA-DR3 and ACPA negative but not ACPA positive RA (Verpoort et al. 2005). These observations are important for two reasons. First, they lend support to genetic influence in disease and more specifically to the role of the immune system as these alleles have functions consistent with immune regulation. Second, they help to define disease categories not solely based on clinical characteristics but on genetic and antibody profiling (McInnes et al. 2011).

Gene-gene and gene-environment interactions are thought to be key determinants of disease pathogenesis. Smoking is the prototypical environmental factor implicated in disease. Smoking is a risk factor for RA and in particular for RF positive disease. The relative risk of RF positive RA in smokers is 2.2 (95% CI 1.7-3.0) compared to a relative risk of RF negative RA of only 0.8 (95% CI 0.6-2). Furthermore, this risk is increased by interactions between this environmental factor and genetic ones. Thus, smokers carrying one copy of the shared epitope have a relative risk of RF positive RA of 7.5 (95% CI 4.2-13.1) whilst those carrying two copies have a relative risk of 15.7 (95% CI 7.2-34.2) (Padyukov et al. 2004). The interaction between smoking and the shared epitope also increases the risk of ACPA positive RA. Smokers with a single copy of the shared epitope have a relative risk of ACPA positive disease of 6.5 (95% CI 3.8-11.4) whilst those with two copies have a relative risk of 21 (95% CI 11.0-40.2) (Klareskog et al. 2006). The study of interactions has been extended to other risk alleles

and to date the highest relative risk of developing ACPA positive RA is conferred by the combination of smoking, double copies of the shared epitope and PTPN22 risk alleles (Kallberg et al. 2007).

Infections represent other notable environmental factors implicated in RA pathogenesis. Molecular mimicry and the ability of some pathogen products to promote protein citrullination have been postulated as possible pathogenic mechanisms. Several studies have demonstrated a positive association between RA and periodontitis (de Pablo et al. 2009;Kinloch et al. 2008;Wegner et al. 2010). Periodontitis is an infectious process initiated by *Porphyromonas gingivalis* and other pathogens and accompanied by a chronic inflammatory response. Common features and potential links between both conditions include their relapsing/remitting nature and similar prevalence, the presence of *P. gingivalis* in synovial fluid of RA patients and genetic factors underlying disease susceptibility (Persson 2012). However, the precise mechanisms that explain this association remain to be elucidated. The human microbiome has also been studied in the context of disease. The microbiome is defined as the collection of microorganisms that populate the human body. As 60-70% of these bacteria reside in the gut, studies have focused on these microorganisms in particular. Of particular interest is the observation that disease is attenuated in murine models of arthritis if animals are raised in germ free conditions. Conversely, introduction of specific gut bacteria induces joint inflammation whilst antibiotic treatment can prevent arthritis development in animal models (Horai et al. 2000;Rath et al. 1996). Data from human studies have very recently added to these longstanding observations. Scher and colleagues undertook sequencing of bacterial DNA in faeces of patients with new onset treatment naïve ACPA positive RA of less than 6 months duration, treated RA patients with disease duration of more than 6

months (chronic RA), treated psoriatic arthritis patients (PsA) and healthy controls and found significant differences in bacterial composition between patient groups. A specific intestinal bacterium *Prevotella copri* was identified in 75% of new onset treatment naïve RA patients compared to 11.5% of chronic RA, 37.5% of PsA and 21% of healthy controls. The expansion of prevotella species was inversely correlated with bacteroides species. To elucidate whether *P.copri* could predispose to increased inflammation, antibiotic treated mice were colonised with the bacteria and colitis was induced. *P. copri* colonised mice demonstrated significantly more severe disease than their control littermates suggesting that *P. copri* may be able to support systemic inflammation (Scher et al. 2013).

The role of autoimmunity in RA has long been proposed owing to the presence of autoantibodies in the sera of these patients. Rheumatoid factors (RF) are autoantibodies against the Fc portion of IgG proteins. They can be present in the sera of patients months or years before the onset of disease and are predictors of joint damage and functional disability (Arend et al. 2012;Scott 2000). Antibodies against citrullinated peptides (ACPA) are directed against a range of citrullinated proteins including fibrinogen, vimentin, α-enolase and type II collagen. They too can be present in the sera of patients for years before disease onset and are prognostic markers that have also been implicated in disease pathogenesis (Willemze et al. 2012). Citrullination is an enzymatic process that results in post-translational modification of proteins. It is catalyzed by peptidylarginine deiminase (PADI) enzymes that convert arginine residues to citrulline (Figure 1.1). Citrullination occurs during several biological processes, including inflammation. In RA, citrullination is thought to occur in a variety of locations including lungs, periodontal tissue and synovial joints (where PADI enzymes have been

found), and may provide a link between genetic and environmental factors and autoimmunity. The analysis of fluid from bronchoalveolar lavages from healthy smokers and smokers with pulmonary pathology revealed citrullinated proteins in smokers but not in non-smokers. The presence of citrullinated proteins was associated with higher levels of PADI2. This observation prompted the hypothesis that long term exposure to smoking may induce citrullination of self-antigens leading to ACPA production in susceptible individuals carrying the shared epitope (Klareskog et al. 2006). Similarly, *P. gingivalis* species express PADI enzymes able to citrullinate fibrin from periodontal tissue. Thus these citrullinated antigens may become immunogenic in patients with periodontitis (de Pablo et al. 2009).

It is likely that other, yet to be defined, autoantibodies against post-translationally modified proteins are present in the sera of RA patients. Indeed, antibodies against carbamylated peptides have recently been identified in the sera of RA patients. Carbamylation is a non-enzymatic post-translational modification that results in the conversion of lysine residues into homocitrulline (Figure 1.1). Homocitrulline and citrulline are similar in structure but differ in length and the modified residue (lysine in the case of homocitrulline and arginine in the case of citrulline). Anticarbamylated protein antibodies have been found in 37-45% of ACPA positive RA and 16-20% of ACPA negative patients. In the latter group they appeared predictive of disease severity (Shi et al. 2011). Unpublished work from our group suggests that autoantibodies against acetylated lysine exist in the sera of patients with very early RA compared to those with resolving and persistent non RA arthritis.

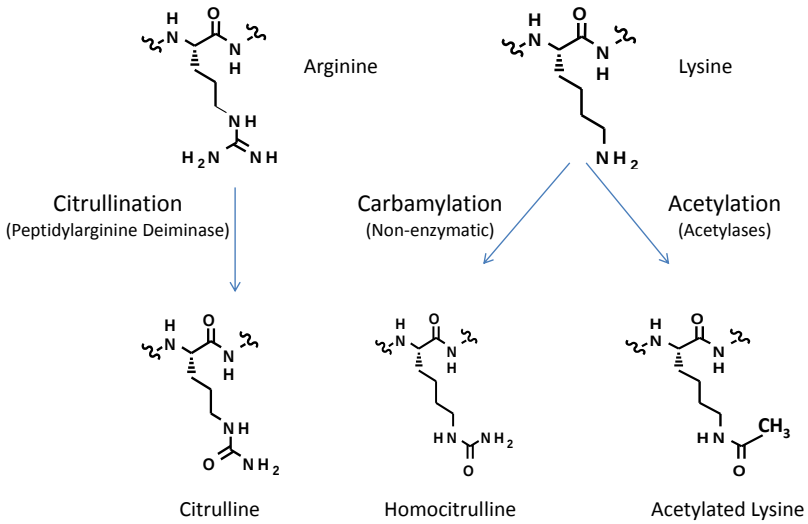

Figure 1.1 Post-translational protein modification. *Diagram depicting the processes of citrullination, carbamylation and acetylation. Citrullination occurs when arginine resides are deaminated to citrulline. Lysine residues can undergo carbamylation through non-enzymatic conversion into homocitrulline or acetylation through addition of acetyl residues. Antibodies against citrullinated, homocitrullinated and acetylated peptides are present in the sera of RA patients.*

1.1.2.2 Synovial architecture in health and disease

Normal synovial tissue consists of two layers: the lining, which is in contact with synovial fluid, and the sublining. The lining is a thin (2-3 cell deep) and avascular layer that lacks a basement membrane and is composed of roughly equal proportions of type A (macrophage-like) synoviocytes and type B (fibroblast-like) synoviocytes (also known as synovial fibroblasts). The sublining is a thicker and more loosely organised layer of type A and type B synoviocytes together with extracellular matrix (ECM) and blood vessels (Mor et al. 2005).

In RA the normal synovial architecture is distorted. The usually thin lining layer is replaced by a hyperplastic 10-15 cells deep layer. At the synovial-cartilage junction this thickened synovial layer can become a mass of “pannus” tissue rich in synovial

fibroblasts and osteoclasts that attaches to and invades the adjacent articular cartilage and subchondral bone. The sublining synovial layer becomes infiltrated with inflammatory cells including T cells, B cells, macrophages, mast cells, and plasma and dendritic cells. Increased activity in the synovium is supported by ECM production and neoangiogenesis (Taylor et al. 2005). A schematic representation of the cells in the RA synovium is shown in Figure 1.2.

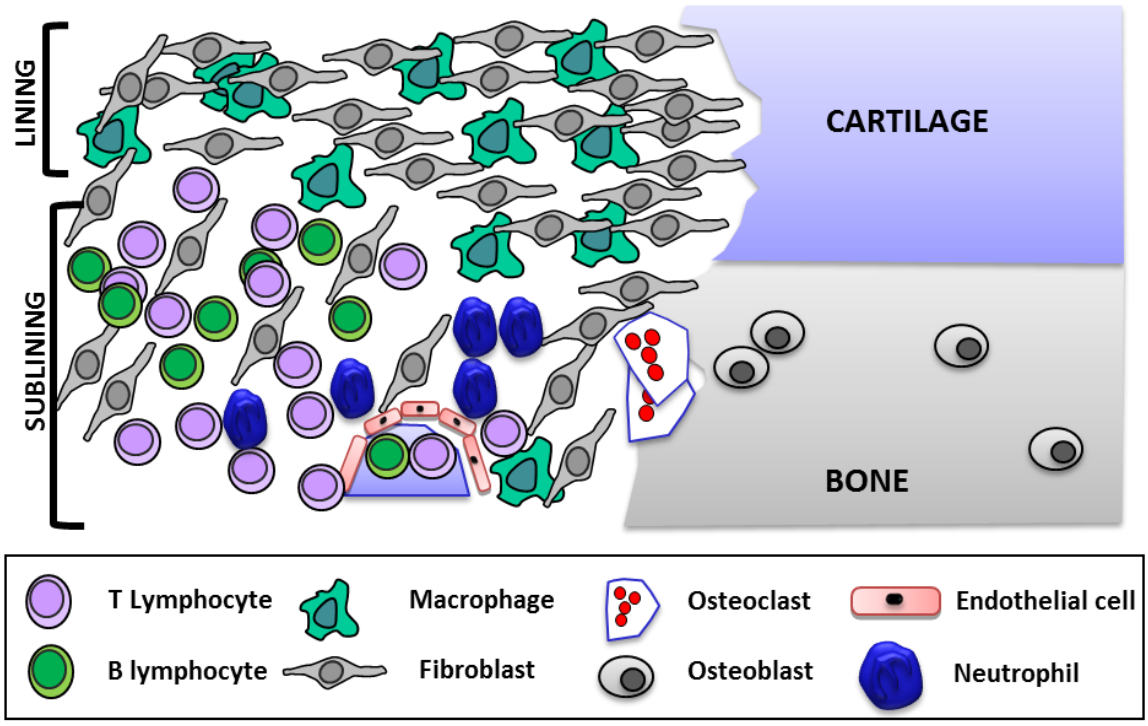

Figure 1.2 Schematic representation of the diversity of cells found in the RA synovium. *The lining layer is mainly composed of macrophages and synovial fibroblasts whilst the sublining layer is composed of these cells as well as other immune inflammatory cells. Reproduced with permission from Juarez et al. 2012.*

This distorted synovial architecture is responsible for one of the main clinical manifestations of disease: joint swelling. Yet somewhat surprisingly, this chronic

inflammatory infiltrate is highly organised and governed by complex interactions between cells of the innate and adaptive immune systems and resident tissue stroma. The role of some of these cells in disease will be discussed next.

1.1.2.3 Cells in the RA synovium

T cells have traditionally been implicated in RA pathogenesis. Their role is suggested by genetic susceptibility factors to RA such as the HLA system, PTPN22 and CTLA4. Additionally, abatacept (a selective co-stimulation modulator that inhibits T cell activation) has demonstrated efficacy in the treatment of RA further emphasising the role of these cells in disease. In RA synovial tissue, CD4 T cells tend to locate around perivascular cuffs whilst CD8 T cells are located throughout synovial tissue (Kurosaka et al. 1983). Historically RA has been considered a predominantly type 1 T helper cell (Th1) disease. This stemmed from the observation that arthritis could be induced in mice by inoculation with IL-12, a cytokine that promotes differentiation of naïve T cells into Th1 cells (Germann et al. 1995). However, it was later shown that it was IL-23 and not IL-12 that played an important role in arthritis induction. IL-12 is composed of p35 and p40 subunits whilst IL-23 is composed of p19 and p40 subunits. To assess the relative contribution of each cytokine to disease, three types of mice were created: one specifically lacking p35 (IL-12 deficient), another lacking p19 (IL-23 deficient) and a third type lacking p40 (IL-12 and IL-23 deficient) and collagen induced arthritis (CIA) induced. IL-23 and combined IL-12 /IL-23 deficient mice were protected against arthritis development whilst IL-12 deficient mice developed severe arthritis. This suggested that IL-23 had a central role in the development of arthritis whilst IL-12 had a protective role. IL-23 and IL-12/IL-23 deficient mice developed no IL-17 producing T

cells whereas IL-12 deficient mice developed an increased number of these cells (Murphy et al. 2003). IL-23 is a cytokine produced by macrophages and dendritic cells that, together with other cytokines, supports type 17 T helper cell (Th17) differentiation whilst suppressing regulatory T cell (Treg) differentiation.

Thus, Th17 responses and IL-17 production by these cells have been implicated in RA pathogenesis. Th17 cells have a key role in the development of autoimmunity in several animal models. For instance, IL-6 deficient mice are resistant to antigen induced arthritis and autoimmune encephalitis owing to altered Th17 activation and differentiation whilst treatment with anti-IL-17 antibodies ameliorates the severity of CIA (Stockinger et al. 2007). IL-17 levels are very low in the sera of healthy individuals but elevated in the sera of RA patients. Co-culture of IL-17 producing T cells with RA synovial fibroblasts induces production of pro-inflammatory cytokines by fibroblasts whilst IL-17 production by T cells is increased in co-culture (Cho et al. 2004). Infiltrating IL-17 producing T cells can be seen in RA synovial tissues (Chabaud et al. 1999) and IL-17 blockade suppresses inflammation in the CIA model (Lubberts 2008). The potential role of IL-17 blockade as a therapeutic target in RA is currently being investigated (Kellner 2013).

In contrast, the regulatory function of RA synovial Treg cells is limited. Tregs have a central role in the maintenance of immune tolerance and prevention of autoimmune disease. They exert this function through secretion of inhibitory cytokines (i.e. IL-10) and reduction of T cell activation through down-regulation of co-stimulatory molecules on antigen presenting cells (Broere et al. 1999). Tregs found in the rheumatoid synovium appear to have limited regulatory function and are unable to suppress

production of pro-inflammatory cytokines by monocytes and activated T cells (Ehrenstein et al. 2004). This limited regulatory function has been associated with their reduced expression of CTLA4 (Flores-Borja et al. 2008). Furthermore, RA synovial fluid effector T cells are less susceptible to suppression than peripheral blood effector T cells (van Amelsfort et al. 2004) which concurs with the observation that strongly activated CD4 T cells are resistant to Treg suppression (Baecher-Allan et al. 2002).

The pathogenic role of B cells in RA is supported in clinical practice by the success of the CD20-B cell depleting therapy rituximab (Edwards et al. 2004). Three distinct patterns of B cell organisation in the RA synovium have been described. In a study of 64 synovial tissue samples, diffuse T and B cell infiltration was seen in 56% of patients. T and B cells formed aggregates lacking follicular dendritic cells and germinal centers in 20% of patients whilst a third subset of patients (24%) showed T and B cell aggregates with germinal center-like structures (Takemura et al. 2001). For years, a role for these cells in disease pathogenesis was proposed owing to their ability to produce antibodies. It is now proposed that their role in disease also extends to antigen presentation and cytokine production. In the RA synovium, B cells produce IL-6, IFNγ and lymphotoxin β which indicates that they may have a pro-inflammatory role and support B cell development (Pistoia 1997).

Neutrophils are present in relatively low numbers in synovial tissue but are the most abundant cell type in synovial fluid. Although their role in disease is not fully elucidated they produce prostaglandins, proteases and reactive oxygen species thought to promote synovial inflammation (Cascao et al. 2010). Very recently, their role has taken centre stage with the description of aberrant NETosis in neutrophils from synovial fluid and

peripheral blood of RA patients (Khandpur et al. 2013). NETosis is a process by which neutrophils release chromatin fibers producing networks termed neutrophil extracellular traps (NETs) that have the capacity to bind pathogens. This process has been described in a number of autoimmune conditions where it is thought to play a pathogenic role by promoting autoimmunity (Woodman 2013). In RA NETs have been shown to contain citrullinated vimentin that is recognised by autoantibodies in these patients. Furthermore, ACPA and RF as well as pro-inflammatory stimuli can induce NETosis in neutrophils. These observations have led to the proposal of NETosis as a key event in disease pathogenesis that promotes and perpetuates autoimmunity and abnormal adaptive and innate immune responses (Khandpur et al. 2013).

Macrophages are very abundant in the lining and sublining layers of RA synovial tissue. Their role in disease pathogenesis is supported by reduction of sublining layer macrophage numbers following successful therapy and positive correlation between this reduction and response to treatment as measured by DAS28 (Haringman et al. 2005). Macrophages in RA produce chemokines including macrophage inflammatory protein 1 and monocyte chemoattractant protein, that attract leucocytes into the joint (Kinne et al. 2000). They also produce pro-inflammatory cytokines such as TNFα and a wide range of members of the interleukin family including IL-1 and IL-6 and the granulocyte macrophage colony stimulating factor (GM-CSF) (Chu et al. 1991;Chu et al. 1992) hence supporting their role in chronic inflammation. Of note, production of some of these factors has been localised to the pannus-cartilage junction suggesting a role in joint destruction. Indeed, it has been proposed that they exert a direct cartilage destructive role through their production of matrix degrading enzymes, an effect that is amplified by co-culture with synovial fibroblasts in murine models (Kinne et al. 2000).

The role of synovial fibroblasts in disease is discussed under a separate heading later in this chapter.

1.1.2.4 Epigenetic regulation

An important role for epigenetic mechanisms in the pathogenesis of RA has been described. Initially coined by developmental biologists to refer to the study of how genotypes give raise to phenotypes during development, the term epigenetics was subsequently used by molecular biologists to refer to heritable changes in gene expression that do not arise from changes in the underlying DNA sequence (Bird 2007). In recent times, the idea that all epigenetic changes are heritable has been the subject of debate (Cortessis et al. 2012) and a broader definition has been proposed that includes non-heritable, environmentally induced and reversible modifications (Bird 2007).

A broad range of epigenetic mechanisms have now been described including DNA methylation, post-translational modification of histones, microRNAs and long non-coding RNAs. Epigenetic marks that are associated with specific cellular gene expression repertoires and are responsible for their maintenance have been defined. At the same time, other epigenetic marks can be dynamic and affected by environmental interactions. Exposure to environmental agents such as cigarette smoke, organic chemicals, metals, nutritional sources and the microbiome have been associated with marked changes in cellular epigenomes, particularly when exposure occurs during key developmental periods (Cortessis et al. 2012). Hence, the epigenome may not only

provide a tool to understand disease pathogenesis but may also explain environmental interactions and provide a powerful tool to modify disease course.

DNA methylation is one of the best studied epigenetic modifications. Addition of a methyl group in position 5 of the cytosine ring within cytosine-phosphate-guanine dinucleotides is associated with gene silencing. RA synovial tissue and cultured RA synovial fibroblasts display global DNA hypomethylation that is associated with up-regulation of disease relevant genes such as adhesion molecules and matrix metalloproteinases (MMPs). Additionally, treatment of normal synovial fibroblasts with the DNA methylation inhibitor 5-aza-2-deoxycytidine leads to up-regulation of disease relevant genes (Karouzakis et al. 2009). A distinct DNA methylation signature has subsequently been demonstrated for RA synovial fibroblasts that is associated with several biological pathways including cell migration, focal adhesion and transmigration (Nakano et al. 2013).

The study of non-protein coding genes that act as modulators of gene function has also attracted attention. Non-coding RNAs are mRNA molecules transcribed from DNA that do not code for proteins. Instead, they are involved in post-transcriptional regulation of gene expression through their ability to regulate the stability of protein coding mRNA (Perkins et al. 2005). Long non-coding RNAs and microRNAs are amongst the most studied non-coding RNAs.

MicroRNAs (miRNAs) are short (21-23bp) RNA fragments that regulate protein translation trough RNA-RNA interactions. They exert their regulatory role through complementarity of 6-8 nucleotides in the miRNA sequence to the same number of

nucleotides in the 3' untranslated region of their target mRNA. The ability to interact with target mRNA on the basis of a small number of nucleotides allows a large number of possible interactions which explains how a single miRNA is able to regulate hundreds of target mRNAs (Strietholt et al. 2008). Several studies have identified altered miRNA expression in plasma of RA patients compared to healthy individuals (Ceribelli et al. 2011) and their study also extends to RA synovial fibroblasts. Increased expression of miR-155 and miR-146a has been described in cultured established RA synovial fibroblasts with the former also being overexpressed in RA synovial tissue and blood monocytes. Whilst overexpression of miR-155 was associated with decreased expression of MMPs (Stanczyk et al. 2008), overexpression of miR-146a has recently been associated with inhibition of osteoclastogenesis in collagen induced arthritis (Nakasa et al. 2011). However, overexpression of miR-146a is not specific to RA and has also been described in osteoarthritis (Yamasaki et al. 2009). Overexpression of miR-203 by RA synovial fibroblasts has also been demonstrated. In this study forced expression of miR-203 in these cells led to up-regulation of MMP1 and IL-6 production via the NF-κB pathway (Stanczyk et al. 2011).

Very recently a potential role for long non-coding RNAs (lncRNAs) in RA pathogenesis has also been proposed. LncRNAs are large (>200bp) RNA molecules that have been implicated in a variety of processes including gene expression regulation and regulation of biological processes such as cell migration, proliferation and invasion (Umekita et al. 2014). Using microarray technology, gene expression patterns of RA and OA synovial fibroblasts were analysed. Two hundred and twenty five differentially expressed transcripts were identified between groups, a hundred of which were lncRNAs. Overexpression of two of these lncRNAs in the RA group was confirmed by

polymerase chain reaction (PCR). The validated lncRNAs were small nucleolar RNA host gene 1 (SNHG1) and RP11-39708. The function of either lncRNA remains unknown at present (Bertoncelj et al. 2013). To assess the effect of pro-inflammatory stimuli on lncRNA expression, the authors subsequently analysed expression levels of lncRNAs following synovial fibroblast stimulation with TNFα and IL-1β for 24 hours. The expression of several lncRNAs was influenced by pro-inflammatory stimulation *in vitro* but this response did not differ between RA and OA synovial fibroblasts. Silencing of one of these lncRNAs, antisense long non-coding RNA in the INK4 locus (ANRIL), resulted in decreased expression of MMP1 and MMP3 mRNA and protein, suggesting a role for ANRIL in the invasive characteristics of RA synovial fibroblasts (Bertoncelj et al. 2014). Although the study of lncRNAs in this context is on its early days and no definite conclusions can yet be drawn from these studies further work continues to be done to determine the role of lncRNAs in RA.

In summary, progression to RA is a multistep process that involves numerous factors. It is postulated that in the earliest phases of disease (before the onset of symptoms) environmental factors affecting susceptible individuals may lead to post-translational modification of self-proteins (i.e. citrullination). These processes are likely to take place in a variety of locations including the lungs, periodontal tissue, the joint and the bone marrow. Such processes may lead to loss of tolerance and development of autoantibodies including RF and ACPA antibodies which can be present years before the onset of clinical disease. Over time and presumably mediated by an as yet, unknown trigger, loss of tolerance progresses to symptomatic disease (McInnes et al. 2011).

1.1.3 Changing concepts: early disease and the window of opportunity

As knowledge of disease pathogenesis has advanced, the management of RA has experienced a parallel shift.

For many years, RA was considered a relatively benign disease where damage occurred late (Raza et al. 2006) Under this premise, aggressive treatment with drugs that, at the time, were felt to be very toxic was not warranted. Instead, cautious introduction of sequential monotherapy with non-steroidal anti-inflammatories as first line and disease modifying agents (DMARDs) as second line was favoured. This invariably resulted in introduction of the most efficacious treatments late in disease (Cush 2007).

Subsequently, longitudinal population based studies changed this perception by revealing a high risk of joint damage, disability and mortality in patients with uncontrolled RA. Of special importance was a seminal publication by Wilske and Healy in 1989 where they proposed "reversing" the treatment pyramid and advocated early disease treatment (Wilske et al. 1989). More recently the concept of a window of opportunity in early disease has been proposed. This suggests that a very early, and yet not fully defined, phase in disease exists in which treatment leads to significantly better outcomes (van der Linden et al. 2010). Using cancer as an analogy, it is postulated that during this early phase, the number of diseased cells is smaller and pathogenic mechanisms may not be fully established hence providing a window of time when cells may be more responsive to treatment (Boers 2003).

Since these concepts were proposed, many clinical trials have proved that early aggressive treatment leads to significantly better clinical outcomes without an unacceptably high adverse side effect profile (Boers et al. 1997;Mottonen et al. 1999). Additionally, bone erosions (an important feature of joint destruction) have been found to occur in early disease and as a result of active synovitis emphasising the need for early aggressive treatment (Raza et al. 2006). Nevertheless the concept of early disease remains poorly defined. Whilst most initial clinical trials assessing aggressive combination therapy defined early RA as disease of less than 2 years symptom duration (Boers et al. 1997;Goekoop-Ruiterman et al. 2005) some lines of evidence suggest that the window of opportunity may be limited to the first few months of disease (Raza et al. 2005). An added difficulty here is the lack of consensus on how disease onset is defined. Various definitions of disease onset have been used in the literature including symptom onset, start of joint swelling, time of fulfilment of classification criteria for RA and time of diagnosis by physician (Raza et al. 2012). Consequently, what might be meant by the first 3 months of disease will be very different depending on how disease onset is defined (Figure 1.3).

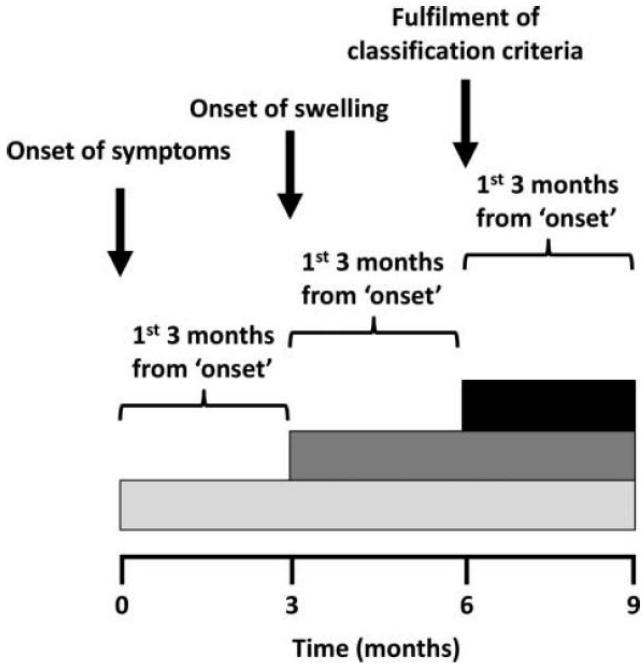

Figure 1.3 Schematic representation of differing definitions of the "first 3 months of disease" depending on how disease onset is defined. *Reproduced with permission from Raza et al. 2012.*

In a prospective observer blinded case control study, patients with very early RA (of less than 3 months symptom duration) in whom DMARD treatment had been initiated at a median disease duration of 3 months were compared with patients with late early RA (of 12-42 months duration) in whom DMARD therapy had been started at a median disease duration of 12 months. Significantly improved clinical and radiographic scores were found in the very early RA group compared to the late early RA group (Nell et al. 2004). At a molecular level, synovial fluid from patients with one or more swollen joints and inflammatory joint symptoms of three months or less duration was characterised revealing a distinct and transient cytokine profile (Raza et al. 2005). At a histological level, changes in microvasculature and synovial tissue have been identified in patients with synovitis of less than 6 weeks duration (Schumacher, Jr. et al. 1994). This expanding knowledge is reflected in a recent survey of rheumatologists where the

majority (84.5%) defined early RA as disease of symptom duration of less than 3 months (Aletaha et al. 2004).

Widespread acceptance of these concepts amongst health care professionals has led to a step change in the management of RA. Early arthritis clinics have been created and identification and treatment of early RA has become a clinical priority. Indeed, current research efforts can be divided into those directed to the development of new therapies and better understanding of disease mechanisms and those dedicated to understanding and bridging barriers to early treatment initiation. Limitations to effective early treatment still exist and issues such as delayed patient presentation and delayed referral to rheumatologists are still being addressed (Raza et al. 2011). In parallel, the search for predictors of disease outcome in early undifferentiated inflammatory arthritis and response to treatment continues in order to achieve early treatment strategies that are tailored to individual patients. In this respect, one of the remaining challenges is the correct early identification of patients that present with undifferentiated arthritis but will go on to develop RA and their distinction from patients with undifferentiated arthritis that will resolve. Whilst the use of the 2010 ACR/EULAR criteria to aid patient diagnosis has led to increased identification of patients with RA at an early stage, it is also recognised that this approach may lead to overdiagnosis of RA in patients with undifferentiated arthritis that is destined to resolve (Cader et al. 2011).

1.1.4 Pre-clinical rheumatoid arthritis and disease chronology

It is not only early RA, but the various phases preceding the clinical manifestations of disease that have attracted interest over the last few years. The observation that raised inflammatory markers and autoantibodies can be present in the sera of patients for some time before the onset of clinical symptoms has led to the suggestion that the preclinical phases leading up to disease may represent important therapeutic windows in their own right.

To facilitate research in this area, unifying terminology has been proposed to describe the phases leading up to the development of RA (Gerlag et al. 2012). These phases are not necessarily sequential and patients do not go through all phases before developing RA. The initial phases (A and B) comprise the presence of susceptibility alleles and exposure to environmental factors such as smoking. Phase C corresponds to asymptomatic autoimmunity. This phase can precede disease onset by up to fifteen years and is characterised by the presence of RF or ACPA in the absence of clinical disease. During this phase systemic inflammation can be detected by the presence of raised inflammatory markers (CRP) and pro-inflammatory cytokines such as TNFα and IL-6 (van Steenbergen et al. 2013). Asymptomatic autoimmunity is sometimes followed by a period of symptoms without clinical or radiological evidence of arthritis (phase D). Alternatively, other individuals may suffer from asymptomatic synovitis characterised by absence of symptoms but presence of histological synovitis (Kraan et al. 1998). Unclassified arthritis and RA complete these phases (phases E and F). A schematic representation of these phases is shown in Figure 1.4.

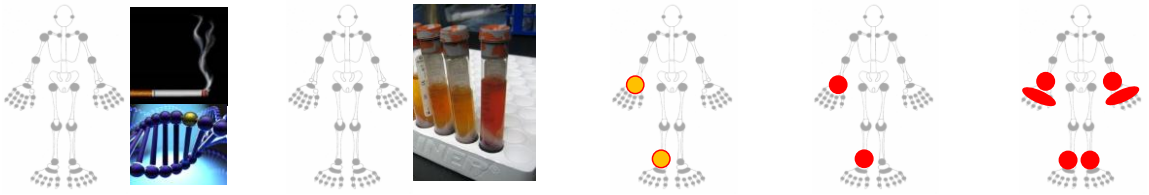

Figure 1.4 Recommendations for terminology to be used to describe specific phases up to the development of RA. *The following definitions are recommended when describing individuals in prospective studies: (a) genetic risk factors for RA, (b) environmental risk factors for RA, (c) systemic autoimmunity associated with RA, (d) symptoms without clinical arthritis, (e) unclassified arthritis, (f) rheumatoid arthritis.*

1.2 The role of synovial fibroblasts in rheumatoid arthritis

Synovial fibroblasts are one of the most abundant cell types in the RA synovium. Traditionally considered to have a landscaping function, they have emerged as key players in disease pathogenesis over recent years.

Synovial fibroblasts are characterised by their spindle-shaped morphology, ability to adhere to plastic *in vitro* and the absence of macrophage and endothelial lineage markers (Wilkinson et al. 1992). Although no specific surface marker for synovial fibroblasts has been identified, antibodies against non-specific markers such as cluster of differentiation 90 (CD90), cluster of differentiation 44 (CD44), decay accelerating factor (DAF), vascular cell adhesion molecule 1 (VCAM1), uridine diphosphoglucose dehydrogenase (UDPGD) and prolyl-4-hydroxylase are commonly used for positive synovial fibroblast identification (Zimmermann et al. 2001).

In recent years, other putative synovial fibroblast markers have been described and the expression of some of these makers has been associated with synovial fibroblasts in different areas of the synovium, suggesting that these may represent distinct subpopulations with specific functions (Figure 1.5). Whilst VCAM1 marks lining layer fibroblasts, CD90 and the recently described endosialin (CD248) mark fibroblasts in the sublining layer. Prolyl-4-hydroxylase and podoplanin (GP38) are expressed by fibroblasts in both layers (Filer 2013). Cadherin-11 is expressed by synovial fibroblasts in the lining layer where it mediates homotypic fibroblast adhesion. Overexpression of cadherin-11 in cultured RA synovial fibroblasts increases their invasiveness *in vitro* an effect that is ameliorated by treatment of cells with antibodies against cadherin-11 (Kiener et al. 2009). Cadherin-11 knockout mice display ameliorated joint inflammation when inflammatory arthritis is induced (Lee et al. 2007). A brief description of these markers is given in Table 1.3.

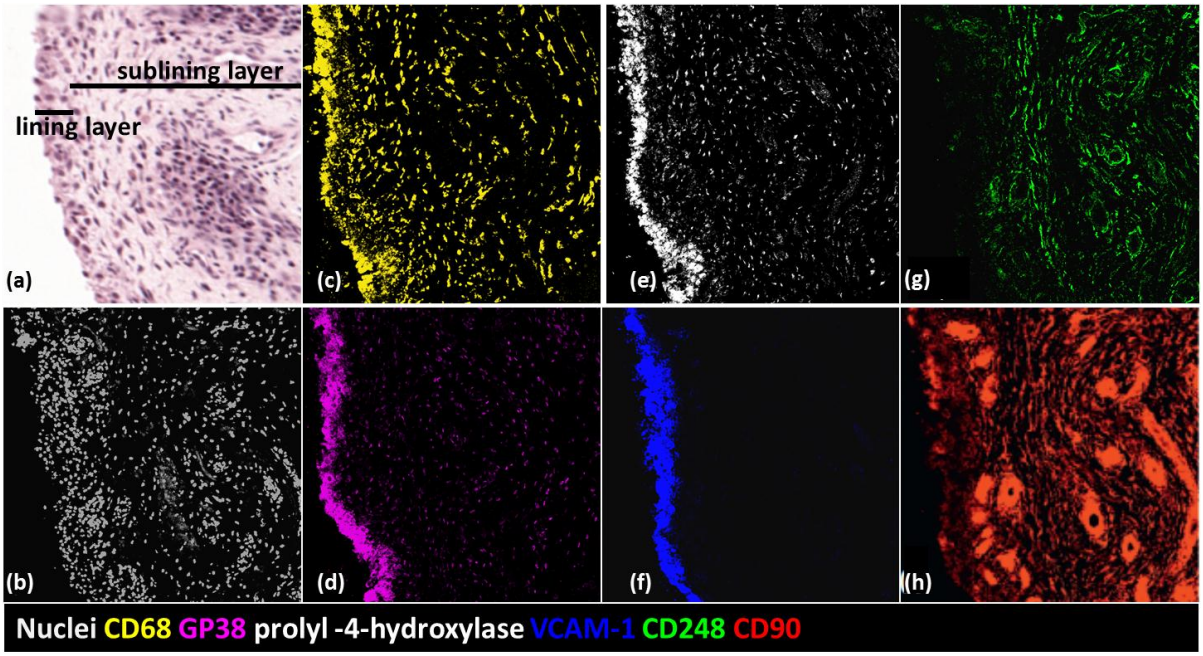

Figure 1.5 Confocal microscopy image of the RA lining and sublining layers. *For reference, the histological structure of the synovium is shown in (a), nuclear staining in (b) and macrophage staining in (c). GP38 (d) and prolyl-4-hydroxylase (e) are expressed by fibroblasts in lining and sublining layers. VCAM-1 is only expressed by synovial fibroblasts in the lining layer (f) whilst CD248 only stains sublining layer fibroblasts (g). CD90 is expressed by sublining layer synovial fibroblasts and endothelial cells (h). Reproduced with permission from Filer 2013.*

Table 1.3 Description of cell surface markers.

Symbol	Synonyms	Name	Description
CD90	Thy-1	Cluster of differentiation 90	Stem cell marker
CD44	HCAM	Cluster of differentiation 44	Cell-cell interactions
DAF	CD55	Decay accelerating factor	Complement system regulation
VCAM1	CD106	Vascular cell adhesion protein 1	Cell adhesion molecule
UDPGD		Uridine diphosphoglucose dehydrogenase	Synthesis of hyaluronan
CD248		Endosialin	Cell-cell adhesion & host defence
Gp38		Podoplanin	Tumour invasion
Cadherin-11		Cadherin-11	Homotypic cell adhesion

1.2.1 RA synovial fibroblasts as mediators of persistent inflammation

The presence of an organised chronic inflammatory infiltrate in the diseased RA synovium has been discussed earlier. Our group and others have suggested that stromal cells may play a central role in the molecular basis for the persistence of this inflammatory response. Just as cancer stroma regulates growth, survival and metastasis of transformed clonal cells (Micke et al. 2004) it was proposed that synovial fibroblasts would play a similar role in the dynamics of the chronic inflammatory infiltrate observed in RA (Buckley et al. 2001).

Normal inflammatory responses are tightly controlled, dynamic processes characterised by rapid response to the inflammatory/infectious trigger, highly specialised interactions between humoral, cellular and connective tissue elements and expansion of effector cells. In the resolution phase of inflammation, the expanded effector cells are cleared and normal tissue homeostasis is resumed. Thus, chronic inflammation can be viewed as a failure of this resolution phase resulting in inappropriate accumulation of cells within tissues (Figure 1.6).

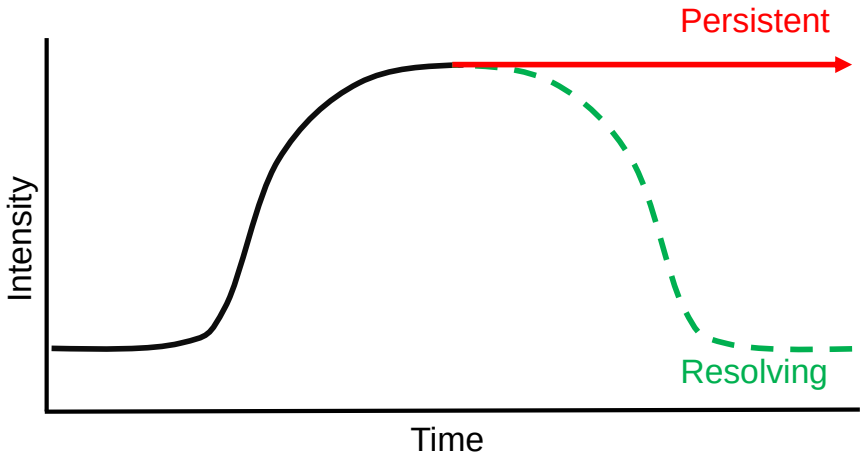

Figure 1.6 Inflammatory response. *Following an insult, an acute inflammatory response takes place. Once the pathogen has been cleared, normal tissue homeostasis is restored by an active process that involves clearance of effector cells. If this resolution phase becomes distorted, persistent chronic inflammation ensues.*

RA synovial fibroblasts promote leucocyte recruitment into the joints and are involved in the persistence of inflammatory infiltrates through their role in leucocyte survival and retention. High levels of neutrophil attracting chemokines including CXCL8 (IL-8), CXCL5 (ENA-78) and CXCL1 are expressed by stimulated cultured RA synovial fibroblasts (Koch et al. 1991;Koch et al. 1994;Koch et al. 1995). Their involvement in monocyte recruitment is supported by constitutive as well as induced expression of monocyte chemoattractant protein 1 (MCP1=CCL2) by cultured RA synovial fibroblasts (Villiger et al. 1992). Synovial fibroblasts also produce CCL4, CCL5 (RANTES) and CXCL16, indicating a role in monocyte, lymphocyte and T cell recruitment (Hosaka et al. 1994;Nanki et al. 2005;Patel et al. 2001). In addition to leucocyte recruitment, synovial fibroblasts support leucocyte survival and accumulation in the joint by a variety of mechanisms including inhibition of T cell apoptosis and expression of pro-survival and pro-retentive signals. Seminal work in this area includes the observation that activated T cells from synovial fluid from RA patients show no

evidence of apoptosis despite having a phenotype suggestive of high susceptibility to this process ($CD45RB^{dull}$, $CD45RO^{bright}$, $Bcl\text{-}2^{low}$, Bax^{high}, Fas^{high}) (Salmon et al. 1994). Interestingly, apoptosis could be induced *in vitro* indicating that the lack of T cell apoptosis observed *ex vivo* was not an intrinsic feature of these cells but rather may be mediated by the microenvironment these cells were in contact with. Indeed, T cells could be rescued from induced apoptosis *in vitro* by co-culture with RA synovial fibroblasts. Subsequently, type 1 interferons produced by RA synovial fibroblasts and macrophages were identified as the main factors mediating this survival (Pilling et al. 1999). *In vitro,* B cell survival is mediated by the expression VCAM1 and CXCL12 (SDF1) (Burger et al. 2001). RA synovial fibroblasts also express B cell activating factor (BAFF) and a proliferation inducing ligand (APRIL) constitutively and in response to toll-like receptor 3 (TLR3) stimulation which further supports their role in B cell function and survival (Bombardieri et al. 2011). RA synovial fibroblasts are also able to support NK cell and neutrophil survival *in vitro* (Chan et al. 2008;Filer et al. 2006). Expression of the constitutive chemokine CXCL12 by RA synovial fibroblasts contributes to T cell retention in a process that involves up-regulation of CXCR4 receptors in T cells (Buckley et al. 2000).

1.2.2 RA synovial fibroblasts as mediators of cartilage and bone destruction

The most compelling piece of evidence supporting a role for RA synovial fibroblasts in cartilage invasion and destruction comes from *in vivo* studies (Lefevre et al. 2009;Muller-Ladner et al. 1996). In their landmark paper, Muller-Ladner and colleagues

cultured RA, OA and normal synovial fibroblasts and dermal fibroblasts and co-implanted them with normal human cartilage under the kidney capsule of severe combined immunodeficient (SCID) mice. As these mice lacked a functional immune system, it provided an optimal environment for the study of interactions between human fibroblasts and human cartilage obviating the risk of transplant rejection. They demonstrated that RA but not OA, normal synovial or dermal fibroblasts attached to and invaded normal cartilage. This work is important for a number of reasons. First, it demonstrates that invasion of cartilage by synovial fibroblast is disease specific. Whilst all RA synovial fibroblast implants (n=5) showed intense invasion into cartilage, OA implants (n=5) only showed small isolated regions of superficial cartilage destruction and neither normal synovial (n=2) nor dermal (n=3) implants showed cartilage destruction. Second, it demonstrates that RA synovial fibroblasts have an intrinsically activated phenotype as they are able to exert their deleterious functions in the absence of cells and cytokines of the immune system. Third, it supports the notion that this phenotype is stable as synovial cells had been cultured for three to six passages prior to co-implantation with cartilage. Following on from this work, the authors have demonstrated that RA synovial fibroblasts are able to transmigrate and invade contralateral intact cell-free cartilage (Lefevre et al. 2009). This has been taken to suggest that synovial fibroblast, at least partly, mediate the well-known clinical feature of disease "spreading" to different joints.

Synovial fibroblasts produce matrix degrading enzymes including cathepsins B, D and L that have been found at sites of invasion in the SCID mouse model (Muller-Ladner et al. 1996). These cells also secrete MMPs including MMP1, 3, 9, 10 and 13 together with aggrecanases all of which have been associated with cartilage destruction (Lindy et

al. 1997;Okada et al. 1989;Tolboom et al. 2002). Production and secretion of some MMPs is regulated by pro-inflammatory stimuli and MAP kinase signalling pathways. MMP1 secretion is regulated by JNK following IL-1 stimulation of cultured synovial fibroblasts (Han et al. 1999). MMP1 and MMP13 secretion is stimulated by IL-1 and TNFα and, in the case of MMP1, mediated by ERK (Pillinger et al. 2003). Additionally, down-regulation of the tumour suppressor gene phosphatase and tensin homolog (PTEN) has been demonstrated to be associated with cartilage invasion. This gene encodes a protein that has tyrosine phosphatase activity. Mutations in this gene have been associated with cancer invasion. The study of PTEN in RA synovial fibroblasts did not reveal gene mutations but demonstrated lack of PTEN expression in the lining layer of RA synovial tissue. This was in contrast with staining of normal synovial tissue that revealed uniform PTEN expression in the lining and sublining layers. The lack of PTEN expression at the sites of invasion (i.e. lining layer) together with the observation of negligible PTEN expression by cartilage invading RA synovial fibroblasts in the SCID mouse model led to the suggestion that PTEN down-regulation contributes to cartilage invasion (Pap et al. 2000a;Pap et al. 2000b).

The pathogenic role of RA synovial fibroblasts extends to bone erosions where they are proposed to play a dual role in promoting bone destruction and preventing bone formation. Osteoclasts have long been implicated as effectors of bone resorption in RA (Fujikawa et al. 1996). Receptor activator of nuclear factor kappa-B ligand (RANKL), a TNF superfamily member, is the only known ligand for the RANK receptor and is a key effector of monocyte to osteoclast differentiation. RANKL mRNA is expressed in RA synovial tissue in the lining layer and at sites of bone destruction and levels of RANKL protein expressed by cultured RA synovial fibroblasts correlate with their ability to

induce monocyte to osteoclast differentiation, thus strongly supporting a central role in joint destruction in RA (Shigeyama et al. 2000).

Dickkopf related protein 1 (DKK1), an inhibitor of the wingless (Wnt) signalling pathway, directly impairs osteoblast differentiation and indirectly enhances bone destruction by increasing RANKL induced osteoclastogenesis (Goldring et al. 2007). Synovial tissue sections of patients with established RA display strong DKK1 expression that localises to synovial fibroblasts (Diarra et al. 2007). Indeed, our group has shown that DKK1 expression by RA synovial fibroblasts is tightly regulated by glucocorticoid metabolism *in vitro* (Hardy et al. 2012). Taken together, these data support a role for Wnt signalling inhibition in RA bone destruction.

1.2.3 RA synovial fibroblasts and synovial hyperplasia

Synovial hyperplasia is associated with overexpansion of synovial fibroblast populations in the lining and sublining layers. Consequently, it has been proposed that RA synovial fibroblasts undergo increased proliferation. In favour of this hypothesis are up-regulation of genes that are associated with cell cycle and mitosis regulation such as ERK and early response gene 1 (EGR1) (Aicher et al. 1994;Schett et al. 2000) and the overexpression in RA joints of a number of growth factors that have been shown to drive synovial fibroblast proliferation *in vitro* (Melnyk et al. 1990). c-myc, a proto-oncogene that has a very important role in cell proliferation, is expressed in RA synovium, especially in areas of cell proliferation and proximity to cartilage suggesting an important role for this gene in synovial fibroblast proliferation and activity (Qu et al. 1994). Nevertheless, increased RA synovial fibroblast proliferation in RA synovial tissue could not be demonstrated (Nykanen et al. 1978), and RA and OA synovial

fibroblasts showed similar growth rates that were slower than that of control dermal fibroblasts *in vitro* (Jacobs et al. 1995). The latter finding is in keeping with our own experience of synovial fibroblast in culture (Chapter 3). Therefore, decreased synovial fibroblast apoptosis has been proposed as an alternative/complementary mechanism to explain fibroblast expansion and dysregulation of several apoptosis pathways has been demonstrated.

Although RA synovial fibroblasts express Fas receptor and are able to undergo Fas mediated apoptosis *in vitro*, Fas-induced apoptosis is rarely observed *in vivo* (Nakajima et al. 1995). Subsequently, TNF induced expression of the anti-apoptotic protein FLIP by synovial fibroblasts has been observed to protect RA synovial fibroblasts from apoptosis. Additionally, down-regulation of FLIP resulted in increased Fas mediated apoptosis (Palao et al. 2004). The proto-oncogene B cell lymphoma 2 (Bcl-2) has anti-apoptotic effects and is expressed in RA synovial tissues where it has been associated with increased cell survival (Perlman et al. 2000). Expression of mutants of the tumour suppressor protein p53 has been demonstrated in RA synovial tissue and cultured synovial fibroblasts that was absent in OA and dermal tissues. Expression was associated with fibroblast survival by preventing apoptosis (Firestein et al. 1996). Furthermore, inhibition of p53 expression in normal and RA synovial fibroblasts resulted in increased cell numbers and enhanced invasive capabilities when these cells were co-implanted with normal cartilage in the SCID mouse model (Pap et al. 2001). These findings suggested important contributions of p53 mutations to synovial hyperplasia and RA synovial fibroblast invasiveness. However, later studies by the same group demonstrated that p53 mutations were present only in a small number of synovial fibroblasts in the lining layer of the RA synovium (Yamanishi et al. 2002).

Subsequent analysis of invasive versus non-invasive synovial fibroblasts revealed no differences in the frequency of p53 mutations. It was thus concluded that it was the proximity to cartilage, as opposed to the presence of p53 mutations, what might determine fibroblast invasiveness (Yamanishi et al. 2005).

The study of TNF induced apoptosis through TNF related apoptosis ligand (TRAIL) has produced somewhat conflicting results. TRAIL can bind to a number of receptors including the death receptors TRAIL-R1 and TRAIL-R2 and the decoy receptors TRAIL-R3 and TRAIL-R4. Some authors have described a lack of TRAIL surface receptors in RA synovial fibroblasts and resistance to apoptosis upon TRAIL stimulation (Perlman et al. 2003) whilst others have found expression of TRAIL-R1 and TRAIL-R2 with low apoptotic rates upon TRAIL stimulation (~30%) and a paradoxical increase in TRAIL mediated proliferation of surviving cells through ERK, p38 and PI3 kinase mediated mechanisms (Morel et al. 2005). Others have reported TRAIL induced apoptosis only when RA synovial fibroblasts are sensitised with the histone deacetylase inhibitor Trichostatin A (Jungel et al. 2006). In contrast, apoptosis rates of up to 80% upon TRAIL stimulation have been reported (Ichikawa et al. 2003). Differences in study design including cleavage of cell surface receptors during trypsinisation and differing reagents could explain the discrepancies between these studies.

1.2.4 Signalling pathways

The altered behaviour of synovial fibroblasts has been associated with changes in signalling pathways and expression of disease related genes.

Evidence for the activation of the transcription factor nuclear factor-κB (NF-κB) in synovial fibroblasts is supported by animal and human studies (Marok et al. 1996;Miagkov et al. 1998). NF-κB is activated by pro-inflammatory stimuli and its activation induces transcription of genes encoding adhesion molecules, pro-inflammatory cytokines and MMPs (Vincenti et al. 1998). NF-κB activation has also been implicated in inhibition of synovial fibroblast apoptosis (Miagkov et al. 1998).

Members of the MAP kinase family have also been shown to be activated in RA synovial fibroblasts. Apart from the above mentioned role of JNK and ERK in MMP expression, JNK and p38 kinases are activated in cultured fibroblasts by pro-inflammatory cytokines and have been implicated in the inflammatory process (Bradley et al. 2004;Sundarrajan et al. 2003). Expression of activated JNK, ERK and p38 MAP kinases in RA synovial tissue has also been demonstrated (Schett et al. 2000). More recently, increased JNK, ERK and p38 activity has been shown in synovial tissues of patients with treatment naïve early RA (<1 year symptom duration) compared to PsA and undifferentiated arthritis. In this study, JNK activation predicted the development of RA (de Launay et al. 2012). Of particular interest is the role of MAP kinases in activator protein 1 (AP-1) system regulation. AP-1 is a heterodimeric transcription factor composed of proteins from the c-fos, c-jun, ATF and JDP families. AP-1 regulates gene expression in response to pro-inflammatory stimuli and has been implicated in up-regulation of MMPs expression by synovial fibroblasts. The study of adherent cell extracts from RA synovial tissues demonstrated high AP-1 binding activity compared to OA tissues. AP-1 binding correlated with c-fos and c-jun expression and disease activity (Asahara et al. 1997).

1.2.5 Known transcriptional profile

RA synovial fibroblasts display an altered transcriptional profile characterised by up-regulation of a number of oncogenes, proto-oncogenes and MMPs together with down-regulation of tumour suppressor genes. Examples have already been described under some of the preceding headings and include c-myc, EGR1 and PTEN to name but a few.

Recent advances in microarray expression profiling technology have been applied to the study of RA synovial tissues and synovial fibroblasts, significantly expanding knowledge in this field. Initial microarray profiling of RA synovial tissue showed significant tissue heterogeneity allowing identification of two major pathogenic subclasses. One of these classes was characterised by expression of genes involved in adaptive immune responses whilst the other featured expression of stromal cell genes (van der Pouw Kraan et al. 2003a;van der Pouw Kraan et al. 2003b). Subsequent analysis of gene expression profiles of 19 cultured RA synovial fibroblasts also identified two main subgroups that matched the tissue findings. Group I synovial fibroblasts showed overexpression of oncogenes and genes involved in complement activation whilst group II showed expression of collagen related genes and smooth muscle actin. These results provide evidence for heterogeneity within RA synovial cultures which may relate to differing clinical pictures and levels of inflammation (Kasperkovitz et al. 2005). Other authors have confirmed observations of heterogeneity within RA tissues and identified relationships between certain RA subsets and response to biologic therapy (Dennis et al. 2014). The transcriptional response of cultured RA and normal synovial fibroblasts to hypoxia has subsequently been examined proving

that hypoxia induces significant changes in transcriptional signatures in both groups (Del Rey et al. 2010).

1.2.6 Unanswered questions: the study of early inflammatory arthritis and the comparison between early and established RA

From the preceding discussion it is clear that the extensive study of the functional and transcriptional characteristics of synovial fibroblasts in patients with established RA strongly implicates them in disease persistence and joint damage. However, the potential involvement of synovial fibroblasts during the early phases of inflammatory arthritis has not been addressed.

When designing this study we took a clinical perspective and focused on the chronology of inflammatory arthritis. A patient presenting with early inflammatory arthritis would have previously had non-inflamed healthy joints. At some point in their life and for incompletely understood reasons they developed an inflammatory arthritis. The natural history of this arthritis may follow a number of paths: (i) it may resolve spontaneously (ii) it may persist as RA or (iii) it may persist as another type of chronic arthritis (Figure 1.7).

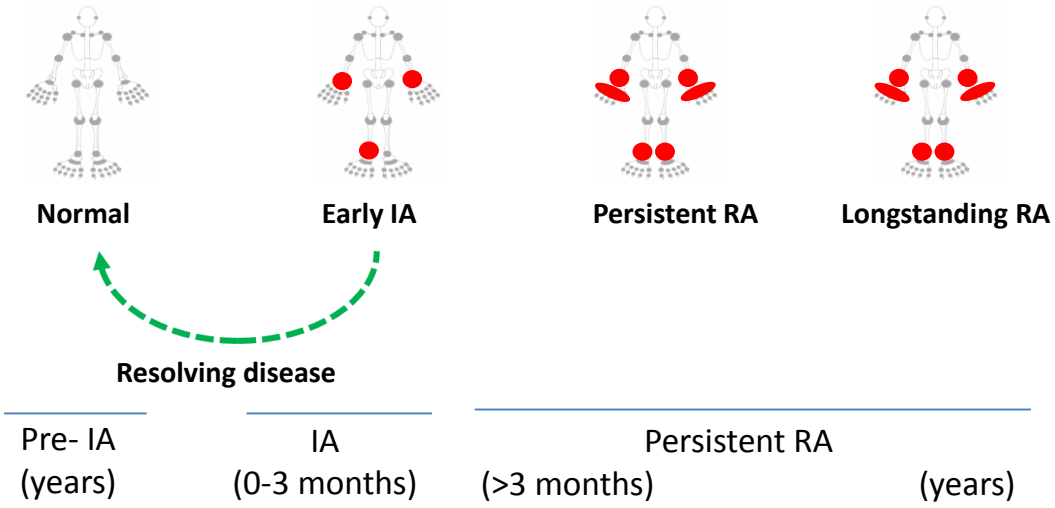

Figure 1.7 Chronology of inflammatory arthritis. *A patient that presents with early inflammatory arthritis (IA) would have had disease free (healthy) joints for years before presentation. At a given point in time (time 0) IA develops which can result in a number of different clinical outcomes. IA may resolve spontaneously and not recur or it may persist in the form of chronic arthritis amongst which RA is included (other types of arthritis excluded from the diagram for simplicity).*

It would thus be very informative to compare and contrast synovial fibroblasts from individuals and patients at these different stages. Owing to the known contribution of synovial fibroblasts to failed resolution of inflammatory infiltrates in established RA, it is tempting to speculate that cells in early disease may play a crucial role in the early stages of inflammatory arthritis and may be involved in critical decisions regarding persistence versus resolution of inflammatory arthritis. At the same time, it is important to define the functional and transcriptional characteristics of fibroblasts from patients with early inflammatory arthritis that persists as RA. In particular, the study of cells from patients during the first three months of disease would help define their characteristics during the early window of opportunity.

Furthermore, as the precise definition of early RA remains elusive, synovial fibroblasts from patients with early RA of more than three months duration will also be studied. The study of cells in individuals with non-inflammatory joint symptoms as well as patients with established RA completes the design. A schematic representation of the five distinct clinical outcome groups to be compared is shown in Figure 1.8. A comprehensive description of these patient groups is provided in Chapter 2.

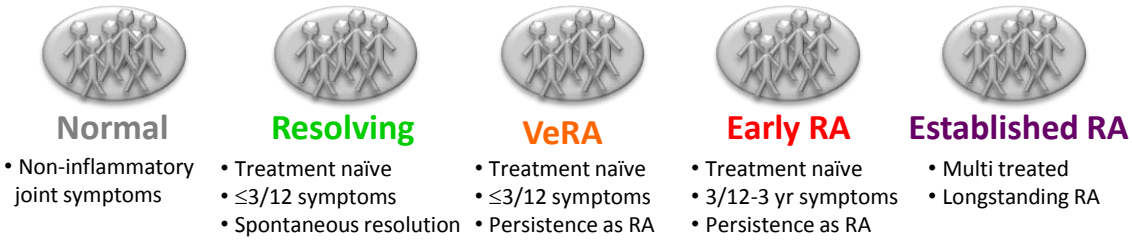

Figure 1.8 Clinical outcome groups. *Schematic representation of the five clinical outcome groups studied in this work. The main differentiating characteristics between groups are shown.*

1.3 Hypothesis and aims

The central hypothesis of this thesis is that synovial fibroblasts from patients in different clinical outcome groups will display different functional characteristics and transcriptomic profiles.

The two subhypotheses of greatest interest that I will test in this thesis are:

(a) That functional and transcriptomic differences exist between synovial fibroblasts in the Resolving and VeRA groups. This comparison is of particular interest as it may

result in identification of key differences between the resolution and persistence of early inflammatory arthritis.

(b) That functional and transcriptomic differences exist between synovial fibroblasts in the VeRA and Established RA groups. With this comparison I aim to gain insights into the progression from early RA to established, destructive disease.

To address these subhypotheses I plan to:

(1) Undertake functional characterisation of synovial fibroblasts in the five clinical outcome groups with a special interest in the comparisons outlined in (a) and (b). Functional characteristics that will be determined include: migration, invasion and proliferation.

(2) Perform transcriptomic analysis of synovial fibroblasts in the five clinical outcome groups, with a special interest in the comparisons outlined in (a) and (b).

2 Patients, materials and methods

2.1 Patient cohorts, sample collection and selection

2.1.1 Patient and outcome group selection

To further our understanding of molecular mechanisms underpinning early inflammatory arthritis, I set out to compare the functional and transcriptional characteristics of synovial fibroblasts in five distinct clinical outcome groups. This approach assumes that any existing differences between samples within each outcome group will not outweigh those differences between samples in different outcome groups, hence allowing identification of clinically significant phenotypes. Thus, outcome groups needed to be composed of clinical cases that were as similar as possible with regards to clinical presentation and biochemical parameters. At the same time, these groups should be representative of the population studied so that results could be generalised back to that population. Appropriate patient sample selection was thus central for the success of this project.

Samples from patients in one of the following five clinical outcome groups were used in this project: Normal, Resolving, very Early RA (VeRA), Early RA and Established RA. Normal controls were defined on the basis of non-inflammatory symptoms in patients undergoing exploratory knee arthroscopy. Resolving arthritis was diagnosed in patients whose arthritis resolved and did not recur at 18 months follow up. The diagnosis of RA was based on fulfilment of the 1987 ARA classification criteria (Arnett et al. 1988). Within the RA groups, further distinctions were made according to disease duration at the time of sample collection. The VeRA group included patients with treatment naïve

inflammatory arthritis of ≤3 months symptom duration at sample collection whilst the Early RA group comprised patients with treatment naïve inflammatory arthritis of symptom duration between 3 months and 3 years at the time of sample collection. A third RA group was composed by patients with longstanding disease of many years duration that were undergoing joint replacement and who had received multiple treatments (Established RA). This group corresponds to the same type of clinical samples upon which most of the synovial fibroblast literature is based. These five outcome groups and their main characteristics are represented in Figure 2.1.

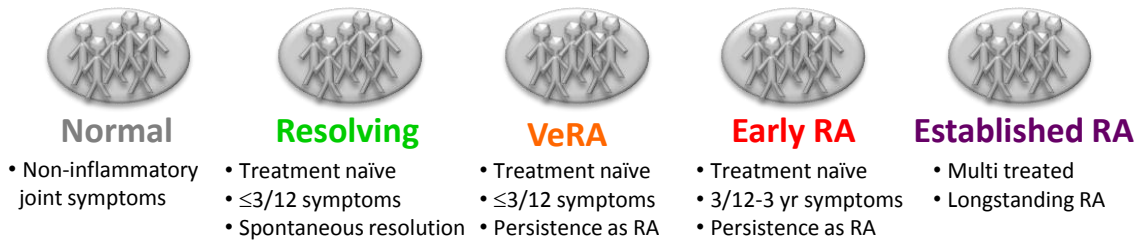

Figure 2.1 Clinical outcome groups. *Schematic representation of the five clinical outcome groups studied in this work. The main differentiating characteristics between groups are shown.*

2.1.2 Patient cohorts

Patient samples originated from one of three patient cohorts described below. At the time of initiation of experiments, all samples had already been collected and were available for use. All participants gave informed, written consent before taking part in the studies and all studies had appropriate ethical approval (LREC references 07/H1203/57, 07Q2706/2 and 07/H1204/191). At the time of sample collection clinical,

biochemical and radiological parameters were recorded including 66 tender and 68 swollen joint counts, ESR and CRP values, RF and anti cyclic citrullinated peptide (CCP) antibody status, 38 joint ultrasound and hand and foot radiographs.

2.1.2.1 Birmingham Early arthritis cohort (BEACON)

Patients were recruited from the rapid access clinic for early arthritis at Sandwell and West Birmingham Hospitals NHS Trust, Birmingham, UK. Treatment naïve patients with early (≤3 months symptom duration) inflammatory arthritis were selected on the criteria of one or more swollen joints and inflammatory symptoms (inflammatory joint pain and/or early morning stiffness and/or joint related soft tissue swelling). Patients with arthralgia but no clinical evidence of joint swelling (assessed by physician) and those with evidence of previous inflammatory joint disease were excluded. Patients were followed up for 18 months at which point they were assigned to their final diagnostic group (Resolving, VeRA or non-RA persistent inflammatory arthritis). The diagnosis of VeRA was based on fulfilment of 1987 ARA criteria (Arnett et al. 1988). Resolving arthritis was defined as no clinically apparent joint swelling at final follow up with no NSAIDs or steroids having been used in the previous three months. Samples from patients with non-RA persistent inflammatory arthritis were not analysed in this work. Treatment naïve patients with RA (as defined by the 1987 ARA criteria) of more than 3 months but less than three years duration were also recruited to this cohort. The same inclusion and exclusion criteria as above were used. Samples originating from this patient group comprised the Early RA group in the work presented in this thesis.

Synovial samples from all patients in this cohort were taken by ultrasound guided synovial biopsy.

2.1.2.2 Established RA cohort

Patients with longstanding RA fulfilling the 1987 ARA classification criteria who were undergoing joint replacement under the care of Mr. Andrew Thomas at the Royal Orthopaedic Hospital NHS Trust were included in the study. Synovial samples were obtained intra-operatively. This was designated the Established RA group.

2.1.2.3 Non-inflammatory cohort

Patients undergoing knee arthroscopy for non-inflammatory symptoms in the absence of clinical and MRI evidence of joint inflammation under the care of Mr. Martyn Snow from the Royal Orthopaedic Hospital were recruited. Most patients were undergoing arthroscopy for meniscal tear repair. Patients with inflammatory arthritis and osteoarthritis were excluded. Synovial samples from macroscopically normal areas of synovium were obtained intra-operatively. Samples were stained with haematoxylin and eosin and observed by light microscopy. Synovial tissue sections were evaluated at low magnification (10X objective) and scored based on the presence and size of mononuclear cell infiltrates. The scoring system was at follows 0: no infiltrates, 1: one small non-focal infiltrate, 2: one diffuse inflammatory infiltrate, 3: small focal aggregates (both perivascular and interstitial) and 4: large focal aggregates with a radial count of at least 10 cells. Only samples with a score of 0 were used in experiments. For simplicity, I will refer to samples originating from this cohort as the Normal group.

The full demographic and clinical characteristics of patients from whom samples used in functional characterisation, proof of concept, SAGE and microarray experiments originated are shown in Tables 2.1 to 2.4.

Table 2.1 Clinical characteristics of patients from whom samples used in functional characterisation experiments originated.

Clinical diagnosis	Code	Age	Gender	Ethnicity	Smoking	Symptom duration	Site	CCP	RF	SJC28	TJC28	VAS	DAS28 ESR	ESR	CRP	Baseline erosions	DMARD treatment
Normal	BX069	22	M	Caucasian	na	na	knee	n	n	0	0	N/A	N/A	na	na	no	none
Normal	BX070	44	M	Caucasian	na	na	knee	n	n	0	0	N/A	N/A	na	na	no	none
Normal	BX081	58	F	Caucasian	na	na	knee	n	n	0	0	N/A	N/A	na	na	no	none
Normal	BX082	49	F	Caucasian	na	na	knee	n	n	0	0	N/A	N/A	na	na	no	none
Normal	BX083	42	M	Asian	na	na	knee	n	n	0	0	N/A	N/A	na	na	no	none
Normal	BX085	38	M	Caucasian	na	na	knee	n	n	0	0	N/A	N/A	na	na	no	none
Normal	BX089	38	F	Caucasian	na	na	knee	n	n	0	0	N/A	N/A	na	na	no	none
Resolving	BX004	33	M	Caucasian	Current	3 wks	knee	n	n	2	1	78	3.6	9	6	no	none
Resolving	BX008	64	M	Caucasian	Ex	6 wks	knee	n	n	2	5	46	4.5	24	15	no	none
Resolving	BX010	40	F	Caucasian	Never	4 wks	knee	n	n	7	7	36	3.9	5	0	no	none
Resolving	BX024	32	M	Caucasian	Current	7 wks	knee	n	n	1	1	35	2.9	10	10	no	none
Resolving	BX038	45	F	Caucasian	Current	1 wks	knee	n	n	5	5	83	4.0	4	0	no	none
Resolving	BX064	35	M	Asian	Current	1 wks	knee	n	n	3	1	6	1.6	2	9	no	none
Resolving	BX071	41	F	Caucasian	Current	4 wks	ankle	n	n	2	0	10	1.7	5	9	no	none
VeRA	BX003	50	M	Caucasian	Current	4 wks	knee	p	p	11	13	28	5.7	31	26	no	none
VeRA	BX005	70	F	Caucasian	Ex	5 wks	knee	n	n	5	4	83	5.9	68	26	no	none
VeRA	BX013	45	F	Black	Current	10 wks	knee	n	n	3	3	12	3.9	24	12	na	none
VeRA	BX015	48	F	Caucasian	Ex	2 wks	knee	n	n	6	8	16	3.5	4	102	na	none
VeRA	BX027	44	F	Caucasian	Current	5 wks	ankle	n	n	2	3	32	3.8	18	10	no	none
VeRA	BX042	55	M	Caucasian	Never	4 wks	knee	p	n	4	0	9	3.5	58	45	yes	none
VeRA	BX063	74	F	Caucasian	Ex	9 wks	knee	p	n	3	3	62	4.4	20	32	no	none
Early RA	BX016	46	M	Caucasian	Current	150 wks	knee	p	p	16	13	75	6.6	38	7	na	none
Early RA	BX066	67	M	Caucasian	Current	38 wks	knee	p	p	1	1	74	4.2	29	48	na	none
Early RA	BX075	22	F	Caucasian	Never	52 wks	knee	n	n	6	6	89	6.4	81	79	na	none
Early RA	BX086	52	F	Caucasian	Current	38 wks	ankle	P	P	8	20	69	6.5	26	52	na	none
Early RA	BX093	65	M	Caucasian	Ex	156 wks	knee	p	p	12	3	28	5.3	72	81	yes	none
Established RA	RA06SY	60	M	Caucasian	na	30 yrs	knee	na	P	11	12	50	6.4	54	75	yes	SSZ
Established RA	RA15SY	37	M	Caucasian	na	22 yrs	knee	na	N	3	1	90	5.0	46	50	yes	MTX,LEF
Established RA	RA18SY	47	M	Caucasian	na	23 yrs	Knee	na	p	1	1	10	3.8	57	45	Yes	ETA
Established RA	RA19SY	63	F	Caucasian	na	20 yrs	knee	na	p	4	7	45	4.1	8	8	yes	ETA
Established RA	RA20SY	73	M	Caucasian	na	20 yrs	knee	na	p	7	9	25	4.8	18	na	na	LEF
Established RA	RA22SY	70	F	Caucasian	na	30 yrs	Knee	Na	p	7	8	0	4.4	20	na	yes	ADA
Established RA	RA23SY	58	F	Indian	na	11 yrs	knee	na	p	17	13	100	6.7	23	na	na	MTX
Established RA	RA28SY	42	F	Caucasian	na	20 yrs	knee	na	n	1	0	na	na	na	na	yes	Gold
Established RA	RA29SY	67	F	Caucasian	na	7 yrs	knee	P	p	13	9	80	6.6	57	66	yes	MTX,ETA

CCP: cyclic citrullinated peptide antibody; RF: rheumatoid factor; ESR: erythrocyte sedimentation rate; CRP: c reactive protein; SJC28: 28 swollen joint count, TJC28: 28 tender joint count; VAS: visual analogue score; DAS28 ESR: 28 joint count disease activity score (ESR); DMARD: disease modifying antirheumatic drug; M: male; F: female; wks: weeks; yrs: years; n: negative; p: positive; na: not available; N/A: not applicable; MTX: methotrexate, LEF: leflunomide; ADA: adalimumab; HCQ: hydroxychloroquine; ETA: etanercept.

Table 2.2 Clinical characteristics of patients from whom samples used in proof of concept experiments originated.

Clinical diagnosis	Code	Age	Gender	Ethnicity	Smoking	Symptom duration	Site	CCP	RF	SJC28	TJC28	VAS	DAS28 ESR	ESR	CRP	Baseline erosions	DMARD treatment
Resolving	BX004	33	M	Caucasian	Current	3 wks	knee	n	n	2	1	78	3.6	9	6	no	none
Resolving	BX008	64	M	Caucasian	Ex	6 wks	knee	n	n	2	5	46	4.5	24	15	no	none
Resolving	BX010	40	F	Caucasian	Never	4 wks	knee	n	n	7	7	36	3.9	5	0	no	none
Resolving	BX024	32	M	Caucasian	Current	7 wks	knee	n	n	1	1	35	2.9	10	10	no	none
Resolving	BX028	74	M	Caucasian	Current	5 wks	knee	n	n	23	0	55	4.8	45	13	na	none
Resolving	BX030	72	M	Caucasian	Never	8 wks	knee	n	n	4	7	34	3.6	5	0	na	none
Resolving	BX038	45	F	Caucasian	Current	1 wks	knee	n	n	5	5	83	4.0	4	0	no	none
Resolving	BX048	35	M	Caucasian	na	2 wks	knee	n	N	1	1	33	4.0	51	7	no	none
Resolving	BX064	35	M	Asian	Current	1 wks	knee	n	n	3	1	6	1.6	2	9	no	none
Resolving	BX071	41	F	Caucasian	Current	4 wks	ankle	n	n	2	0	10	1.7	5	9	no	none
Resolving	BX076	28	M	Black	Current	6 wks	knee	n	n	1	2	99	4.5	18	8	na	none
VeRA	BX003	50	M	Caucasian	Current	4 wks	knee	p	p	11	13	28	5.7	31	26	no	none
VeRA	BX005	70	F	Caucasian	Ex	5 wks	knee	n	n	5	4	83	5.9	68	26	no	none
VeRA	BX011	49	F	Caucasian	Never	2 wks	knee	n	n	8	9	35	4.7	12	8	na	none
VeRA	BX013	45	F	Black	Current	10 wks	knee	n	n	3	3	12	3.9	24	12	na	none
VeRA	BX027	44	F	Caucasian	Current	5 wks	ankle	n	n	2	3	32	3.8	18	10	no	none
VeRA	BX031	43	M	Caucasian	Ex	9 wks	knee	n	n	4	19	76	6.9	58	0	na	none
VeRA	BX040	56	M	Caucasian	Current	10 wks	mcp	n	p	21	14	50	5.2	5	0	no	none
VeRA	BX042	55	M	Caucasian	Never	4 wks	knee	p	n	4	0	9	3.5	58	45	yes	none
VeRA	BX049	48	F	Caucasian	na	3 wks	ankle	p	p	3	6	29	3.9	10	0	no	none
VeRA	BX059	62	F	Caucasian	Current	16 wks	ankle	p	p	2	4	16	5.32	40	5	yes	none
VeRA	BX063	74	F	Caucasian	Ex	9 wks	knee	p	n	3	3	62	4.4	20	32	no	none
VeRA	BX084	49	M	Caucasian	Never	6 wks	mcp	p	p	12	17	87	6.8	25	18	no	none
Early RA	BX016	46	M	Caucasian	Current	150 wks	knee	p	p	16	13	75	6.6	38	7	na	none
Early RA	BX017	61	F	Caucasian	Ex	30 wks	knee	n	n	6	15	45	4.9	8	9	na	none
Early RA	BX021	57	M	Caucasian	Ex	14 wks	knee	p	p	14	21	50	7.1	56	16	na	none
Early RA	BX022	58	M	Caucasian	Current	16 wks	knee	p	p	7	7	33	4.1	7	0	yes	none
Early RA	BX032	46	F	Caucasian	Current	30 wks	ankle	p	n	4	10	47	5.2	24	32	na	none
Early RA	BX055	64	M	Caucasian	Current	26 wks	knee	n	n	16	14	30	5.4	13	17	na	none
Early RA	BX066	67	M	Caucasian	Current	38 wks	knee	p	p	1	1	74	4.2	29	48	na	none
Early RA	BX075	22	F	Caucasian	Never	52 wks	knee	n	n	6	6	89	6.4	81	79	na	none
Early RA	BX077	72	F	Caucasian	Never	38 wks	knee	n	n	16	21	70	7.5	53	43	na	none

CCP: cyclic citrullinated peptide antibody; RF: rheumatoid factor; ESR: erythrocyte sedimentation rate; CRP: c reactive protein; SJC28: 28 swollen joint count, TJC28: 28 tender joint count; VAS: visual analogue score; DAS28 ESR: 28 joint count disease activity score (ESR); DMARD: disease modifying antirheumatic drug; M: male; F: female; wks: weeks; yrs: years; n: negative; p: positive; na: not available; N/A: not applicable; MTX: methotrexate, LEF: leflunomide; ADA: adalimumab; HCQ: hydroxychloroquine; ETA: etanercept.

Table 2.3 Clinical characteristics of patients from whom samples used in SAGE experiments originated.

Clinical diagnosis	Code	Age	Gender	Ethnicity	Smoking	Symptom duration	Site	CCP	RF	SJC28	TJC28	VAS	DAS28 ESR	ESR	CRP	Baseline erosions	DMARD treatment
Normal	BX069	22	M	Caucasian	na	na	knee	n	n	0	0	N/A	N/A	na	na	no	none
Normal	BX070	44	M	Caucasian	na	na	knee	n	n	0	0	N/A	N/A	na	na	no	none
Normal	BX081	58	F	Caucasian	na	na	knee	n	n	0	0	N/A	N/A	na	na	no	none
Normal	BX082	49	F	Caucasian	na	na	knee	n	n	0	0	N/A	N/A	na	na	no	none
Normal	BX083	42	M	Asian	na	na	knee	n	n	0	0	N/A	N/A	na	na	no	none
Normal	BX088	34	M	Caucasian	na	na	knee	n	n	0	0	N/A	N/A	na	na	no	none
Normal	BX089	38	F	Caucasian	na	na	knee	n	n	0	0	N/A	N/A	na	na	no	none
Normal	BX095	46	F	Caucasian	na	na	knee	n	n	0	0	N/A	N/A	na	na	no	none
Resolving	BX004	33	M	Caucasian	Current	3 wks	knee	n	n	2	1	78	3.6	9	6	no	none
Resolving	BX008	64	M	Caucasian	Ex	6 wks	knee	n	n	2	5	46	4.5	24	15	no	none
Resolving	BX010	40	F	Caucasian	Never	4 wks	knee	n	n	7	7	36	3.9	5	0	no	none
Resolving	BX033	81	F	Caucasian	Never	7 wks	ankle	n	n	11	16	50	6.7	60	52	no	none
Resolving	BX038	45	F	Caucasian	Current	1 wks	knee	n	n	5	5	83	4.0	4	0	no	none
Resolving	BX048	35	M	Caucasian	na	2 wks	knee	n	N	1	1	33	4.0	51	7	no	none
Resolving	BX064	35	M	Asian	Current	1 wks	knee	n	n	3	1	6	1.6	2	9	no	none
Resolving	BX076	28	M	Black	Current	6 wks	knee	n	n	1	2	99	4.5	18	8	na	none
VeRA	BX003	50	M	Caucasian	Current	4 wks	knee	p	p	11	13	28	5.7	31	26	no	none
VeRA	BX005	70	F	Caucasian	Ex	5 wks	knee	n	n	5	4	83	5.9	68	26	no	none
VeRA	BX013	45	F	Black	Current	10 wks	knee	n	n	3	3	12	3.9	24	12	na	none
VeRA	BX014	63	F	Caucasian	Never	4 wks	knee	n	n	5	1	50	5.1	104	9	na	none
VeRA	BX015	48	F	Caucasian	Ex	2 wks	knee	n	n	6	8	16	3.5	4	102	na	none
VeRA	BX027	44	F	Caucasian	Current	5 wks	ankle	n	n	2	3	32	3.8	18	10	no	none
VeRA	BX031	43	M	Caucasian	Ex	9 wks	knee	n	n	4	19	76	6.9	58	0	na	none
VeRA	BX042	55	M	Caucasian	Never	4 wks	knee	p	n	4	0	9	3.5	58	45	yes	none
VeRA	BX063	74	F	Caucasian	Ex	9 wks	knee	p	n	3	3	62	4.4	20	32	no	none
Early RA	BX016	46	M	Caucasian	Current	150 wks	knee	p	p	16	13	75	6.6	38	7	na	none
Early RA	BX018	69	F	Caucasian	Never	52 wks	knee	n	n	7	7	52	4.6	11	0	yes	none
Early RA	BX022	58	M	Caucasian	Current	16 wks	knee	p	p	7	7	33	4.1	7	0	yes	none
Early RA	BX055	64	M	Caucasian	Current	26 wks	knee	n	n	16	14	30	5.4	13	17	na	none
Early RA	BX066	67	M	Caucasian	Current	38 wks	knee	p	p	1	1	74	4.2	29	48	na	none
Early RA	BX075	22	F	Caucasian	Never	52 wks	knee	n	n	6	6	89	6.4	81	79	na	none
Early RA	BX077	72	F	Caucasian	Never	38 wks	knee	n	n	16	21	70	7.5	53	43	na	none
Early RA	BX093	65	M	Caucasian	Ex	156 wks	knee	p	p	12	3	28	5.3	72	81	yes	none
Established RA	RA06SY	60	M	Caucasian	na	30 yrs	knee	na	P	11	12	50	6.4	54	75	yes	SSZ
Established RA	RA15SY	37	M	Caucasian	na	22 yrs	knee	na	N	3	1	90	5.0	46	50	yes	MTX,LEF
Established RA	RA20SY	73	M	Caucasian	na	20 yrs	knee	na	p	7	9	25	4.8	18	na	na	LEF
Established RA	RA23SY	58	F	Indian	na	11 yrs	knee	na	p	17	13	100	6.7	23	na	na	MTX
Established RA	RA25SY	53	F	Caucasian	na	30 yrs	knee	na	n	8	11	na	na	na	na	yes	HCQ
Established RA	RA28SY	42	F	Caucasian	na	20 yrs	knee	na	n	1	0	na	na	na	na	yes	Gold
Established RA	RA29SY	67	F	Caucasian	na	7 yrs	knee	p	p	13	9	80	6.6	57	66	yes	MTX,ETA

Established RA	RA37SY	55	F	Caucasian	na	23 yrs	knee	p	n	8	5	85	5.9	45	57	yes	none

CCP: cyclic citrullinated peptide antibody; RF: rheumatoid factor; ESR: erythrocyte sedimentation rate; CRP: c reactive protein; SJC28: 28 swollen joint count, TJC28: 28 tender joint count; VAS: visual analogue score; DAS28 ESR: 28 joint count disease activity score (ESR); DMARD: disease modifying antirheumatic drug; M: male; F: female; wks: weeks; yrs: years; n: negative; p: positive; na: not available; N/A: not applicable; MTX: methotrexate, LEF: leflunomide; ADA: adalimumab; HCQ: hydroxychloroquine; ETA: etanercept.

Table 2.4 Clinical characteristics of patients from whom samples used in microarray experiments originated.

Clinical diagnosis	Code	Age	Gender	Ethnicity	Smoking	Symptom duration	Site	CCP	RF	SJC28	TJC28	VAS	DAS28 ESR	ESR	CRP	Baseline erosions	DMARD treatment
Normal	BX070	44	M	Caucasian	na	na	knee	n	n	0	0	N/A	N/A	na	na	no	none
Normal	BX081	58	F	Caucasian	na	na	knee	n	n	0	0	N/A	N/A	na	na	no	none
Normal	BX082	49	F	Caucasian	na	na	knee	n	n	0	0	N/A	N/A	na	na	no	none
Normal	BX083	42	M	Asian	na	na	knee	n	n	0	0	N/A	N/A	na	na	no	none
Normal	BX085	38	M	Caucasian	na	na	knee	n	n	0	0	N/A	N/A	na	na	no	none
Normal	BX088	34	M	Caucasian	na	na	knee	n	n	0	0	N/A	N/A	na	na	no	none
Normal	BX089	38	F	Caucasian	na	na	knee	n	n	0	0	N/A	N/A	na	na	no	none
Normal	BX095	46	F	Caucasian	na	na	knee	n	n	0	0	N/A	N/A	na	na	no	none
Resolving	BX004	33	M	Caucasian	Current	3 wks	knee	n	n	2	1	78	3.6	9	6	no	none
Resolving	BX008	64	M	Caucasian	Ex	6 wks	knee	n	n	2	5	46	4.5	24	15	no	none
Resolving	BX010	40	F	Caucasian	Never	4 wks	knee	n	n	7	7	36	3.9	5	0	no	none
Resolving	BX024	32	M	Caucasian	Current	7 wks	knee	n	n	1	1	35	2.9	10	10	na	none
Resolving	BX028	74	M	Caucasian	Current	5 wks	knee	n	n	23	0	55	4.8	45	13	na	none
Resolving	BX030	72	M	Caucasian	Never	8 wks	knee	n	n	4	7	34	3.6	5	0	na	none
Resolving	BX033	81	F	Caucasian	Never	7 wks	ankle	n	n	11	16	50	6.7	60	52	no	none
Resolving	BX038	45	F	Caucasian	Current	1 wks	knee	n	n	5	5	83	4.0	4	0	no	none
Resolving	BX048	35	M	Caucasian	na	2 wks	knee	n	n	1	1	33	4.0	51	7	no	none
Resolving	BX054	55	M	Caucasian	Never	6 wks	ankle	n	n	5	4	91	3.5	2	6	no	none
Resolving	BX064	35	M	Asian	Current	1 wks	knee	n	n	3	1	6	1.6	2	9	no	none
Resolving	BX065	37	F	Asian	Never	7 wks	knee	n	n	2	8	10	3.3	7	0	no	none
Resolving	BX071	41	F	Caucasian	Current	4 wks	ankle	n	n	2	0	10	1.7	5	9	no	none
Resolving	BX072	32	M	Caucasian	Current	10 wks	knee	n	n	1	3	60	3.7	15	0	no	none
Resolving	BX076	28	M	Black	Current	6 wks	knee	n	n	1	2	99	4.5	18	8	no	none
Resolving	BX087	27	M	Asian	Current	4 wks	ankle	n	n	2	2	20	3.8	27	28	no	none
VeRA	BX003	50	M	Caucasian	Current	4 wks	knee	p	p	11	13	28	5.7	31	26	no	none
VeRA	BX005	70	F	Caucasian	Ex	5 wks	knee	n	n	5	4	83	6.0	68	26	no	none
VeRA	BX011	49	F	Caucasian	Never	2 wks	knee	n	n	8	9	35	4.7	12	8	na	none
VeRA	BX013	45	F	Black	Current	10 wks	knee	n	n	3	3	12	3.9	24	12	na	none
VeRA	BX015	48	F	Caucasian	Ex	2 wks	knee	n	n	6	8	16	3.5	4	102	na	none
VeRA	BX020	59	M	Caucasian	na	6 wks	knee	n	n	20	4	50	4.9	14	22	na	none
VeRA	BX031	43	M	Caucasian	Ex	9 wks	knee	n	n	4	19	76	6.9	58	0	na	none
VeRA	BX040	56	M	Caucasian	Current	10 wks	mcp	n	p	21	14	50	5.2	5	0	no	none
VeRA	BX042	55	M	Caucasian	Never	4 wks	knee	p	n	4	0	9	3.5	58	45	yes	none
VeRA	BX045	42	F	Asian	Never	2 wks	ankle	p	p	18	28	100	8.3	54	40	no	none
VeRA	BX049	48	F	Caucasian	na	3 wks	ankle	p	p	3	6	29	3.9	10	0	no	none
VeRA	BX063	74	F	Caucasian	Ex	9 wks	knee	p	n	3	3	62	4.4	20	32	no	none
VeRA	BX084	49	M	Caucasian	Never	6 wks	mcp	p	p	12	17	87	6.8	25	18	no	none
VeRA	BX092	48	M	Caucasian	Ex	4 wks	mcp	p	p	9	8	50	6.0	63	38	no	none

Established RA	RA06SY	60	M	Caucasian	na	30 yrs	knee	na	p	11	12	50	6.4	54	75	yes	SSZ
Established RA	RA15SY	37	M	Caucasian	na	22 yrs	knee	na	n	3	1	50	5.0	46	50	yes	MTX,LEF
Established RA	RA20SY	73	M	Caucasian	na	20 yrs	knee	na	p	7	9	90	4.8	18	na	na	LEF
Established RA	RA23SY	58	F	Indian	na	11 yrs	knee	na	p	17	13	25	6.7	23	na	na	MTX
Established RA	RA25SY	53	F	Caucasian	na	30 yrs	knee	na	n	8	11	100	na	na	na	yes	HCQ
Established RA	RA28SY	42	F	Caucasian	na	20 yrs	knee	na	p	1	0	na	na	na	na	yes	Gold
Established RA	RA29SY	67	F	Caucasian	na	7 yrs	knee	p	p	13	9	na	6.6	57	66	yes	MTX,ETA
Established RA	RA37SY	55	F	Caucasian	na	23 yrs	knee	p	n	8	5	85	5.9	45	57	yes	none

CCP: cyclic citrullinated peptide antibody; RF: rheumatoid factor; ESR: erythrocyte sedimentation rate; CRP: c reactive protein; SJC28: 28 swollen joint count, TJC28: 28 tender joint count; VAS: visual analogue score; DAS28 ESR: 28 joint count disease activity score (ESR); DMARD: disease modifying antirheumatic drug; M: male; F: female; wks: weeks; yrs: years; n: negative; p: positive; na: not available; N/A: not applicable; MTX: methotrexate, LEF: leflunomide; ADA: adalimumab; HCQ: hydroxychloroquine; ETA: etanercept.

2.1.3 Sample collection, coding and validation of phenotype

Synovial samples collected at the time of biopsy or surgery were transferred to universal containers and kept on ice until processing (typically within 3 hours of collection). Primary synovial fibroblast cell lines were established from these samples as specified in the materials and methods section. Each cell line received a unique code comprising a prefix (BX, abbreviation for biopsy) and a number (sequentially given according to when the sample was collected). This code was used for all lines irrespective of their clinical outcome. The only exception to this rule was the code given to Established RA samples obtained from joint replacement surgery where the code comprised the prefix RA (for rheumatoid arthritis) a number (sequentially given according to when sample was collected) and suffix SY (synovial).

The phenotype of all fibroblasts used in this work was validated to confirm that the cells being cultured were indeed synovial fibroblasts and not other adherent cells present in synovial tissue such as macrophages or endothelial cells. Two criteria were used for validation. Synovial fibroblasts were identified by light microscopy on the basis of their spindle-shaped morphology (Image 2-1). Additionally, cell surface markers were assessed by flow cytometry. Cultured synovial fibroblasts did not express markers of macrophage (CD68) or endothelial (CD31) lineage but expressed the synovial fibroblast marker CD90 (Zimmermann et al. 2001).

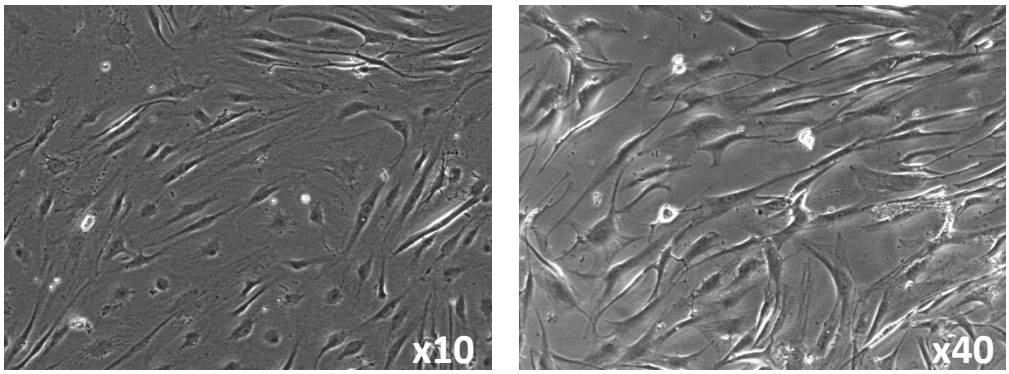

Image 2-1 Morphology of synovial fibroblasts. *Light microscopy images showing spindle-shaped morphology. x10 and x40 images shown.*

2.1.4 Testing of long term cultures for infection

Whenever cells are cultured, a risk of infection exists. Every effort is made to minimise this risk by handling cultures under sterile conditions in laminar flow cabinets and by adding antibiotics to culture medium. Nevertheless, the risk still exists and is particularly high if cells remain in culture for prolonged time periods. Infections may not only affect the viability of cultured cells, but if gone unnoticed, they may affect experimental results. Mycoplasma species are common contaminants of cell cultures. They are resistant to commonly used antibiotics and small and difficult to detect by microscopy, hence specific testing for these agents is required. Thus, regular mycoplasma testing was carried out on cell cultures used in this work. Testing was performed using a commercially available mycoplasma PCR kit as described in the methods section. None of the cultures used in this thesis tested positive. A typical image of a negative test is shown in Image 2-2.

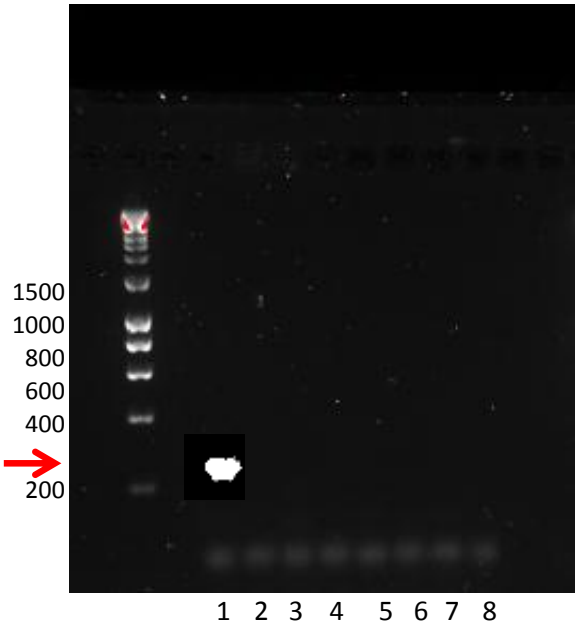

Image 2-2 Mycoplasma testing. *Agarose gel image of an experiment in which seven cell lines were tested. A positive control (lane 1) and seven samples (lanes 2 to 8) are shown. The size of the mycoplasma DNA fragment amplified (if present) should be 270bp (represented by red arrow in the ladder and the white band seen in lane 1). None of the samples tested positive.*

2.2 Cell culture

2.2.1 Tissue culture reagents

Reagents were purchased from Sigma-Aldrich unless otherwise specified. Reagents used to make culture medium included: RPMI 1640 (R0883), 100mM Sodium ortho-pyruvate (SOP) (S8636), L-glutamine-penicillin-streptomycin solution (GPS) (G1146) containing 200mM L-glutamine, 10,000 units of penicillin and 10mg/ml streptomycin, non-essential amino acids (NEAA) (M7145) and fetal calf serum (FCS) (F7524). Other reagents used in cell culture, recovery, maintenance and storage of cell lines included: 10x stock solution of trypsin-EDTA (PAA, L11-003) and dimethyl sulfoxide (DMSO) (D2879). Phosphate buffered saline (PBS) was made by dissolving PBS tablets (Oxoid BR0014) in distilled water at a ratio of 1 tablet

per 100ml of water. PBS was autoclaved prior to use. Where required for sterilization, solutions were filtered through 0.22μm filters (Millipore SLGP033RS). Syringes were purchased from BD Plastipak. Tissue culture plastics, tubes and flasks were purchased from Sarstedt. Cryovials were purchased from Grainer bio-one. For mycoplasma testing the EZ-PCR mycoplasma test kit (Geneflow 20-700-20) was used. Amplification was performed in the BioRad T100 thermal cycler. Materials used for gel electrophoresis included: SYBR safe DNA staining (Life Technologies S33102), UltraPure agarose (Life Technologies 16500500), UltraPure 10x TBE buffer (Life Technologies 15581-044) and HyperLadder 1kb (Bioline BIO-33053).

2.2.2 Medium

Synovial fibroblasts were cultured with complete fibroblast medium composed of: RPMI 1640, 10% FCS, 1% NEEA, 1% SOP and 1% GPS.

2.2.3 Primary cell cultures

Primary synovial fibroblast cultures were established at the time of biopsy or surgery. Each clinical sample originating from a patient gave rise to a cell line. Tissue samples were cut into small sections of approximately $1mm^3$ using a sterile scalpel. Sections were suspended in 6ml of complete fibroblast medium and transferred into T25 flasks. Lines were incubated at 37°C in 5%CO_2 and left undisturbed for a week. Subsequently medium was changed weekly.

2.2.4 Cell line maintenance in culture

Synovial fibroblasts were fed once weekly and maintained in culture until confluence. At feeding, 66% of the culture medium (referred to as conditioned medium) was discarded and replaced with fresh complete medium. Once cells reached confluence they were trypsinised.

2.2.5 Fibroblast trypsinisation (splitting)

Conditioned medium was removed and cells washed with PBS once. The cell monolayer was treated with trypsin (diluted 1:5 in PBS) for 5 minutes at 37°C in 5%CO_2. Cells were further detached mechanically by gently tapping the edge of the flask. They were then observed by microscopy to ensure complete detachment from plastic and collected in fresh complete fibroblast medium and centrifuged at 300*g* for 6 minutes. The supernatants were discarded and the cell pellets re-suspended in fresh medium and seeded into new flasks. Cells were reseeded into new flasks at a lower density applying a 1:3 ratio. Every time a culture was split the passage number increased by 1.

2.2.6 Freezing, storage and recovery of samples

At any given time during culture, if cells were not required for immediate use, they were stored in liquid nitrogen. Cells were trypsinised as above and washed with fresh medium and centrifuged at 300*g* for 6 minutes. They were subsequently re-suspended in freezing medium (composed of 90%FCS and 10% DMSO) and transferred to cryovials. The cryovials were placed in a freezing tray to allow gradual temperature reduction and placed in -80°C for at least 3 hours. Cells were subsequently transferred to the liquid nitrogen facility. Usually cells

were stored at a 1:3 ratio, that is, cells obtained from one confluent T75 flask would be split into three cryovials. Some lines were stored at "high density" meaning that all cells from a confluent T75 flask would be frozen into one cryovial. Freezing at high density allowed faster recovery of cell lines.

When required for culture, cells were retrieved from liquid nitrogen, quickly thawed in a water bath at 37°C and re-suspended in fresh complete medium. Cells were centrifuged at 300*g* for 6 minutes, supernatants were discarded and cells re-suspended in fresh medium and transferred to a T75 culture flask and incubated at 37°C in 5%CO_2. Cells were left undisturbed for a week before feeding.

2.2.7 Passage number of cells used

One of the advantages of cell culture is that it enables researchers to increase cell numbers. However, it has been shown that the gene expression patterns of cultured synovial fibroblasts change with increased cell passaging (Neumann et al. 2010). In consequence, all the work presented in this thesis was undertaken at low passage numbers. Cells used in functional assays were between passage 4 and 6 inclusive. For SAGE experiments cells were cultured to passage 5 and stored in liquid nitrogen in preparation for the experiments. Cells used in microarray experiments were at passage 3.

2.2.8 Testing of long term cultures for infection

To ensure that cultures were free from infection, mycoplasma testing of cultured lines was performed regularly. The EZ-PCR mycoplasma test kit (Geneflow 20-700-20) was used to

analyse the supernatants of cultured lines as per manufacturer's instructions. Briefly, PCR amplification was carried out by preparing a reaction mix containing 17.5µl of nuclease free water, 5µl of reaction mix and 2.5µl of the test line's supernatant. Test tubes were placed in the thermal cycler and run with the following parameters: one cycle at 94°C for 30 seconds, 35 cycles at 94°C for 30 seconds followed by 60°C for 120 seconds followed by 72°C for 60 seconds, one cycle at 94°C for 30 seconds, one cycle at 60°C for 120 seconds and a final cycle at 72°C for 5 minutes. Amplified products were subsequently analysed using gel electrophoresis. A 2% agarose gel was made by mixing 3g of agarose, 150ml of TBE buffer and 135ml of double distilled water. 6µl of SYBR safe DNA gel stain were added to the agarose mixture and poured into the cassette and covered with 1xTBE buffer. 5µl of PCR products and ladder were loaded to corresponding ports in the gel and electrophoresis run at 120v for one hour.

2.3 Methods: Chapter 3

2.3.1 Experimental set up and workflow

A minimum of 5 lines per clinical outcome group were analysed in each functional assay with the exception of the proliferation assay where 3 lines per outcome group were assessed. To maximise the use of cell lines and maintain passage numbers consistent within assays, a workflow system was established whereby cells were sequentially analysed in different assays following the same order (Figure 2.2). If after analysis in all assays, cells were still viable they were stored at high density for any potential future experiments.

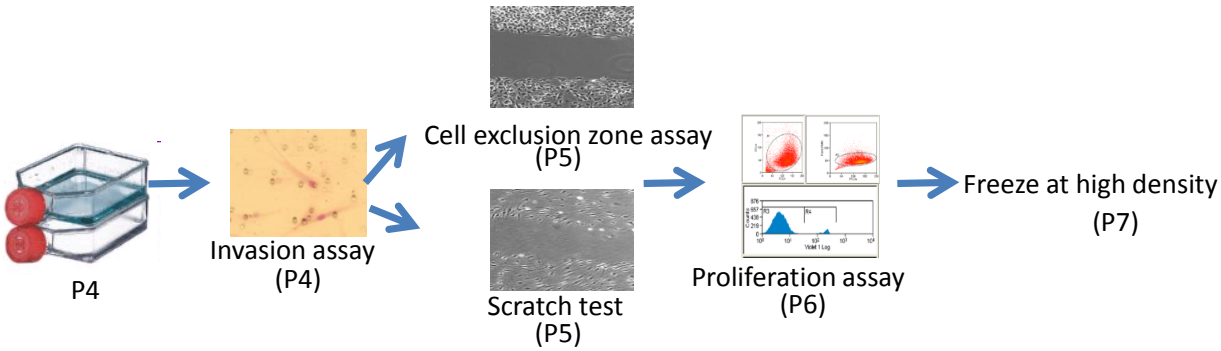

Figure 2.2 Functional assays workflow. *For each patient line, one passage 4 (P4) T75 flask was cultured. Cells were first used in the invasion assay (at passage 4). Next cells were analysed in parallel cell exclusion zone assay and scratch tests at passage 5. Subsequently, cell proliferation was assessed (at passage 6). If remaining cells were viable, they were frozen at high density for future use if needed. Between each experiment remaining cells were returned to the incubator to allow growth prior to the next experiment.*

2.3.2 Materials used in functional experiments

For both the cell exclusion zone and scratch test experiments, 6-well plates (BD Falcon 353046) were used throughout. Tissue culture inserts (Ibidi 80209) were used for creation of cell monolayers. Tumour necrosis alpha (TNFα) (R&D systems 210-TA-010), transforming growth factor beta (TGFβ) (Peprotech 100-21) and platelet derived growth factor (PDGF) (Peprotech 100-14B) were used for stimulation and chemoattraction. Growth factor reduced matrigel coated invasion chambers (BD 354483) and 24-well flat bottom with low evaporation lid plates (BD Falcon 353504) were used in the invasion assay. Staining of invading cells was performed with Diff-Quick (Reagena 102164) after fixation with methanol (VWR 20847.307). DIPX mounting medium (Thermo Scientific Raymond Lamb 12658646) was used to fix membranes to microscope slides. The medium used in the invasion assay was Dulbecco's modified eagle medium (DMEM) (Sigma-Aldrich D6546) supplemented with 1%

GPS and 0.5% bovine serum albumin (BSA) (Sigma-Aldrich A2153). The click-iT EdU flow cytometry assay kit (Invitrogen C10418) was used to assess cell proliferation.

2.3.3 Methods used in functional experiments

2.3.3.1 Scratch test

Cell monolayers were seeded on 6-well plates. Grids were taped to the base of the plates to serve as reference point. Cells were seeded at a density of $8x10^4$ per well and cultured at 37°C in 5% CO_2 for a week. At day 8 a single scratch wound was created with a sterile 20μL pipet tip. Images of the denuded areas were taken with a digital Olympus inverted phase contrast microscope at baseline (Time 0) and 18 hours later (Time 1). The grids at the back of the plate were used to divide the wound into 3 longitudinal frames that were recorded. The cell-free area was measured using Image J software analysis. The average of three frames was taken. The percentage of area covered in 18 hours was calculated using Microsoft Excel with the formula:

$$\frac{A0 - A1}{A0} \, 100$$

where A0 denotes area at Time 0 and A1 area at Time 1. A schematic representation of this assay is presented in Figure 2.3.

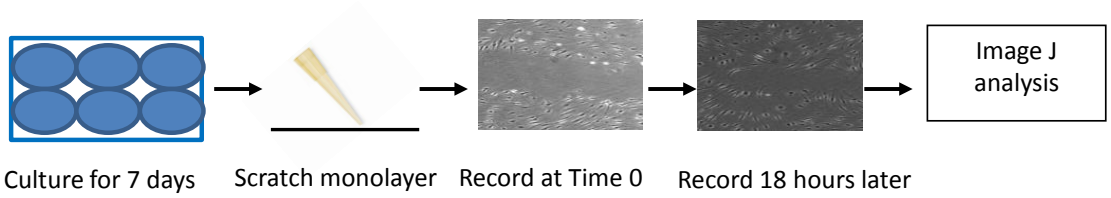

Figure 2.3 Schematic representation of the scratch test assay. *After culturing cell monolayers for seven days a scratch was created with a sterile pipet tip. Images of the cell denuded area were taken at baseline and 18 hours later. Image J software was used to measure the area and the percentage of area covered was calculated using Microsoft Excel. Image of pipet tip reproduced from http://www.usascientific.com/200ul-tipone-yellow-stacks.aspx.*

2.3.3.2 Cell exclusion zone assay

Cell monolayers were created in 6-well plates by aliquoting cell suspensions either side of a tissue culture insert. On day one, a grid was secured to the base of the plate. Culture inserts were positioned into the centre of each well and 70µl of cells at a density of $3x10^5$cells/ml were aliquoted to each port of the insert and incubated at 37°C in 5% CO_2 for 24 hours to allow adherence. At day 2, inserts were removed and images were taken at Time 0 (baseline) and Time 1 (18 hours later) as specified for the scratch test. A schematic representation of this assay is shown in Figure 2.4. For the stimulated assay, the experiments were repeated stimulating cells with TNFα (10ng/ml) or TGFβ (1ng/ml) for 48 hours. In these experiments, cells were seeded into culture inserts as specified and allowed to adhere for 24 hours. Conditioned medium was removed and replaced with fresh complete medium containing stimulants. 30 hours later inserts were removed and images taken at Time 0 and 18 hours later. Cells were stimulated for a total of 48 hours. Image analysis and area calculation was done as specified for the scratch test.

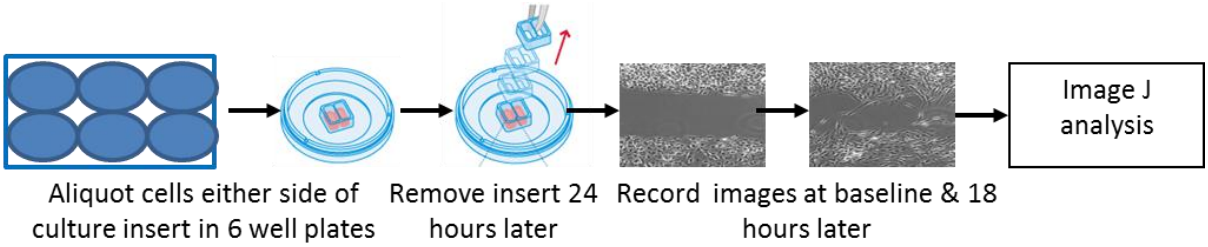

Figure 2.4 Schematic representation of the cell exclusion zone assay. *Cells were aliquoted either side of a culture insert and cultured for 24 hours. After removal of the insert a gap had formed between both cell monolayers. The cell free gap was imaged at Time 0 and 18 hours later. Data were subsequently analysed with image J and Microsoft Excel. Image of tissue culture inserts reproduced from http://ibidi.com/xtproducts/en/ibidi-Labware/Open-Slides-Dishes:-Removable-hambers/Culture-Insert-Family.*

2.3.3.3 Assessment of cell proliferation

The Click It EdU cell proliferation kit (Invitrogen C10418) was used according to manufacturer's instructions. As the aim of these experiments was to assess cell proliferation under the same conditions to which cells were subjected in the cell exclusion zone assay, the same experimental set up was used. Hence, culture inserts were positioned in the centre of wells in 6-well plates and 70µl of cells at a density of $3x10^5$cells/ml were aliquoted to each port of the insert. Cells were incubated at 37°C in 5% CO_2 for 24 hours to allow adherence. At day 2, culture inserts were removed and 2µM 5-ethynyl-2-deoxyuridine (EdU) added to the culture medium. Cells were incubated at 37°C in 5% CO_2 for 18 hours and subsequently prepared for proliferation analysis. Cells were washed with PBS, trypsinised and re-suspended in complete fibroblast medium. They were washed with 1% BSA in PBS and fixed with 100µl of 4% paraformaldehyde for 15 minutes. Cells were centrifuged at 500*g* for 5 minutes and re-suspended in 100µl of saponin wash reagent for a further 15 minutes. After another centrifugation step, they were incubated for 30 minutes with pacific blue, washed with saponin, filtered and analysed by flow cytometry (Dako Cyan ADP High Performance

(Dako, Ely, UK)). Data were analysed using SUMMIT software (Dako). Cell proliferation was expressed as percentage of stained cells.

2.3.3.4 Invasion assay

In vitro cell invasion was assessed with a transwell assay. Matrigel coated invasion chambers were used for this purpose (Figure 2.5). They consist of a 24-well companion plate with cell culture inserts that contain an 8µm pore size membrane coated with a thin layer of matrigel matrix. Chambers were used as per manufacturer's instructions. Briefly, $5x10^4$ cells suspended in 500µl of serum free 1% GPS, 0.5% BSA DMEM were seeded into each culture insert. The lower chambers were filled with 1%GPS, 0.5%BSA DMEM with 50ng/ml of PDGF, the latter acting as a chemoattractant. Chambers were incubated at 37°C in 5% CO_2 for 72 hours. Non-invading cells were scraped from the inside of the inserts using a cotton bud. Invading cells on the under surface of the membrane were fixed with methanol and stained with Diff Quick (Reagena 102164). Membranes were removed with a scalpel blade and fixed on microscope slides using DIPX. Cells were observed and counted using a non-inverted light microscope (Zeiss Axiostar plus). Eight ocular fields per membrane were counted.

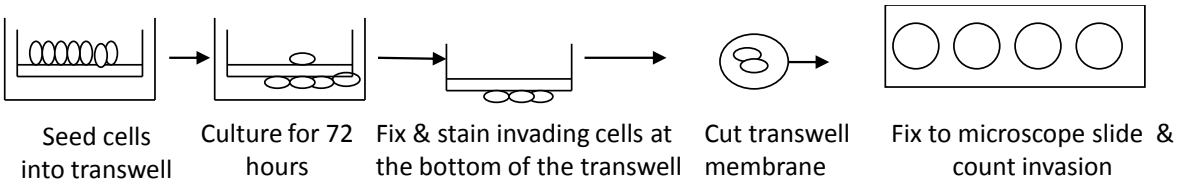

Figure 2.5 Schematic representation of the invasion assay. *Cells were seeded into invasion chambers. Cells were cultured for 72 hours to allow invading cells to digest matrigel and migrate to the bottom of the transwell. After fixing and staining cells attached to the bottom of the membrane, membranes were cut and fixed onto microscope slides that were visualised by light microscopy.*

2.4 Methods: Chapter 4

2.4.1 Candidate gene expression analysis with microfluidic cards

384-well custom made microfluidic cards were used to perform 48 gene expression assays (Life technologies, TaqMan gene expression arrays). The design of these cards is such that the specific gene probes and primers are pre-loaded and stable in the card so that gene expression analysis is quick and reliable. The list of gene targets selected for these cards is given in Appendix Table 9.1 together with a brief explanation of the relevance of the assessment of each target.

2.4.1.1 Sample preparation and RNA isolation for candidate gene analysis

All samples used in these experiments were cultured and treated under identical conditions. When cell lines achieved confluence at passage 3, two T75 flasks were taken. Conditioned medium was discarded and cells were washed with PBS once. Subsequently one flask was treated with 6ml of complete fibroblast medium supplemented with TNFα (10ng/ml) whilst the other was treated with 6ml of un-supplemented complete fibroblast medium. Cells were

cultured at 37°C in 5% CO_2 for 24 hours. Following the incubation time, supernatants were collected and stored. Cells monolayers were washed with PBS and trypsinised as described in section 2.2.5. A series of cell aliquots was created for several purposes. Amongst these, an aliquot was created with $1x10^4$ cells that were suspended in 350µl of RLT lysis buffer (containing guanidine isothiocyanate to immediately inactivate RNases) and stored -80°C for subsequent RNA isolation and analysis using microfluidic cards.

Cells that had been stored in 350µl of RLT buffer at -80°C were thawed and RNA extracted using the RNeasy kit (Qiagen 74104) according to manufacturer's instructions. Briefly, cells were thawed and 350µl of 70% ethanol added. Samples were applied to the columns and centrifuged at 13000*g* for 5 minutes. Samples were washed with two wash buffers (700µl of RW1 and 500µl of RPE) and RNA eluted in 30µl of RNase free water. Eluted RNA was further treated with DNA *free* (Ambion 1906) according to manufacturer's protocol to ensure that only pure RNA was obtained. 1µl of DNAse and 3.5µl of DNAse buffer were added to the eluted mRNA sample and incubated at 37°C for 30 minutes. 5µl of DNase inactivation reagent was added and incubated with the sample at room temperature for 2 minutes. After centrifugation (13000*g* for 1 minute) the supernatant (RNA) was collected and used in the microfluidic experiments.

2.4.1.2 Reverse transcription and real time PCR in microfluidic cards

The Quantitec Probe RT PCR kit (Qiagen 204443) was used for reverse transcription and real time PCR according to manufacturer's instructions. The reaction mix for each sample contained: 15µL of RNA, 1µL of reverse transcriptase, 50µL of RT PCR master mix and 34µL of RNA free water. Each 95µL reaction was loaded into the corresponding port of the

card. Cards were centrifuged at 300*g* for 1 minute, sealed and run in the Applied Biosytems 7900 HT fast real time PCR cycler. The programme used consisted of 1 cycle at 50°C for 30 minutes, 1 cycle at 94.5°C for 15 seconds, 40 cycles at 96°C for 30 seconds and 59.7°C for 1 minute.

2.4.1.3 Gene expression analysis

Three housekeeping genes were assayed in the cards: glyceraldehyde-3-phosphate dehydrogenase (GAPDH), β2 microglobulin and 18S ribosomal RNA (18S). The variation in expression levels of each housekeeper was calculated using the coefficient of variation method with the formula:

$$\frac{IQR}{M}\ 100$$

where IQR represents interquartile range and M median. This coefficient of variation was lowest for GAPDH (5.5%) followed by 18S (6.3%) and β2 microglobulin (6.4%). Consequently, gene expression was normalised to GAPDH.

Gene expression was quantified using the 2-delta Ct method (2^{-dCt}). First, the threshold cycle (Ct) value was set for each gene. Then the delta Ct (dCt) value was calculated by subtracting the GAPDH Ct value from the Ct value of the gene of interest. Subsequently a 2^{-dCt} value was calculated. Gene expression data were plotted as scattered dot plots. Differential gene expression between groups was calculated using Kruskal Wallis and Dunn's post-test analysis on median values.

2.4.2 DKK1 ELISA

DKK1 protein levels were measured using the DKK1 ELISA duo set (R&D DY1906) according to manufacturer's instructions. A brief description is given here. All incubations were done at room temperature and all samples were done in triplicate. A Nunc maxisorp 96-well plate was coated with 100µl/well of capture antibody and incubated overnight. The plate was washed and coated with 300µl/well of reagent diluent and incubated for 1 hour. Standards were diluted in reagent diluent and samples in complete fibroblast medium at a 25 fold dilution. 100µl/well of standard or sample were added to the plate and incubated for 2 hours. The plate was washed and 100µl/well of detection antibody were added and incubated for 2 hours. After another washing step, 100µl/well of streptavidin/HRP were added and the plate incubated for 20 minutes away from the light. After a wash, 100µl/well of substrate solution were added and incubated for 30 minutes away from the light. 50µl/well of sulphuric acid was added and the plate read at 450 nm.

Results were calculated as follows. A standard curve was created by plotting the mean absorbance of each standard against their concentration and drawing a best fit curve. Using regression analysis, the formula for the best fit curve was calculated and applied to each unknown sample. Results were multiplied by the dilution factor used (x25). Data were expressed as median and interquartile range.

2.4.3 Osteoblast differentiation and bone nodule formation experiments

2.4.3.1 Collection of supernatants from cultured synovial fibroblasts

One Resolving (BX010) and one VeRA line (BX040) were cultured in T75 flasks until confluence. Conditioned medium was discarded and cells washed with PBS. Conditioned medium was replaced with 6ml of fresh fibroblast medium and cells cultured for 48 hours. Subsequently, conditioned medium was collected and stored in 200µl aliquots at -80°C for use in osteoblast differentiation experiments.

2.4.3.2 Osteoblast differentiation experiments

Commercially available osteoblast precursors (Promocell C-12720) were used in these experiments. $2x10^4$cells/well were seeded on 6-well plates with 2ml/well of mineralisation medium (Promocell C-27020) to induce osteoblast differentiation. Cells were kept in culture for 21 days before assessing mineralised bone nodule formation as a surrogate marker of osteoblast differentiation. The experimental set up was as follows: positive and negative osteoblast precursor differentiation controls were created by culturing osteoblasts precursors with mineralisation and growth medium (Promocell Germany, C-27001) respectively. The expected effect was for the mineralisation but not the growth medium to induce osteoblast differentiation and mineralised bone nodule formation. A DKK1 positive control was created by adding 50ng/ml of recombinant DKK1 (R&D systems 5439-DK-010) to osteoblast mineralisation medium. Test samples were treated with osteoblast mineralisation medium

containing 25µl of conditioned fibroblast medium from either Resolving or VeRA cell lines as appropriate. Following culture for 21 days, cells were stained with alizarin red. Briefly, cell medium was discarded and cells washed with PBS twice. Cells were fixed with 10% buffered formalin (Sigma HT50-1-1) for 15 minutes and stained with 0.5% alizarin red (Sigma A5533) in water (pH4.2) for 15 minutes. Staining was followed by a washing step (using tap water) repeated 5 times. Direct observation under light microscopy (Leica inverted light microscope) was performed. The number of nodules formed in a 20x field was counted in triplicate and the mean of these triplicates taken. To confirm osteoblast differentiation, osteocalcin mRNA expression was measured by RT PCR using a Taqman osteocalcin gene assay (Life Technologies Hs-01587814_g1).

2.4.4 Synovial fibroblasts-HUVEC co-cultures in flow capture assays

Synovial fibroblasts were cultured onto inverted 6-well 0.4µm transwell filter inserts at a density of $5x10^5$ for 24 hours. Human umbilical vein endothelial cells (HUVEC) were seeded into the inner surface of the inserts at a concentration that would produce confluent monolayers in 24 hours. Cells were co-cultured for 48 hours in complete fibroblast medium prior to treatment with 100U/ml of TNFα and 10ng/ml IFNγ for a further 24 hours. Inserts were secured to a plate in a flow chamber system and lymphocytes (at a concentration of $2x10^6$/ml in PBS containing 0.15% bovine serum albumin and 5mM glucose) perfused for 4 minutes over HUVEC. The perfusion flow rate used was 0.099ml/min which is equivalent to a wall shear rate of $140s^{-1}$ and wall shear stress of 0.1Pa. After 2 minutes of washout, video clips were taken of a number of fields in the central area of the flow chamber. Analysis of the

images determined whether lymphocytes were rolling adherent, firmly adherent or transmigrating. Lymphocytes were isolated from venous blood from healthy donors.

For analysis of DKK1 levels in co-culture supernatants the R&D systems VersaMAP immunoassay was used as per manufacturer's instructions. Supernatants from cell co-cultures were diluted 1:3 in complete fibroblast medium. All incubations were done at room temperature on a plate shaker. Briefly, plates were washed with 100µl/well of wash buffer. 50µl/well of microparticle cocktail were added and incubated for 2 hours followed by 3 washing steps. 50µl/well of standard or sample were added and incubated for 2 hours. After another 3 washes, 50µl/well of antibody cocktail were added and the plate incubated for 1 hour. After 3 additional washes, 50µl/well of streptavidin-PE were added and incubated for 30 minutes. After three washes, 100µl/well of wash buffer were added and analysed in the Luminex100 instrument using the following settings: 50 events/bead, minimum events: 0, flow rate: 60µl/min, sample size: 50µl, doublet discriminator gates at 7500 and 15,500.

2.5 Methods: Chapter 5

2.5.1 Description of SAGE method

Total RNA is isolated using Trizol. Subsequently mRNA is isolated using Oligo (dT) magnetic beads. These beads contain oligodT sequences that bind to the polyA tail of mRNAs enabling mRNA isolation by magnetic separation. At the same time, the oligodT sequence is used as primer for reverse transcription and thus cDNA conversion also takes place on the beads. Next the cDNA transcripts are digested using the enzyme Nla III. This endonuclease cleaves transcripts at sites where the sequence GTAC is present. As this sequence occurs at

approximately every 250bp this is the approximate size of the resulting fragments. Following this, barcode adaptor A is ligated to the samples. This adaptor contains a unique barcode that enables identification of all transcripts originating from a given sample. It also contains a truncated internal adaptor sequence and an EcoP151 restriction enzyme recognition site. When EcoIP15I is added, it binds to the recognition sequence and cleaves cDNA 25-27bp downstream from the adaptor hence generating a 27bp sequence. The next step is the ligation of adaptor B that contains the primers for emulsion PCR. Samples are deposited on glass slides where amplification by emulsion PCR takes place. Next, sequencing by ligation is performed. This type of sequencing is based on the ability of DNA ligases to bind oligonucleotides of complementary DNA strands. Fluorescently labelled oligonucleotides are used to probe the unknown DNA sequences. Hybridisation of unknown nucleotides to complementary fluorescently labelled nucleotides results in fluorescence emission. Different bases can be identified as different colours in the emitted spectrum.

The newly obtained nucleotide sequences (called reads) are then mapped to a reference nucleotide sequence database (Reference Sequence database, RefSeq) using specific software. This process allows identification of the gene of origin of the tag. By quantifying the number of reads available for a given transcript, expression levels can be determined and compared between samples (Matsumura et al. 2005). Following sequencing experiments, independent confirmation of results is usually performed by validating target gene expression with quantitative methods such as real time quantitative PCR (Rajeevan et al. 2001).

2.5.2 **Reagents and materials used in Chapter 5**

Preparation of samples for SAGE analysis was done with the following reagents. Total RNA purification was performed with Trizol (Ambion 15596-018). Polyadenylated RNA was purified by magnetic selection using µMacs mRNA isolation kits (Miltenyi Biotech 130-075-201). Library generation was performed with the SOLiD SAGE kit with barcoding adaptor module (Life Technologies 4452811) and the SOLiD RNA barcode kit, module 1-16 (Life Technologies 4427046). Emulsion PCR was performed using the SOLiD EZ bead amplifier E20 accessories kit (Life Technologies 4453077) and the SOLiD ePCR kit (Life Technologies 4400834). Bead enrichment was performed with the SOLiD XD bead enrichment kit (Life Technologies 4453663) and components from SOLiD buffer kit (Life Technologies 4387918). Bead pre-deposition modification was done with SOLiD pre deposition kit (Life Technologies 4472967) and slide deposition with SOLiD XD slide and deposition kit v2 (Life Technologies 4456997) and components from SOLiD buffer kit (Life Technologies 4387918). Sequencing was performed using the SOLiD ToP fragment barcoded sequencing kit, MM35/5 (Life Technologies 4452696) and components from the SOLiD ToP instrument buffer kit (Life Technologies 4452688). Other reagents used in these experiments included: DEPC-treated and sterile filtered water for molecular biology (Sigma Life Science 95284), formaldehyde solution 37% (Sigma-Aldrich F15587), protease inhibitor cocktail tablets (Roche complete mini tablets 11836153001) and ethanol absolute (VWR International 20821.330). RNA quantity and quality were assessed with the Qubit dsDNA HS assay kit (Life Technologies Q32851) and the Quant-iT RNA assay kit **(**Life Technologies Q32852). PCR tube strips of 8 (Fisher Scientific 14230210) were used for real time PCR.

2.5.3 Cell culture and storage for SAGE experiments

Culture and processing of cell lines for SAGE experiments was performed in a standardised fashion. Eight different cell lines were cultured from each outcome group (making a total of 40 cell lines). Cells were grown under the same conditions until a minimum of $2x10^6$ cells per line were obtained. To obtain the RNA quantity required for the SAGE experiments $1x10^6$ cells per line per experiment was required. Hence, an arbitrary minimum cell number of $2x10^6$ cells per line was established in order to have spare samples in case any of them were lost or damaged during subsequent sample preparation and sequencing. All cell lines were at passage 5. Once cultured cells were ready to be processed, lines were harvested and counted. Volumes were adjusted to $1x10^6$ per ml, washed with 1 ml of PBS once and stored as cell pellets at -80°C.

2.5.4 RNA isolation, polyA RNA purification and library generation

Following the SOLiD 4 SAGE protocol, total RNA extraction was performed using Trizol followed by polyadenylated (polyA) RNA purification with µMacs columns as per manufacturer's instructions. Briefly, samples were thawed and homogenised with 1ml of Trizol. They were incubated at room temperature for 5 minutes and 0.2ml of chloroform added followed by vigorous shaking, incubation at room temperature for 3 minutes and centrifugation at 12,000*g* for 15 minutes at 4°C to obtain phase separation. The aqueous phase was collected and RNA isolation performed by adding 0.5ml of 100% isopropanol, followed by incubation at room temperature for 10 minutes and centrifugation at 12,000*g* for 10 minutes at 4°C. Supernatants were discarded and pellets washed in 1ml of 75% ethanol, vortexed and centrifuged at 7500*g* for 5 minutes at 4°C. Pellets were air dried and re-

suspended in 20µl of RNase free water. After incubation at 60°C for 15 minutes the RNA was used for polyA RNA purification by magnetic selection using µMacs columns. RNA was denaturated by heating at 70°C for 5 minutes. µMacs columns were prepared by rinsing with 100µl of lysis buffer and 50µl of magnetic oligodT beads were added to the samples. Samples were applied to the column where magnetically labelled polyA RNA was isolated by placing the columns in the MAC separator. Contaminants were removed through six washing steps and cDNA was synthesised. 43.5µl of first strand reaction mixture was added to the beads and incubated at 42°C for 3 minutes. 1.5µl of reverse transcriptase was added and incubated at 42°C for 2 hours with mild mixing every 15 minutes. This first cDNA strand was chilled in ice for 2 minutes and the second strand synthetised by adding the second strand reaction mixture and incubating at 16°C for 3 hours. The reaction was stopped by adding 0.5M EDTA and incubated with wash buffer for 15 minutes. Next Nla III and barcode adaptor A ligation was undertaken followed by EcoP15l digestion and barcode adaptor B ligation. A PCR was then performed and run to determine the optimal PCR cycles for emulsion PCR.

2.5.5 Assessment of RNA quantity and quality

RNA quantitation was performed with the Qubit fluorometer and the Quant-iT RNA Assay kit. Firstly, calibration was undertaken using standards 1 and 2 (included in the kit). Each sample was then quantitated sequentially in triplicate, and the mean of triplicates recorded. For quality assessment, Agilent RNA 6000 Pico chips were set up and primed as per manufacturer's instructions. RNA samples were diluted to achieve concentrations between 1ng/µl and 5ng/µl. Samples were heat denaturated and 1µl of each sample was loaded, together with the provided RNA 6000 Pico ladder into the chip. The chip was vortexed at

2400 rpm, and run on the Agilent 2100 bioanalyser. RNA quality was assessed by means of the RNA integrity number (RIN); a RIN value between 8.0 and 10.0 was considered optimal.

2.5.6 Emulsion PCR

SAGE libraries were pooled into groups of 8, using barcodes 1-8 for two of the pooled sample sets, and barcodes 9-16 for the other two. Pooled library sets were quantitated with the Qubit dsDNA HS assay kit, and diluted to a concentration of 43pg/µl. Emulsion PCR was performed in each pooled library as per manufacturer's protocol with a library concentration of 0.5pM. Following emulsion PCR, libraries were enriched for P2-containing beads, and the 3' ends modified with a terminal transferase reaction. Enriched beads were quantitated with the Nanodrop ND-100 spectrophotometer and compared to a previously prepared standard curve.

2.5.7 Sequencing

Beads were deposited on chambers as per Applied Biosystems SOLiD 4 system instrument's operation guide. $132x10^6$ beads from each pooled library were deposited on SOLiD slides using a 4-well deposition chamber. Beads were left to adhere at 37°C for 1 hour. Following deposition, non-adhered beads were pipetted off, and the chamber flushed with deposition buffer. Slides were washed with slide storage buffer, and fitted into a clean flow cell in the SOLiD 4 analyser, which was then filled with prepared 1x instrument buffer. All other sequencing buffers were prepared and fitted as per protocol and a 35bp forward/5bp barcode SAGE sequencing run initiated.

2.5.8 Analysis of SAGE data

Tags were mapped to the Reference Sequence (Ref Seq) database using the Bioscope analysis pipeline. Normalisation and gene expression profiling was performed using SOLiD SAGE analysis software. Statistical analysis of SAGE expression data was done using edgeR run under Bioconductor.

2.5.9 SAGE target validation methods

Materials used for RNA isolation and reverse transcription included: µMacs mRNA isolation kits (Miltenyi Biotech 130-075-201), isopropanol (AnalaR 102246L), sodium acetate (Sigma 71196) and glycogen (Invitrogen 10814-010). Reverse transcription was performed using SSII reverse transcriptase (Invitrogen 100004925), 5x FS Buffer (Invitrogen y0232), Rnease out (Invitrogen 100000840), 0.1M DTT (Invitrogen y00147), 10mM dNTP (Invitrogen 10297-018) and oligodT beads (Invitrogen 58862). Reagents used in real time quantitative PCR included: primer pairs designed by myself and manufactured by Eurofins Operon, absolute qPCR SYBR green ROX mix (Thermo Scientific AB-1163/A) and water for molecular biology (Sigma-Aldrich 95284).

2.5.10 RNA isolation, precipitation and reverse transcription for real time PCR

RNA isolation was performed using the µMacs mRNA isolation kit as per manufacturer's instructions. Samples were thawed and 500µl of lysis buffer added. Samples were thoroughly mixed to ensure complete dissolution and centrifuged at 13,000*g* at 4°C for 3 minutes.

Magnetic columns were placed in the MACS separator and equilibrated by rinsing with 100µl of lysis buffer. 50µl of magnetic oligodT beads were added to the samples and mixed. Samples were applied to the columns where magnetically labelled polyA RNA was isolated. Contaminants were removed with two washing steps with 200µl of lysis buffer and a further four washes with 100µl of wash buffer. 70µl of elution buffer were added and eluted RNA was collected in tubes and kept in ice. Subsequently, RNA was precipitated using isopropanol. 70µl of isopropanol, 7µl of sodium acetate and 1µl of glycogen were added to each sample and incubated at -80°C for at least 15 minutes. Samples were centrifuged at 13,000*g* at 4°C for 15 minutes. Supernatants were discarded and samples washed with 150µl of 70% alcohol and centrifuged again. Supernatants were discarded and samples left to air dry. Once dried, pellets were re-suspended in 10µl of RNase free water and 1µl of oligodT. 39µl of reverse transcriptase reaction mix containing 17µl RNase free water, 10µl 5xFS buffer, 5µl of DTT, 5µl of dNTP, 1µl of RNase out and 1µl of reverse transcriptase were added. Samples were run in the BioRad T100 thermal cycler with the following parameters: 25°C for 5 minutes, 42°C for 30 minutes and 85°C for 5 minutes.

2.5.11 Real time PCR primer design

For each gene to be validated, a specific primer pair was designed using the primer design tool in the National centre for biotechnology information (NCBI) website. The unique NM number for each gene was entered in the search area and a series of primer pairs were obtained. In order to select a good quality primer pair a number of parameters were used including: PCR product size of 80-250bp, primer pairs separated by at least one intron and a GC content of approximately 55% in each strand (Chuang et al. 2013).

Primer pairs selected according to these parameters were tested on Amplifx software (available for free download at: http://download.cnet.com/AmplifX/3000-2054_4-53766.html) before ordering. First, the cDNA sequence of the target gene was introduced in the sequence tab. Next, the sequences of the forward and reverse primers were entered in the primer list and a "virtual" PCR was run. This allowed identification of the size and position of the product and provided information on the quality of the primers with regards to GC content, stability and self-annealing. A screenshot of a representative example is shown in Figure 2.6. Primer pair sequences were ordered from Eurofins Operon. The primer pair sequences of primer pairs used in this work are shown in Appendix Table 9.2.

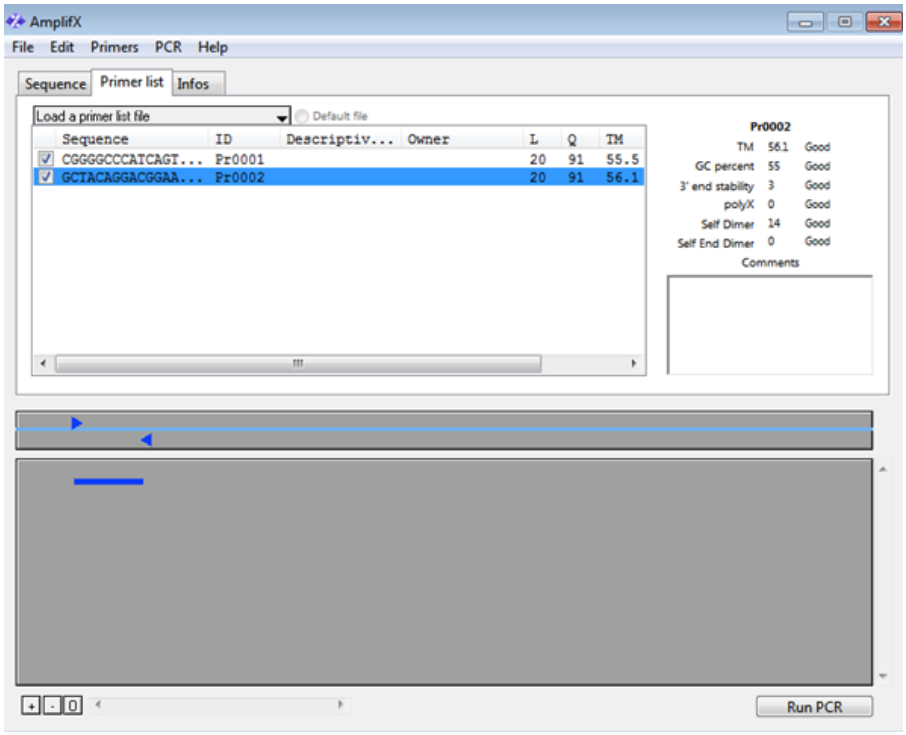

Figure 2.6 Screenshot showing the use of Amplifx to test primer pair quality. *Primer pair sequences can be seen in the screenshot in the primer list tab and the PCR product produced from these primer pair can be seen at the bottom of the image in blue. On the right hand side quality control parameters are displayed including GC content, self-annealing and primer stability. All these parameters are satisfactory for the primer pair shown.*

2.5.12 Real time PCR

Real time PCR experiments were performed in 384-well plates using the Light Cycler 480 PCR system (Roche). All samples were done in triplicate. Two reaction mixes were created: a sample and a primer mix. Sample mixes contained 0.1µl of cDNA, 2.9µl of water and 5µl of SYBR green ROX mix (which contained all components required for PCR with the exception of the primer templates) per sample per test. Primer mixes contained 0.1µl of forward and 0.1µl of reverse primer and 1.8µl of water per test. 8µl of sample mix and 2µl of primer mix were pipetted into each well to make a total 10µl per test. As a hot-start DNA polymerase was used, an activation step (95°C for 15 minutes) was included in the PCR reaction protocol. The PCR reaction was carried out with the following parameters: one cycle at 95°C for 15 minutes (hot-start), 40 amplification cycles at 95°C for 15 seconds followed by 60°C for 1 minute and a final cycle for the melting curves that consisted of 95°C for 15 seconds, 60°C for 1 minute and 95°C for 15 seconds. Gene expression was normalised to GAPDH using the 2-delta Ct method (2^{-dCt}) as previously described. Differential gene expression between groups was calculated using Kruskal Wallis and Dunn's post-test analysis on median values.

Quality control of primer pairs was performed by analysing primer pair products on a gel. For each primer pair, a PCR using human genomic DNA (Promega G3041) and Go Taq master mix (Promega M7122) was performed. For each primer pair a reaction was made in a PCR tube that contained 4µl of cDNA (diluted 1:10), 5µl of Go Taq master mix, 0.5µl of forward and 0.5µl of reverse primers. Samples were run on the BioRad T100 thermal cycler using the following cycling parameters: 95°C for 3 minutes, 95°C for 30 seconds, 60°C for 30 seconds, 72°C for 30 seconds, 40 cycles at 95°C for 30 seconds, 72°C for 5 minutes and 4°C thereafter.

Once complete, PCR products were run on a 2% agarose gel and run at 120v for one hour as specified in section 2.2.8.

2.5.13 TRAIL-R4 Flow cytometry

Expression of TRAIL-R4 protein was determined by flow cytometry. Reagents used in these experiments included: PE conjugated anti human TRAIL-R4 (R&D FAB633P), IgG isotype control (R&D, IC002P) and cell dissociation buffer (Gibco 13151014). Three Resolving (BX004, BX033, BX038) and three VeRA (BX011, BX013, BX063) lines were used in these experiments. The TRAIL-R4 expressing hepatic epithelial cell line (AKN-1) was used as positive control.

To dissociate cells from their flasks without cleaving cell surface receptors, 12ml of cell dissociation buffer were added to T75 flasks and cells incubated at room temperature on a plate shaker for 35 minutes. Detached cells were re-suspended in 8ml of medium and centrifuged at 500*g* for 5 minutes. Cell volumes were adjusted to $6x10^4$/ml. 700µl of cell suspension were transferred to a tube and washed 3 times with 0.5% BSA PBS. 100µl of sample were transferred to each well of a flexiplate and incubated with the corresponding TRAIL-R4 or IgG isotype at a concentration of 1:50 and incubated in the dark at 4°C for 45 minutes. Cells were washed with PBS and re-suspended in 100µl of PBS and transferred to flow cytometry tubes containing 400µl of PBS for analysis. Cells were filtered prior to analysis in the Dako Cyan ADP High Performance flow cytometer (Dako, Ely, UK). Data were analysed using SUMMIT version 4.3 software (Dako).

2.6 Methods: Chapter 6

2.6.1 Reagents and materials used in Chapter 6

For RNA isolation and preparation of samples for microarray analysis the following reagents were used: RNeasy Mini kit (Qiagen 74106), QIAshredder (Qiagen 79656), RNA clean and concentrator 25 (Cambridge Biosciences R1018) and 1.5ml LoBind tubes (Eppendorf 022431021). RNA quantity and quality were assessed with the Nanodrop 2000 spectrophotometer (Thermo Scientific). For labelling and creation of cRNA the Low Input Quick Amp Labeling Kit, Two-Color (Agilent Technologies 5190-2306) was used. Samples were hybridised onto Sure Print G3 gene expression 8x60k v2 microarrays (Agilent Technologies 039494) and scanned in the Agilent G2505C scanner. Reverse transcription of RNA for real time PCR was performed with the iScript cDNA Synthesis Kit (BioRad 170-8891).

2.6.2 Cell culture, treatment and storage for microarray experiments

All samples were cultured and treated under identical conditions. When cell lines achieved confluence at passage 3, two T75 flasks were taken. Conditioned medium was discarded and cells were washed with PBS once. Subsequently one flask was treated with 6ml of complete fibroblast medium supplemented with TNFα (10ng/ml) whilst the other was treated with 6ml of un-supplemented complete fibroblast medium. Cells were cultured at 37°C in 5% CO_2 for 24 hours. Supernatants were stored and cells washed with PBS and trypsinised as directed. $0.5x10^6$ cells were stored as pellets at -80°C for subsequent RNA isolation and analysis using microarrays.

2.6.3 RNA isolation and preparation of samples for microarray analysis

RNA isolation was performed with the Qiagen RNeasy and QIAshredder kits as per manufacturer's protocol. Briefly, cell pellets were treated with 350µl of RLT buffer and mixed thoroughly to ensure complete dissolution of pellets. Samples were transferred to QIAshredder columns and centrifuged for 2 minutes at 16,100*g*. All subsequent centrifugation steps were performed at 10,000*g*. 350µl of 70% ethanol were added to lysates, mixed thoroughly and transferred to RNeasy mini spin columns. Columns were centrifuged for 15seconds. Flow-throughs were discarded and 700µl of RW1 buffer added. Samples were centrifuged for 15seconds. After discarding the flow-through, 500µl of RPE buffer were added and samples centrifuged for 15seconds. This step was repeated with a further 500µl of RPE buffer and columns centrifuged for 2 minutes. Collection tubes were replaced with new ones and samples centrifuged for 1 minute. Columns were placed in 1.5ml LoBind tubes and 50µl of RNase free water added to elute RNA. Samples were centrifuged for 1 minute. Columns were removed and the eluted RNA was kept in ice and subsequently treated with RNA clean and concentrator kit as per protocol. 100µl of RNA binding buffer were added to each sample and mixed well. An additional 150µl of 100% ethanol were added, mixed and transferred to Zymo-spin column. Samples were centrifuged at 14,000*g* for 1 minute (the same speed was used for all centrifugation steps except the last one). After discarding the flow-through 400µl of RNA prep buffer were added and samples centrifuged for 1 minute. This was followed by two washing steps with 800µl and 400µl of RNA wash buffer respectively and centrifugation for 30 seconds. Columns were centrifuged again in empty collection tubes for 2 minutes. Columns were then transferred to 1.5ml LoBind tubes and

30µl of RNase free water added to elute RNA. Samples were left to stand at room temperature for 1 minute and subsequently centrifuged at 10,000*g* for 30 seconds. Eluted RNA was stored at -80°C. RNA quantity and quality were measured with the Nanodrop 2000 spectrophotomer. RNA quality was assessed by reporting the 260/280 and 260/230 ratios. 2µl of each sample were applied to the sensor for testing with 2µl of RNase free water being applied between readings to re-calibrate the instrument.

2.6.4 Microarray experiment

Sample labelling and microarray hybridisation and scanning were performed by Oxford Gene Technology Ltd (Oxford, UK). Briefly, RNA was converted to cDNA and labelled with Cy3 using the Low Input Quick Amp Two-Color Labeling Kit as per manufacturers protocol. At the same time, a control reference RNA (Stratagene human Ref) was labelled with Cy5. Equal amounts of test and control cDNA were mixed and hybridised onto Agilent Sure Print G3 gene expression 8x60k v2 microarrays. Arrays were scanned in the Agilent G2505C scanner. Scanned images were analysed with Agilent Feature Extraction Software 10.7.3.1. Platform specific pre-processing and normalisation of data using loess normalisation and background correction were performed during feature extraction. Loess normalisation is a regression technique for dye bias correction that is used in preference to total intensity normalisation when test mRNA originates from samples that are closely related. Background correction is applied to subtract background from foreground intensity. Quality control report files were produced by the external provider and reviewed by myself. All quality control metrics were within satisfactory ranges.

2.6.5 Analysis of microarray data with Partek Genomic suite

Feature extracted data files were analysed with Partek Genomic suite 6.6. The gene expression workflow was used for analysis. Files were imported on green to red ratio processed signal and log2 transformed. Attributes for each sample were added including age, gender, clinical diagnosis (outcome group), joint of origin and antibody status. After assessing sources of variation in the data set, a one way fixed non nested ANOVA model was created to identify differentially expressed probes according to different attributes. The significance of the differential expression was given by a p value. A false discovery rate (FDR) of <0.05 was set to control for multiple testing using the Benjamini Hochberg method (Benjamini et al. 1995). A fold change for the difference in gene expression was also obtained. Antibody status was found not to contribute to variance in the dataset and was thus not included in the ANOVA model.

2.6.6 Data visualisation using Genesis software

The publicly available Genesis platform (available for download at https://genome.tugraz.at/genesisclient/genesisclient_description.shtml) was used for visualisation of datasets as heat maps. The green/red expression data of the samples of interest was transformed to text format. Gene expression was normalised and genes sorted by expression value on trend.

2.6.7 Mapping of probes to genome of reference using Ensembl

Mapping of probes to the reference genome was performed with the Ensembl genome database project website (available at http://www.ensembl.org/index.html). Probe unique identification numbers were entered in the search field and the chromosomal location of the probe was identified. Probes with multiple chromosomal locations were excluded from candidate gene selection. Next, the chromosomal region was assessed in detail to ascertain whether the probe corresponded to annotated genes and whether the gene associated to the probe was protein coding (Figure 2.7). Only protein coding genes were included in candidate gene selection.

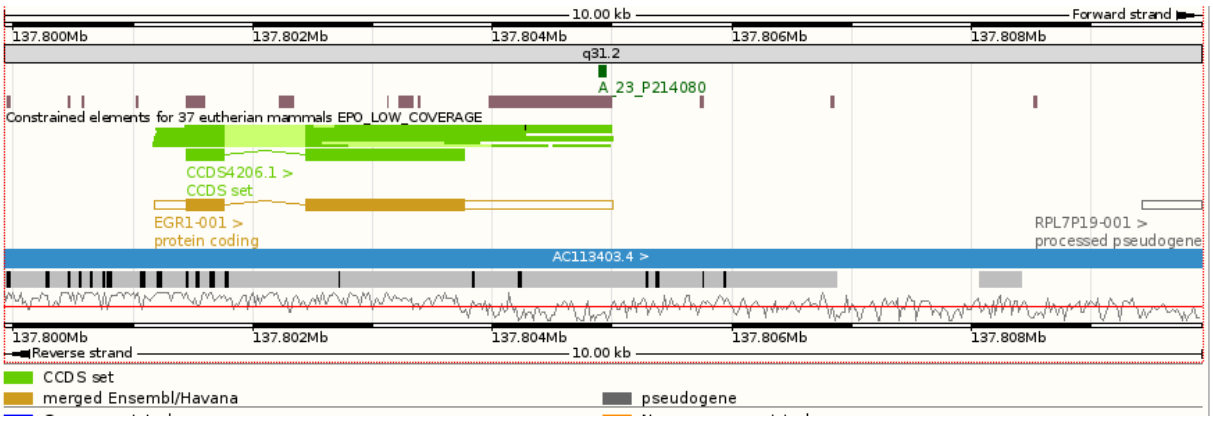

Figure 2.7 Detailed analysis of chromosomal region of origin of probes. *In this example probe number A_23_P214080 was mapped to the reference genome (shown as a green square at the top of the image). Below the probe, the gene associated with this probe can be seen (yellow boxes). In this example this corresponded to early growth response protein 1 (EGR1). Note that information regarding transcript variant (number 001 in this case) and whether the gene is protein coding or not is also displayed.*

2.6.8 Primer pair design and testing

Primer design was performed using Primer 3 software (available at http://bioinfo.ut.ee/primer3-0.4.0/primer3/). Once key genes of interest were identified, their cDNA sequence was obtained from Ensembl and entered in the corresponding search filed in Primer 3. Where possible, primers were designed on the 3'UTR to avoid truncated sequences. Parameters applied to primer pair design and quality testing using Amplifx were as described in section 2.5.10. Primer pair sequences were ordered from Eurofins Operon. The primer pair sequences of primers used in these work are shown in Appendix Table 9.3.

2.6.9 Reverse transcription and real time PCR

Reverse transcription of RNA was performed with the iScript cDNA synthesis kit as per manufacturer's instructions. From each sample a 10µl reaction mix containing 5µl of RNA, 0.5µl of reverse transcriptase, 2.5µl of reaction mix and 2µl of water was crated. Samples were run on the BioRad T100 thermal cycler using the following parameters: 25°C for 5 minutes, 42°C for 30 minutes and 85°C for 5 minutes. Once converted, cDNA samples were diluted 1:5 in RNase free water. Real time PCR was performed as described in section 2.4.11.

Quality control of primer pairs was performed using the melting curve analysis method. For each primer pair, a PCR using human genomic DNA (Promega G3041) was performed in triplicate as specified in section 2.4.11. The melting curves for the primer pairs used in Chapter 6 are shown in Appendix Figure 9.1 and Appendix Figure 9.2. All primer pairs demonstrated single peak indicating that only a single PCR product was amplified.

3 Functional characterisation of fibroblasts

3.1 Introduction

The *in vitro* migratory and invasive characteristics of RA synovial fibroblasts have been explored in the published literature. In these studies, the cells characterised originated from patients with longstanding RA who had received multiple treatments undergoing joint replacement for severe disease. Their functional profiles were compared to that of osteoarthritis synovial fibroblasts (with a small number of studies using normal synovial fibroblasts as comparators).

By functionally characterising synovial fibroblasts I aimed to add to existing knowledge in two ways. Firstly, I wished to compare a range of functional characteristics of synovial fibroblasts in five distinct clinical outcome groups: Normal, Resolving, Very early, Early and Established RA. If successful, this approach might not only allow identification of functional differences between cells from patients with differing clinical fates but could also allow description of new biomarkers to identify patients at risk of RA at inflammatory arthritis onset. This in turn would allow early targeted treatment of patients at risk and avoidance of treatment in patients with markers of resolving disease. The study of synovial fibroblasts from patients with resolving arthritis as well as those from patients with very early and early RA is a novel approach. Despite the wealth of evidence that treatment of RA at very early stages results in significantly better long term outcomes, there is a distinct lack of data on the function of synovial fibroblasts in early disease. The study of cells at these early stages has been hampered by a number of limitations including difficulties identifying and recruiting patients with very early and resolving arthritis and the lack of required expertise to obtain

tissue samples from these patients. The Birmingham Early Arthritis cohort was conceived to overcome these limitations and the systematic collection of early samples has allowed the work undertaken in this thesis. The analysis of samples from resolving arthritis deserves special mention as this is designed to answer a question that has not previously been posed in the literature: what are the functional differences between synovial fibroblasts from patients with resolving and persistent inflammatory arthritis?

Secondly, I wished to describe well defined cellular functions using well characterised assays. Within the existing literature, several assays have been used interchangeably to describe a given cellular function leading to confusion and sometimes contradictory results. For instance, synovial fibroblast migration has been assessed by means of scratch tests, transwell migration and matrigel invasion assays (Denk et al. 2010;Ng et al. 2010;Tolboom et al. 2005). I set out to use assays that would be more suited to the cellular function under study and to describe any differences that might be observed between cells from patients in different clinical outcome groups.

3.2 Functional characterisation of fibroblasts: Experimental design

To determine the *in vitro* migratory and invasive characteristics of synovial fibroblasts three different assays were used. The protocols for these assays have been outlined in the methods section and the optimisation and results of these experiments are described under subsequent headings in this chapter.

To ensure that differences between outcome groups could be ascertained, a minimum of five cell lines were included in each outcome group. These lines were selected on the basis of relative homogeneity of clinical parameters within a given outcome group and all assays were performed on the same samples. As it will be seen below, for some groups, the number of samples assessed exceeded this minimum. This was done in order to strengthen statistical robustness and ensure that observed differences were indeed conclusive. The full clinical characteristics of patients whose samples were used in these experiments are given in Table 2.1. As far as possible passage numbers were kept constant amongst all cell lines used in each functional assay. Hence, cells used in the invasion assay were mostly at passage 4, those used in the scratch test and cell exclusion zone assays were at passage 5 and those used in the proliferation assay were at passage 6 (see Figure 2.2 for schematic representation). A maximum difference of 1 passage was allowed between cell lines used in a given functional assay.

3.3 Functional characterisation of fibroblasts: Results

3.3.1 Assessment of fibroblast migration

Cell migration is central to the development and maintenance of multicellular organisms. In health, cell migration is central to embryonic development, immune responses and wound healing. In contrast, abnormal or inappropriate cell migration can contribute to disease (Horwitz et al. 2003). In RA, inappropriate migration and retention of lymphocytes leads to persistent joint inflammation (Buckley et al. 2001). In the context of synovial fibroblasts, migration and attachment of fibroblasts in the lining layer of the synovium to adjacent

cartilage results in cartilage damage (Muller-Ladner et al. 1996). The description of synovial fibroblast migration in different clinical outcome groups may thus unravel important disease mechanisms. I studied synovial fibroblast migration by means of two different assays: a scratch test and a cell exclusion zone assay.

3.3.2 Scratch test

Scratch tests have been used in other disciplines as models of wound healing for epithelial and mesenchymal cells and to assess the effect of pharmaceutical compounds (Hulkower 2011). In the context of the study of synovial fibroblasts, this test has been used to assess the effect of hypoxia and lysophosphatidic acid stimulation and T cell derived conditioned medium on migration rates of cultured synovial fibroblasts (Ng et al. 2010;Zhao et al. 2008;Zhu et al. 2011). The scratch test is one of the simplest approaches to the study of cell migration and relies on mechanical disruption of a cell monolayer to create a cell free area that is subsequently "filled" by the remaining cells in the monolayer. By measuring the surface area of the cell-denuded zone at baseline and a fixed time later, migration rates can be assessed and contrasted between different conditions. In these experiments, cell monolayers were seeded on 6-well plates and cultured for seven days. At day 8, a scratch was created in the cell monolayer with a sterile 20µL pipet tip. The cell-denuded area was recorded at baseline and 18 hours later. Cell migration was expressed as percentage of area covered in 18 hours (for schematic representation see Figure 2.3).

3.3.2.1 Assay Optimisation

Although the basic protocol for this assay is well described (Hulkower 2011;Zhu et al. 2011), some optimisation steps of this protocol were required for these experiments and are described here. Scratch tests have been performed in a variety of multi-well plates containing 96 wells or fewer. A disadvantage of plates with large numbers of wells is that, at the level of magnification required to view the whole length of the cell-denuded area, only one field has appropriate optical quality under microscopy for quantification of percentage of area covered. As I wished to record and measure at least three optical fields per well (to cover most of the length of the cell-denuded area) a 6-well plate format was favoured.

The choice of seeding density ($8x10^4$ cells/well) was based on previous experience from our study of optimal seeding densities to create synovial fibroblast monolayers on 6 well-plates. A series of time-course experiments using two different cell lines (BX089 and BX085) was carried out to determine the optimal time point at which cell migration should be assessed (Figure 3.1). The aim was to select a time point that would not result in complete coverage of the denuded area as that would make comparisons of percentage of area covered between samples difficult. A time point of 18 hours was selected on this basis.

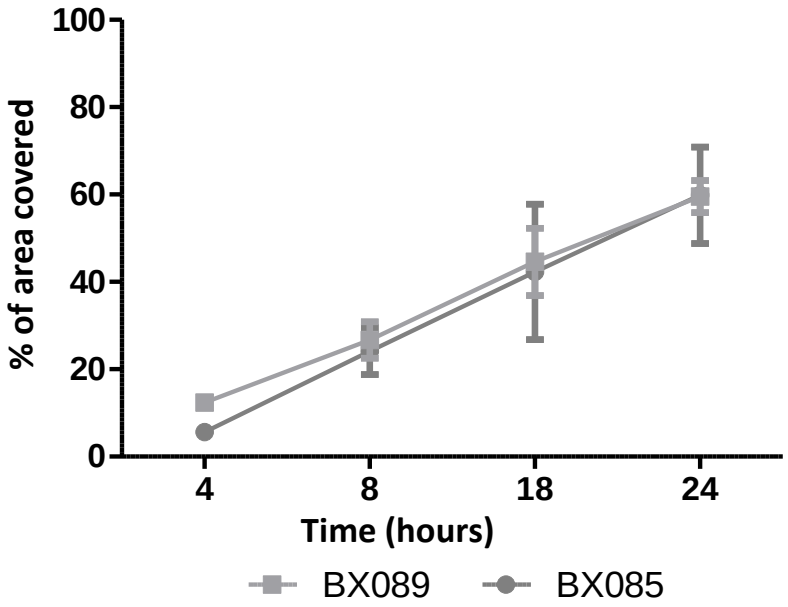

Figure 3.1 Scratch test time-course experiments. *Percentage of denuded area covered at each time point is represented. Two different cell lines assayed (BX089 and BX085) in duplicate. Median and range shown.*

Given that the read out of this assay was the percentage of cell-free area covered in 18 hours, it was essential to ensure that the identical cell-denuded area was measured at both time points. To achieve this, each wound was artificially divided into 25mm longitudinal frames using a grid secured to the base of the plate. Each of these frames was labelled A-G (Figure 3.2). Images of the same three longitudinal frames per experiment were obtained at both time points by aligning the rectangles seen through the microscope's eye piece to the labelled frames. Three frames per well were recorded at each time point using a digital Olympus inverted phase contrast microscope with a 4x objective lens.

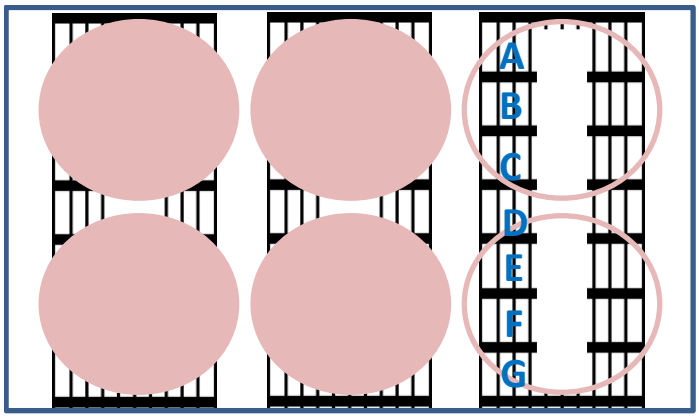

Figure 3.2 Diagram representing the use of a grid to enable measurement of identical frames at both time points. *25mm grids were photocopied onto acetate, cut to size and taped to the base of the 6-well plate. By labelling each frame with a letter and aligning this with the rectangles seen through the microscope's eye piece, the same frames were recorded at both time points.*

3.3.2.2 Scratch test: Results

The results of the assay are shown in Figure 3.3. Within a given clinical outcome group migration ranged from 15-20% to 40-45% of area covered in 18 hours. Median migration values were very similar across clinical outcome groups and ranged from 31 to 44.5%. These findings suggested that the rate of migration in response to injury of samples within an outcome group was the same as that between samples from different outcome groups. In other words, synovial fibroblasts from patients with differing pathologies could not be differentiated on the basis of their migratory characteristics when assessed using a scratch test. Whilst this might be a true reflection of these cells' biology I was surprised by the lack of differences between outcome groups and set out to find a possible explanation for this.

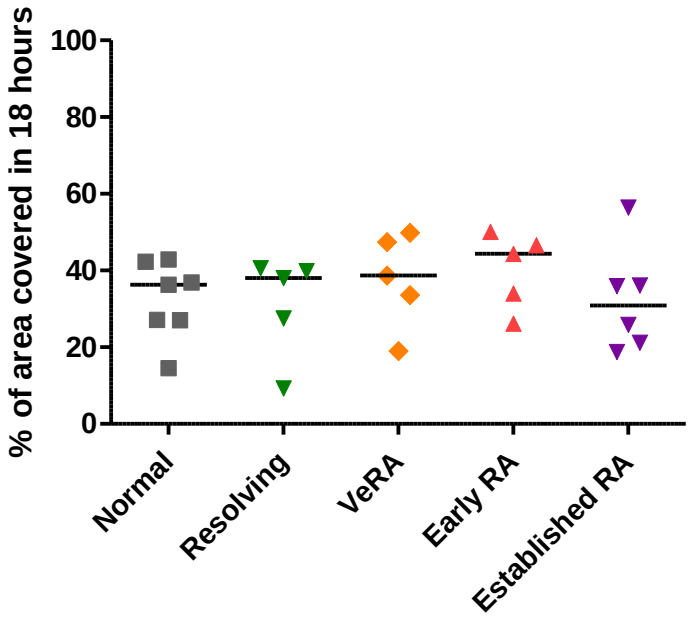

Figure 3.3 No differential migration between outcome groups in response to injury. *Cell migration expressed as percentage of area covered in 18 hours. Each dot represents mean of duplicates for each cell line. Horizontal bars represent median value for each outcome group. Statistical significance assessed by Kruskal-Wallis test with Dunn's post-test analysis for multiple comparisons.*

Although scratch tests are simple to perform and allow assessment of cell motility in real time, they have been criticised as they suffer from a number of limitations. One such limitation is that it can be difficult to reproduce scratches consistently between wells hence leading to cell-denuded areas that vary in size and shape (Hulkower 2011). To assess whether this limitation might have affected the results, I plotted the scratches' surface area in all replicates (Figure 3.4A). In this histogram, the y axis shows the number of wells and the x axis the surface area of the scratches expressed in μm^2. By doing this, I was able to confirm that the surface area of the scratches generated varied widely between replicates and ranged from a minimum value of 312,558μm^2 to a maximum of 642,015μm^2. This is further represented in Figure 3.4B, where two representative images of scratches with very different surface areas are shown.

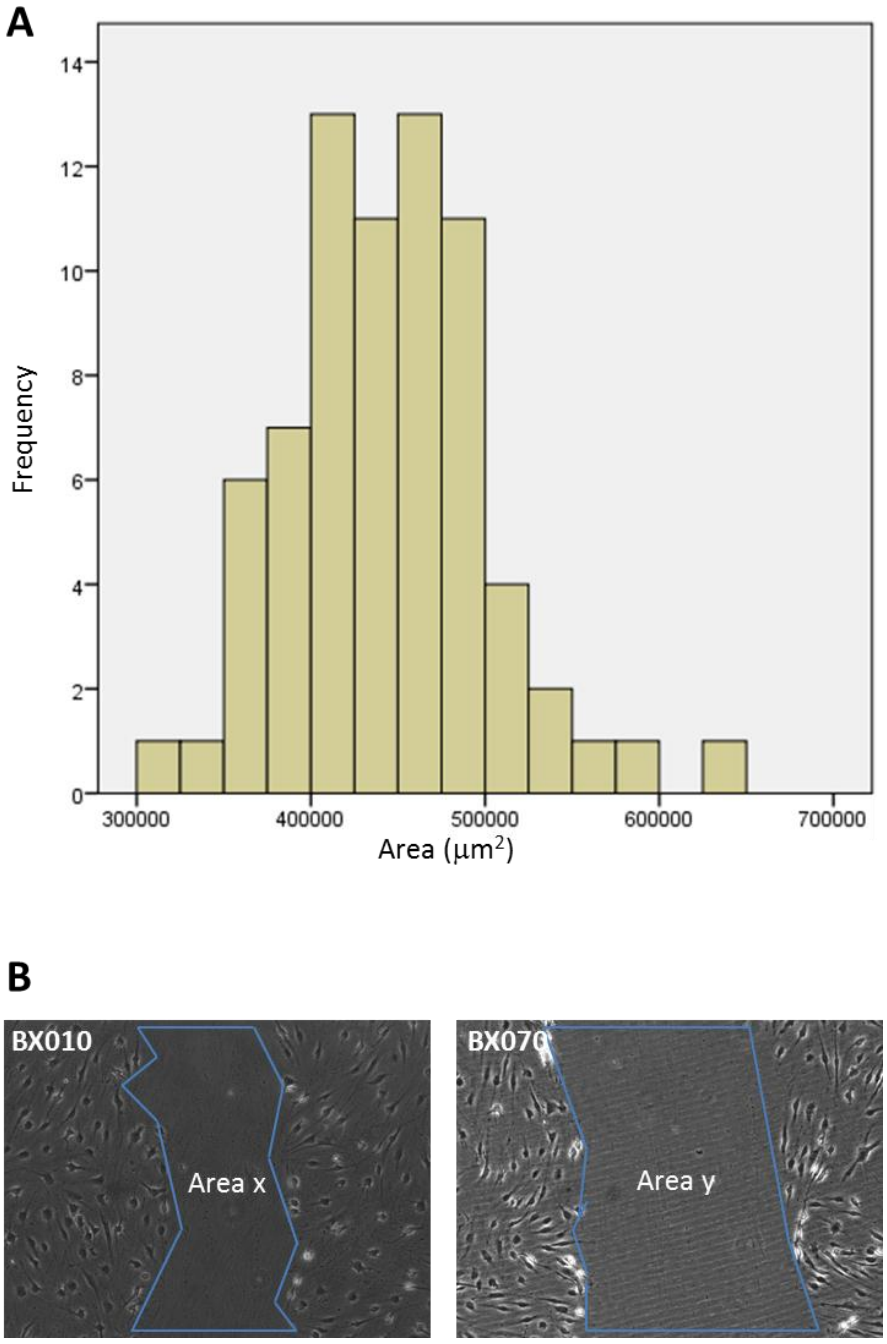

Figure 3.4 Discrepancies in the shape and surface area of scratches between wells. ***A,*** *Histogram representing the distribution of the scratches' surface area in all samples. The y axis shows the number of wells, the x axis shows the area expressed in* μm^2*. The area of the scratches ranged from 312,558*μm^2 *to 642,015*μm^2*. Clear variability in surface area between wells is demonstrated.* ***B,*** *Representative images depicting differences in shape and surface area of scratches between two samples. Area x corresponds to the area of the scratch in a given sample (BX010) and measures 312,558*μm^2 *whilst area y corresponds to the area of the scratch in another sample (BX070) and measures 480,633*μm^2*.*

This highlighted a significant experimental limitation: by producing different starting conditions for different samples, direct comparisons between these samples were compromised as we could not ascertain whether any differences or indeed similarities between samples were due to the cells' behaviour or the experimental conditions.

Another factor taken into consideration was the effect that mechanically scratching a cell monolayer might have on cell migration. When a cell-denuded area is artificially created by scratching, the cells at the edges of this area are damaged. This may result in release of factors that may affect migration and may even lead to altered migration of these damaged cells (Staton et al. 2009). A number of alternative scratching methods have been proposed to overcome this problem such as laser photoablation or electrical wounding (Hulkower 2011). It has also been proposed that a washing step between cell wounding and study of cell migration may attenuate these effects by removing any released factors and potentially the damaged cells at the edges of the cell-free area. The protocol I developed lacked such a step and in retrospect I wonder whether the inclusion of a washing step would have improved the assay's performance. In practice this observation meant that assessment of cell migration following injury might simply not be the same as assessment of cell migration in the absence of such insult, hence I decided to develop an assay that would allow assessment of cell migration in the absence of injury.

3.3.3 Cell exclusion zone assay

The main objectives during the development of this assay were to create identical experimental conditions between samples and to avoid mechanical disruption of cells at the edge of the cell-free area. To achieve this, I used tissue culture inserts to create a cell exclusion zone assay. Culture inserts consisting of two ports separated by a membrane were placed in the centre of wells in 6-well plates. Cells were aliquoted into both ports and left to adhere for 24 hours. After removal of the inserts, two cell monolayers had been created either side of the artificial gap created by the insert's membrane and migration could be measured (for schematic representation see Figure 2.4)

By using this method, the cell-free zone created was of very similar surface area between samples. The surface areas of cell-denuded zones created with this and the scratch test are contrasted in Figure 3.5. Whilst surface area varied widely between samples using the scratch test, this variation was minimised by using the tissue culture inserts method, with surface areas ranging from 252,868μm^2 to 353,854μm^2.

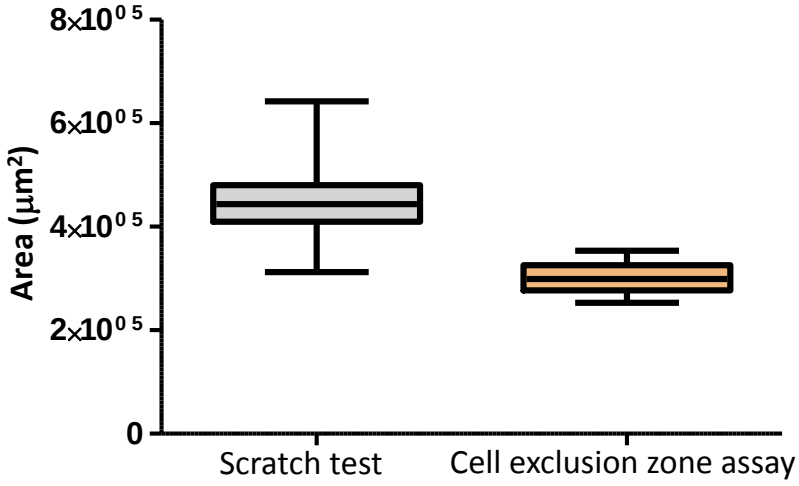

Figure 3.5 Representation of the surface area of the cell-free zone in the scratch test and the cell exclusion zone assay. *Whilst the surface area of scratches varied widely between different samples using the scratch test, such variation was minimal when using a tissue culture insert to create the cell-denuded area in the cell exclusion zone assay. Box and whisker plots where box represents median and interquartile range and vertical lines represent maximum and minimum values.*

3.3.3.1 Cell exclusion zone assay optimisation

A first series of experiments was carried out to determine the optimal seeding density for the assay. The manufacturer's protocol for the tissue culture inserts recommended densities of 3-7x10^5cells/ml to achieve confluent monolayers in 24 hours. As in these experiments the optimal seeding density should not only be determined by confluence at 24 hours but also by ability of achieving complete coverage of the artificial gap between monolayers, a time-course experiment was designed. Using the same cell line (RA28SY) three seeding densities (3x10^5, 5x10^5 and 7x10^5 cells/ml) were assayed over six time points (18, 24, 36, 48, 66, 72 hours) (Figure 3.6). Confluence at 24 hours was achieved with all densities. The percentage of area covered was very similar in all time points with all seeding densities. Complete coverage of the gap was achieved at 72 hours with all seeding densities. As the results for all parameters were fairly similar between seeding densities, the lowest seeding density (3x10^5cells/ml) was selected for subsequent experiments to minimise cell wastage.

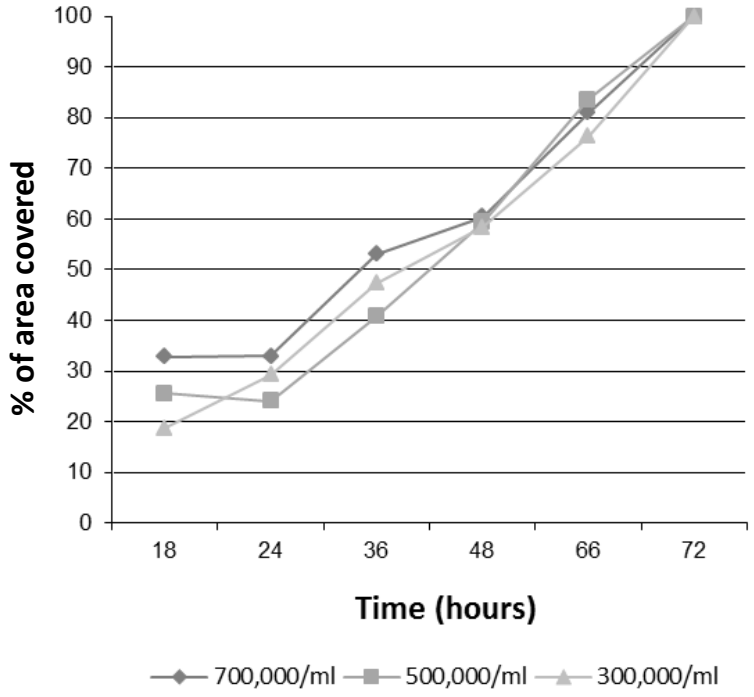

Figure 3.6 Cell exclusion zone assay: determination of optimal seeding density. *Percentage of area covered at different time points with different seeding densities was assessed. Results obtained were very similar for all densities.*

Next, a series of time-course experiments was performed to determine the optimal time point for assessment of cell migration. Two cell lines (RA19SY and BX081) were assayed. The aim was to select a time point that would not result in complete coverage of the cell-free gap as that would make comparisons of percentage of area covered between samples difficult. Cell lines were assessed over six time points ranging from 18 to 72 hours. Both lines showed migration at the minimal time point of 18 hours with one of them achieving 70% of area coverage at 24 hours (and complete coverage at 48 hours). These results indicated variability in area covered between samples but also that some lines might be very fast migrators achieving a significant amount of area covered at 18 hours. On this basis and to avoid

achieving complete confluence at migration assessment, a time point of 18 hours was selected (Figure 3.7).

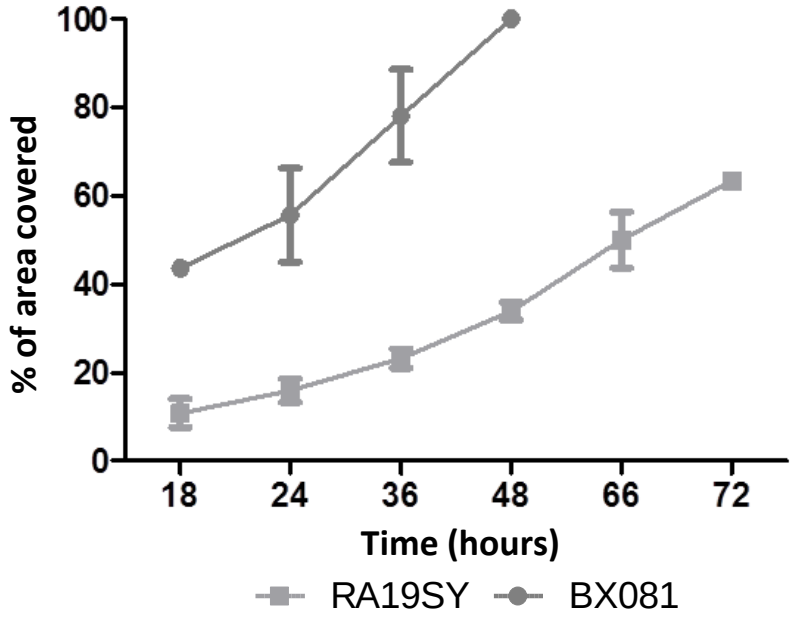

Figure 3.7 Cell exclusion zone assay: time-course experiment. *To determine optimal time point for migration assessment, two different cell lines were assayed (RA19SY and BX081) in duplicate over six time points. Median and rage represented. Note BX081 achieved 100% of area covered at 48 hours and hence there were no further measurements available after that time point.*

3.3.3.2 Cell exclusion zone assay: Results

Image 3-1 shows the typical images obtained with this assay and Figure 3.8 the overall results.

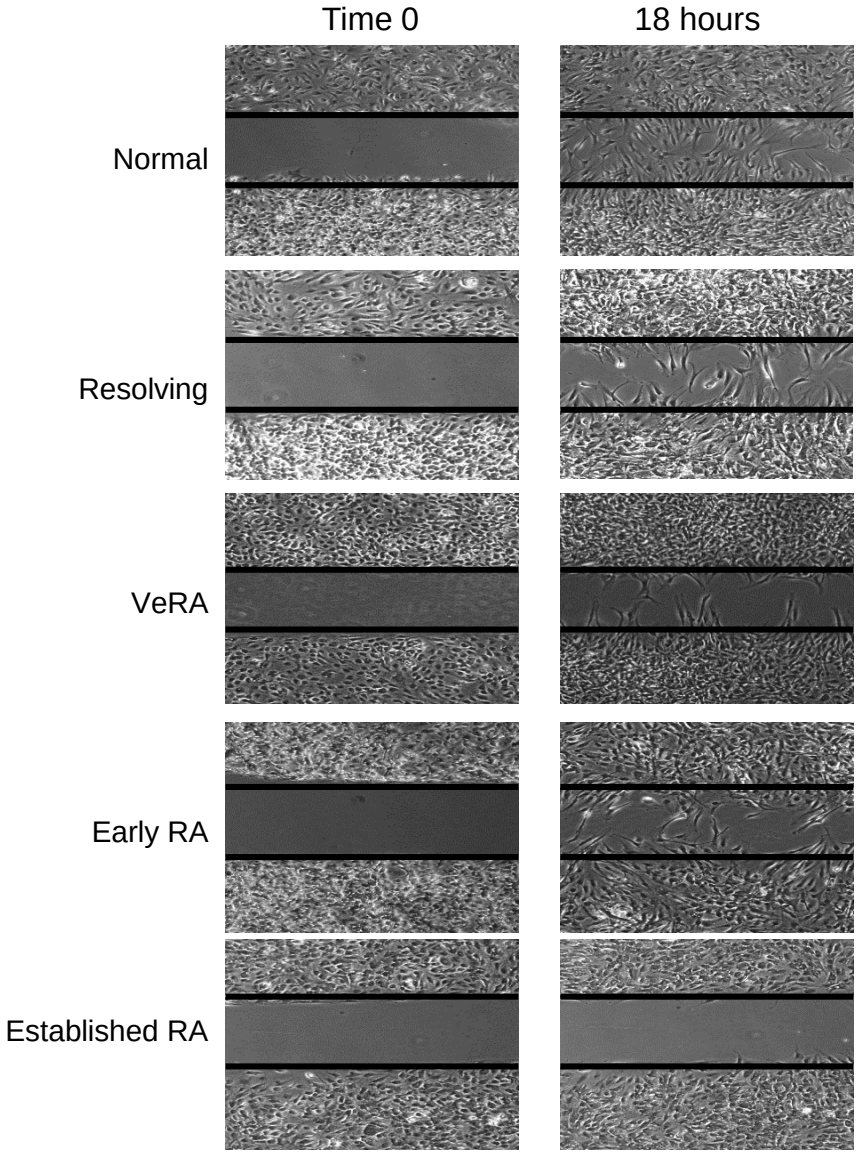

Image 3-1 Phase contrast microscope images showing differences in cell migration at 18 hours between clinical outcome groups. *Maximal differences are observed between Normal and longstanding multi-treated Established RA lines.*

Statistically significant differences in migration were observed between the five clinical outcome groups (Kruskal-Wallis, p=0.002). Normal and resolving lines migrated faster than RA lines. Median migration ranged from 73.9% in the Normal group, through 60% in the Resolving, 45% in Early RA to 20% in VeRA and just under 16% in Established RA. Dunn's post-test analysis showed that statistically significant differences existed between the Normal

and Established RA (73.9% vs. 15.9%, $p<0.05$) and Normal and VeRA (73.9% vs. 20%, $p<0.05$) groups.

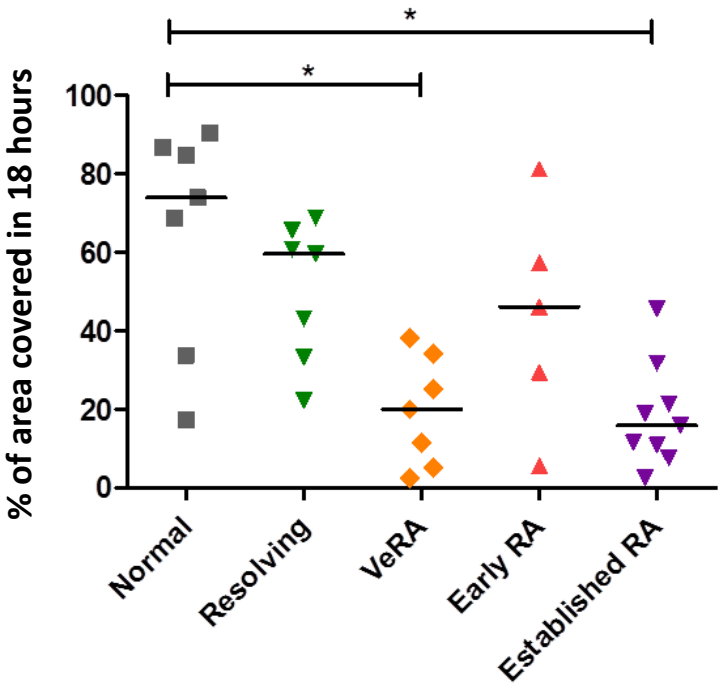

Figure 3.8 Differential cell migration between clinical outcome groups. *Decreasing gradient of cell migration as outcome group progresses from Normal to disease was observed. Statistically significant differences demonstrated between Normal and very early RA (VeRA) and Normal and longstanding multi-treated RA lines (Established RA). Cell migration expressed as percentage of area covered in 18 hours. All lines done in duplicate. Each dot represents the median value for duplicates for each cell line. Horizontal bars represent median value for each clinical outcome group. Statistical significance assessed by Kruskal-Wallis test with Dunn's post-test analysis for multiple comparisons. *p<0.05.*

As the synovial microenvironment in RA is distorted and characterised by abundance of pro-inflammatory cytokines such as tumour necrosis factor α (TNFα) and transforming growth factor β (TGFβ), I wished to ascertain whether treatment of synovial fibroblasts with these cytokines would have an effect on cell migration. I thus repeated the cell exclusion zone experiments following stimulation of cells with TNFα (10ng/ml) or TGFβ (1ng/ml) for 48

hours and found no significant differences in migration when compared to the unstimulated system. Figure 3.9 shows the results of these experiments. Migration of cells treated with the different stimulants has been plotted as fold change relative to the unstimulated controls. A fold change of 1 indicates no difference in migration between the test, stimulated sample and the unstimulated control.

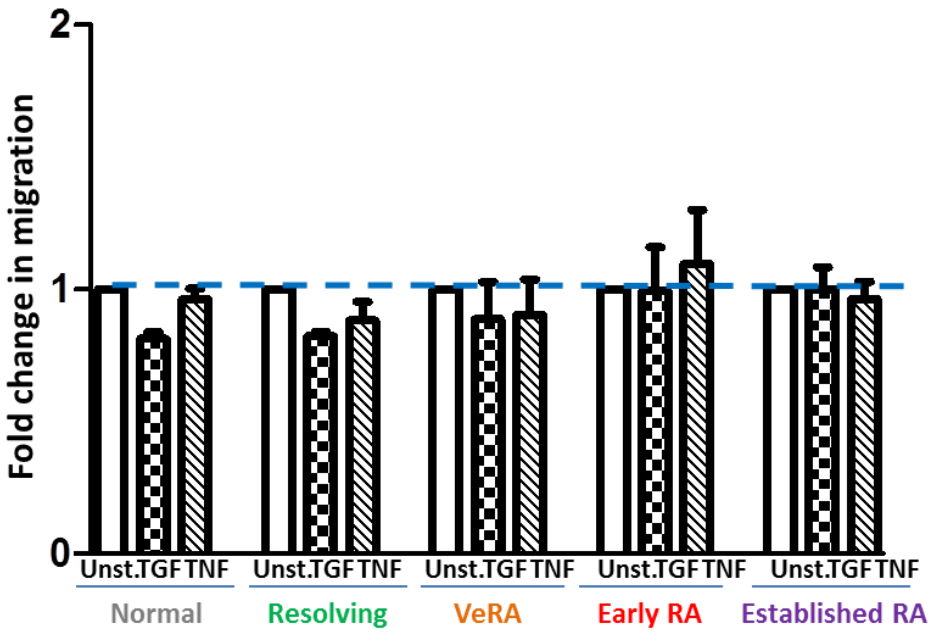

Figure 3.9 Comparison of stimulated and unstimulated migration between clinical outcome groups. *Results are expressed as fold change relative to unstimulated control (white bars). Bars represent median and interquartile range. Four lines per outcome group assessed.*

3.3.3.3 Assessment of synovial fibroblast proliferation in different outcome groups

To confirm that the observed differences were a reflection of differential cell migration rather than of differential cell proliferation, the proliferation rate of fibroblasts in the different outcome groups was assessed at 18 hours by EdU incorporation. EdU (5-ethynyl-2-

deosyuridine) is a thymidine analogue that is incorporated into newly synthetised DNA during cell proliferation. EdU is fluorescently labelled allowing identification of proliferating cells by flow cytometry (Figure 3.10).

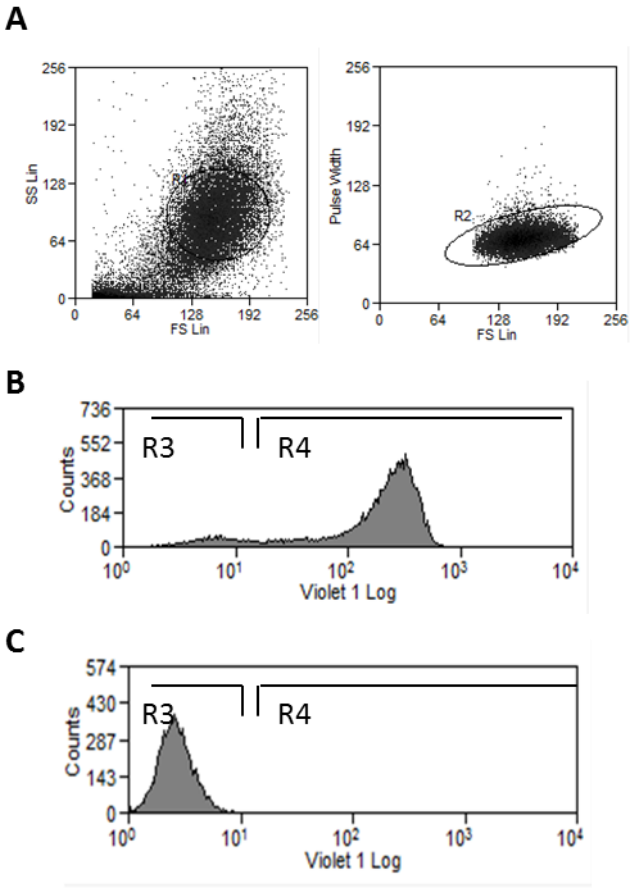

Figure 3.10 Proliferation assay: flow cytometry plots. A, *Cells were identified on size and granularity properties using forward scatter versus side scatter plot. Doublets were excluded by gating on forward scatter versus pulse width plot.* ***B,*** *Representative image of positive control (MDCK cell line) proliferation at 18 hours. Violet 1 plot shows peak in region 4 (R4) that represents cells that have taken up dye.* ***C,*** *Representative image of synovial fibroblast proliferation at 18 hours. Violet 1 plot shows that cells have not taken up dye, indicating no proliferation at 18 hours.*

Prior to undertaking these experiments and to ascertain the optimal EdU concentration to be used, an EdU titration experiment was done. One cell line (BX086) was used for this

experiment. Cells were seeded on a 6 well-plate at a density f $8x10^4$cells/well and treated with increasing EdU concentrations ranging from 2 to 10µM as suggested in the manufacturer's protocol. Cell proliferation was assessed at 96 hours (Figure 3.11). The percentage of proliferating cells (ranging from 4.8% to 5.4%) was very similar with all EdU concentrations. As a result, the lowest concentration of 2µM was selected for subsequent experiments in order to minimise reagents' wastage.

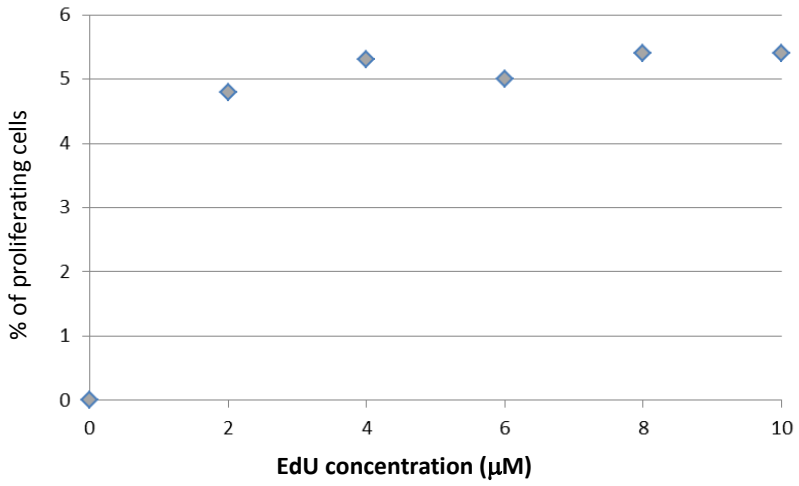

Figure 3.11 EdU titration. *Cells were treated with increasing EdU concentrations (2-10µM) for 96 hours to determine optimal concentration. As proliferation rates were very similar at all concentrations, the lowest 2µM concentration was selected for subsequent experiments.*

Subsequent experiments were performed to determine fibroblasts proliferation rates. These experiments were undertaken under the same conditions as the cell exclusion zone assay: 70µl of cell suspension (at a density of $3x10^5$cells/ml cells) were aliquoted either side of a tissue culture insert and allowed to adhere for 24 hours. Tissue culture inserts were removed at Time 0, EdU added to culture medium and proliferation assessed 18 hours later. The highly proliferative Madin-Darby canine kidney epithelial cell line (MDCK) was used as positive

control. The percentage of proliferating synovial fibroblasts in different outcome groups ranged from 0% to 0.9%. This was in sharp contrast with the percentage of proliferating cells observed in the positive control group (53-78%) (Figure 3.12). These experiments confirmed that the observed differences in cell migration were thus not attributable to differential cell proliferation.

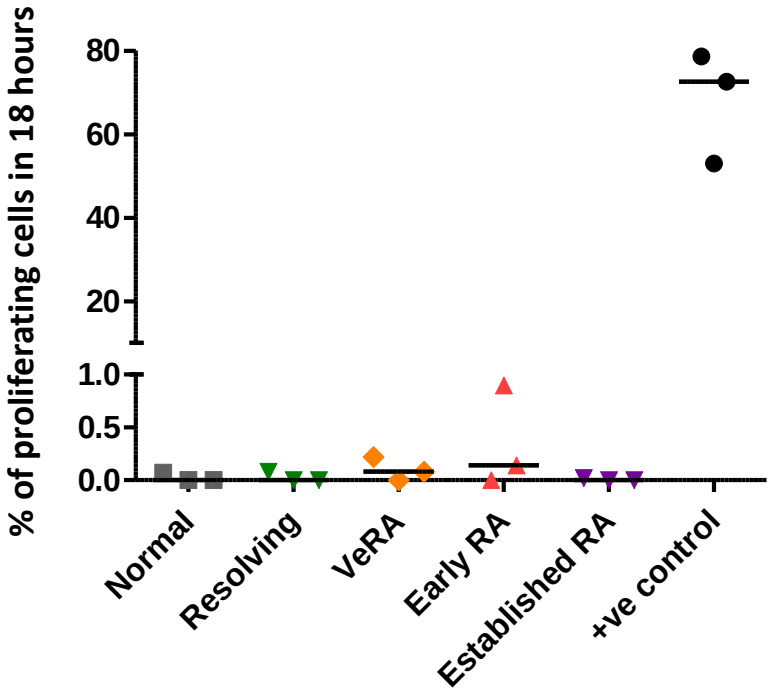

Figure 3.12 Synovial fibroblasts in all outcome groups display very low and comparable proliferation rates at 18 hours. *Minimal fibroblast proliferation is seen at 18 hours in all outcome groups. Dots represent median value of triplicates for each line. Each dot represents one cell line. Horizontal bars represent median values within outcome groups. Three lines per outcome group were tested. Note split y axis to include proliferation of positive control.*

3.3.4 Assessment of fibroblast invasion

A key pathogenic characteristic of RA synovial fibroblasts is their ability to attach to and invade cartilage. These properties have been demonstrated *in vivo* and *in vitro*. Direct invasion of cartilage by RA synovial fibroblasts but not by OA, normal or dermal fibroblasts was shown in the SCID mouse model where invading cells produced matrix degrading enzymes including cathepsins B, D and L (Muller-Ladner et al. 1996).

In vitro studies have been used to assess the invasive characteristics of human RA synovial fibroblasts and synovial fibroblasts from murine inflammatory arthritis models (Kiener et al. 2009;Laragione et al. 2008;Laragione et al. 2010;Tolboom et al. 2002;Tolboom et al. 2005). Human RA synovial fibroblasts displayed higher *in vitro* invasion rates than OA synovial fibroblasts, a feature that correlated with the rate of radiographic joint damage and expression of MMPs 1, 3 and 10 (Tolboom et al. 2002;Tolboom et al. 2005).

Building on this knowledge, my aim was to compare the invasive properties of cells in the five clinical outcome groups. I hypothesised that synovial fibroblasts from RA patients would display more invasive characteristics than those from the Resolving arthritis and Normal groups.

The invasive characteristics of cells in the five outcome groups were assessed by means of matrigel coated chambers as described in the methods section. Briefly, transwells that had 8µm pores in their membrane and were coated with matrigel matrix were inserted in wells of 24-well plates. Synovial fibroblasts were seeded onto the inner surface of transwells and cultured for 72 hours. Non invading cells on the inner surface of the transwells were removed

and membranes detached from the transwells, stained and mounted onto microscope slides. Invading cells that had been able to digest the matrigel layer and migrate through the pores attaching to the under-surface of the membrane were observed by light microscopy. The number of invading cells was compared between groups (for schematic representation see Figure 2.5).

3.3.4.1 Invasion assay optimisation

In order for invasion rates to be compared between samples, a robust and reproducible method of measuring cell invasion had to be developed. As the pattern of cell invasion in matrigel chambers is known to be uneven, with greater invasion at the membrane edges than at the centre, it is usually recommended that assessment of cell invasion is done from the central membrane area. However, the published literature and the manufacturers' protocol for the assay were imprecise on this point, failing to detail how these measurements should be taken and only indicating that counts were taken from the "central membrane area". As I wanted to ensure that in my experiments the identical central area was assessed in all replicates, I developed a device that would facilitate this. This "centering device" consisted of a coverslip in which the whole membrane area had been drawn with a square in its centre that represented the area of the membrane to be counted. By positioning the centering device over each of the membranes, I ensured that exactly the same area was counted in all samples (Figure 3.13). Eight ocular fields within this square were counted at x20 magnification for each sample. This represented 15% of the surface area of the membrane.

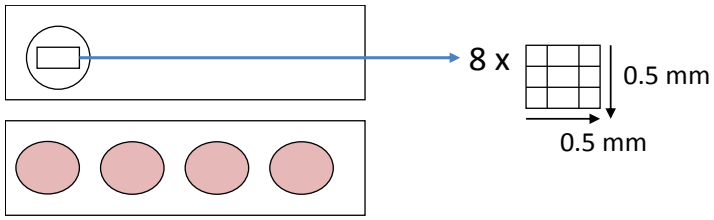

Figure 3.13 Diagram of the centering device used to assess cell invasion. *Bottom rectangle represents a microscope slide with four invasion membranes (light pink circles). The top rectangle represents a cover slip in which the membrane area has been drawn together with a rectangle inside it. By positioning the cover slip so that the edges of the circle coincide with that of the invasion membrane, the exact same area was measured in all samples. Eight ocular fields inside the rectangle (corresponding to 2mm^2) were measured for each sample.*

Next, a series of time-course experiments was carried out to determine the optimal time point to assess cell invasion. Two lines (RA19SY and BX085) were assayed at 24, 48 and 72 hours. Minimal invasion was observed at the earlier time point of 24 hours with invasion increasing over time reaching the highest invading cell numbers for both lines at 72 hours (Figure 3.14). Thus a time point of 72 hours was selected to allow for maximal invasion. This time point also coincided with that used in some of the published literature (Tolboom et al. 2002;Tolboom et al. 2005).

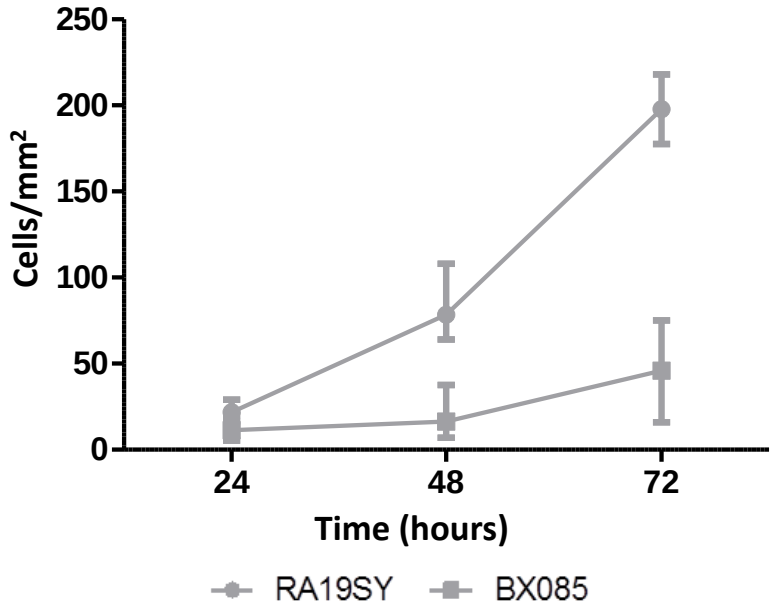

Figure 3.14 Invasion assay: time-course experiment. *Two different lines were assayed (RA19SY and BX085) in triplicate at three different time points (24, 48 and 72 hours). Median and range represented. A time point of 72 hours was selected on the basis that it showed maximal invasion.*

3.3.4.2 Invasion assay: Results

Figure 3.15A shows a typical image obtained in this assay. Under light microscopy and after Diff-Quick staining synovial fibroblasts can be visualised as nucleated cells with elongated cytoplasm. The pores in the membrane through which cells have migrated are seen as circles in the background.

The results of this assay are displayed in Figure 3.15B. Although some lines in the longstanding multi-treated RA group displayed very invasive characteristics (with one line achieving a migration rate of 460 cells/mm^2 in 72 hours), overall no statistically significant differences between outcome groups were demonstrated (Kruskal-Wallis, p=0.79).

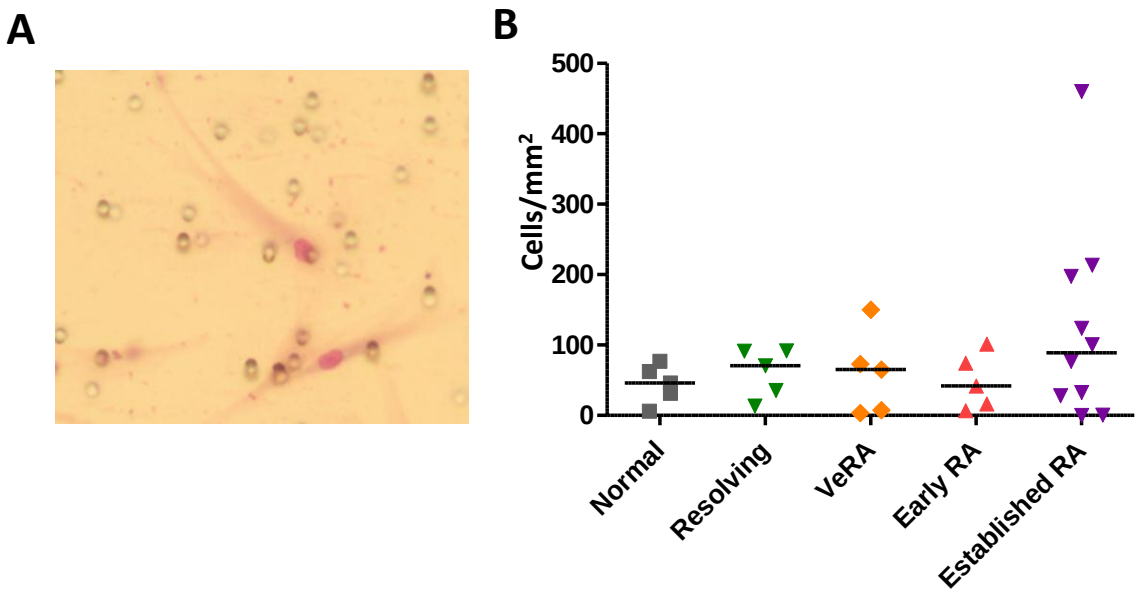

Figure 3.15 Invasion assay. ***A,*** *Invading synovial fibroblasts are seen in the undersurface of the invasion membrane as nucleated cells with elongated cytoplasm.* ***B,*** *No statistically significant differences in cell invasion between different clinical outcome groups were observed. All experiments were done in triplicate. Dots represent medians of triplicates for each cell line. Horizontal bars represent median invasion value for the clinical outcome group. Invasiveness is expressed as number of cells invading the matrigel coated membrane/mm^2 in 72 hours. Statistical significance assessed by Kruskal-Wallis test with Dunn's post-test analysis for multiple comparisons.*

3.4 Functional characterisation of fibroblasts: Overall discussion

This is the first body of work to systematically examine, compare and contrast the functional characteristics of synovial fibroblasts in five distinct clinical outcome groups.

The use of a cell exclusion zone assay to study migration of human synovial fibroblasts is a novel approach that to the best of my knowledge has not previously been used in this context. Using this assay, I observed differential migration between cells from patients in different outcome groups that was not secondary to differential cell proliferation. Interestingly, lines from very early RA patients (≤3 months symptom duration) and Established RA behaved

similarly with comparable migration rates (20% and 15.9% respectively, p=0.9 by Mann Whitney test). Statistically significant differences between these migration rates and those from Normal synovial fibroblasts (73.9%) existed indicating that synovial fibroblasts from RA patients in these two outcome groups migrate much slower than healthy cells.

When considering these results two immediate questions arise from this observation: (a) what are the clinical consequences (if any) of differential migration? and (b) what causes migration to be different?

Potential clinical consequences of this behaviour can be hypothesised. As discussed in the introductory pages of this thesis, the hyperplastic RA synovium is characterised by expansion of fibroblast populations. This effect is thought to be due to a combination of decreased apoptosis and increased local cellular proliferation (although evidence of *in vivo* proliferation is scarce) (Mor et al. 2005). In the light of our results we can also speculate that decreased cell migration might contribute to pathological accumulation of synovial fibroblasts in the RA synovium. Such a suggestion is of course purely speculative and would require verification of differential cell migration *in vivo*.

In order to explore the potential causes of differential migration we need to briefly consider the biological processes underlying migration of adherent cells (Friedl et al. 2012;Yamazaki et al. 2005). Cell migration in 2D substrates consists of four successive processes that are regulated by key molecules, in particular members of the Rho family of small GTPases (Rac, Rho and Cdc42). In response to extracellular stimuli cells are polarised and actin polymerisation occurs that results in formation of membrane protrusions (filopodia and

lamellipodia). Phosphatidylinositide 3-kinase (PI3K) contributes to cell polarisation whilst Rac and Cdc42 proteins are involved in production of membrane protrusions (Etienne-Manneville et al. 2002). Next, adhesion of the protrusions to the substrate occurs through complex integrin-dependent cell-substrate adhesions which are regulated by Rac. Subsequently, the nucleus and cell body are translocated by acto-myosin contractile forces. Rho has a fundamental role here as it regulates the assembly of contractile acto-myosin filaments. Finally, during retraction adhesive structures at the trailing edge are disassembled. In 3D migration, ECM remodelling also takes place. Alterations in cell migration can result from distortion in any of these steps. There are thus a number of targets we could further study to elucidate differential migration mechanisms. Experiments involving inhibition or gain of function of Rac, Rho and PI3K would be very informative. Indeed work from Chan and colleagues found that Rac is necessary for lamellipodia formation in RA synovial fibroblasts (Chan et al. 2007) and the role of PI3K signalling in RA is an area of increasing research interest (Reedquist et al. 2006). Further study of integrins, that are already known to mediate adhesion of synovial fibroblasts to cartilage (Ishikawa et al. 1996), would also be of value in unravelling the causes of differential migration.

The study of the transcriptomic profiles of synovial fibroblasts during migration would be of special interest in this context. Gene expression is a dynamic process that varies depending on external conditions. For example, as it will be seen in Chapter 6, TNF stimulation significantly modified gene expression patterns of synovial fibroblasts in all groups under study. Thus, the analysis of gene expression patterns in these cells during migration might not only indicate generic pathways involved in synovial fibroblast migration but may provide clues to disruption of key migration checkpoints in disease.

In contrast to the results of the cell exclusion assay, no differences in cell migration in response to scratching were observed. Scratch tests have been used to assess RA synovial fibroblast migration under different experimental conditions. Ng and colleagues reported increased migration when synovial fibroblasts were cultured under hypoxic conditions (1% oxygen). This effect was not observed when cells were cultured under normoxic conditions or at 3% and 5% oxygen (Ng et al. 2010). A different group used this assay to assess the effect of the signalling molecule lysophosphatidic acid (LPA) on RA synovial fibroblast migration reporting increased migration rates upon LPA stimulation (Zhao et al. 2008). Whilst these studies were designed to assess differences before and after specific treatments, neither of them reported on migration rates of resting RA synovial fibroblasts thus not allowing for direct comparison with our results. The potential limitations of this assay have been discussed. Regardless of whether these limitations had any effect in experimental conditions, it is clear that migration following disruption of a cell monolayer (scratch test) and in the absence of such stimuli (cell exclusion zone assay) are different biological processes that are likely to require engagement of different cellular networks and machinery. These differences may explain why differing cell migration rates between groups were observed with the former but not with the latter.

There were no significant differences in cell invasion between outcome groups. The invasive characteristics of synovial fibroblasts *in vitro* have been assessed in human and animal studies. Of particular interest in terms of similarity with the work we present, Tolboom and colleagues used this assay to compare the invasive characteristics of fibroblasts from patients with longstanding multi-treated RA (the equivalent of the Established RA group in this work) and control OA fibroblasts (Tolboom et al. 2002;Tolboom et al. 2005). They concluded that

RA synovial fibroblasts were significantly more invasive than OA fibroblasts, a feature that correlated with the rate of radiographic joint damage. Careful analysis of the results of their work reveals that a large variation in cell invasion between lines within a given outcome group existed. This variability led the authors to use large numbers of cell lines in each outcome group, ranging from 30 to 72 in the RA group and from 17 to 49 in the OA group (depending on the study), in order to demonstrate statistically significant differences between groups. Variability in invasion rates within outcome groups is also seen in my results. This is particularly marked in the Established RA group were invasion rates range from 0 to 460 cells/mm^2. Taking this into account it could be argued that in order for us to fully characterise differential invasion between these groups a much larger sample size per outcome group would be required. In the context of this assay it is also worth noting that although no statistically significant differences in invasion between outcome groups were identified, a more invasive phenotype is suggested for the Established RA group when looking at the raw data (Figure 3.15). If instead of using the absolute cells/mm^2 data, invasion is assessed as percentage of cell lines achieving an invasion cut off of 100 cells/mm^2 at 18 hours, we find that 0% for the Normal, Resolving and Early RA groups achieve this cut off with 20% VeRA group and 50% for the Established RA group.

Alternative methods to assess *in vitro* synovial fibroblast invasion exist. These include co-culture of synovial fibroblasts with cartilage particles for 15 days followed by measurement of cartilage degradation products (Neidhart et al. 2003) and co-culture of synovial fibroblasts with cartilage discs for 14 days followed by histological and immunohistochemical analysis (Pretzel et al. 2009). Although it could be argued that the use of these approaches in my experimental set up may have been of greater biological relevance, several drawbacks

precluded their use. These included the fact that these experiments are lengthy and technically challenging and the need to identify a source of cartilage. Chamber systems coated with reconstituted cartilage matrix have been used extensively for the assessment of synovial fibroblast invasion (Frye et al. 1996;Ray et al. 2001;Tolboom et al. 2002;Tolboom et al. 2005). The decision to use coated chambers in this work, stemmed from the need to have a simple and reproducible assay that would allow high throughput given the large number of samples that I wished to assess.

It is also worth noting here that all *in vitro* experimental designs suffer from limitations as they invariably are imperfect substitutes for the *in vivo* situation. However, whilst *in vivo* experiments may be more physiologically relevant, they are expensive, time consuming, technically challenging and ill-suited for the analysis of multiple samples from several outcome groups. For these reasons, an *in vitro* experimental design was favoured to assess the functional characteristics of synovial fibroblasts in the five outcome groups of interest.

4 Proof of concept: candidate gene approach

4.1 Introduction

Before embarking on time consuming, high cost experiments to determine the full transcriptomic profile of synovial fibroblasts in the five different clinical outcome groups, a series of smaller scale, candidate gene approach experiments was performed to establish proof of concept.

Custom made microfluidic cards were used to perform 48 gene expression assays. Cell lines from patients in three clinical outcome groups were assayed: Resolving (n=9), VeRA (n=12) and Early RA (n=9). Gene expression analysis was performed on unstimulated synovial fibroblasts and parallel samples exposed to TNFα (10ng/ml) for 24 hours. A candidate gene approach was used during microfluidic card design. Targets already known to be associated with key fibroblast functions were selected. These included adhesion molecules (VCAM1), chemokines (CXCL12 and CXCL16), cell surface markers (CD248 and PDPN) and matrix metalloproteinases (MMP1, MMP2, MMP3, MMP9, MMP13 and MMP14) amongst others. A full list of gene expression targets assayed is shown in Appendix Table 8.1. The clinical characteristics of patients in each outcome group are shown in Table 2.2.

4.2 Candidate gene approach: Results

Out of the 48 genes assayed, three were housekeeping genes (GAPDH, 18S, β2microglobulin) and for another one (PADI4) levels expressed by synovial fibroblasts were below the limit of

detection of the assay. The results for the remaining 44 genes assayed are shown in Figure 4.1 and Figure 4.2 (unstimulated and TNF stimulated samples respectively). For certain genes, the results were inconclusive because expression values were below the lower limit of detection of the assay for several fibroblast lines in each group. In the unstimulated samples these included: TLR2, TNSF11, SHOX, LGALS3, MMP9 and MMP13 and in the TNF stimulated samples: LGALS12 and SHOX. Statistically significant differences in gene expression profiles between outcome groups were observed for three genes: DKK1, SLIT3 and EGF in unstimulated samples. No differences in gene expression were observed between different outcome groups in the TNF stimulated samples.

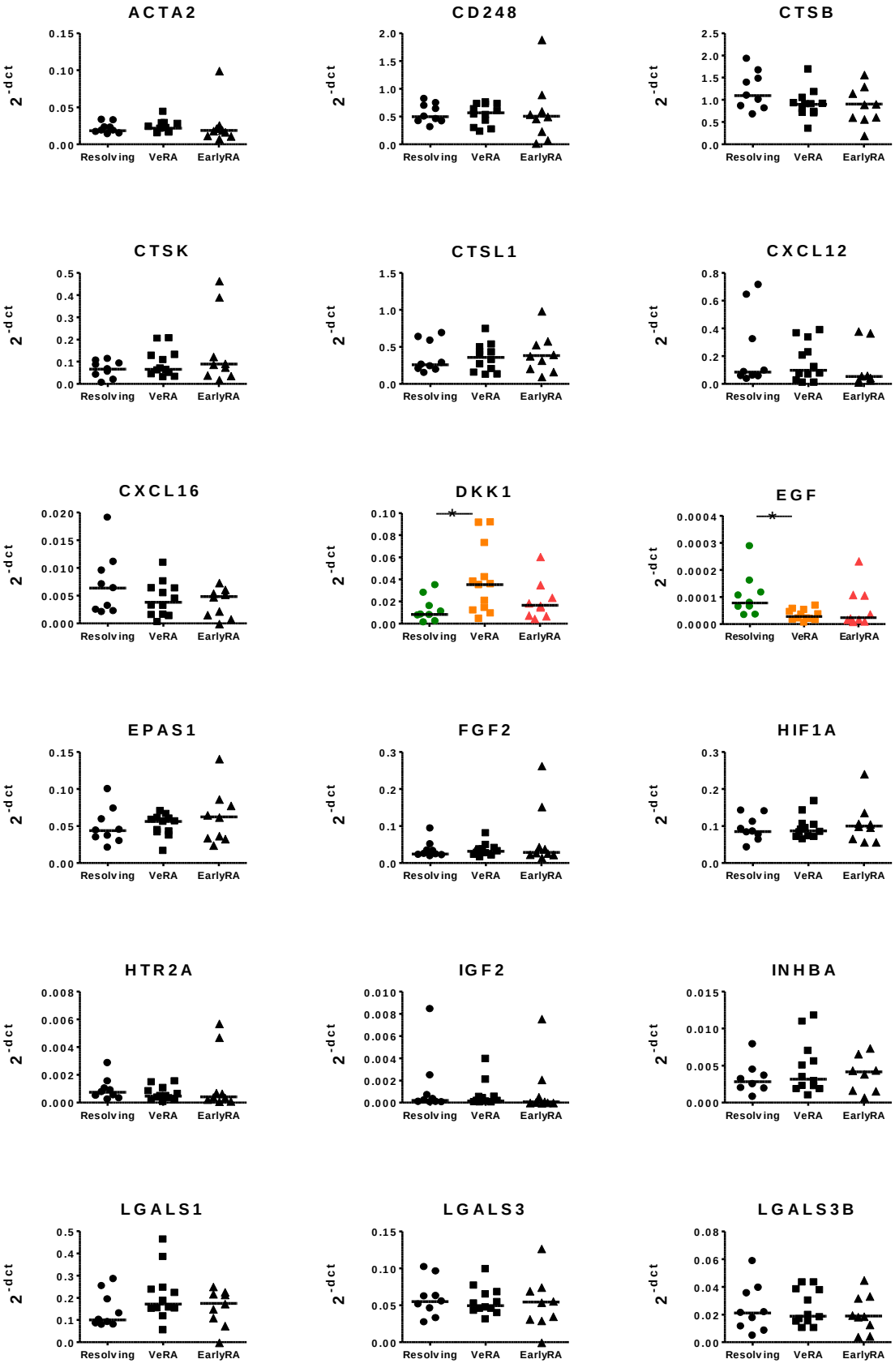
ACTA2
CD248
CTSB
CTSK
CTSL1
CXCL12
CXCL16
DKK1
EGF
EPAS1
FGF2
HIF1A
HTR2A
IGF2
INHBA
LGALS1
LGALS3
LGALS3B
2-dct
Resolving
VeRA
EarlyRA

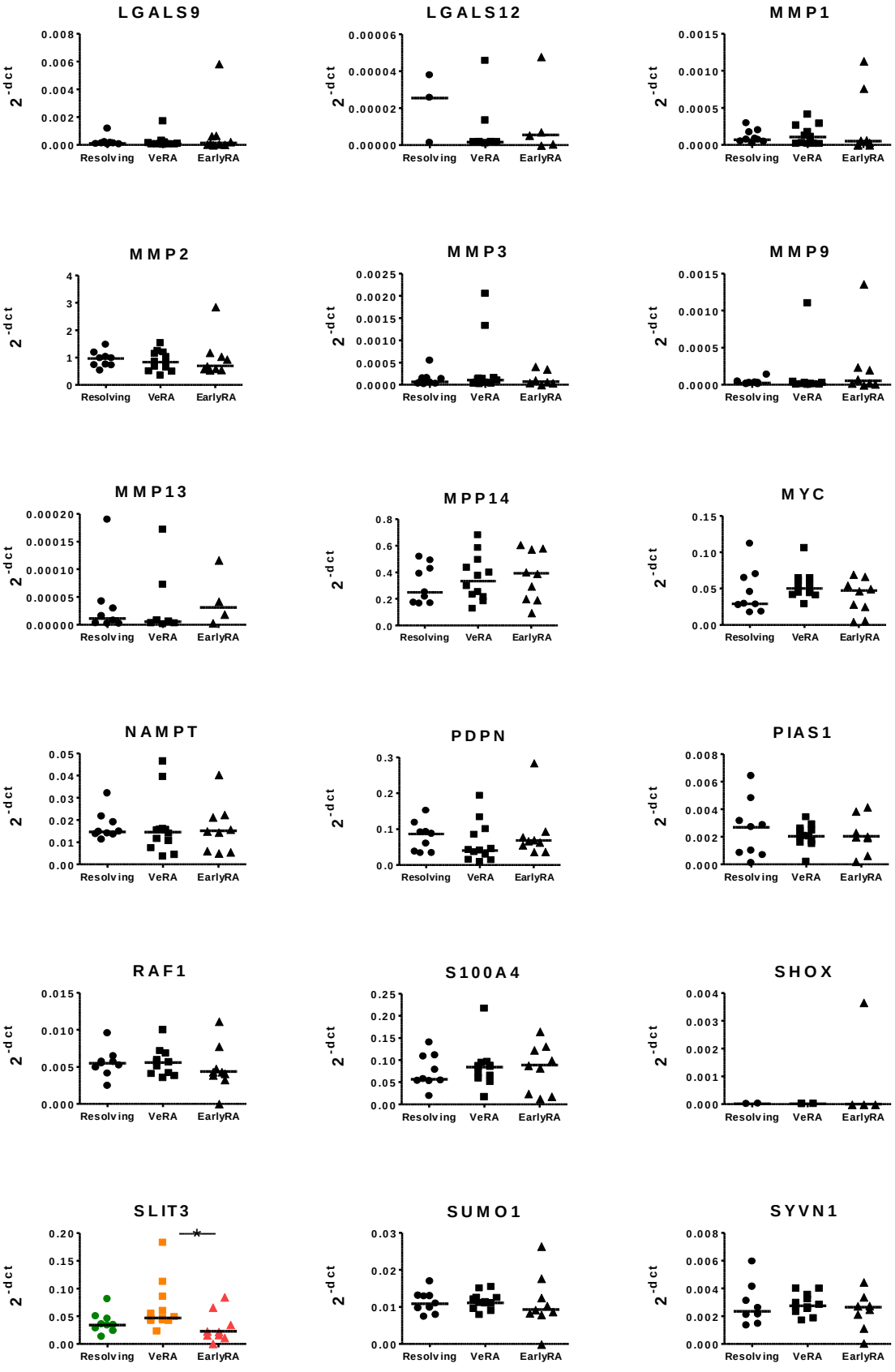
LGALS9
LGALS12
MMP1
MMP2
MMP3
MMP9
MMP13
MPP14
MYC
NAMPT
PDPN
PIAS1
RAF1
S100A4
SHOX
SLIT3
SUMO1
SYVN1
2-dct
Resolving
VeRA
EarlyRA

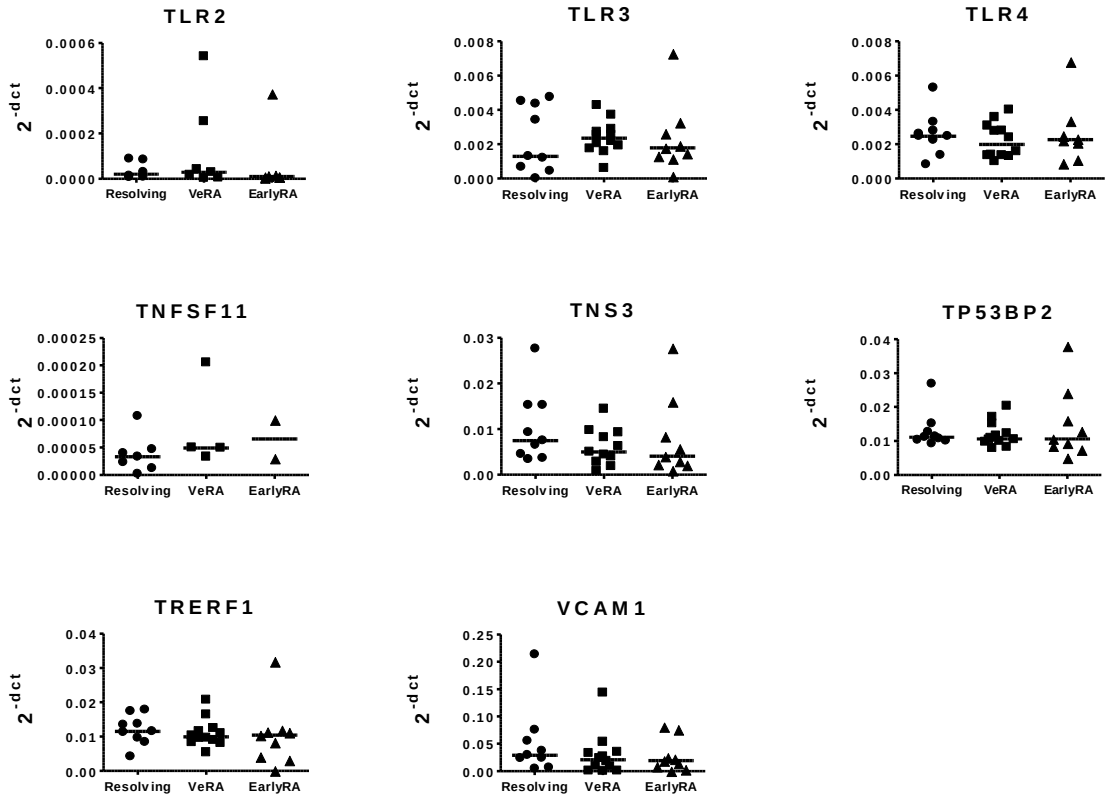

Figure 4.1 Gene expression patterns in unstimulated synovial fibroblasts samples. *The expression patterns of 44 genes in Resolving (n=9), VeRA (n=12) and Early RA (n=9) unstimulated samples are shown. Kruskal Wallis test with Dunn's post-test analysis for multiple comparisons. *p<0.05.*

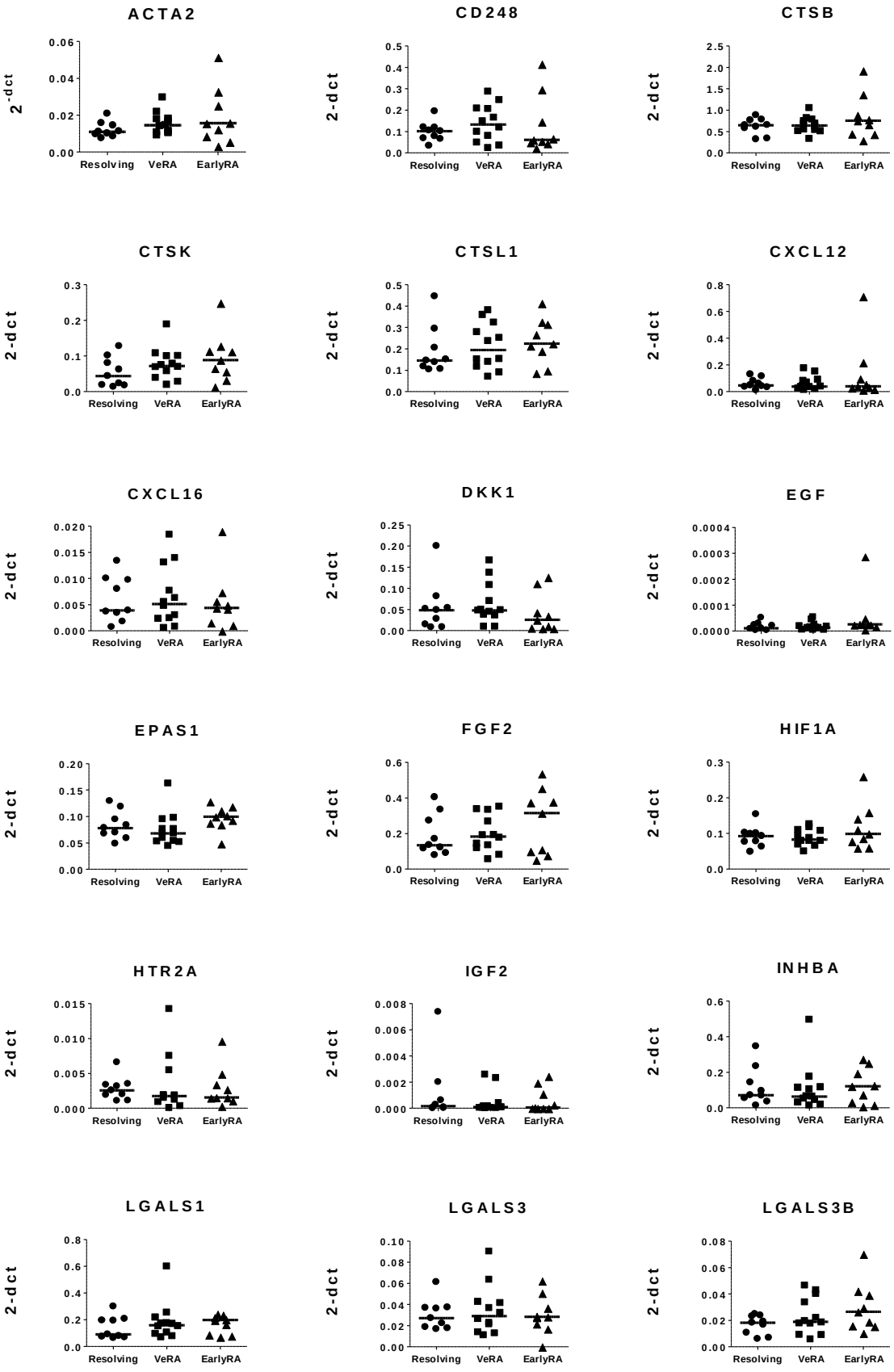
ACTA2
2-dct
0.06
0.04
0.02
0.00
Resolving
VeRA
EarlyRA
CD248
0.5
0.4
0.3
0.2
0.1
0.0
CTSB
2.5
2.0
1.5
1.0
0.5
0.0
CTSK
0.3
0.2
0.1
0.0
CTSL1
CXCL12
0.8
0.6
0.4
0.2
0.0
CXCL16
0.020
0.015
0.010
0.005
0.000
DKK1
0.25
0.20
0.15
0.10
0.05
0.00
EGF
0.0004
0.0003
0.0002
0.0001
0.0000
EPAS1
FGF2
HIF1A
HTR2A
IGF2
0.008
0.006
0.004
0.002
0.000
INHBA
LGALS1
LGALS3
LGALS3B

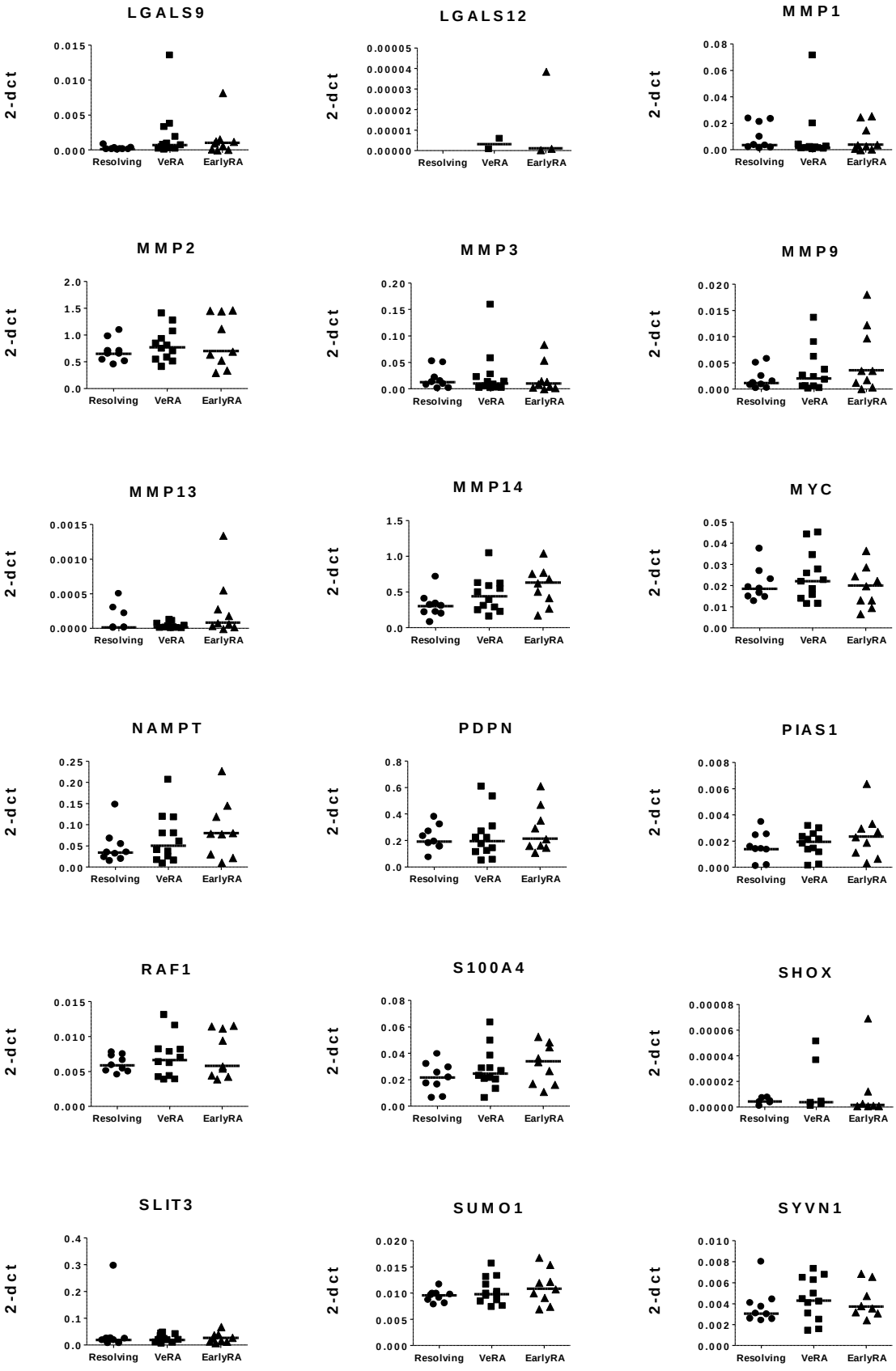
LGALS9
LGALS12
MMP1
MMP2
MMP3
MMP9
MMP13
MMP14
MYC
NAMPT
PDPN
PIAS1
RAF1
S100A4
SHOX
SLIT3
SUMO1
SYVN1
2-dct
Resolving
VeRA
EarlyRA

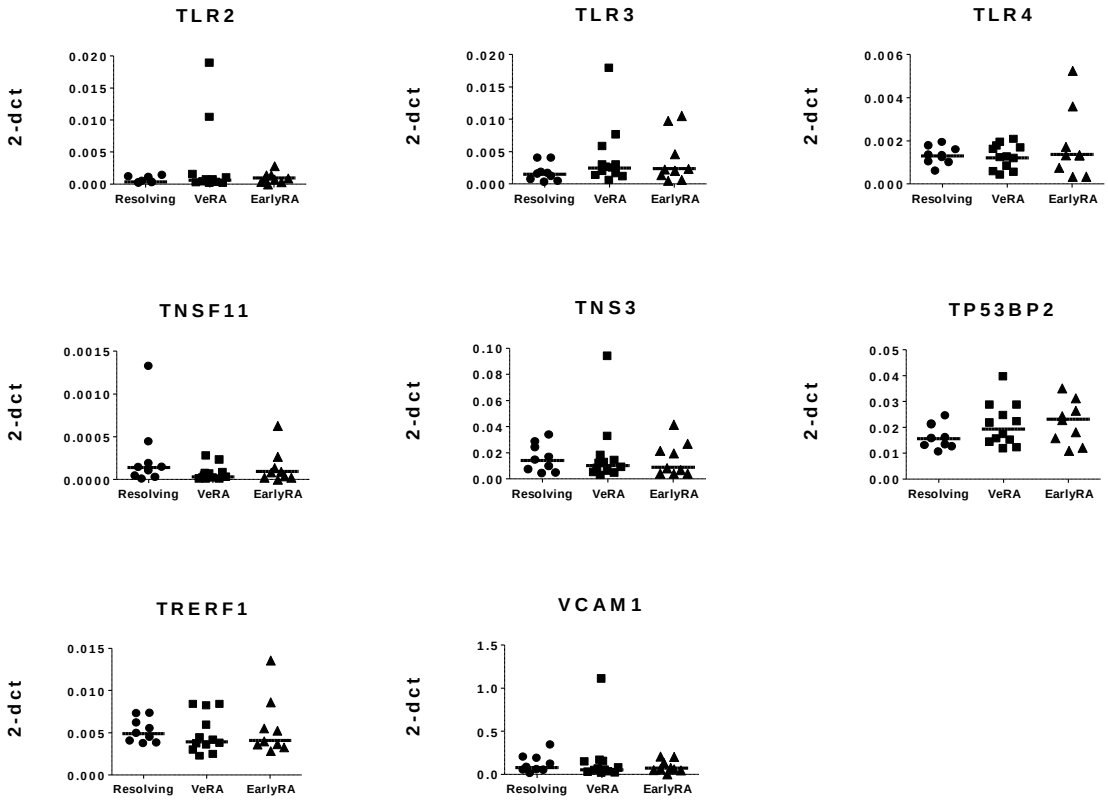

Figure 4.2 Gene expression patterns in TNF stimulated synovial fibroblasts samples. *The expression patterns of 44 genes in Resolving (n=9), VeRA (n=12) and Early RA (n=9) TNF stimulated samples are shown. Kruskal Wallis test with Dunn's post-test analysis for multiple comparisons.*

The observation that Dickkopf related protein 1 (DKK1) was differentially expressed between outcome groups was of particular interest for two reasons. First, the difference in expression was observed between the Resolving and VeRA groups, thus lending support to the hypothesis that the study of early samples might provide clues to key genes involved in the switch from resolving to persistent disease. Second, DKK1 is an inhibitor of the Wnt signalling pathway that has been proposed as a "master regulator of joint remodelling" (Diarra et al. 2007). Wnt signalling plays a critical role in osteoblast differentiation and activity, driving bone formation. Inhibition of Wnt signalling via DKK1 directly impairs osteoblast

differentiation and indirectly enhances bone destruction by increasing RANKL induced osteoclastogenesis (Goldring et al. 2007). In RA patients, serum DKK1 levels are higher than in healthy controls or patients with other rheumatic diseases (Wang et al. 2011). Patients carrying a genetic variant in the DKK1 gene have higher serum DKK1 levels and more progressive joint destruction (de Rooy 2012) suggesting a fundamental role for DKK1 in RA. Treatment of murine models of arthritis with anti DKK1 antibodies has shown promise in restoring bone loss. Furthermore, synovial tissue sections of patients with established RA show strong expression of DKK1 localising to synovial fibroblast (Diarra et al. 2007). Our group also recently reported that expression of DKK1 by synovial fibroblasts is closely regulated by the local glucocorticoid metabolism (Hardy et al. 2012). Wnt signalling inhibition by DKK1 may therefore be an as yet undefined pathway through which synovial fibroblasts influence bone destruction in RA. I therefore decided to investigate this target in more detail by determining DKK1 protein levels and by assessing the potential functional consequences of differential DKK1 expression between the Resolving and VeRA groups.

4.3 Determination of DKK1 protein levels

DKK1 protein levels in the supernatants of cultured synovial fibroblasts were determined by ELISA. Although the results appeared encouraging with supernatants from fibroblasts from VeRA patients showing higher overall DKK1 levels than those from patients with Resolving arthritis, levels of variability within groups were high and differences between groups did not achieve statistical significance (median: 23.2 ng/ml vs. 6.6 ng/ml respectively, p=0.07) (Figure 4.3).

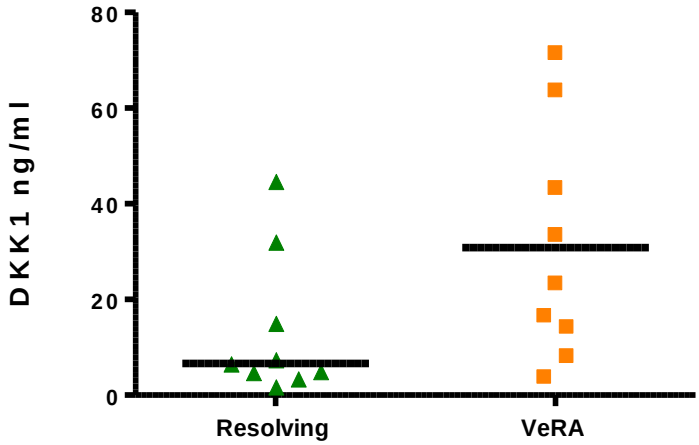

Figure 4.3 DKK1 protein levels in supernatants of cultured synovial fibroblasts. *DKK1 levels were measured in the supernatants of cultured synovial fibroblast from Resolving (n=9) and VeRA (n=9) groups by ELISA. Box and whisker plot where box represents median and interquartile range and vertical lines represent maximum and minimum values. Mann Whitney test: p=0.07.*

4.4 Osteoblast differentiation and bone nodule formation experiments

Overexpression of DKK1 mRNA in cultured VeRA synovial fibroblasts compared to Resolving synovial fibroblasts with a similar trend at the protein level had been observed so far. DKK1 promotes an imbalance in bone homeostasis in favour of bone destruction by impairing osteoblast differentiation. We thus hypothesised that co-culture of osteoblast precursors with conditioned medium from cultured VeRA synovial fibroblasts would result in decreased osteoblast differentiation and bone nodule formation compared to co-culture with conditioned medium from Resolving synovial fibroblasts. These experiments were designed in collaboration with Professor Mark Cooper (Professor of Medicine, Sydney University) and Dr Rowan Hardy (Research Fellow in Endocrinology, Diabetes and Metabolism, University of Birmingham). Dr Rowan Hardy performed the experiments.

Briefly, commercially available osteoblast precursors were cultured in osteoblast mineralisation medium (containing ascorbic acid) in the presence of conditioned medium obtained from cultured synovial fibroblasts in the Resolving and VeRA groups. To assess the effect of DKK1 on osteoblast differentiation, a DKK1 control was created with recombinant DKK1. Positive differentiation controls were established using osteoblast mineralisation medium containing non-conditioned fibroblast medium. Negative controls consisted of osteoblast growth medium containing non-conditioned fibroblast medium. Formation of mineralised bone nodules stained using alizarin red was used as a surrogate marker of osteoblast differentiation. Positively stained nodules were observed in the positive control and were absent in the negative control as expected. Low numbers of nodules were identified in the DKK1 control, indicating that osteoblast differentiation was inhibited.

Nodule formation was observed when osteoblast precursors were co-cultured with conditioned medium from both, Resolving and VeRA synovial fibroblasts (Image 4-1). Nodule counts were higher in co-cultures with conditioned medium from VeRA synovial fibroblasts, a finding that directly opposed our hypothesis. Due to time constraints, these experiments had to be abandoned before further replicates could be added to this n=1 in each group experiment. Therefore, definite conclusions cannot be drawn from these experiments. Furthermore, potential limitations of these experiments must be acknowledged. A possible significant experimental drawback was the use of relatively small amounts of fibroblast condition medium (25µl). *In vitro* effects are reported with DKK1 concentrations of 40-100ng/ml which would not have been achieved in the amount of conditioned medium used. Additionally, other soluble factors present in the medium may have had an effect on

osteoblast differentiation (i.e. IL-6). It is therefore likely that if these experiments had been continued, changes to the experimental protocol would have been made to optimise this assay.

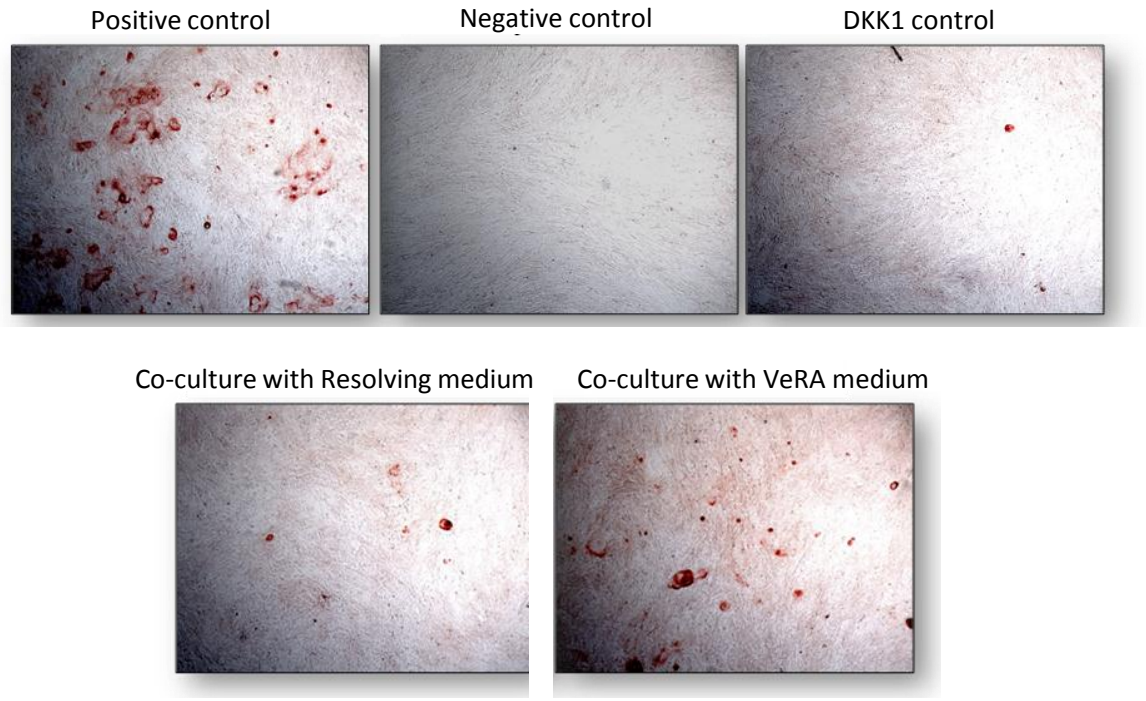

Image 4-1 Osteoblast differentiation and mineralised bone nodule formation. *Light microscopy images of mineralised bone nodules produced by differentiated osteoblasts under different conditions. Higher bone nodule formation is observed with VeRA medium co-culture compared to co-culture with Resolving medium. Images are representative of one experiment with two replicates in each outcome group.*

4.5 Synovial fibroblast-HUVEC co-cultures in flow capture assays

Our group has previously demonstrated that stromal cells regulate lymphocyte adhesion to endothelium in an *in vitro* flow-based migration model. Fibroblasts and human umbilical vein endothelial cells (HUVEC) were cultured either side of a 0.4µm pore filter. Co-cultures were

stimulated with of TNFα and IFNγ for 24 hours. Filters were transferred to a flow chamber system through which lymphocytes were perfused. Increased lymphocyte migration through the filter was observed when HUVEC were co-cultured with synovial fibroblasts but not with dermal fibroblasts controls (McGettrick et al. 2009). In collaboration with Dr Helen McGettrick (Arthritis Research UK Career Development Fellow) we decided to analyse DKK1 protein levels in the co-culture flow system. These experiments were carried out by Dr McGettrick.

DKK1 levels in the supernatants of synovial fibroblast-HUVEC co-cultures were determined with a bead based multiplex technique as specified in the methods section. DKK1 protein levels were determined in the supernatants of HUVEC alone (n=7) or co-cultured with Resolving (n=5) or VeRA (n=5) synovial fibroblasts. DKK1 levels in the supernatant of co-cultures of HUVEC and Resolving fibroblasts did not differ from those found when HUVEC were cultured alone. However, statistically significantly higher levels of DKK1 were observed in the supernatant of co-cultures of HUVEC with VeRA synovial fibroblasts compared to HUVEC alone (median 1094pg/ml vs. 244.9pg/ml respectively, $p<0.01$) (Figure 4.4A). Furthermore, DKK1 levels in supernatants positively correlated with lymphocyte adhesion (Figure 4.4B). Other cytokines assayed in these experiments included IL-8, RANTES, IL-4, GRO-alpha, IL-6, IL-1β, ENA78, MMP13 and IL-1α, none of which showed differences.

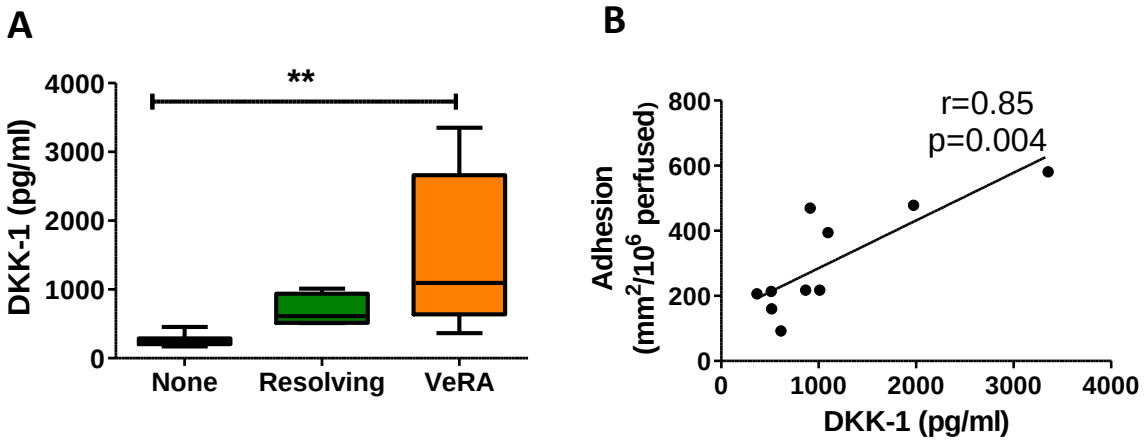

Figure 4.4 Synovial fibroblast-HUVEC co-cultures. A, *DKK1 levels were determined in the supernatant of HUVEC cultured alone (n=7) or co-cultured with Resolving (n=5) or VeRA (n=5) synovial fibroblasts. No differences in DKK1 levels were observed between HUVEC alone and Resolving-HUVEC co-cultures. Significantly higher DKK1 levels were observed in the supernatant of VeRA-HUVEC co-cultures than HUVEC alone. Box and whisker plot where box represents median and interquartile range and vertical lines represent maximum and minimum values. Differences in DKK1 levels between groups assessed with Kruskal Wallis test. **p<0.01.* ***B,*** *DKK1 levels positively correlated with lymphocyte adhesion. Correlation assessed with Spearman test.*

4.6 Proof of concept: candidate gene approach: Discussion

Proof of concept experiments demonstrated that gene expression profiles of cultured synovial fibroblasts segregate according to outcome. These differences were observed in unstimulated but not in TNF stimulated cells. Of the 48 genes assayed in the unstimulated samples, 38 provided robust data. Three out of these 38 genes demonstrated differences in expression according to outcome. This gave us confidence that a larger unbiased mRNA transcriptomic analysis of these cells would yield interesting results.

Additionally, these data suggest that increased DKK1 production could be a key event in progression to RA and occurs early in the disease process. In order to conclusively prove this, further work would need to be undertaken that is beyond the scope of this project.

5 Transcriptomic analysis by Serial Analysis of Gene Expression

5.1 Introduction

Encouraged by the results of the proof of concept experiments, I set out to determine whether synovial fibroblasts from patients in the five clinical outcome groups displayed differential transcriptional profiles. Serial Analysis of Gene Expression (SAGE) is a high throughput Next Generation Sequencing (NGS) technique that enables sequencing of mRNA fragments in a parallel fashion. At the time these experiments were designed, this technology (using the SOLiD platform from Applied Biosystems) was available through a collaboration with the Molecular Development Department that had, together with the Technology Hub, taken over joint running of this platform. This, together with bioinformatics expertise available from the Technology Hub and Systems Science for Health initiatives, represented an attractive approach to experimental design and data analysis. However, this approach proved unfruitful and no conclusive results were obtained from these experiments. Nevertheless, the work undertaken has been included as a chapter in this thesis as a significant amount of time and resources were invested on this venture and key learning points emerged from this process.

5.2 Serial Analysis of Gene Expression: The technology

The ability to sequence DNA has been an important contribution to the advancement of all disciplines of biological sciences. The initial Sanger sequencing methods were developed in the 1970s (Sanger et al. 1975;Sanger et al. 1977) and became the sequencing methods of

choice for the subsequent 25 years still remaining in use today. Nevertheless, this field was revolutionised in the 2000s with the development of NGS technologies. A variety of NGS platforms exist that share a common advantage over the traditional Sanger methods: these high-throughput, large scale automated methods enable sequencing of large cDNA volumes in short periods of time at a fraction of the cost. NGS platforms include reversible terminator technology (Illumina), sequencing by ligation (SOLiD platform from Applied Biosystems), pyrosequencing (Roche) and semi-conductor sequencing (Ion Torrent and Proton). The major difference between them is the underlying sequencing method which lends each platform their characteristic advantages and disadvantages. Regardless of the method used, NGS platforms offer diverse applications including whole genome sequencing, mRNA sequencing, targeted sequencing and chromatin immunoprecipitation sequencing. The choice of application is dictated by the biological question being addressed. Our goal was to determine the transcriptional profile of synovial fibroblasts at mRNA level and thus we used an mRNA sequencing pipeline.

Serial Analysis of Gene Expression (SAGE) produces a snapshot of the mRNA populations in a given sample. A modified version of the original method developed by Velculescu and colleagues in 1995 (Velculescu et al. 1995) was used in the experiments described in this thesis (Matsumura et al. 2005). The SAGE method is based on two principles: (i) a short (27bp) nucleotide sequence, referred to as a tag, from a defined position within a transcript is enough to uniquely identify that transcript and (ii) the expression level of this transcript can be determined by the number of times this tag is identified. A simplified schematic representation of the SAGE method is shown in Figure 5.1.

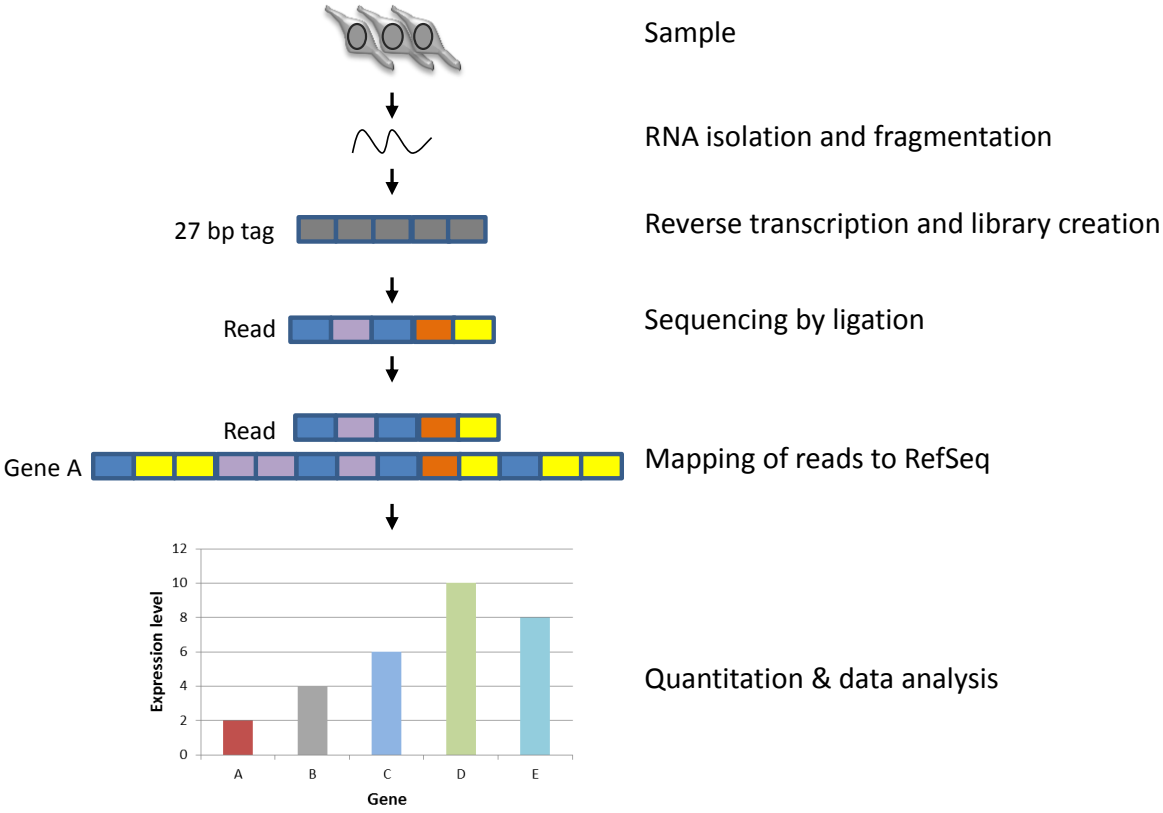

Figure 5.1 Schematic representation of the SAGE method. *mRNA is isolated from the samples of interest, fragmented, reverse transcribed and amplified creating cDNA libraries. The cDNA fragments are sequenced and the resulting reads are mapped to a reference nucleotide sequence database (RefSeq). The number of reads for a given transcript (i.e. gene A) is quantified providing information about expression levels for that gene. Expression data from different samples can subsequently be compared during further data analysis.*

5.3 Serial Analysis of Gene Expression: Experimental design

To ascertain whether differences in gene expression between synovial fibroblasts in the different outcome groups existed, transcriptomic analyses of cell lines in all five outcome groups were performed using the SAGE method.

In proposing that differences in gene expression between outcome groups would be identified, an assumption was made that any differences in expression between samples within each outcome group would not outweigh those differences between samples in different outcome groups. However, biological variation between samples of the same and differing outcome groups must be considered from the outset and, where possible, strategies to minimise this variation should be adopted. A way of strengthening experimental design in this context is by increasing the number of biological replicates (samples) in each outcome group. The optimal number of samples will vary depending on the biological variability associated with that sample. In practice, this consideration often needs to be balanced with cost implications associated with these technologies. An accepted approach is to use the same number of replicates as that used in prior microarray analysis experiments. Previous experience of synovial fibroblast transcriptome analysis in our group demonstrated that six samples per group were sufficient for statistical analysis of microarrays to identify differentially expressed genes. With this in mind and to increase the strength of the analyses, eight samples per group were selected and used in these experiments (making a total of 40 samples). To further minimise biological variability, clinical groups were made as homogeneous as possible by selecting patients and controls of similar ages, gender and disease duration within and between groups. A summary of the clinical characteristics of patients in each outcome group is shown in Table 5.1. The full clinical characteristics of these patients are shown in Table 2.3.

Table 5.1 Summary of patient characteristics.

Clinical Outcome	Joint of origin	Antibody positive	Disease duration	Gender (female)	Mean age (yrs)
Normal (n=8)	8 knee (100%)	N/A	N/A	4 (50%)	41.8
Resolving (n=8)	7 knee (87.5%) 1 ankle (12.5%)	0 (0%)	3.8 wks	3 (37.5%)	45.1
VeRA (n=8)	8 knee (100%)	3 (37.5%)	5.8 wks	5 (62.5%)	56
Early RA (n=8)	8 knee (100%)	4 (50%)	66 wks	3 (37.5%)	57.8
Established RA (n=8)	8 knee (100%)	5 (62.5%)	20 yrs	5 (62.5%)	55.6

Antibody status defined as either RF or CCP positivity; N/A: not available; wks: weeks; yrs: years

Synovial cells lines were created from samples from each of these patients. Subsequently, lines were cultured under the same conditions and to the same level of confluence and stored at passage five as cell pellets for subsequent SAGE processing and analysis. Sample selection, culture and preparation for SAGE experiments were performed by myself. RNA extraction was performed by myself and Mr Stephen Kissane (Senior Technician at the Technology Hub, University of Birmingham). Creation of cDNA, amplification and sample sequencing were performed by Mr Stephen Kissane as mandated by the Technology Hub.

5.3.1 Sample quality control

The quality and quantity of the RNA isolated from each sample are key to obtaining good quality libraries and sequencing data. Quality control was performed for each sample as specified in the materials and methods section. Briefly, RNA integrity was assessed by determining the 18S and 28S RNA fractions using gel electrophoresis run in a chip. In the absence of RNA degradation, 18S and 28S appear as two distinct electrophoretic bands. If degradation has occurred, other bands appear between the two ribosomal bands and before the 18S band. In addition to visualising the bands, the software associated to the chip calculates

an RNA integrity number (RIN) using an algorithm that takes into account not only the ratio between ribosomal bands but also the presence of degradation products. RIN values are optimal between 8.0 and 10.0. RNA quantity was measured using a Qubit fluorometer (Invitrogen) as described. 0.5µg of RNA per sample were used. The mean measured RNA amount and RIN value for each sample are shown in Appendix Table 9.4.

Next, cDNA library creation and sequencing was performed as specified in the methods section. Following sequencing, a large number of reads per sample were obtained that required mapping to the genome of reference and further analysis.

5.4 SAGE data: Analysis

Mapping of reads to the genome (also referred to as alignment) and data analysis were performed by Dr Paul Badenhorst (Senior Lecturer, Molecular Development Department, University of Birmingham). Sequenced reads were mapped to the reference nucleotide sequencing database (RefSeq) using the SOLiD SAGE mapping tool software. A brief description of the analyses undertaken is given here.

5.4.1 Read alignment and data normalisation

Sequencing of a given sample generates a list of all the reads observed in that sample (representing transcripts of the genome of origin) and the number of times each of those reads is observed (counts). To identify the transcript of origin of a given read, mapping to a

reference genome must be performed. The SOLiD SAGE platform we used typically produces reads that are 50-75bp in length. Alignment of such short sequences to the whole genome can be challenging as there may be a number of equally likely places where these short reads might originate from. At the same time, if perfect alignment is performed, biological variation (i.e. single nucleotide polymorphisms) will not be identified. Thus, a certain degree of mismatch tolerance must be allowed during alignment. One to three mismatches are commonly allowed during read alignment. However, with increasing number of mismatches the number of mapped reads is increased but the accuracy of mapping is decreased. Up to two mismatches were allowed during mapping of these experiments. The output files generated following alignment contained the list of each tag, its frequency of occurrence, its RefSeq identifier number and (where applicable) a brief description of the identified gene. Three transcript categories were identified and represented by three different RefSeq identifier numbers known as accession numbers. These were: NM accession numbers (representing mRNA products), NR accession numbers (representing non coding RNA) and XR accession numbers (representing predicted non coding RNA). The expression levels of each of these transcripts were given by the frequency of their occurrence (number of counts).

In order for the counts of a given transcript to represent expression levels of that transcript two conditions must be fulfilled: (i) the amount of input material (i.e. mRNA) must be the same for all sequenced samples and (ii) the size of the cDNA library must be the same in all samples so that the total number of mapped reads is the same in all samples. The first of these conditions is achieved during library preparation by sampling equal amounts of material in all samples. It is thus essential that library preparation is accurate as this is a common source of error in sequencing experiments. As the size of the total number of mapped reads often differs

between samples following sequencing experiments, normalisation to total read count is usually performed (Dillies et al. 2013). Using EdgeR Bioconductor, data were normalised to total read count by applying the following formula to each sample:

$$\frac{n}{r}\ \bar{x}$$

where n represents the number of counts for a given read, r the total number of reads in that sample and $\bar{x}$ the mean total read count across all samples in the dataset. Following normalisation, the counts obtained were a linear representation of the expression levels of a given transcript. Following total count normalisation two samples were identified as outliers within their given groups as their expression patterns differed significantly from those of the remaining samples in their groups. These were: one sample in the VeRA group (BX005) and one sample in the Early RA group (BX077). These samples were excluded from subsequent differential expression analysis.

5.4.2 Differential expression analysis

Data analysis, like experimental design, is determined by the biological question being addressed. Given the large number of samples and groups examined in the SAGE experiments, a variety of analyses could potentially be conducted. Differential expression analysis was thus focused on addressing two questions: (i) what are the differences in transcriptional profile between very early RA and resolving disease? In other words, what are the key genes responsible for the resolution of early inflammatory arthritis? (ii) do RA

synovial fibroblasts display the same transcriptional characteristics in early and late disease? A schematic representation of the biological question and the clinical outcome groups to be compared during analyses is shown in Figure 5.2.

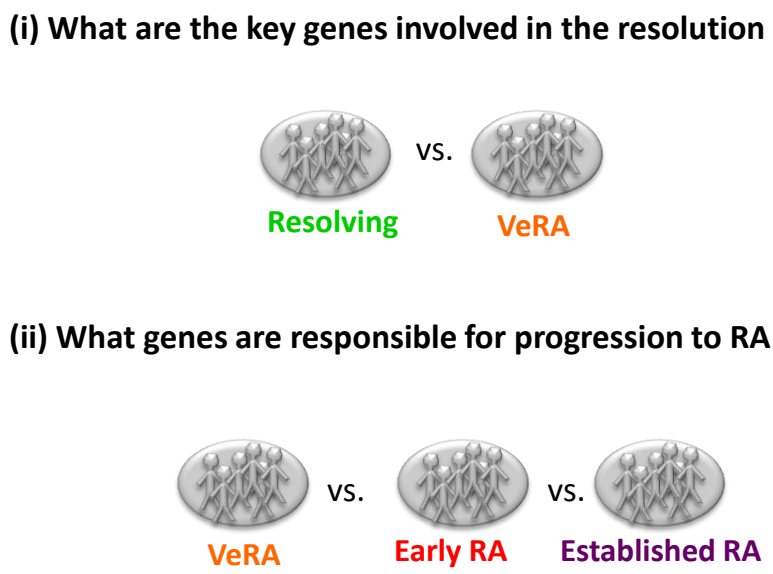

Figure 5.2 Schematic representation of the proposed differential expression analyses. *To identify key genes involved in the resolution of early inflammatory arthritis, transcriptomic data from Resolving and VeRA groups should be compared. To unravel genes responsible for progression to RA and disease chronicity such comparison should involve, VeRA, Early RA and Established RA groups.*

Prior to undertaking differential expression analysis, data were visualised using principal component analysis (PCA) to ascertain the degree of clustering within outcome groups. A PCA plot representative of these analyses is shown in Figure 5.3. Clear clustering of Established RA samples along the second component (or dimension) was observed. A degree of clustering of VeRA and Early RA samples along the first dimension was also observed. However, no clustering of Normal samples, which appeared to be distributed randomly along the first dimension, was seen. The lack of clustering raised concerns about the high degree of

heterogeneity that may be present in the samples of this outcome group. As a result of this observation, all Normal samples were excluded from subsequent data analyses.

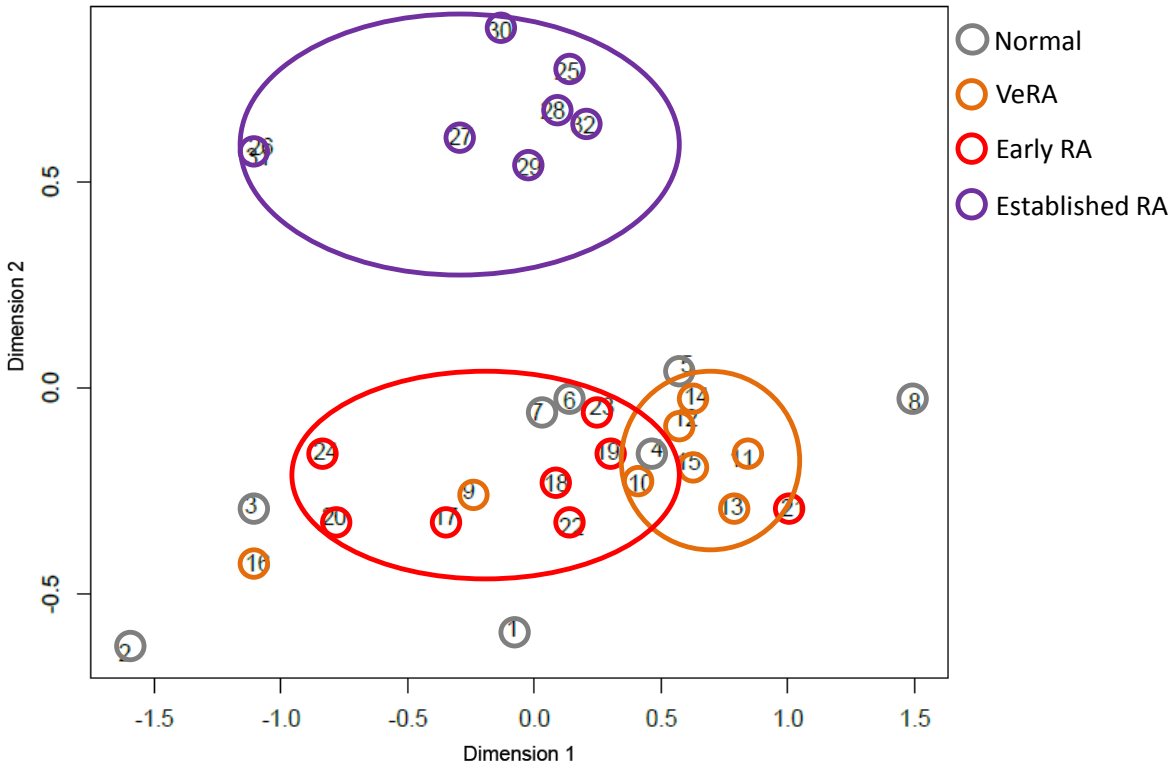

Figure 5.3 Principal component analysis plot of Normal, VeRA, Early RA and Established RA samples. *Clustering of Established RA samples along the second dimension is seen. Some clustering of Early RA and VeRA samples along the first dimension is also observed. Normal samples are randomly distributed along the first dimension. Samples are represented by numbers (Normal:1-8, VeRA: 9-16, Early RA: 17-24, Established RA: 25-32) and surrounded by coloured circles denoting outcome group of origin (grey: Normal, orange: VeRA, red: Early RA, purple: Established RA).*

Next, a general linear model was built to identify significantly differentially expressed transcripts between outcome groups. Multiple testing correction was performed and a false discovery rate (FDR) of 0.01 was set. The results of these analyses are discussed below,

starting with the analysis of Resolving versus RA persistent early inflammatory arthritis (Resolving vs. VeRA comparison). Data mining, pathway analysis and target validation were performed by myself.

5.5 Differential expression data analysis: Results

5.5.1 Resolving versus VeRA comparison

Principal component analysis of the transcriptional profile of synovial fibroblasts in the Resolving and VeRA groups revealed differences along the first principal component (Figure 5.4).

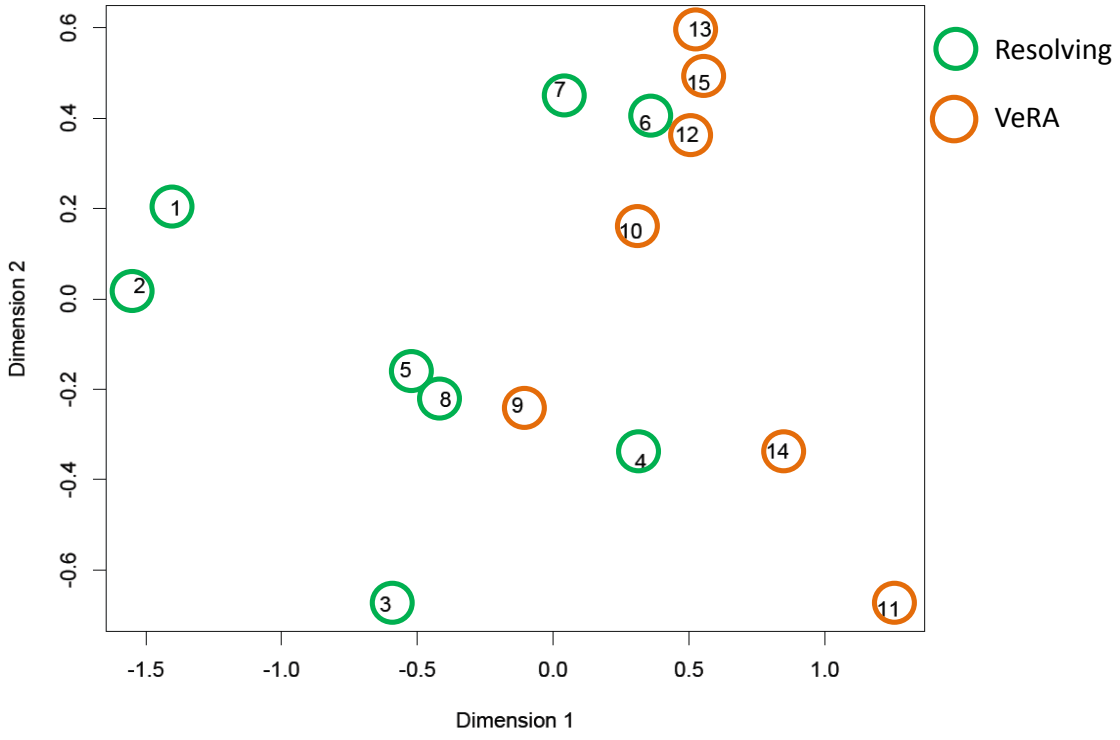

Figure 5.4 Principal component analysis plot of Resolving and VeRA samples. *Separation between samples in each outcome group is seen along the first principal component. Each sample is represented by a number (Resolving: 1-8, VeRA: 9-15). Each number is surrounded by a green (Resolving) or orange (VeRA) circle representing the outcome group to which they belong.*

5.5.2 Data mining strategy

A total of 701 transcripts were differentially expressed between both groups (FDR: 0.01). To reduce this data set to a manageable set of key differentially expressed genes for validation, a series of data mining strategies was employed. These strategies were employed independently and results obtained by all three were combined to select a final set of targets for quantitative real time PCR validation. As the purpose of data mining was to identify targets for further validation at mRNA and protein levels, non-protein coding RNA and predicted non-coding RNA transcripts were excluded from this analysis. In total, 564 transcripts representing protein coding genes were analysed.

First, differentially expressed genes were sorted by p value (lowest to highest) and fold change (highest to lowest). An arbitrary cut off of 100 was set and the top 100 genes were further investigated. Second, a "candidate gene" approach was used whereby I reviewed the description of all differentially expressed transcripts and those that seemed interesting in the light of published literature of RA and synovial fibroblasts were selected (i.e. CXCL16, TNFRSF9). An example of the typical results obtained using these two approaches is shown in Figure 5.5. Third, differentially expressed genes were classified into biological categories using pathway analysis.

A

	A	B	C	D	E
1	**Tag**	**PValue**	**Fod change**	**NM number**	**Gene symbol**
2	CATGTTGGTCAGGCTGGTCTCCAACTC	1.11801E-09	-4.499210781	NM_003879.5	CFLAR tv1
3	CATGTTGGTCAAGCTGGTCTCGAACTC	1.39578E-09	-4.564281304	NM_181742.3	ORC4 tv 1-6
4	CATGTTGGTCAGGCTGCTCTCAAACTC	1.86588E-09	-4.840221171	NM_003643.3	GCM1
5	CATGTTGGGGAGGCTGGTCTCGAACTC	3.56891E-09	-5.508151405	NM_003099.3	SNX1 tv1-2
6	CATGTTGGTCAGGCTGCTCTCGAACTC	3.577E-09	-4.245516917	NM_018962.2	DSCR6
7	CATGTTGGTCAGGCTGGTCTAGAACTC	3.8478E-09	-4.536040841	NM_001077206.2	SEC31 tv1, 3, 4-6
8	CATGTTGGTCAGGCTGGTCTCAAACAC	4.00054E-09	-4.598142786	NM_032316.3	NICN1
9	CATGTTGGTCAGGCTGGTTTCAAACTC	4.2261E-09	-4.990569303	NM_032875.2	FBXL20 tv 1-2
10	CATGTTGGTCAGGCTGTTCTCGAACTC	4.71809E-09	-4.504212808	NM_003999.2	OSMR tv 1-2
11	CATGTTGGTCAGGCTGGGCTCAAACTC	4.73253E-09	-4.935171553	NM_003574.5	VAMP tv 1-2
12	CATGTTGGTCAGGCTGGTTTCGAACTC	5.0357E-09	-4.364406469	NM_001745.3	CAMLG
13	CATGTTGTTCAGGCTGGTCTCAAACTC	5.07911E-09	-4.704706354	NM_016298.3	FBX040
14	CATGATTTATAGTCATTTGGGTATATA	5.3021E-09	-6.176050188	NM_001040440.2	CCDC112 tv 1-2
15	CATGTTGGTTAGGCTGGTCTCAAACTC	5.42601E-09	-4.415691719	NM_178836.3	PLD6
16	CATGTGGTTTTTGTCTTTGGTTCTGTT	5.56958E-09	-6.170984583	NM_004956.4	ETV1 tv 1-3
17	CATGTTGGTCGGGCTGGTCTCAAACTC	8.6895E-09	-4.630918189	NM_016946.4	F11R
18	CATGTTGGTTAGGCTGGTCTCGAACTC	1.10344E-08	-4.307055808	NM_144567.3	ANGEL2
19	CATGGAATGTTCTTCCATTTGTTTGTA	1.39357E-08	-6.438613835	NM_001449.4	FHL1 tv 1-9
20	CATGTTGATCAGGCTGGTCTTGAACTC	1.86196E-08	-3.954772541	NM_001025780.1	FAM108B1 tv2
21	CATGTTGGCCAGGGTGGTCTTGAACTC	1.94095E-08	-4.478867453	NM_022894.3	PAPOLG
22	CATGTTGGTCAGGCTGGTCTTGAATTC	2.12429E-08	-4.3986401	NM_178819.3	AGPAT6 tv
23	CATGTAGTTGAGCGGTTTTGAGTGAGT	2.14968E-08	-5.938671207	NM_001171637.1	CCDC148 tv2
24	CATGATTTATAATCCTTTGGGTACATA	2.46634E-08	-5.105864127	NM_021627.2	SENP2
25	CATGTTGGTCAGACTGGTCTTGAACTC	2.76576E-08	-4.316867747	NM_018097.2	HAUS2 tv 1-2
26	CATGTTGGTCAGGCTGGTCATGAACTC	3.22737E-08	-4.570927864	NM_000393.3	COL5A2
27	CATGTTGGTCAGGCTGGTCGTGAACTC	3.27131E-08	-4.532116418	NM_031904.3	FRMD8
28	CATGTTGGTCAGGCTGTTCTTGAACTC	3.27934E-08	-4.470982979	NM_173511.3	FAM117B
29	CATGTTAACCAGGCTGGTCTCGAACTC	3.29495E-08	-3.486990211	NM_002572.3	PAFAH1B2 tv1
30	CATGTTGGTCAAGCTGGTCTTGAACTC	3.35154E-08	-4.502134077	NM_013390.2	TMEM2 tv1-2
31	CATGTTGGTCAGGCTGGTCTTGAACGC	3.35516E-08	-4.418535053	NM_014358.2	?CLEC4E
32	CATGTGTTTTTTGTCTTTGGCTCTGTT	3.39049E-08	-7.500373069	NM_001190478.1	MTRNR2L5
33	CATGATTTATAGTCCTTTGGGTATATA	3.60983E-08	-4.667986007	NM_001127500.1	MET tv1
34	CATGTTGGTCAGGCTGGCCTTGAACTC	3.8059E-08	-4.44649681	NM_014235.3	UBL4A
35	CATGGAGTCAGGAGATCGAGACCATCC	3.86301E-08	-3.527510739	NM_003190.4	TAPBP tv1,3
36	CATGTTGGTCAGGCTGGCTTTGAACTC	4.06483E-08	-4.550423634	NM_001012514.1	ITM2C tv 1-3
37	CATGTTAGCCAGGCTGGTCTTGAACTC	4.72036E-08	-3.984401436	NM_001079512.2	FAM18A
38	CATGGTACTGGTGCCAAAACAGATATA	4.9708E-08	-6.602089026	NM_000922.3	PDE3B
39	CATGTTGGTCAGGTTGGTCTTGAACTC	5.6226E-08	-3.734605841	NM_003423.2	STEAP2 tv 1-2
40	CATGTTCTCACTCATAGGTGGGAATTG	6.2893E-08	-4.914127408	NM_030912.2	TRIM8
41	CATGTTCTCACTCATAAGTGGGAATTG	6.31018E-08	-5.690740308	NM_006058.3	TNIP1
42	CATGCTCTCACTCATAGGTGGGAATTG	7.04637E-08	-6.309385012	NM_022901.2	U2AF2 tv 1-2
43	CATGTTGGCCAGGCTGGTCTTGGACTC	7.53131E-08	-4.591334543	NM_032842.3	ALG9 tv 1-4
44	CATGGAATGTTTTTCCATTTGTTTGTG	8.28613E-08	-6.207044876	NM_024086.3	OSMR tv 1-2
45	CATGTTCTCACTCACAGGTGGGAATTG	8.52917E-08	-6.118464106	NM_016396.2	CTDSPL2
46	CATGTTAGCCAAGATGGTCTCGATCTC	9.39615E-08	-4.604680635	NM_024947.3	HSD17B13 tv A-B
47	CATGCTGTTTTGGTTACTGTAGTCTTG	1.0222E-07	-4.954222333	NM_024536.3	CA12 tv 1-2
48	CATGTTGGCCAGGCTGGTCTCGAACGC	1.0596E-07	-4.813215263	NM_022901.2	LRRC19
49	CATGTTGGCCAGGCTGGTCCCGAACTC	1.06244E-07	-4.59687786	NM_032842.3	TMEM209
50	CATGTTGGCCAGGCTAATCTCGAACTC	1.08774E-07	-5.586369213	NM_024086.3	METTL16
51	CATGTTGGCCAGGCTGGTCACAAACTC	1.10133E-07	-3.750463042	NM_004226.3	STK17B

B

	A	B	C	D	E
1	**Tag**	**PValue**	**Fod change**	**NM number**	**Gene symbol**
2	CATGTTGACCAGGCTGGTCTCGAACTC	2.56735E-08	6.947687011	NM_019067.5	CXCL16
3	CATGTTGTACAGGCTGGTCTCAAACTC	1.71862E-07	3.228975153	NM_001561.5	TNFRSF9
4	CATGTTGGCCAGGCTGCTCTTGAACTC	1.35671E-06	4.201637344	NM_005099.4	ADAMTS4
5	CATGTTGGCCATGCTGGTCTCAAACTC	2.46163E-06	2.548628153	NM_001145320.1	ADAMTSL2
6	CATGTTGGCCAGGCTAGTCTCAAACTT	9.54252E-05	3.515767909	NR_024106.1	ADAM3A
7	CATGTTGGCCAGGCCGGTCTCAAACTC	1.85163E-06	2.836510941	NM_000243.2	MEFV
8	CATGTTCACCAGGCTGGTCTTGAACTC	6.54418E-06	2.822874522	NM_005204.2	MAP3K8
9	CATGCCTGTAATCCCAGCACTTCAGGA	0.00012994	7.376093222	NM_080876.3	DUSP19
10	CATGCCTGTAATCCTAGCACCTTGGGA	0.000175657	4.490544905	NM_001946.2	DUSP6
11	CATGATCACACCACTGCACTCCAGCCT	0.000144603	5.360849871	NM_001001671.3	MAP3K15

Figure 5.5 Data mining strategy. *Screenshots showing***: *A, Top 100 (only top 51 in this screenshot) differentially expressed genes ranked by p value and fold change.* ***B,*** *Candidate gene approach where functionally interesting genes have been selected for further consideration as potential validation targets.*

5.5.3 Pathway analysis

Using the DAVID functional annotation tool (open online resource available at http://david.abcc.ncifcrf.gov/) categorisation of genes into biological groups was performed. All 564 differentially expressed transcripts were entered into the software. These transcripts were functionally annotated and grouped into functional pathways using the Kyoto Encyclopedia of Genes and Genomes (KEGG). Eight functional pathways were identified. These pathways related to cellular functions (apoptosis, focal adhesion and tight junctions), malignancies (chronic myeloid leukaemia, prostate cancer and melanoma) and cell signalling (insulin and TGF beta signalling pathways). Once identified, each pathway was individually visualised and those genes within the pathway that had arisen from the list of differentially expressed transcripts between Resolving and VeRA synovial fibroblasts were identified and selected for further assessment as potential validation targets (Figure 5.6).

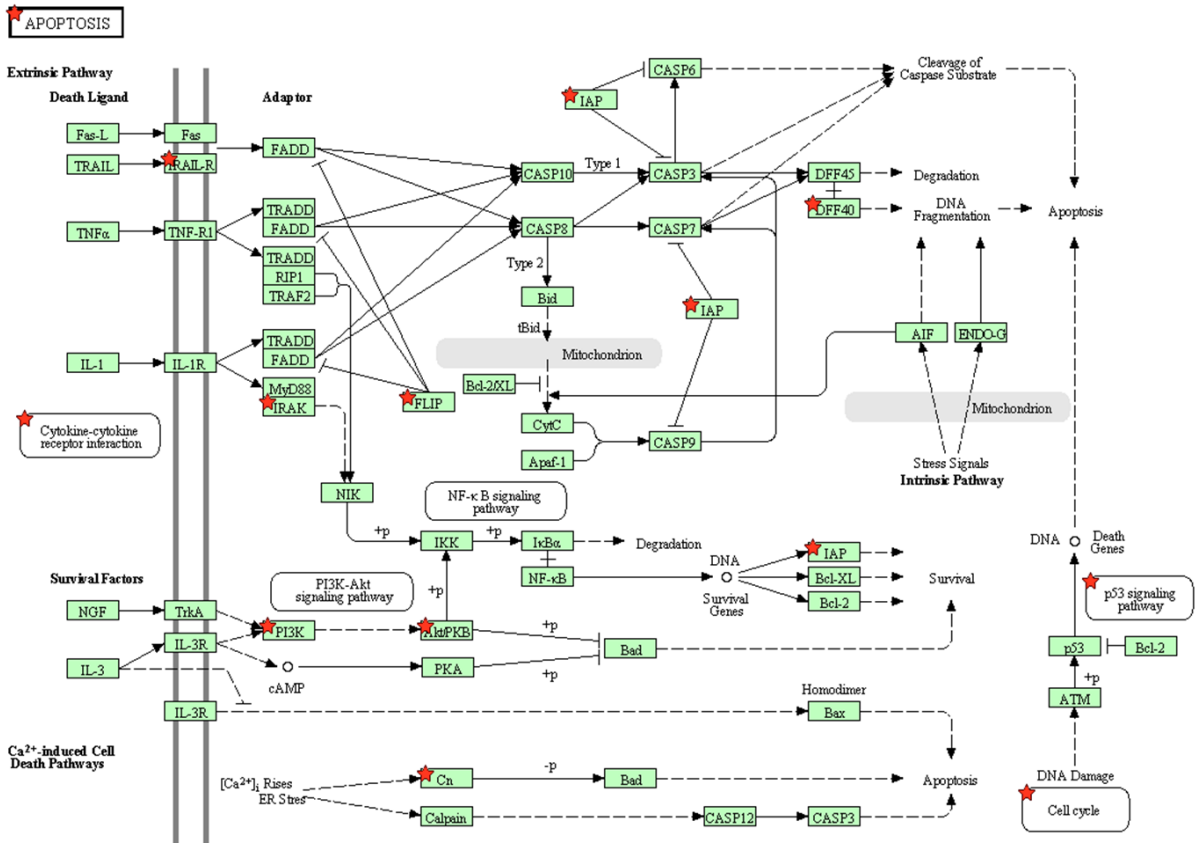

Figure 5.6 Pathway analysis. *Sample image showing apoptosis pathway. Each green square represents a gene in the pathway. Those genes marked with a red star arise from the list of differentially expressed genes between Resolving and VeRA synovial fibroblasts. For each pathway, the starred genes were identified and added to the final list of potential validation targets.*

5.6 Target validation

Using a combination of these three data mining strategies, 25 protein coding genes were selected for final target validation. The protein products of these genes and a description of their function are shown in Table 5.2. The fold change in expression levels between Resolving and VeRA lines are also given together with the statistical significance of the change expressed as p value. All targets were overexpressed in the VeRA compared to the

Resolving group. Primer pairs for these targets were designed and quality control tested as specified in the methods section.

Table 5.2 Gene targets selected for PCR validation.

Symbol	Product	Description/Function	Fold difference	P value
CAMLG	Calcium signal modulating cyclophilin ligand	B and T cell homeostasis	-4.365	5.04E-09
CHRD	Chordin	Bone morphogenetic protein antagonist	-4.499	1.12E-09
COMP	Cartilage oligomeric protein	Non-collagenous ECM component	-4.504	2.41E-06
COL5A2	Collagen type 5 alpha 2	Collagen assembly regulator	-4.570	6.03E-06
DFFB	DNA fragmentation factor B	DNA fragmentation & chromatin condensation	-4.935	2.32E-06
E2F2	Transcription factor E2F2	Tumour suppressor & cell cycle regulator	-4.631	8.69E-09
F11R	Junctional adhesion molecule A	Regulator of tight junction assembly	-4.571	6.31E-06
FGF5	Fibroblast growth factor 5	Oncogene	-4.667	6.35E-06
FGFR1	Fibroblast growth factor receptor 1	Receptor for several of FGF ligands	-2.651	1.13E-04
IRAK3	IL1 receptor associated kinase	Negative regulator of TLR signalling	-4.176	6.09E-07
cMET	Hepatocyte growth factor receptor	Proto-oncogene	-5.515	2.62E-07
MDM2	Mouse double minute 2 homolog	Negative regulator of p53	-4.038	2.66E-07
OSMR	Oncostatin M receptor	Promotes EMT transition	-4.504	4.72E-09
PAK2	P21 activated kinase	Apoptosis regulator, cell migration	-4.410	6.15E-07
PDPK1	3-phosphoinositide dependent protein kinase-1	Activator of the AKT/PKB pathway	-4.137	2.66E-07
PIK3CD	PI 3 kinase catalytic subunit delta	Growth, proliferation, differentiation, motility	-4.247	4.37E-06
PRKCI	Protein kinase C iota	Negative regulator of apoptosis	-2.555	8.82E-05
PTK2	Protein tyrosine kinase 2	Focal adhesion	-2.717	1.61E-04
RAB3B	Ras related protein 3B	Oncogene	-2.578	5.09E-05
SNX1	Sorting nexin 1	Epidermal growth factor expression regulator	-4.410	4.13E-06
SOCS3	Suppressor of cytokine signalling 3	Negative regulator of STAT signalling	-2.922	7.21E06
TGFBR1	Transforming growth factor beta receptor 1	TGF beta signalling transduction	-2.399	1.79E05
TRAIL-R4	TRAIL receptor 4	Inhibitor of TRAIL induced apoptosis	-2.342	4.52E-05
VAMP A	Vesicle associated membrane protein A	Regulation of tight junctions	-2.579	5.09E-05
XIAP	X linked inhibitor of apoptosis	Regulation of apoptosis, invasion & proliferation	-2.741	8.12E-05

Fold difference refers to Resolving vs. VeRA

5.6.1 Real time PCR: Results

Real time quantitative PCR was used for independent target validation, with 21 out of the 25 primers designed passing quality control testing. The expression levels of these 21 genes were tested in all eight samples in each outcome group (Figure 5.7). Levels of expression of TNF related apoptosis inducing ligand receptor 4 (TRAIL-R4) were significantly higher in the VeRA samples than in the Resolving ones (median: 0.21 vs. 0.05, p=0.04; fold difference: 4.4). No statistically significant differences were observed between groups in the expression of the remaining genes. Whilst the observed validation yield (1 out of 21) was lower than expected, given that TRAIL-R4 seemed a plausible and attractive target, subsequent efforts were directed to its validation at protein level.

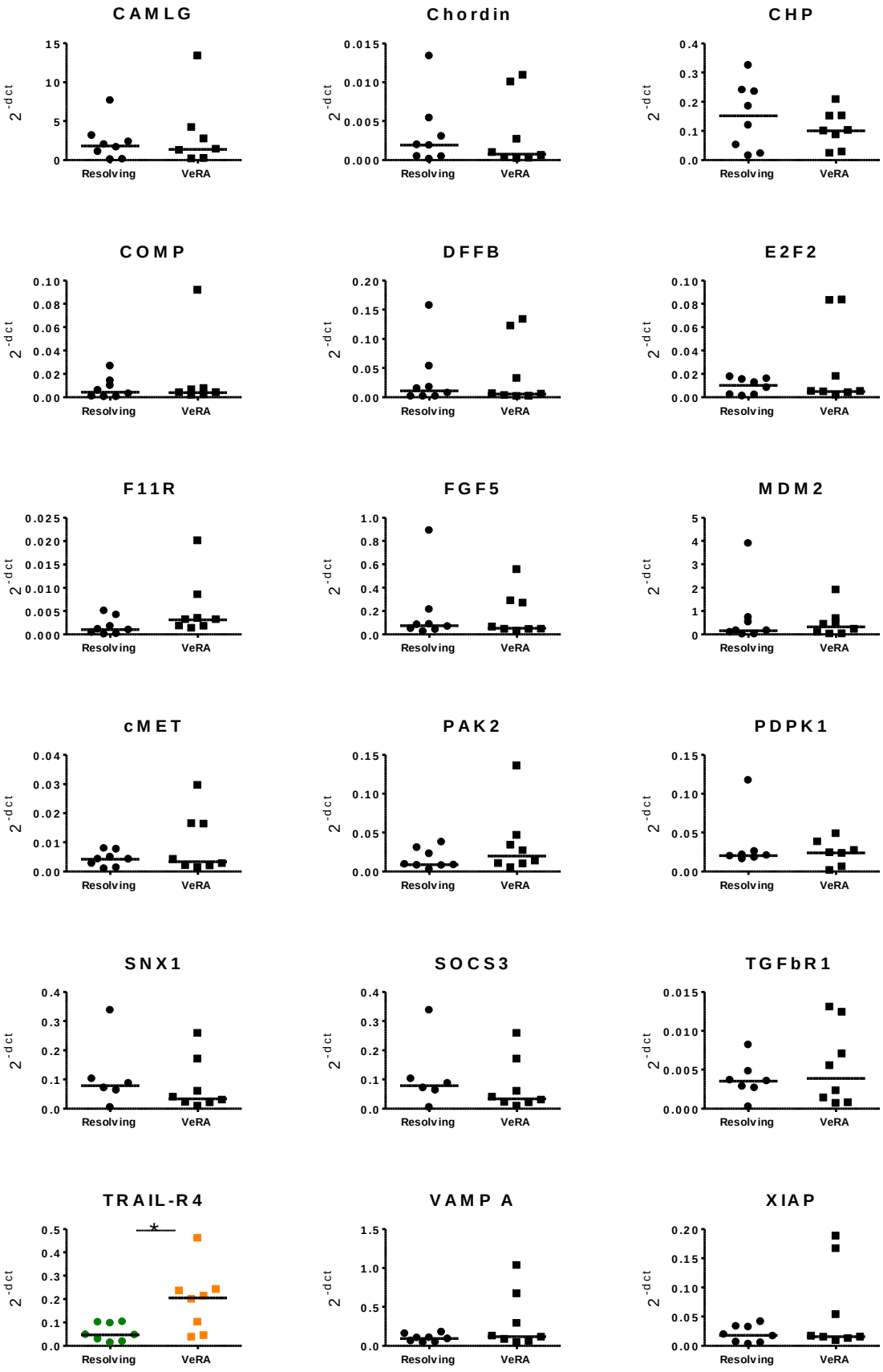
CAMLG
Chordin
CHP
COMP
DFFB
E2F2
F11R
FGF5
MDM2
cMET
PAK2
PDPK1
SNX1
SOCS3
TGFbR1
TRAIL-R4
VAMP A
XIAP
2-dct
Resolving
VeRA
*

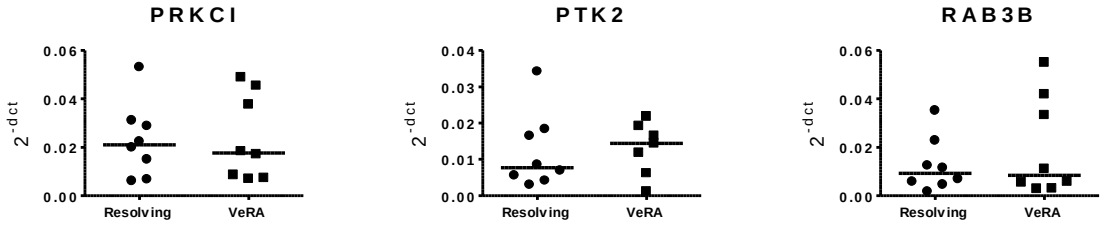

Figure 5.7 Target validation. *Expression levels of 21 selected genes were assessed by PCR in Resolving (n=8) and VeRA (n=8) samples. The expression of TRAIL-R4 was significantly higher in VeRA samples than in Resolving ones (median: 0.21 vs. 0.05, p=0.04). Expression levels normalised to GADPH using the* 2^{-dCt} *method. Data shown in scattered dot plots where horizontal lines represent medians. Differences in expression between groups assessed with Mann-Whitney test. *p<0.05.*

5.6.1.1 TRAIL-R4 validation

TRAIL-R4 (also known as TRAIL decoy receptor 2 (TRAIL-DcR2)) is a member of the TRAIL family of receptors that in contrast to the better studied TRAIL receptors 1 and 2, has an inhibitory role in TRAIL induced apoptosis (Degli-Esposti et al. 1997).

TRAIL induced apoptosis of RA synovial fibroblasts has been previously investigated with conflicting results. Whilst some authors observed apoptosis rates of up to 80% following TRAIL stimulation of RA synovial fibroblasts (Ichikawa et al. 2003), others failed to demonstrate apoptosis of these cells upon TRAIL stimulation (Perlman et al. 2003). The potential role of TRAIL-R4 has not been studied in this context and thus represented a novel and attractive approach. The observation that TRAIL-R4 was overexpressed by VeRA samples suggested that inhibition of TRAIL induced apoptosis might be an early event in the development of RA and might contribute to the failed resolution of inflammatory arthritis.

TRAIL-R4 expression levels were determined by flow cytometry as specified in the methods section. To avoid cleavage of this cell surface receptor, an EDTA based cell dissociation buffer was used instead of trypsin for cell detachment prior to cytometry. The TRAIL-R4 expressing hepatic epithelial like cell line (AKN-1) was used as positive control. The three lines that showed highest TRAIL-R4 expression in the VeRA group (BX014, BX013 and BX063) and the three that demonstrated lowest TRAIL-R4 expression in the Resolving group (BX038, BX033 and BX010) were selected for protein validation. The results of these experiments are shown in Figure 5.8. TRAIL-R4 expression was observed in the positive control as expected. The percentage of synovial fibroblasts expressing TRAIL-R4 in the Resolving and VeRA groups was the same (2.5% and 2.6% respectively) and did not differ from values obtained for the isotype control (2.3%), indicating no TRAIL-R4 surface expression by synovial fibroblasts in either group.

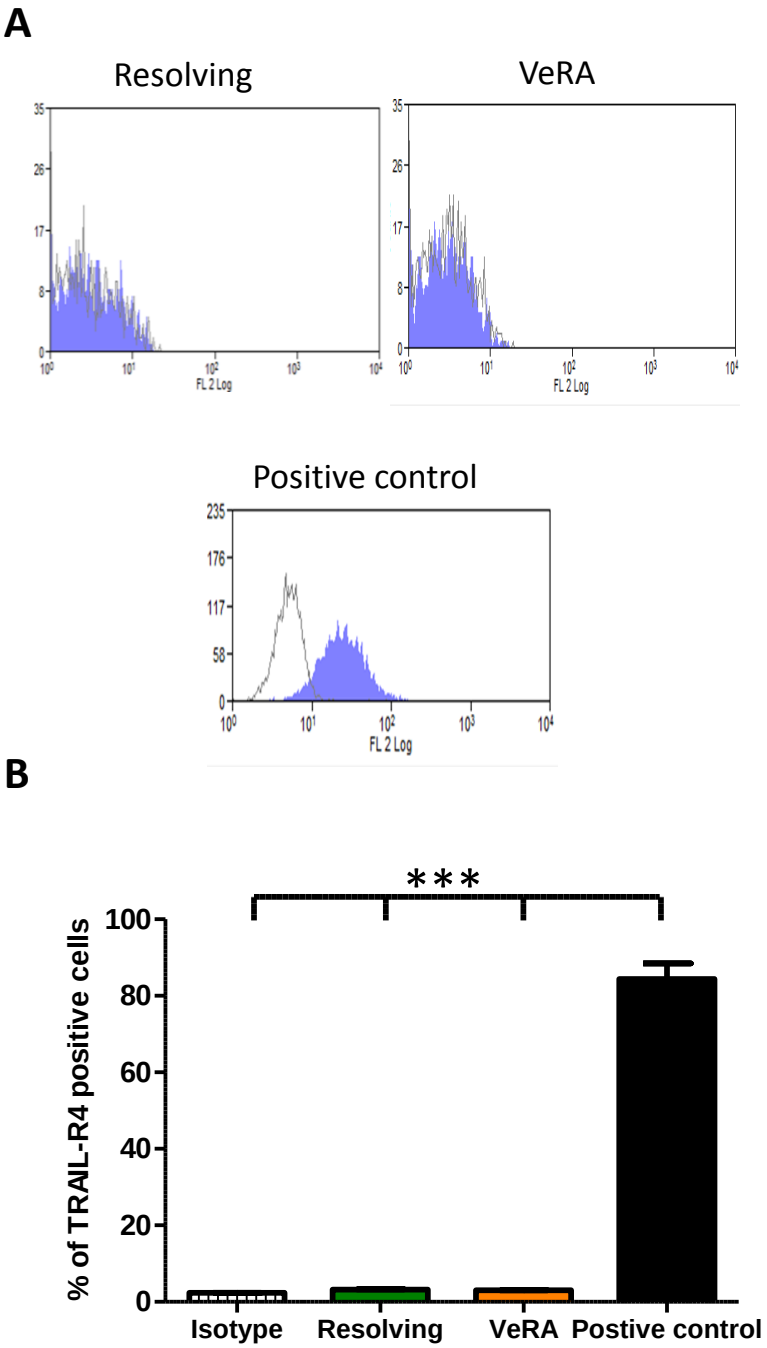

Figure 5.8 TRAIL-R4 protein expression assessed by flow cytometry. *Levels of TRAIL-R4 were determined in Resolving (n=3) and VeRA (n=3) samples.* ***A,*** *Representative flow cytometry plot showing TRAIL-R4 expression in positive control samples but not in synovial fibroblasts from either group. Test samples shown in light purple, isotype control shown as a grey line.* ***B,*** *Graphical representation of results: the percentage of TRAIL-R4 positive cells did not differ between isotype control, Resolving and VeRA samples. Statistically significant differences in percentage of positive cells were seen between the positive control group and all other groups. Data represented as mean±SD. One way ANOVA, ***p<0.001.*

Although mRNA expression is not always a reflection of protein production, the inability to validate TRAIL-R4 at protein level together with the low validation yield at mRNA level raised suspicions regarding the quality, accuracy and validity of the result obtained from the SAGE experiments. A troubleshooting process was consequently started to determine any potential sources of errors.

5.7 SAGE experiments: Troubleshooting

Potential and not mutually exclusive sources of error considered included:

1. Errors during library amplification. For example, if clonal artefacts occurred during library amplification, sequencing of such artefacts rather than "real" sample tags could have taken place leading to inaccurate results.
2. Errors during sequencing and mapping of reads to the reference genome.
3. Errors introduced during data analysis: for example during statistical analysis of differentially expressed genes or during application of data mining strategies.
4. Errors during PCR validation.

This list is by no means exhaustive but used as an illustration of potential sources of bias. It also illustrates how identifying some of these biases may not be entirely straightforward. The aim of the troubleshooting exercise was to ascertain whether the SAGE experiment results were accurate or whether alternative methods of acquiring transcriptional profiles (for example by undertaking microarray experiments) should be sought. To ascertain this, a final

attempt to validate SAGE data was made based on observations made by Dr Paul Badenhorst during data analysis.

During PCA analysis it had been noted that samples from the Established RA group quite clearly clustered away from the remaining samples in the data set. Concerns arose that these may be the only samples that were biologically different from a transcriptional profile perspective and that differences between other groups had artefactually arisen during statistical analysis (Type I error). Under this premise the only samples that were biologically different from the rest were those belonging to the Established RA group. Thus it followed that if the data obtained from SAGE experiments were correct and regardless of whether spurious differences had been identified between other groups (i.e. Resolving and VeRA), robust differences between Established RA and other groups existed and could be independently confirmed.

To test this hypothesis I attempted independent validation by PCR of differentially expressed genes between the Resolving and Established RA group. The list of differentially expressed transcripts between these groups was ranked by p value (lowest to highest) and fold change (highest to lowest). Protein coding genes with the highest statistical confidence and highest fold change were selected as PCR targets to improve the yield of PCR validation. This strategy yielded the following targets: beta actin (β-actin), 18S ribosomal RNA (18S), calcium binding protein P22 (CHP), glyceraldehyde-3-phosphate dehydrogenase (GAPDH), hepatocyte growth factor receptor (cMET), 3-phosphoinositide dependent protein kinase-1 (PDPK1) and Ras related protein 3B (RAB3B).

Reviewing these targets, a striking observation was made: three genes traditionally considered as reference housekeeping genes (β-actin, 18S and GAPDH) were differentially expressed between outcome groups. If independently verified by PCR, this may be the reason for the failed attempt to validate SAGE data at PCR level as quantitation of PCR data was done relative to GAPDH. Hence, efforts were directed to determine an optimal housekeeping gene for quantitation of PCR data on synovial fibroblasts.

5.7.1 Determining an optimal housekeeper

The relative quantitation method 2-delta Ct method (2^{-dCt}) was used for the quantification of results obtained from PCR experiments. Here, expression levels of the gene of interest are expressed relative to expression levels of a reference housekeeping gene. An optimal housekeeping gene will be expressed at constant levels in all cells under study and under different conditions. In practice this means that the choice of optimal housekeeper depends on the cells being studied. Determining an optimal housekeeper should thus be an integral part of PCR quantitation.

To determine expression levels of housekeeping genes a comparative method could not be used as a circular problem would arise whereby expression levels of one housekeeping gene would be calculated relative to another housekeeping gene with no knowledge of the gold standard. To overcome this limitation expression levels were assessed in two ways: by looking at the distribution of cycle threshold (Ct) values and by calculating the average fold change in expression from the mean. First, the Ct values of all samples for a given gene were

plotted to assess their distribution (displaying median, 25^{th} and 75^{th} percentile and range). An optimal housekeeper would be one that showed minimal variation in its distribution across all samples. It is important to note here that although Ct values will vary with RNA amounts, by analysing all samples in the same experiment, the effect of differing RNA amounts would be the same in all genes. Second, average fold changes in expression from the mean were calculated. At a PCR reaction efficiency of 100%, 1 cycle (expressed as Ct in real time PCR) corresponds to a 2 fold change in gene expression (as PCR is an exponential reaction: gene expression is 2^n where n is the number of cycles=Ct). An optimal housekeeper will not have more than a two-fold change in expression between samples (corresponding to one PCR cycle) and the smallest maximum fold change. Variability in gene expression was thus expressed as average fold change from the mean and maximum fold change representing standard deviation and ranges respectively (Dheda et al. 2004).

Commonly used housekeeping genes were selected for the experiment. These included: β-actin, 18S, GAPDH, ubiquitin C (UBC), hydroxymethylbilane synthetase (HMBS), ribosomal protein L13a (RPL13a), β2-microglobulin (B2M), hypoxanthine phosphorybosyltransferase 1(HPRT1) and succinate dehydrogenase complex subunit A (SDHA). Some of them (β-actin, GADPDH and 18S) had been identified as differentially expressed between Resolving and Established RA synovial fibroblasts during SAGE analysis.

Results are shown in Figure 5.9. When variability in gene expression was plotted as a distribution of Ct values, small variation was seen for 18s, GAPDH, UBC and RPL13with larger variation being observed for β-actin and SDHA. However, it was difficult to determine which housekeeper showed the least variation on the basis of the distribution alone. Analysis

of fold change data gave an answer to this. Genes displaying fold changes of ≤2 included 18S, GAPDH, UBC, HMBS, and RPL13a. Of these GAPDH showed the lowest maximum fold change (1.7) and was thus selected as optimal housekeeper for subsequent PCR quantitation.

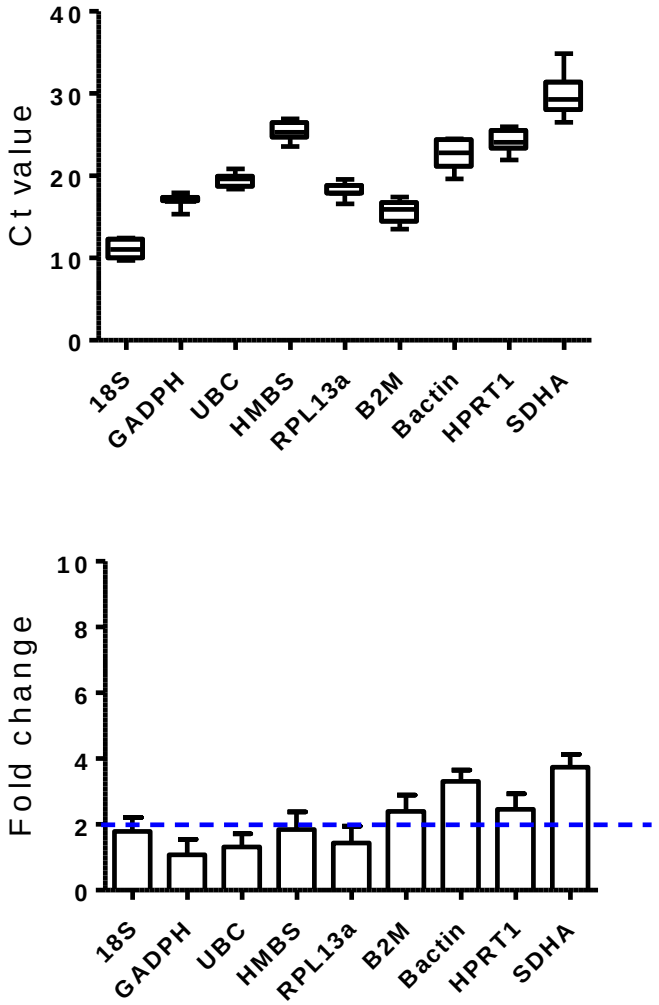

Figure 5.9 Housekeeping genes real time PCR results*. Expression levels of housekeeping genes were assessed in Normal (n=3), Resolving (n=3), VeRA (n=3), Early RA (n=3) and Established RA (n=3) samples. Top graph: the distribution of Ct values for each gene is shown in a box and whisker plots (box: median, 25th and 75th percentile; whiskers: maximum and minimum values). Genes showing least variation in distribution include 18S, GAPDH, UBC and PRL13a. Bottom graph: variability in gene expression represented in bar graphs where the columns represent average fold change from the mean and the error bars the maximum fold change. Horizontal discontinued blue line represented the cut off fold change value of 2. GAPDH displays the lowest variability followed by UBC, RPL13a and 18S. For gene abbreviations see text.*

5.7.2 Resolving versus Established RA comparison

In addition to aiding selection of an optimal housekeeper, these experiments demonstrated small variation on two of the housekeepers identified as differentially expressed between Resolving and Established RA samples by SAGE (18S and GAPDH) and marginally larger variation in another (β-actin: average fold change from the mean: 2.4, maximum fold change:3). These observations contradicted the SAGE results and suggested that the results obtained from SAGE experiments might not be accurate. Nevertheless to fully confirm this, expression levels of putative differentially expressed genes between Resolving and Established RA samples derived from SAGE data were assessed by PCR. No differences in gene expression between groups were seen for any of these genes (Figure 5.10).

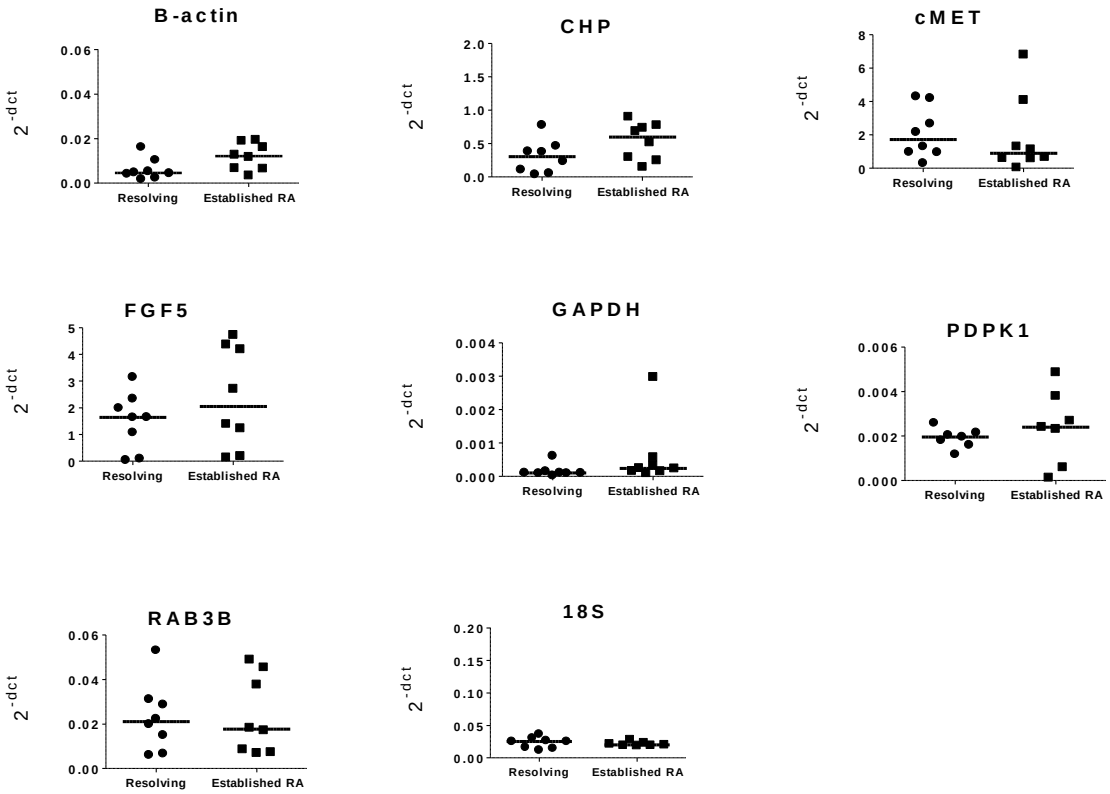

Figure 5.10 Assessment of differentially expressed genes between Resolving and Established RA. *Expression levels of the top 8 genes identified as differentially expressed between both groups were assessed by PCR in Resolving (n=8) and Established RA (n=8) samples. Expression levels normalised to GADPH using the 2^{-dCt} method with the exception of GAPDH that was normalised to 18S. Data shown in scattered dot plots where horizontal lines represent medians. No differences in expression of any of the genes were seen between groups. Differences in expression between groups assessed with Mann-Whitney test.*

5.8 SAGE data: discussion

The results obtained from the SAGE experiments were not possible to validate and appeared to contradict unbiased assessment of housekeeping gene expression. It was therefore decided that conclusions regarding the transcriptomic profile of the samples analysed could not be drawn. It is likely that a combination of errors occurred during these experiments that rendered these data unusable. It is worth noting that in the twelve months that have passed since these experiments were undertaken this platform has been abandoned at the University of Birmingham in favour of the Illumina system that provides higher coverage and more accurate results. This is in keeping with current trends in the sequencing field where the reversible terminator technology platform developed by Illumina is superseding other platforms.

A number of learning points emerged from this process. The importance of determining an optimal housekeeping before embarking on quantification of PCR data is perhaps one of the most valuable ones. We also learnt that when outsourcing experiments, it is important to ensure that strict quality control is applied to all experimental steps by the external provider. The ability to troubleshoot and identify any deviation from correct protocols should also be available as well as accountability for such deviations.

The failure of this approach meant that an alternative method of performing transcriptomic analyses had to be sought.

6 Transcriptomic analysis using microarray technology

6.1 Introduction

Given the difficulties encountered with SAGE technology, an alternative method for undertaking transcriptomic analysis was sought. Microarray technology has long been established as a powerful method for the study of gene expression (Trevino et al. 2007). Microarrays produce a snapshot of the transcriptome of a given sample with high accuracy and resolution and allow comparisons of gene expression patterns between samples. At the time these experiments were designed, experience of microarray use in our group included the transcriptomic analysis of paired synovial, dermal and bone marrow fibroblast samples in RA and osteoarthritis and the transcriptomic analysis of macrophages from wild type and dual specificity protein phosphatase 1deficient mice. All experimental work and analyses described in this chapter were carried out by myself except where indicated.

6.2 Microarray technology

A two colour microarray was used as described in the materials and methods section. Hybridisation of samples and scanning of microarrays were performed by an external provider (Oxford Gene Technology Ltd, UK). Briefly, mRNA was reverse transcribed to cDNA and labelled with a fluorescent dye: Cy3 for the labelling of test samples (emitting green fluorescence on excitation) and Cy5 (emitting red fluorescence on excitation) for the labelling of the reference cDNA control (Stratagene human reference DNA). Equal amounts

of both test and control cDNA were simultaneously hybridised onto arrays containing 50,599 long (60-mer) features. After hybridisation and scanning, green/red fluorescence ratios were obtained that represented the expression levels of each feature in the test samples relative to the controls.

6.3 Microarray technology: Experimental design

The importance of biological replicates within outcome groups to strengthen experimental design has already been discussed in the context of SAGE experiments. A study of the effect of replication on microarray experiments suggested that a minimum of five replicates per condition should be used to obtain reliable statistical results (Pavlidis et al. 2003). Previous experience of human synovial fibroblast transcriptome analysis in our group demonstrated that six samples per group were sufficient for statistical analysis of microarrays to identify differentially expressed genes. Thus, we set six as the minimum number of samples per group to be analysed but decided to study as many samples as available in each outcome group to increase representativeness within groups. At the same time, we chose not to include samples from the Early RA group (disease of >3 months duration at presentation) in the analysis. This helped in reduction of heterogeneity in the RA group whilst still enabling us to address the two main research questions: (i) what are the differences in transcriptional profile between very early RA and resolving disease? (ii) do RA synovial fibroblasts display the same transcriptional characteristics in early and late disease?

In contrast to the SAGE experiments, microarray experiments were performed on unstimulated samples as well as parallel samples exposed to TNFα (10ng/ml) for 24 hours. The rationale for this approach was to study resting cultured synovial fibroblasts as well as fibroblasts that had been cultured in a pro-inflammatory environment that resembled the inflammatory milieu seen in the synovium in inflammatory joint disease. Moreover, the addition of these samples to the experimental design allowed us to address a third research question: (iii) what effect does TNF stimulation have on the transcriptomic profiles of synovial fibroblast in different outcome groups?

A schematic description of the four outcome groups studied is shown in Figure 6.1. The biological questions being addressed and the clinical outcome groups to be compared during differential expression analyses are shown in Figure 6.2. A summary of the clinical characteristics of patients in each outcome group is shown in Table 6.1. The full clinical characteristics are shown in Table 2.4.

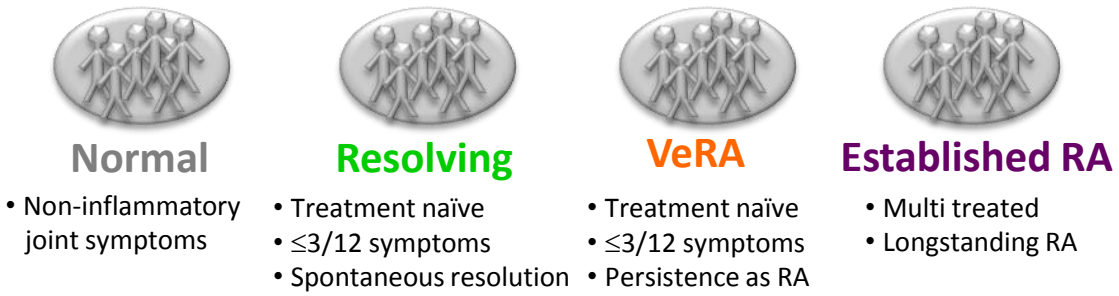

Figure 6.1 Representation of the four groups compared in microarray experiments. *Samples in Normal (n=8), Resolving (n=16), VeRA (n=14) and Established RA (n=8) groups were compared. The main differentiating attributes between groups are shown in the figure. Parallel unstimulated and TNF stimulated samples were processed.*

(i) What are the key genes involved in the resolution of early inflammatory arthritis?

(ii) What genes differentiate early from late RA?

(iii) What effect does TNF stimulation have on different outcome groups?

Unstimulated vs. TNF stimulated

Figure 6.2 Schematic representation of the proposed differential expression analyses. *To identify key genes involved in the resolution of early inflammatory arthritis, transcriptomic data from Resolving and VeRA groups will be compared. To unravel genes responsible for differences between early and late RA analyses will involve VeRA and Established RA groups. To compare responses to TNF stimulation between groups, differential expression analysis of unstimulated and TNF stimulated samples in each group will be performed.*

Table 6.1 Summary of patient characteristics.

	Normal (n=8)	**Resolving (n=16)**	**VeRA (n=14)**	**Established RA (n=8)**
Mean age (yrs)	43.6	45.6	52.5	55.6
Female gender	4 (50%)	5 (31%)	7 (50%)	5 (63%)
Joint of origin	8 Knee (100%)	12 Knee (75%) 4 Ankle (25%)	9 Knee (64%) 2 Ankle (14%) 3 MCP (22%)	8 Knee (100%)
Antibody positive	0 (0%)	0 (0%)	8 (57%)	6 (75%)
Mean DAS28ESR	-	3.8	4.8	5.9
Disease duration	N/A	5 weeks	5 weeks	20 years

Antibody status defined as either RF or CCP positivity; N/A: not available.

Sample preparation and RNA extraction for microarray experiments were performed as specified in the methods section. All samples analysed were at passage 3.

6.3.1 Sample quality control

RNA isolation was performed prior to outsourcing of samples for microarray processing. The initial RNA isolation and clean up experiment is described here.

Specific RNA quantity and quality requirements were determined by the external provider. RNA quality was determined using the absorbance method by the 260/280 and 260/230 indexes. Requirements per sample were as follows: 500ng of total RNA, 260/280 ratio >1.8 and 260/230 ratio >1.5.

In the initial experiment, RNA was isolated from four samples and its quantity and quality measured with the Nanodrop 2000 spectrophotomer (Table 6.2). Whilst the amount of RNA recovered was sufficient in all cases and all samples displayed a 260/280 ratio >1.8, two of them had unsatisfactory 260/230 ratios (below the 1.5 cut off).

Table 6.2 Measured RNA concentration, volume and 260/280 and 260/230 ratios of initial four samples. *Blue rows indicate samples that achieved the quality cut off, red ones represent samples that did not.*

Sample	Total RNA Concentration (ng/µl)	Volume (µl)	260/280 ratio	260/230 ratio
1	128.6	30	2.04	2.03
2	138.5	30	2.04	1.73
3	158.2	30	2.05	0.84
4	152.7	30	2.08	0.33

These results led us to perform an additional cleaning step after RNA isolation to improve sample quality. We used a column based cleaning kit that consisted of a unique cleaning buffer that was added to each sample together with ethanol to create optimal binding conditions and was run on a fast spin column. After cleaning, the 260/230 ratios improved to 2.22 and 2.04 (samples 3 and 4 respectively). This cleaning step was applied to all samples to ensure consistency in sample preparation. The total RNA concentration and ratios for all samples are represented in Appendix Table 9.5.

6.4 Microarray experiments: Data analysis

Following processing of samples by the external provider, microarray data were analysed using a commercial software package (Partek Genomics Suite, version 6.6) and the publicly available Genesis platform and Ensembl genome database project website.

Before describing data analyses and results, it is important to highlight the following. Agilent probes are designed to detect specific transcripts. Assuming that they function correctly,

increased signal intensity from a given probe indicates an increased level of expression of a specific transcript. Throughout this chapter I will refer to changes in expression of transcripts rather than the more correct, but awkward, description of changes in probe signal intensity.

6.4.1 Microarray data analysis with Partek Genomic Suite

Data analyses were performed using the gene expression workflow in Partek Genomic Suite. Agilent human gene expression microarray raw data files were imported into Partek Genomic Suite using the green/red ratio input parameter and applying log2 transformation to the output values. The green/red ratio was used to ensure sample data (green) were normalised to reference data (red). A log2 transformation was applied for ease of interpretation of ratio values <1. Next, attributes specifying the characteristics of the patients from whom the samples were obtained were added to each sample. These included: age, gender, clinical diagnosis (outcome group), joint of origin of the sample and antibody status. Exploratory data analysis was performed by means of principal component analysis (PCA), histogram plots and quality control metrics. Differential expression analyses were done with the analysis of variance (ANOVA) technique. A one way fixed non-nested ANOVA model was built on the entire dataset to identify differentially expressed transcripts according to different attributes. The significance of the differential expression was given by a p value. A false discovery rate (FDR) of <0.05 was set to control for multiple testing using the Benjamini Hochberg method. A fold change for the difference in gene expression was also obtained. Antibody status was found not to contribute to variance in the dataset and was thus not included in the ANOVA model.

6.5 Microarray experiments: Unstimulated samples results

6.5.1 Principal component analysis

The PCA plot of all unstimulated samples, colour coded according to clinical outcome group of origin, is shown in Figure 6.3. Although some degree of clustering was seen amongst samples in the Normal group, clustering according to outcome group was not clear cut. This indicated that outcome group was not responsible for the biggest variation in the dataset, with other attribute or attributes being responsible for this. PCA data were visualised according to age, gender, antibody positivity and joint of origin in turn, but no clear clustering could be seen in the PCA plots according to any of these attributes (Figure 6.4).

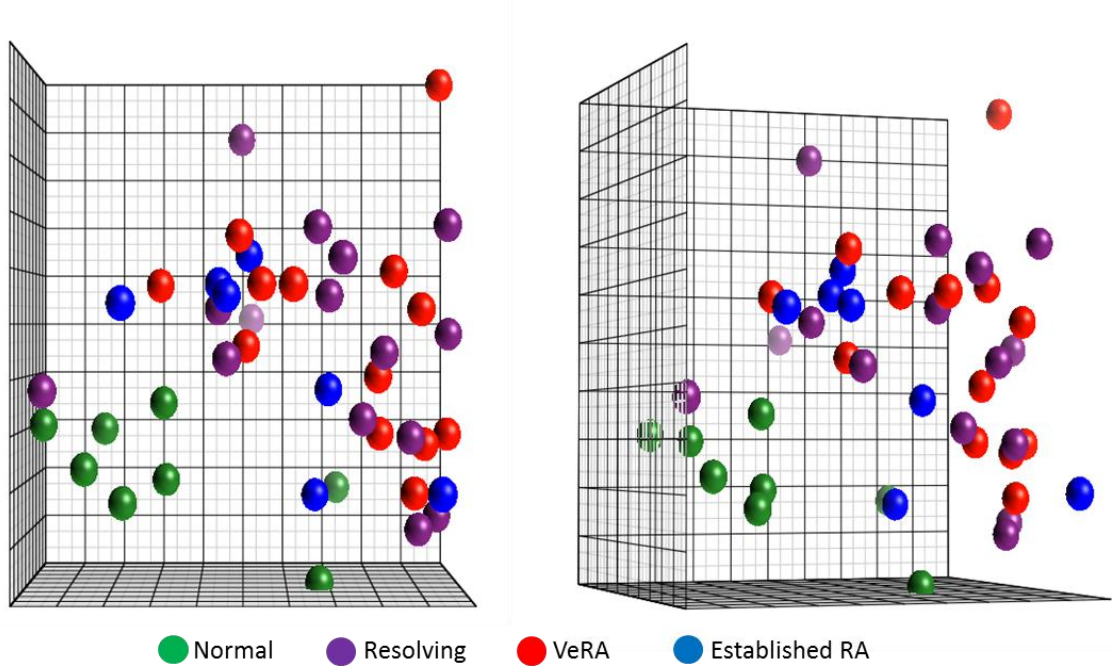

Figure 6.3 PCA plot of Normal, Resolving, VeRA and Established RA unstimulated samples (two different rotation angles of the same plot shown). *A degree of clustering was seen amongst Normal samples although clustering was not clear cut. This suggested that attribute or attributes other than clinical diagnosis contributed to the biggest variation in the dataset. Normal (n=8), Resolving (n=15), VeRA (n=13) and Established RA (n=7).*

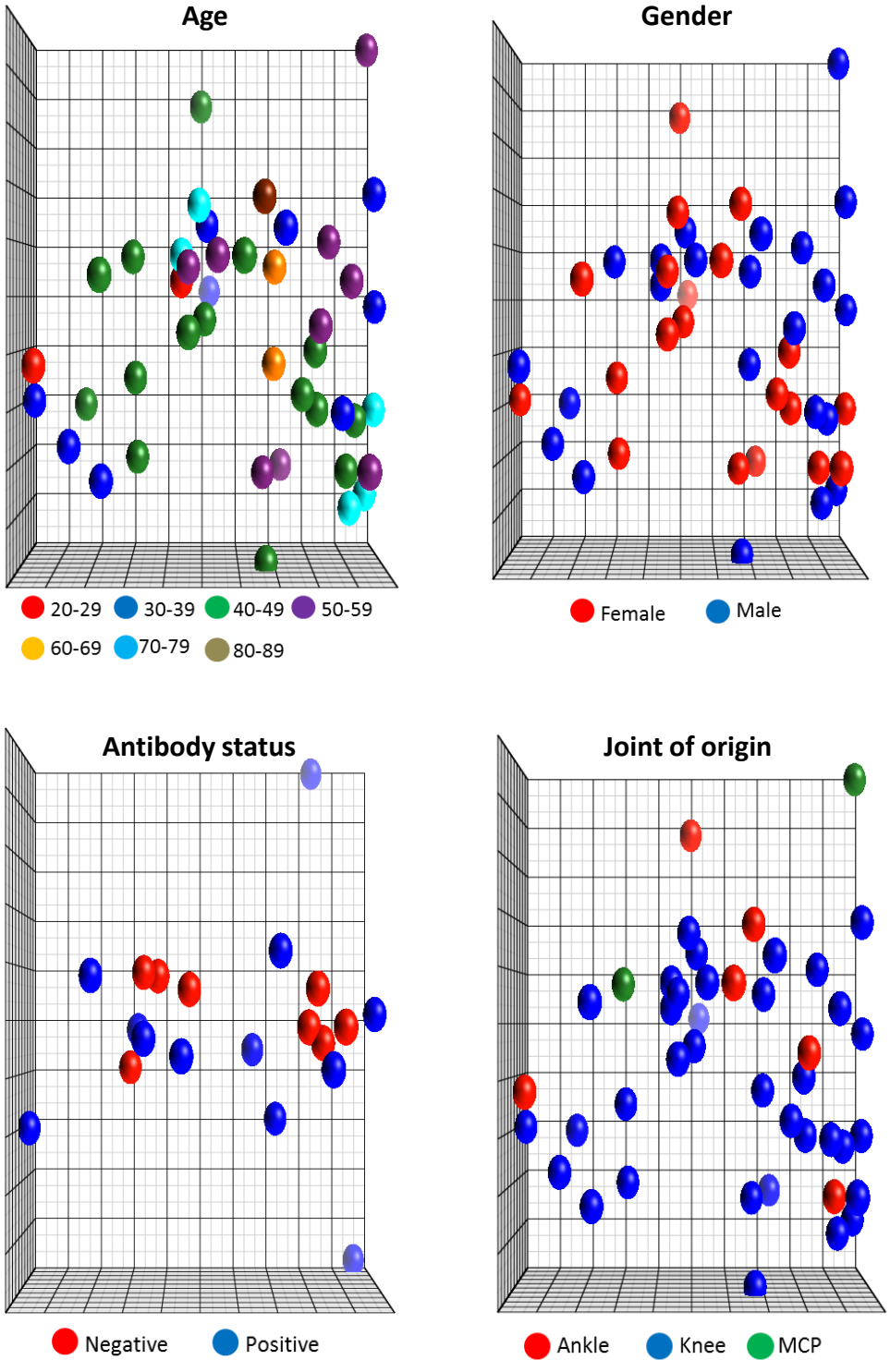

Figure 6.4 PCA plots of unstimulated samples visualised according to other attributes. *Samples represented according to Age, Gender (Female n=20, Male n=23), Antibody status (Positive defined as positive to either RF or CCP; Positive n=12, Negative n=8, only VeRA and Established RA samples depicted) and joint of origin (Ankle n=6, Knee=35, MCP=2). No clustering was seen according to any of the attributes. MCP: metacarpophalangeal joints.*

The sources of variation in the dataset were plotted in a pie chart (Figure 6.5). Clinical diagnosis (outcome group) accounted for 24% of the variation, joint of origin for 7% and gender and age for 1% each. Antibody status did not have an effect in the observed variation. 67% of the variation was unexplained suggesting that other attributes not included in the model were responsible for a significant amount of data variation. This unexplained variation includes inherent inter-individual biological variation between samples.

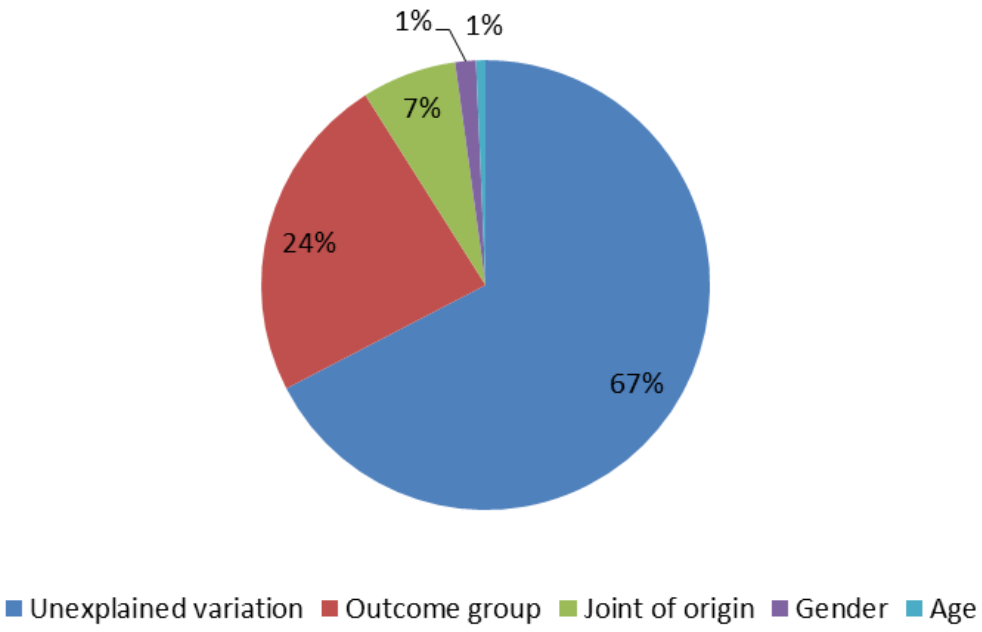

Figure 6.5 Sources of variation in the unstimulated samples data set. *Pie chart representing sources of variation. Clinical diagnosis (outcome group) accounted for 24% of the variation, joint of origin for 7% and age and gender for 1% each. 67% of the variation remained unexplained. Unexplained variation most likely represents inter-individual biological variation.*

6.5.2 Differential expression analysis

To identify differentially expressed transcripts according to different attributes, differential expression analysis was performed. The number of differentially expressed transcripts according to each of the attributes is shown in Table 6.3. By doing this analysis, in addition to the number of transcripts differentially expressed, an output file with the transcript's identifier number, fold difference in expression and p value was obtained.

Table 6.3 Differential expression analysis of unstimulated samples. *Attributes are shown in the first column with the number of differentially expressed transcripts according to varying attributes in the second column.*

Attribute	Number of differentially expressed transcripts
Gender	69
Joint	317
Age	32
All outcome groups	1096

Differential expression analysis according to gender and joint of origin is represented graphically in Figure 6.6. Clear differences in expression patterns could be seen between samples from female and male patients and between samples from different joints of origin.

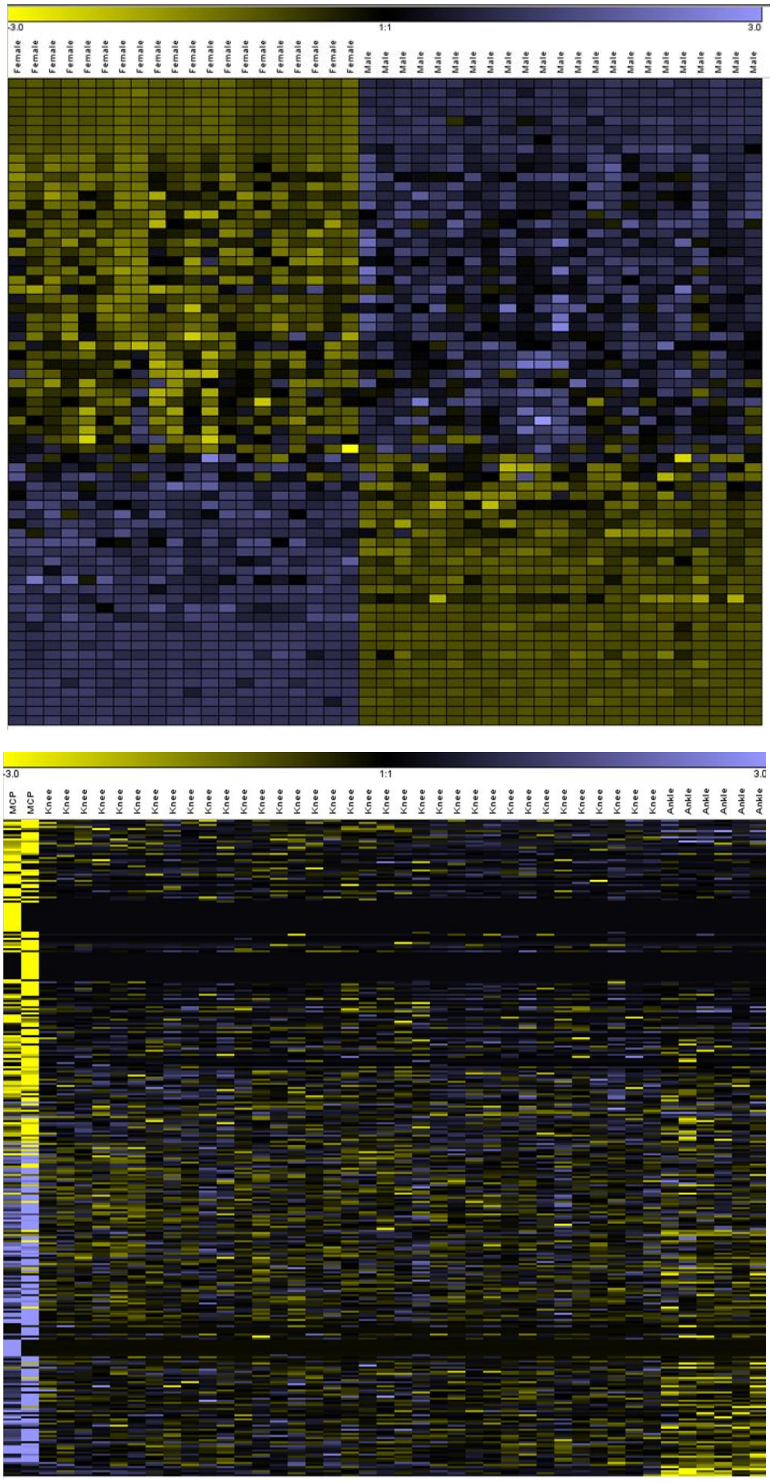

Figure 6.6 Graphical representation of differential expression analysis. *Top: heat map depicting differential expression between samples from female (n=20) and male (n=23) patients. Bottom: heat map representing differential expression between metacarpophalangeal (MCP) (n=2), knee (n=35) and ankle (n=6) joints. Three clear patterns of gene expression can be seen depending on the joint of origin. Columns represent samples, rows represent transcripts. Yellow represents underexpressed transcripts, blue overexpressed ones.*

Upon examination of the results of the differential expression analysis according to gender an interesting observation was made. Two samples originating from male patients and one from a female patient appeared to have opposite expression patterns to the remaining samples in their respective groups. Figure 6.7 shows a representative example of this phenomenon with two genes. X inactive specific transcript (XIST) is a gene involved in X chromosome inactivation which is normally up-regulated in females. Zinc finger protein Y linked (ZFY) encodes a transcriptional factor that is usually up-regulated in males. In the example shown, the pattern of gene expression is reversed in two "male" and one "female" samples. The characteristics of the patient samples were checked in the patient database and it was ascertained that these samples indeed belonged to a female and two males respectively. Thus, it was assumed that mislabelling had occurred at some stage during sample preparation. In consequence these three samples were excluded from subsequent analysis of both unstimulated and TNF stimulated data. They corresponded to one Resolving (BX072), one VeRA (BX084) and one Established RA (RA29SY) samples. In consequence the final number of samples analysed were as follows Normal (n=8), Resolving (n=15), VeRA (n=13) and Established RA (n=7).

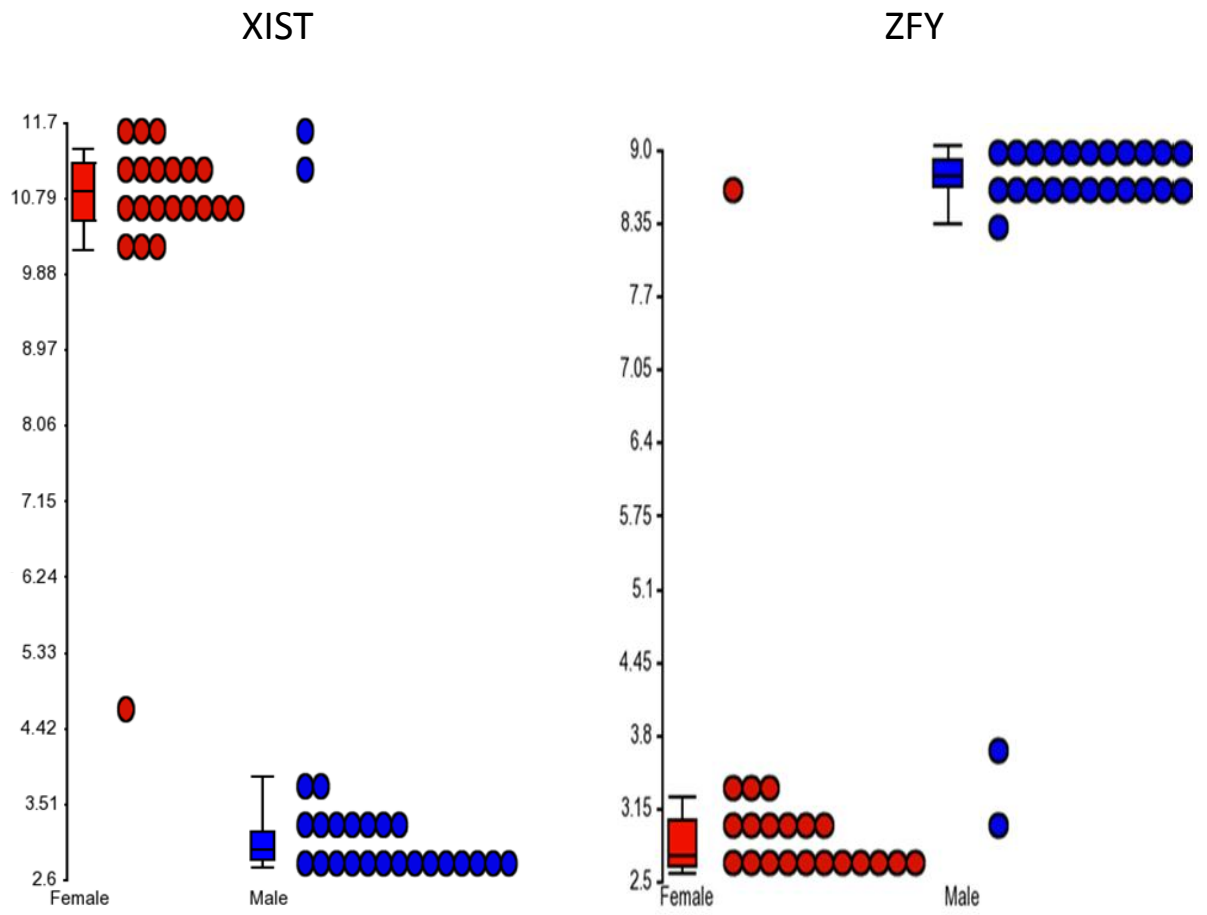

Figure 6.7 Differential expression of XIST and ZFY in female and male samples. *X inactive specific transcript (XIST) and Zinc finger protein Y linked (ZFY) were identified as differentially expressed between male and female samples. XIST expression was higher in females than males whilst the expression of ZFY was higher in males. However, one of the samples in the female group and two in the male group displayed expression patterns that were opposite to those of the remaining samples in their group. Each dot represents a sample. Red dots represent samples from female patients, blue dots samples from male patients.*

The observation of differentially expressed transcripts according to joint of origin was of particular interest. Seminal work from Chang and colleagues demonstrated that fibroblasts from different organs display characteristic gene expression patterns suggesting that they are distinct differentiated cell types (Chang et al. 2002). More intriguingly, when gene expression profiles of fibroblasts from the same organ are analysed by unsupervised hierarchical

clustering, clear differences in expression programmes are seen according to their anatomical origin. For instance, dermal fibroblasts from upper limbs cluster together and separately from those from lower limbs. When dermal fibroblasts from multiple locations in same individuals are analysed, instead of clustering together (as they belong to the same organ from the same individual) they cluster with cells from different individuals but from an equivalent anatomical location. This positional demarcation is associated with specific patterns of homeobox (HOX) gene expression (Rinn et al. 2006). The homeobox family of genes is involved in determining positional identity along the antero-posterior axis during development of invertebrate and vertebrate animals (Krumlauf 1994). In humans the HOX genes are located in clusters (denoted A to D) on four different chromosomes (HOXA chromosome 7, HOXB chromosome 17, HOXC chromosome 12, and HOX D chromosome 2) (Scott 1992).

The finding of a gene expression signature according to joint of origin was both novel and in keeping with this previous work and suggested that synovial fibroblasts also possess positional identity and that differences exist between cells from different joints. I decided to capitalise on this observation and attempt independent verification by PCR. To select key genes for verification, the list of 317 differentially expressed transcripts was ranked by p value (lowest to highest) and the top four differentially expressed genes (four members of the HOX family of genes located in the C cluster: HOXC10, HOXC6, HOXC9 and HOXC8) were selected for target validation.

The microarray expression data for these genes are plotted in Figure 6.8. Higher expression levels of the four target genes were seen in samples originating from ankle and knee joints compared to metacarpophalangeal (MCP) joints.

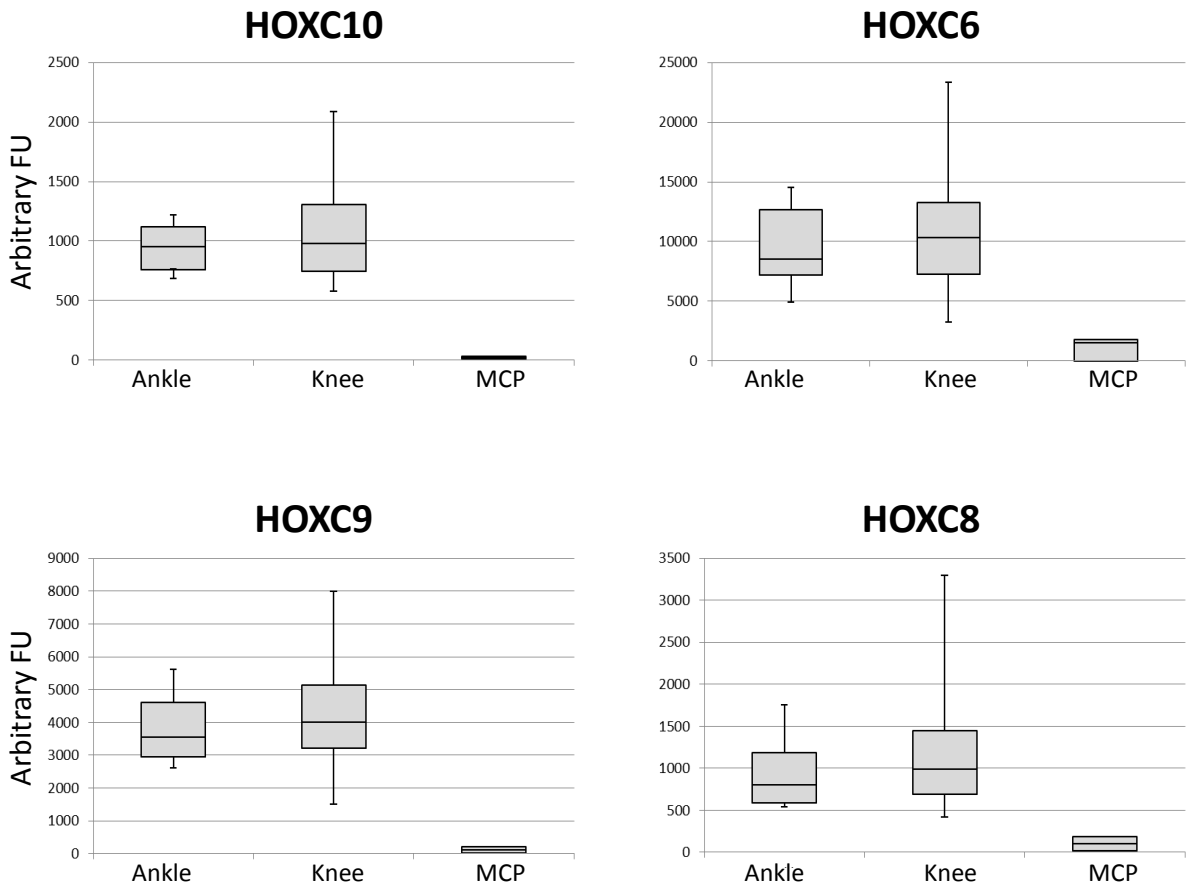

Figure 6.8 Expression levels of selected target HOXC genes assessed by microarray. *Raw microarray data representing expression levels of HOXC10, HOXC6, HOXC9 and HOXC8 in ankle (n=6), knee (n=35) and MCP (n=2) joints. Higher expression levels of all genes were seen in samples originating from ankle and knee joints compared to MCP joints. Expression levels expressed as arbitrary fluorescence units (FU).*

Encouragingly similar results were obtained on PCR analysis. Expression levels of all four genes were higher in samples originating from ankle and knee joints compared to MCP joints

(Figure 6.9). Although these differences did not achieve statistical significance, the results gave an indication that independent validation may be achieved if sample numbers were increased.

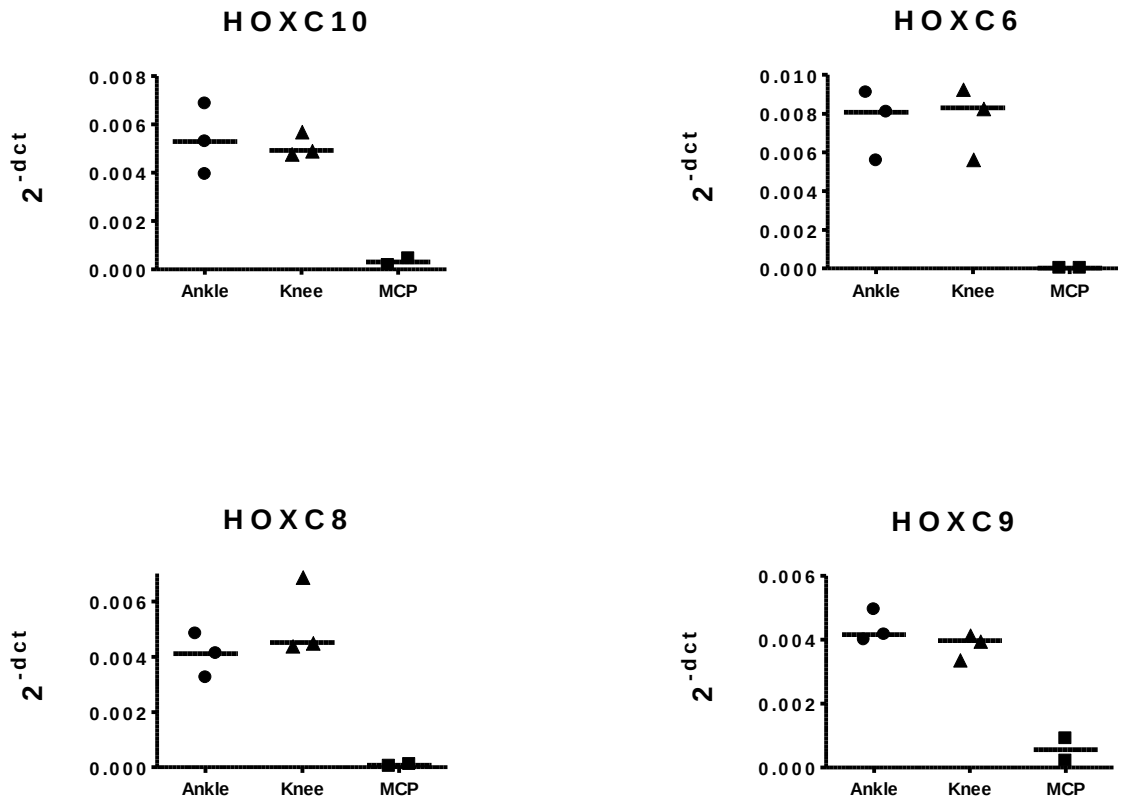

Figure 6.9 Expression levels of selected target HOXC genes assessed by PCR. *Expression levels of HOXC10, HOXC6, HOXC9 and HOXC8 were assessed in ankle (n=3), knee (n=3) and MCP (n=2) joint samples by PCR. Higher expression levels of all genes were seen in samples originating form ankle and knee joints. Expression levels expressed with the* 2^{-dct} *method relative to GAPDH.*

6.5.3 Differential expression analysis: Resolving versus VeRA comparison

We hypothesised that synovial fibroblasts may be involved in failed resolution of inflammation in early inflammatory arthritis and would retain an imprint of this involvement after *in vitro* culture. To test this hypothesis I compared the transcriptomic profile of Resolving and VeRA synovial fibroblasts. No transcripts were identified as differentially expressed between these groups. The lack of differences between both outcome groups is further emphasised when these groups are visualised using PCA (Figure 6.10).

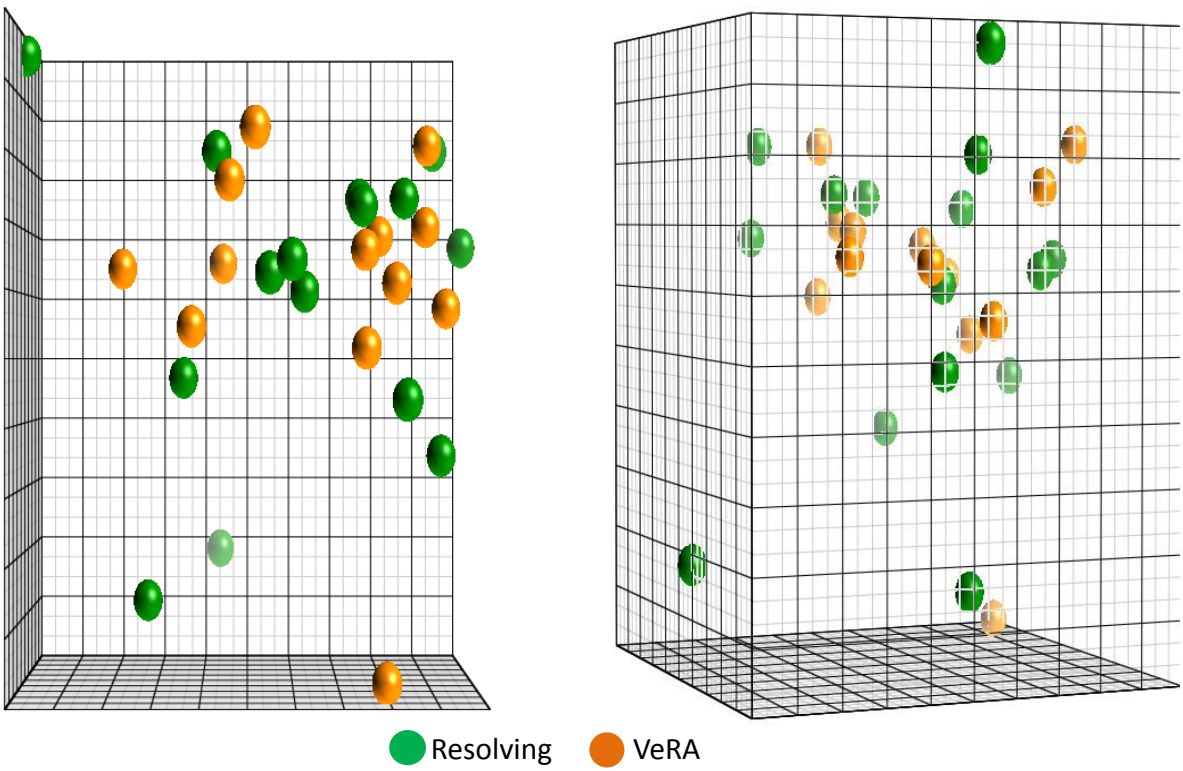

Figure 6.10 PCA plot of Resolving and VeRA unstimulated samples (two different rotation angles of the same plot shown). *No clustering of samples within the same outcome group was seen. Resolving (n=15), VeRA (n=13).*

6.5.4 Differential expression analysis: Early versus Late RA comparison

We also hypothesised that differences exist in gene expression patterns of synovial fibroblasts in very early (VeRA) and Established RA that may be responsible for or a consequence of the progression to disease chronicity. Differentially expressed transcripts between these groups were demonstrated in this analysis.

The number of differentially expressed transcripts varied depending on the fold difference cut off applied: from 73 transcripts at a fold difference of 1.5 to 40 transcripts at a fold difference of two.

6.5.5 Data filtering and identification of protein coding genes

Independent validation of results by PCR is an important component in the pathway leading to the verification of results in microarray experiments. To select key genes for PCR validation, data were filtered according to two commonly used approaches. First, transcripts were selected on the basis of fold difference and only those transcripts that showed a fold difference in expression of ±2 between both outcome groups were selected for validation. Second, transcripts not denoting protein coding genes were filtered out. The rationale for this approach was to select targets for which commercially available reagents existed so that we might be able to validate findings at the protein level in tissue samples. To ascertain whether probes corresponded to protein or non-protein coding genes, the Ensembl genome database

project website (http://www.ensembl.org/index.html) was used to map probes to the reference genome. An example of a non-protein coding probe is shown in Figure 6.11.

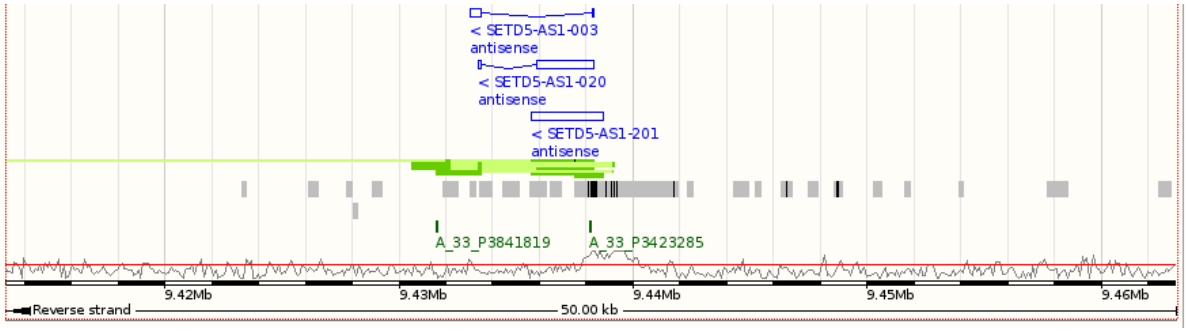

Figure 6.11 Mapping of a probe to the reference genome identifies a non-protein coding gene. *Example of non-protein coding gene identified through genome mapping. Differential expression analysis between VeRA and Established RA identified probe A_33_P3423285 (green square box at the bottom of the image). This probe was mapped to three transcript variants of the same gene (SETD5-antisense RNA 1). All these variants were long non coding RNAs and did not code for protein products. Subsequently, SETD5-anstisense RNA 1 was not selected for target validation.*

Using these filtering and mapping strategies, 20 protein coding genes were identified. 11 of these were overexpressed and 9 underexpressed in VeRA compared to Established RA. The raw microarray expression data for these genes are shown in Figure 6.12. The full list of differentially expressed transcripts (including non-protein coding ones) at a fold difference of 2 is shown in Appendix Table 9.6. The raw microarray expression data for these genes in all outcome groups are shown in Appendix Figure 9.3.

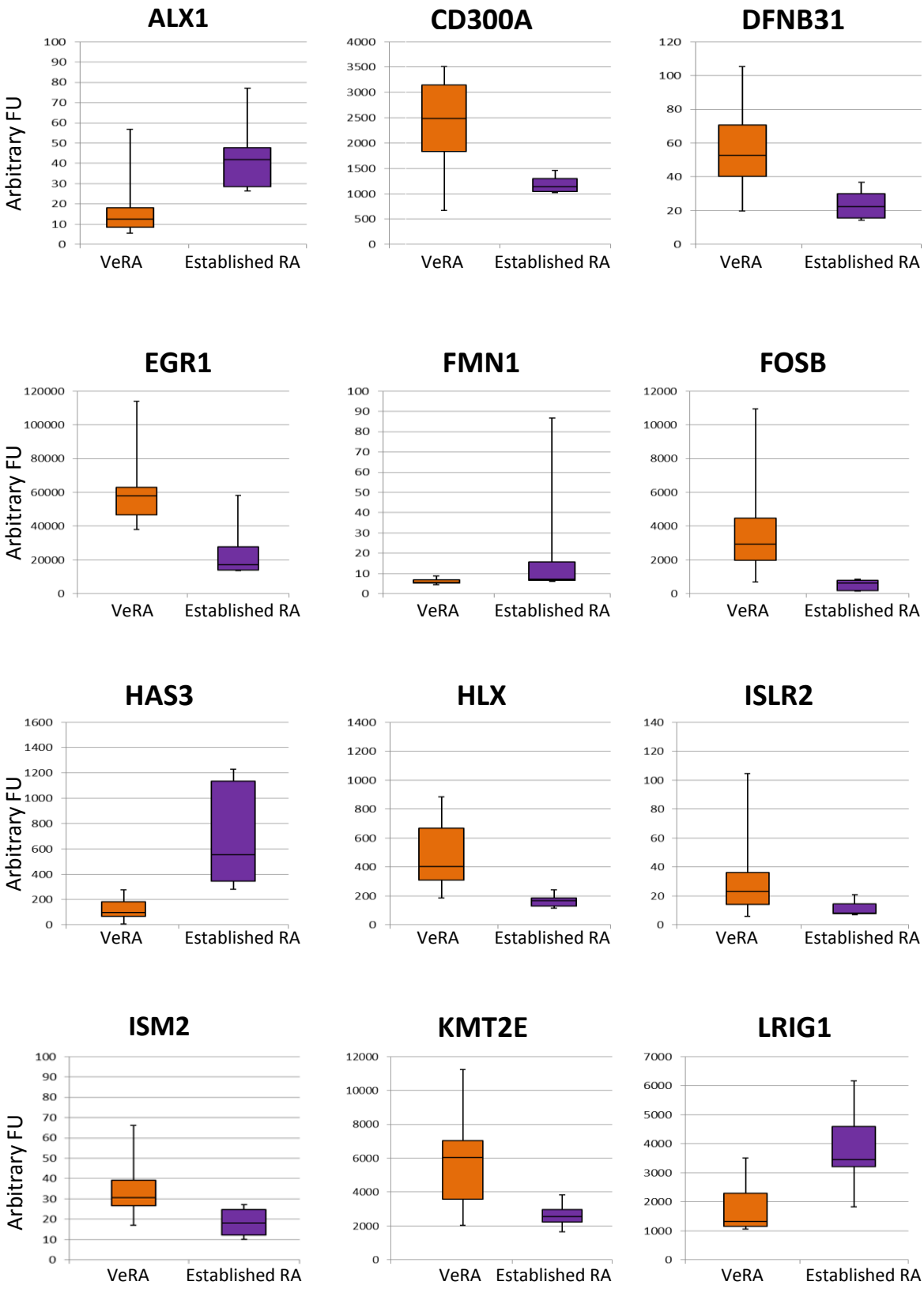
ALX1
CD300A
DFNB31
EGR1
FMN1
FOSB
HAS3
HLX
ISLR2
ISM2
KMT2E
LRIG1
Arbitrary FU
VeRA
Established RA

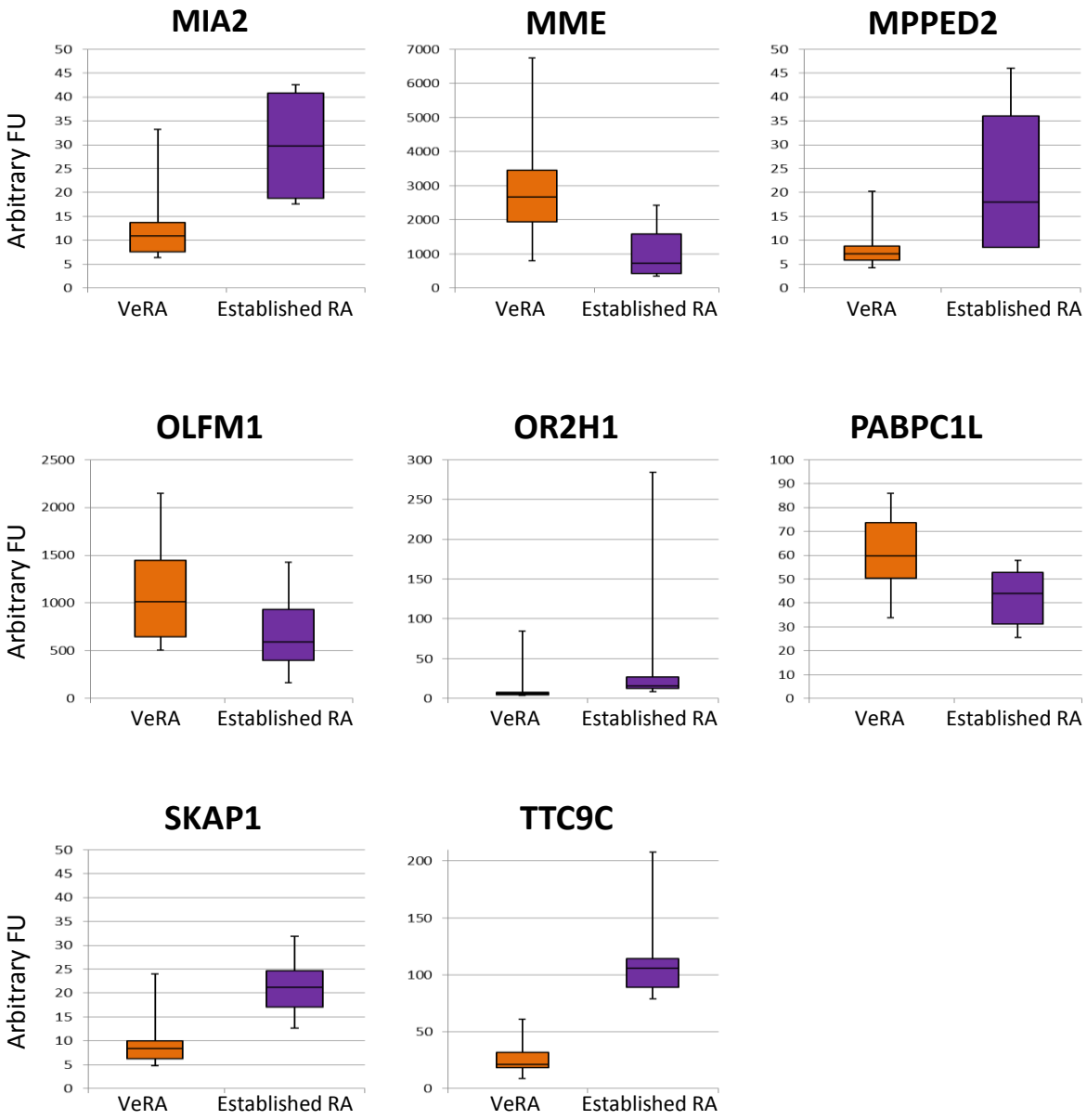

Figure 6.12 Expression levels of selected target genes assessed by microarray in unstimulated samples. *Raw microarray data representing expression levels of 20 target genes in unstimulated VeRA (n=13) and Established RA (n=7) samples are represented. Expression levels expressed as arbitrary fluorescence units (FU).*

Primer pairs for each gene were designed using Primer 3 and quality control tested using the melting curve method as specified in the materials and methods section. The expression levels of these 20 genes were tested in eight samples in each outcome group by PCR and are shown in Figure 6.13.

.

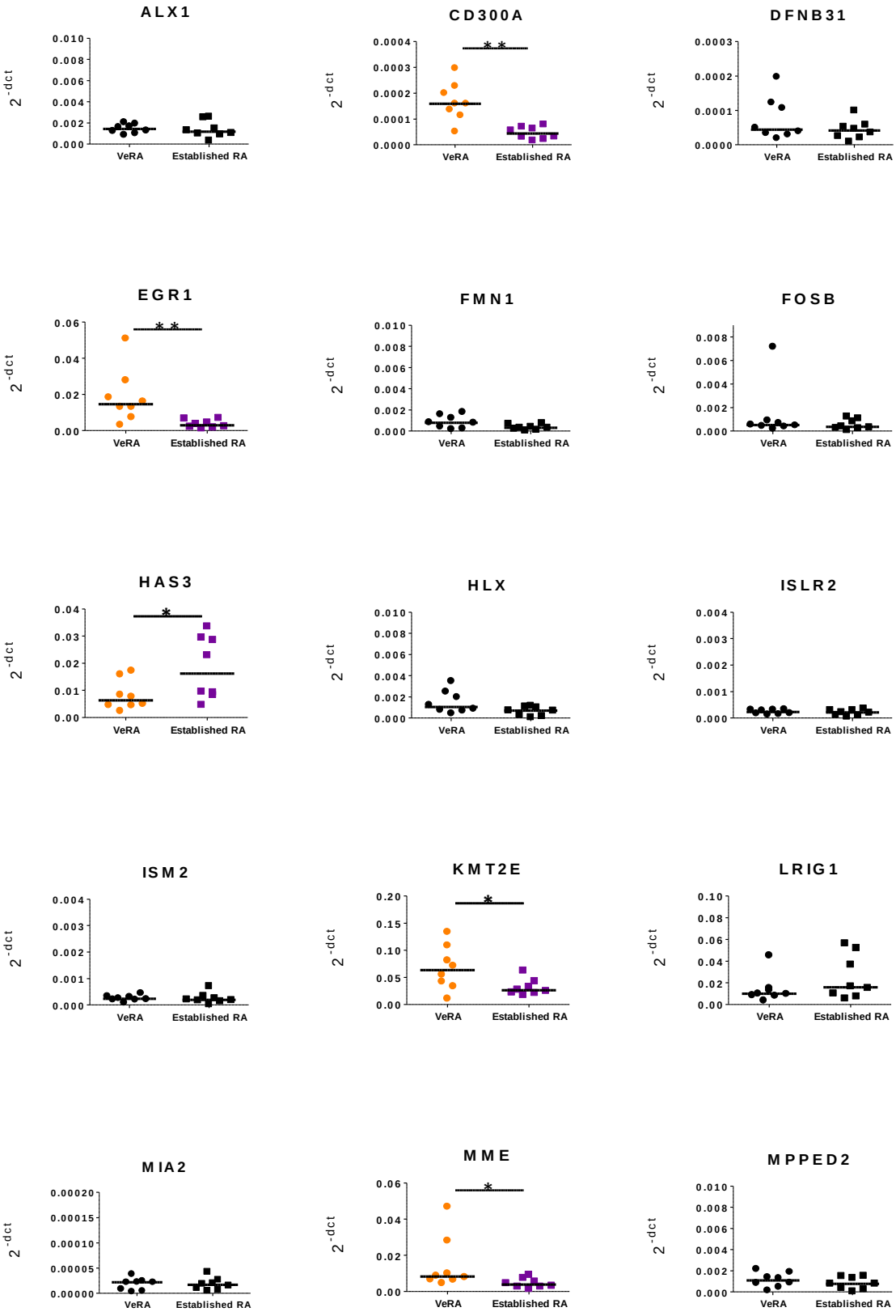
ALX1
CD300A
DFNB31
EGR1
FMN1
FOSB
HAS3
HLX
ISLR2
ISM2
KMT2E
LRIG1
MIA2
MME
MPPED2
2-dct
VeRA
Established RA
*
**

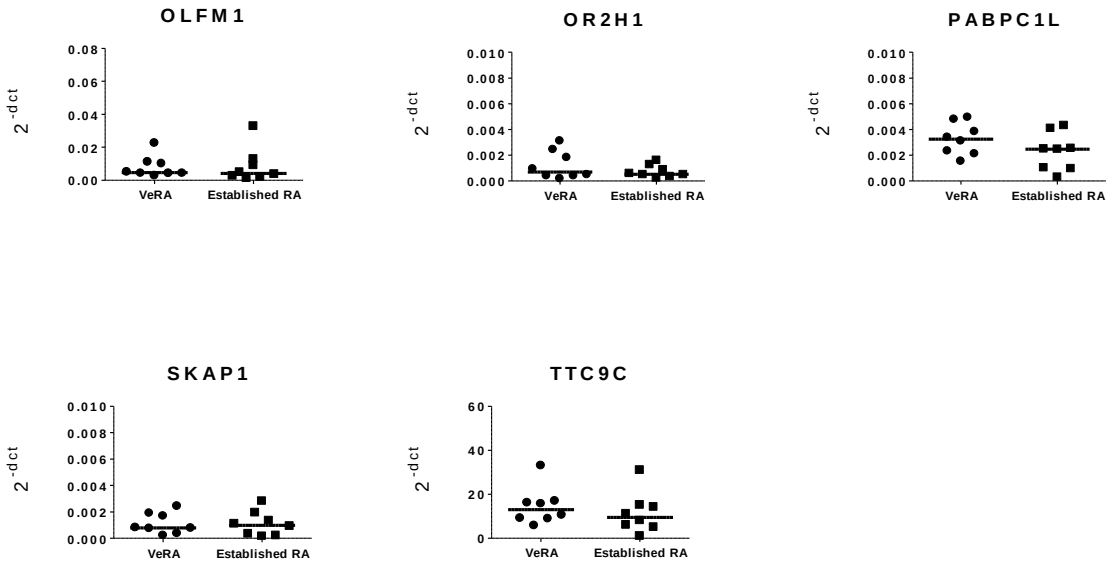

Figure 6.13 Expression levels of 20 selected target genes assessed by PCR. *Differences in gene expression levels were assessed in unstimulated VeRA (n=8) and Established RA (n=8) samples. Expression levels of CD300A, EGR1, KMT2E and MME were significantly higher in VeRA than in Established RA samples. Expression levels of HAS3 were significantly higher in Established RA than VeRA samples. Expression levels represented with the 2^{-dct} method relative to GAPDH. Data shown in scattered dot plots where horizontal lines represent medians. Differences in expression between groups assessed with Mann-Whitney test. *p<0.05, **<0.01.*

Five genes were independently verified by PCR as differentially expressed between VeRA and Established RA samples. Four of them were overexpressed in VeRA compared to Established RA samples. These were: early growth response protein 1 (EGR1), membrane metalloendopeptidase (MME), cluster of differentiation 300A (CD300A) and lysine specific methyltransferase 2E (KMT2E). In contrast, the expression of hyaluronan synthase 3 (HAS3) was lower in VeRA compared to Established RA samples. Table 6.4 shows the tested genes with their chromosomal location, fold difference in expression levels between VeRA and Established RA lines, the statistical significance of the difference (expressed as p value) as well as the fold difference and p value of the difference of those genes validated by PCR.

Table 6.4 Chromosomal location, fold change and p value of 20 selected differentially expressed genes between unstimulated VeRA and Established RA.

Name	Chromosomal location	Fold difference VeRA vs. Est. RA	p value	Validates in RT PCR (fold difference, p value)
CD300A	17: 72,477,870-72,477,929	2.582	3.955E-05	Yes (3.664, 0.0039)
EGR1	5: 137,804,891-137,804,950	2.875	2.579E-05	Yes (5.271, 0.0019)
HAS3	16: 69,151,369-69,151,428	-4.179	6.410E-05	Yes (-2.223, 0.0379)
KMT2E	7: 104,654,395-104,654,454	9.405	3.175E-05	Yes (2.155, 0.0499)
MME	3: 154,898,216-154,898,275	4.004	1.403E-05	Yes (3.289, 0.0148)
ALX1	12: 85,677,449-85,677,508	-3.132	1.614E-06	No (1.047, 0.7209)
DFNB31	9: 117,240,601-117,240,660	2.622	3.888E-05	No (1.721, 0.4412)
FMN1	15: 33,442,032-33,442,091	-2.232	2.722E-05	No (2.492, 0.0621)
FOSB	19: 45,978,205-45,978,264	4.479	3.152E-05	No (2.432, 0.5054)
HLX	1: 221,055,600-221,055,659	3.001	1.823E-06	No (2.294, 0.1049)
ISLR2	15: 74,428,824-74,428,883	4.578	5.649E-06	No (1.145, 0.5737)
ISM2	14: 77,941,303-77,941,362	2.347	6.897E-05	No (1.010, 0.5054)
LRIG1	3: 66,429,597-66,429,656	-2.507	6.478E-05	No (-1.767, 0.2345)
MIA2	14: 39,716,981-39,717,040	-2.132	1.558E-05	No (1.001, 0.9591)
MPPED2	11: 30,601,870-30,601,929	-2.23	1.013E-05	No (1.382, 0.3821)
OLFM1	9: 137,987,788-137,987,847	2.161	2.936E-05	No (1.071, 0.5054)
OR2H1	6: 29,431,909-29,431,968	-2.716	3.261E-06	No (1.690, 0.6454)
PABPC1L	20: 43,550,312-43,550,371	2.437	1.309E-06	No (1.436, 0.2786)
SKAP1	17: 46,210,830-46,210,889	-2.179	2.163E-06	No (-1.010, 0.9591)
TTC9C	11: 62,503,254-62,503,313	-3.671	3.897E-05	No (0.2786, 1.274)

6.6 Microarray experiments: TNF stimulated samples results

The same analyses were applied to TNF stimulated samples. As the rationale for these analyses has already been described, only the results are discussed below.

6.6.1 Principal component analysis

Samples did not cluster according to outcome group when PCA was performed (Figure 6.14) suggesting that unidentified attributes other than outcome group account for the greatest variation in this data set. Data were also visualised using PCA plots according to age, gender, antibody positivity and joint of origin in turn but no clustering was observed in the PCA plots according to any of these attributes (Figure 6.15).

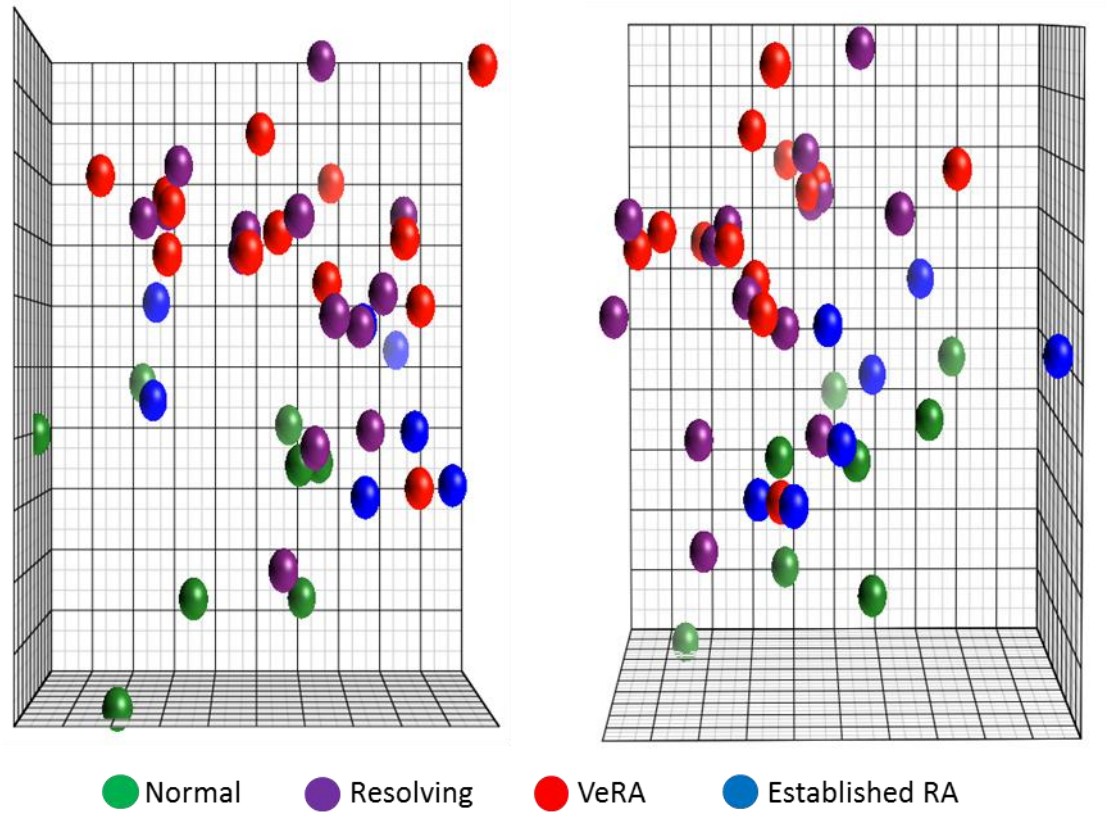

Figure 6.14 PCA plot of Normal, Resolving, VeRA and Established RA TNF stimulated samples (two different rotation angles of the same plot shown). *No clear clustering of samples according to outcome group was seen along the two principal components. This suggested that attributes other than clinical diagnosis contributed to the biggest variation in the dataset. Normal (n=8), Resolving (n=15), VeRA (n=13) and Established RA (n=7).*

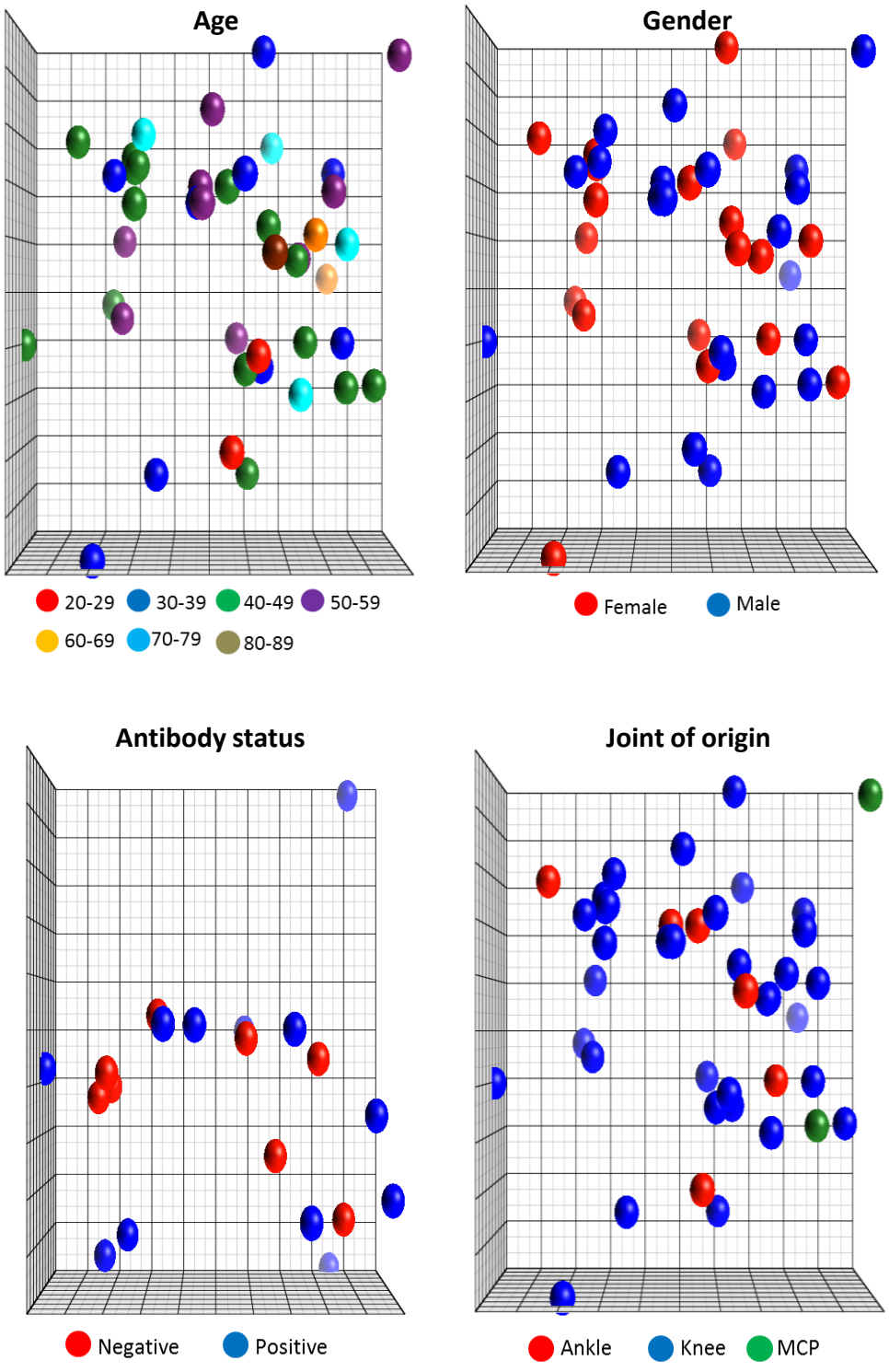

Figure 6.15 PCA plots of TNF stimulated samples visualised according to other attributes. *Samples represented according to Age, Gender (Female n=20, Male n=23), Antibody status (Positive defined as positive to either RF or CCP; Positive n=12, Negative n=8, only VeRA and Established RA samples depicted) and joint of origin (Ankle n=6, Knee=35, MCP=2). No clustering was seen according to any of the attributes. MCP: metacarpophalangeal joints.*

The sources of variation in the dataset were plotted in a pie chart (Figure 6.16). Clinical diagnosis (outcome group) accounted for 26% of the variation, joint of origin for 7% and gender and age for 1% each. 65% of the variation remained unexplained suggesting that other attributes not included in the model accounted for data variation (including inter-individual biological variation between samples). Antibody status did not contribute to variation.

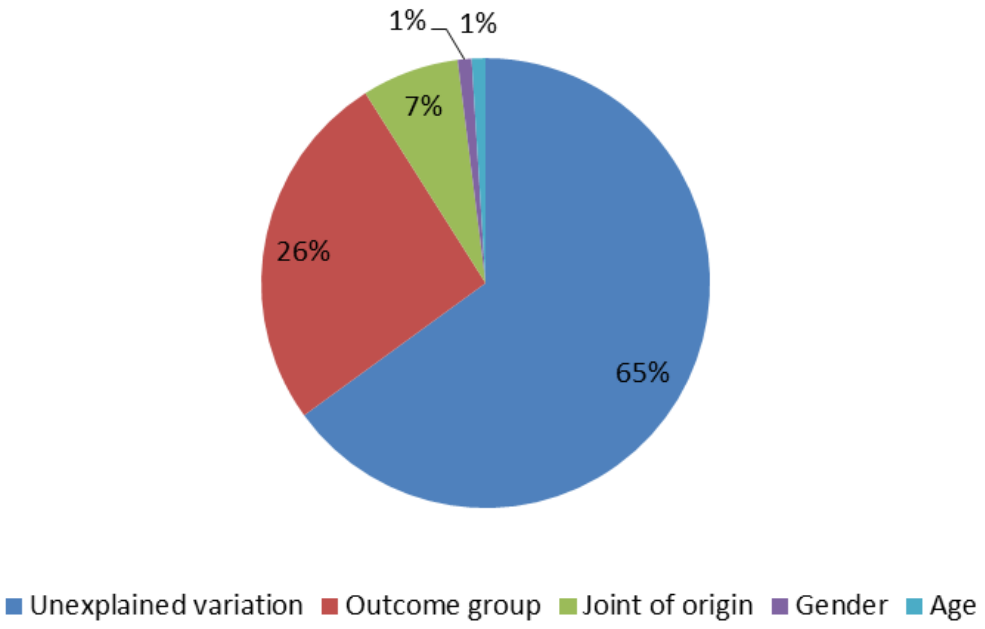

Figure 6.16 Sources of variation in TNF stimulated samples. *Pie chart representing sources of variation. Clinical diagnosis (outcome group) accounted for 26% of the variation, joint of origin for 7% and age and gender for 1% each. 65% of the variation remained unexplained.*

6.6.2 Differential expression analysis

The results of differential expression analysis are shown in Table 6.5.

Table 6.5 Differential expression analysis of TNF stimulated samples. *Attributes are shown in the first column and the number of differentially expressed transcripts according to varying attributes in the second column.*

Attribute	Number of differentially expressed transcripts
Gender	67
Joint	249
Age	16
All outcome groups	1336

To focus analysis on answering the two main questions of interest, two group differential expression analyses were performed.

6.6.3 Differential expression analysis: Resolving versus VeRA comparison (TNF stimulated samples)

To test the hypothesis that synovial fibroblasts may be involved in failed resolution of early inflammatory arthritis, we compared the transcriptomic profile of synovial fibroblasts in the Resolving and VeRA groups. No differentially expressed transcripts were identified. The lack of differences between both outcome groups was further emphasised when these groups were visualised using PCA (Figure 6.17). This was in keeping with results obtained from the analyses of unstimulated samples.

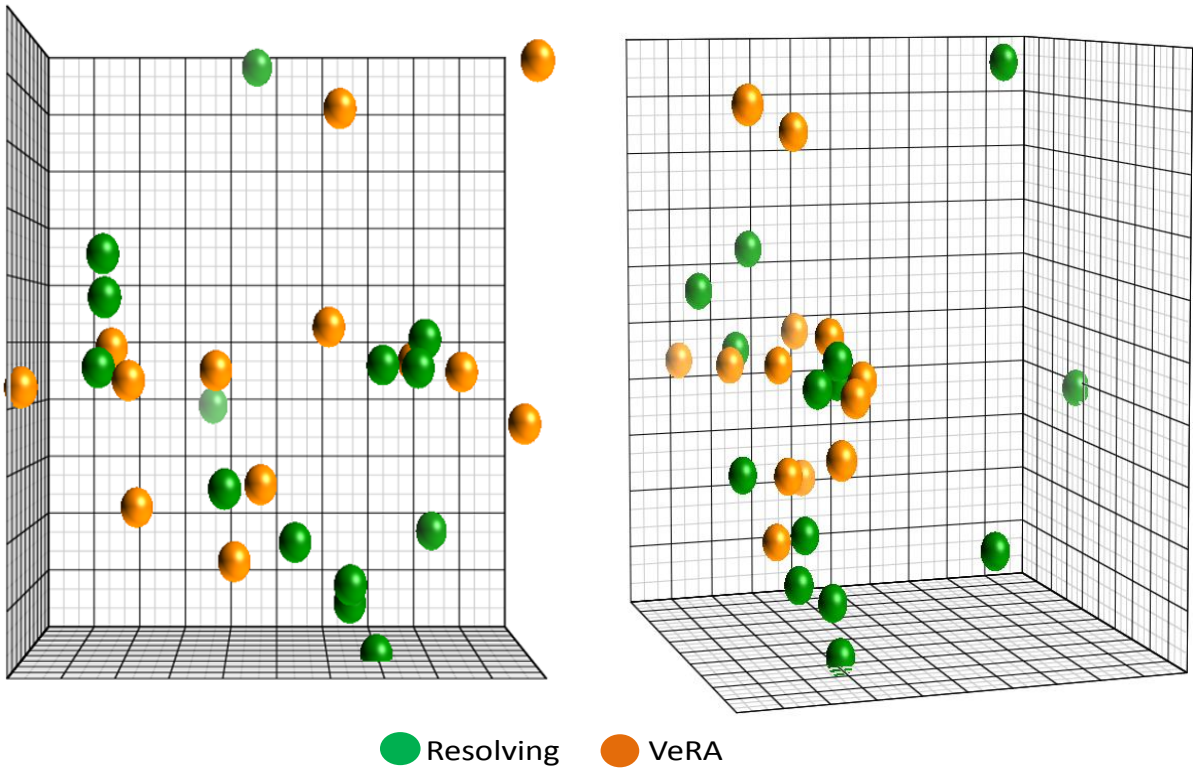

Figure 6.17 PCA plot of Resolving and VeRA TNF stimulated samples (two different rotation angles of the same plot shown). *No clustering of samples within the same outcome group was seen. Resolving (n=15), VeRA (n=13).*

6.6.4 Differential expression analysis: Early versus Late RA comparison (TNF stimulated samples)

Next, the comparison between both RA groups was performed to ascertain key differentially expressed genes between early and late disease. This comparison yielded 184 transcripts when a fold difference of 1.5 was used as a cut off and 79 transcripts at a fold difference of 2. A heat map representing the 79 differentially expressed transcripts at a fold difference of 2 is shown in Figure 6.18.

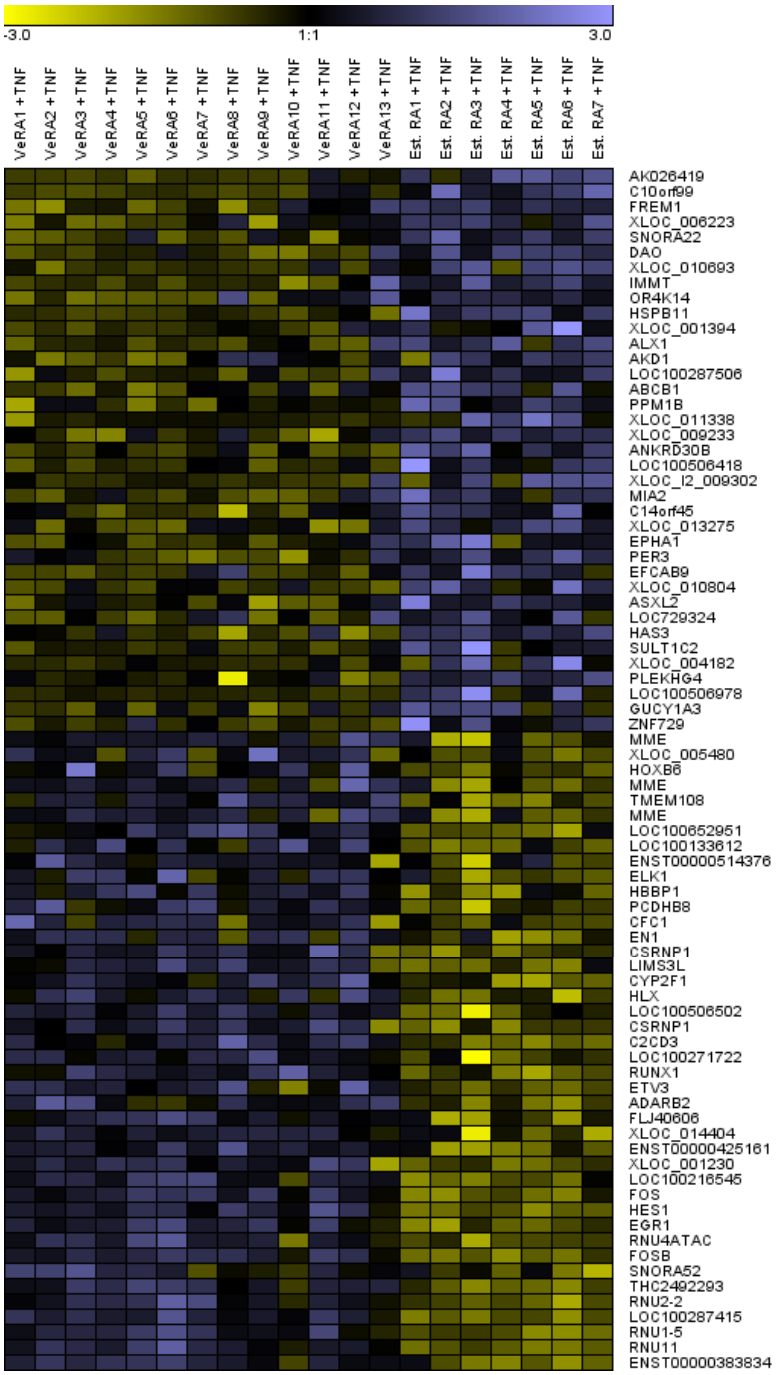

Figure 6.18 Graphical representation of differentially expressed transcripts at a fold difference of 2. *Heat map depicting differential expression between TNF stimulated samples from VeRA (n=13) and Established RA (n=7) patients. At a fold difference of 2, 79 transcripts are differentially expressed between the groups. This can be seen as two clearly differing patterns between outcome groups. Columns represent samples, rows represent transcripts.*

6.6.5 Data filtering and identification of protein coding genes

Data filtering and selection of protein coding genes were done as specified for the unstimulated samples. An additional filtering strategy was applied to target selection based on what was learnt from previous PCR validation of unstimulated samples. I observed that none of the genes that had expression values below 100 in the raw microarray data were validated by PCR. As one of the known limitations of microarrays is that they are unable to accurately measure weakly expressed genes (Tarca et al. 2006), the apparent difference in expression might have represented background expression. Hence I did not include weakly expressed genes (with intensity values below 100) in the target selection process. Data filtering yielded 14 protein coding genes with a fold difference in expression between groups of 2 and expression levels above 100 fluorescence units. The microarray expression data for these 14 genes are shown in Figure 6.19. Five of these genes (MME, HAS3, EGR1, FOSB and HLX) were in common with those from unstimulated data analysis. The full list of differentially expressed transcripts (including non-protein coding ones) at a fold difference of 2 is shown in Appendix Table 9.7. The raw microarray expression data for these genes in all outcome groups are shown in Appendix Figure 9.4.

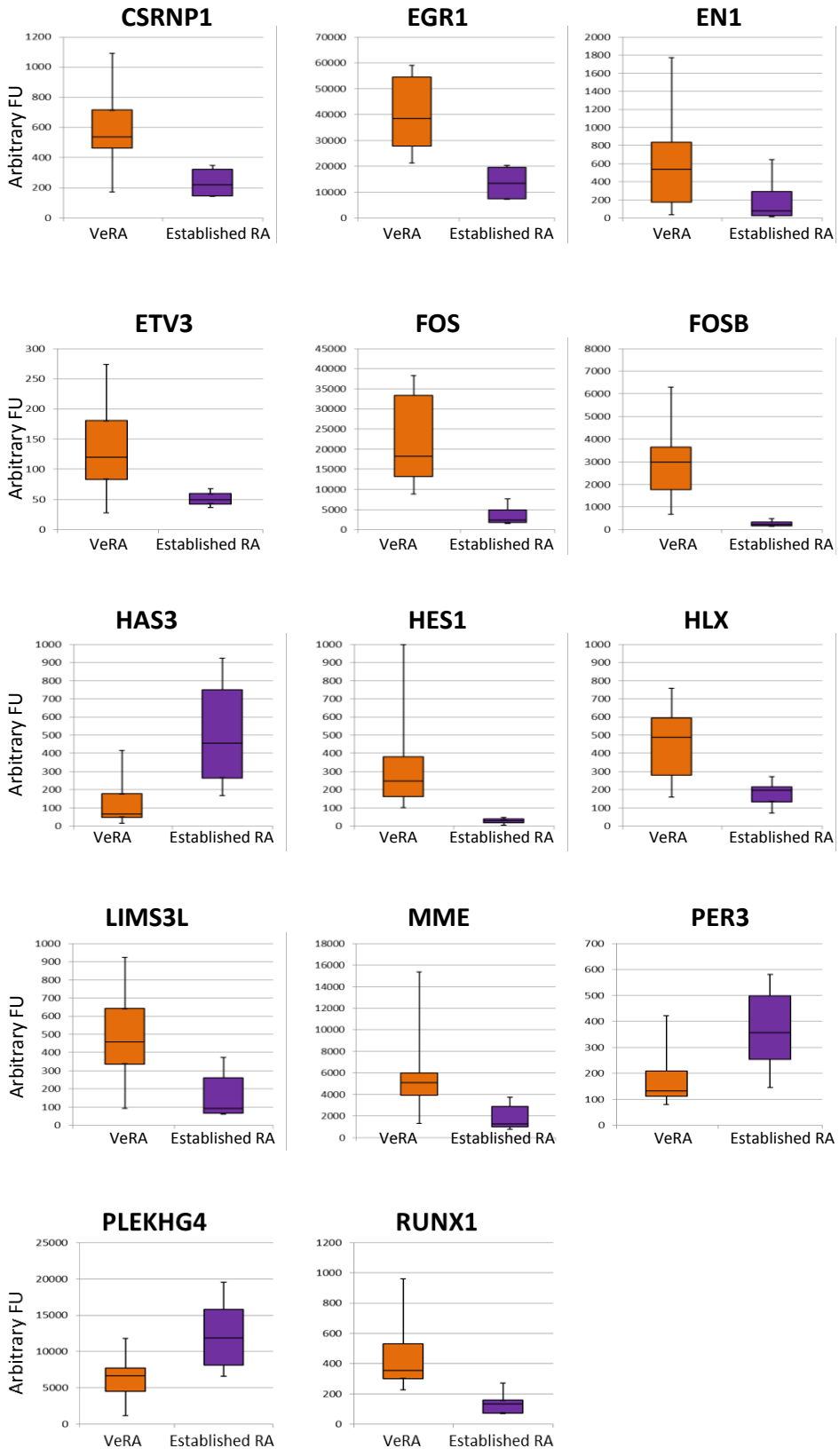

Figure 6.19 Expression levels of selected target genes assessed by microarray in TNF stimulated samples. *Raw microarray data representing expression levels of 14 target genes in TNF stimulated VeRA (n=13) and Established RA (n=7) samples are represented. Expression levels expressed as arbitrary fluorescence units (FU).*

PCR primers were designed and quality control tested as described. PCR was performed using eight samples in each outcome group and results are shown in Figure 6.20. Six out of the 14 genes were independently validated by PCR. Expression levels of all these genes were higher in VeRA than in Established RA samples. The validated genes included early growth response protein 1 (EGR1), c-FOS (FOS), homeobox protein engrailed 1 (EN1), hairy and enhancer of split 1(HES1), LIM and senescent cell antigen like domain 3-like (LIMS3L) and cysteine serine rich nuclear protein 1 (CSRNP1).

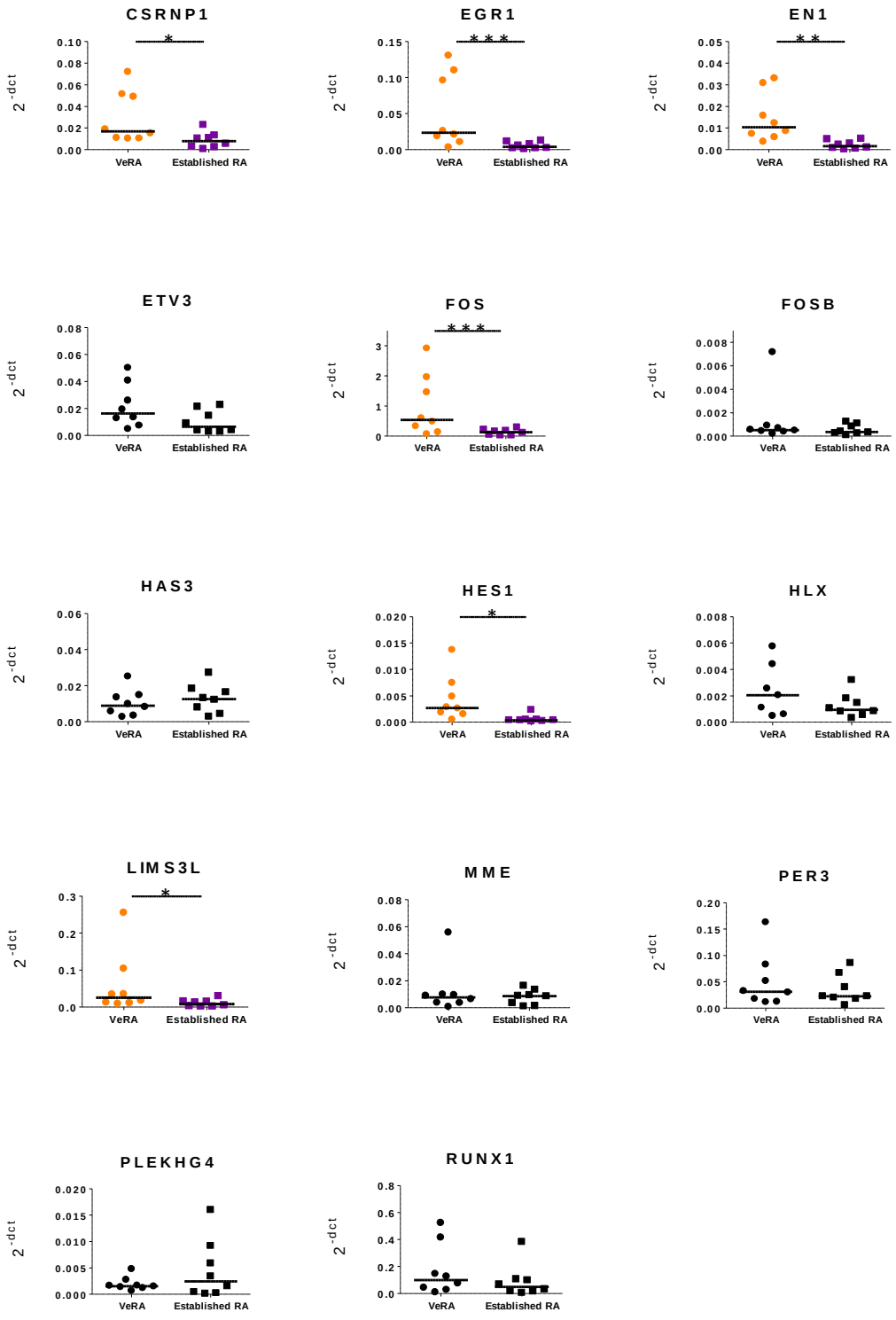

Figure 6.20 Expression levels of 14 selected genes assessed by PCR. *Differences in gene expression levels were assessed in TNF stimulated VeRA (n=8) and Established RA (n=8) samples. Expression levels of CSRNP1, EGR1, EN1, FOS, HES1 and LIMS3L were significantly higher in VeRA than in Established RA samples. Expression levels expressed with the* 2^{-dct} *method relative to GAPDH. Data shown in scattered dot plots where horizontal lines represent medians. Differences in expression between groups assessed with Mann-Whitney test. *p<0.05, **<0.01, ***<0.001.*

6.7 Microarray analysis: Effect of TNF stimulation on gene expression signatures

To assess the effect of TNF stimulation on gene expression, differential expression analysis of unstimulated and TNF stimulated samples within each outcome group were performed. Clear separation between unstimulated and TNF stimulated samples in each outcome group was demonstrated using PCA (Figure 6.21).

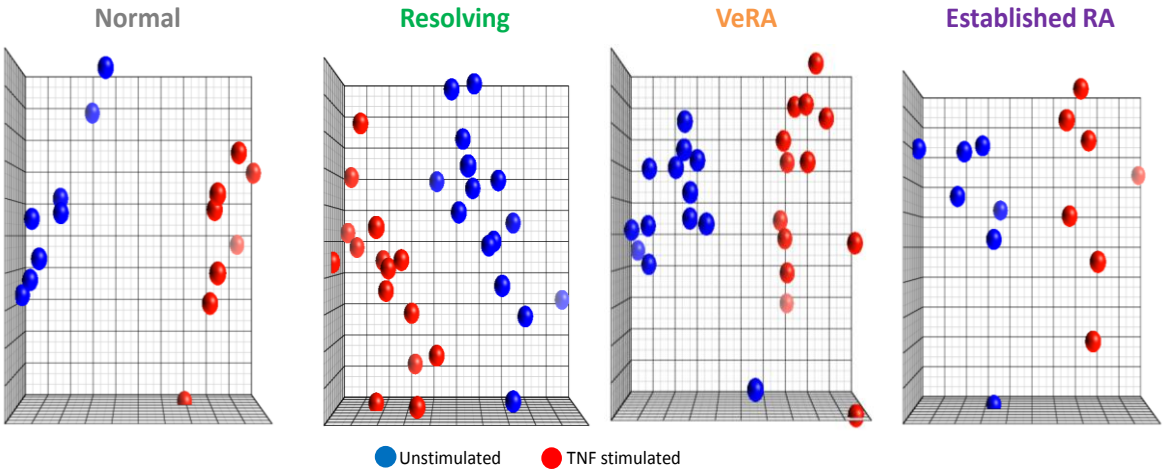

Figure 6.21 PCA plots visualised according to TNF status. *Clear separation of unstimulated and TNF stimulated samples within each group was seen. Normal (n=16), Resolving (n=30), VeRA (n=26) and Established RA (n=14).*

Differential expression analysis allowed identification of differentially expressed transcripts according to defined attributes. A summary of the results of these analyses is shown in Table 6.6.

Table 6.6 Differential expression analysis of unstimulated versus TNF stimulated samples in each outcome group. *Attributes are shown in the first column and the number of differentially expressed transcripts according to varying attributes are shown in subsequent columns.*

Attribute	Number of differentially expressed transcripts			
	Normal	Resolving	VeRA	Established RA
Gender	57	554	271	109
Age	20	2412	1879	1985
TNF status	2767	1910	1764	1308
Joint of origin	-	221	762	-

Next, pathway analysis was performed using the DAVID functional annotation tool as described. Transcripts where expression had changed in response to TNF stimulation in each group were entered in the functional annotation tool. Pathways identified as involved in TNF response in each outcome group are shown in Table 6.7. Many of the pathways were in common between the four outcome groups (i.e. signalling through IL1R and HIV-I-Nef, cells and molecules involved in acute inflammatory response), or were common to three or two of the groups, whilst some were unique to certain groups.

Table 6.7 Pathway analysis of differentially expressed transcripts between unstimulated and TNF stimulated samples in each group.

Pathway	Normal	Resolving	VeRA	Established RA
Erythrocyte differentiation	✓	✓	✓	✓
HIV-I-Nef	✓	✓	✓	✓
Signal transduction through IL1R	✓	✓	✓	✓
LDL pathway during atherogenesis	✓			
Cells and molecules involved in acute inflammatory response	✓	✓	✓	✓
Adhesion and diapedesis of granulocytes	✓	✓	✓	✓
NF-κB activation by nontypeable haemophilus influenzae	✓	✓	✓	✓
Induction of apoptosis through DR3 and DR4/5 death receptors	✓	✓	✓	✓
Cadmium induces DNA synthesis and proliferation in macrophages	✓	✓	✓	
Selective expression of chemokine receptors during T cell polarization	✓		✓	✓
Phospholipase Cd1 in phospholipid associated cell signalling	✓			
Keratinocyte differentiation	✓	✓	✓	
Pertussis toxin intensive CCR5 signalling in macrophage	✓	✓		
Cytokines and inflammatory response	✓	✓	✓	✓
Regulation of haematopoiesis by cytokines	✓	✓	✓	✓
Adhesion and diapedesis of lymphocytes	✓	✓	✓	✓
TNFR2 signalling		✓	✓	✓
Activation of PKC through G protein coupled receptor		✓	✓	
Cytokine network		✓	✓	
NF-κB signalling		✓	✓	
CD40L signalling		✓	✓	✓
The 41BB dependent immune response			✓	✓
TACI and BCMA stimulation of B cell immune responses				✓

To further dissect TNF responses in each outcome group, the lists of transcripts whose expression had changed in response to TNF (2767 transcripts in the Normal group, 1910 transcripts in Resolving, 1764 transcripts in VeRA and 1308 in the Established RA group) were compared. The number of transcripts up- and down-regulated in response to TNF in each outcome group is shown in Figure 6.22.

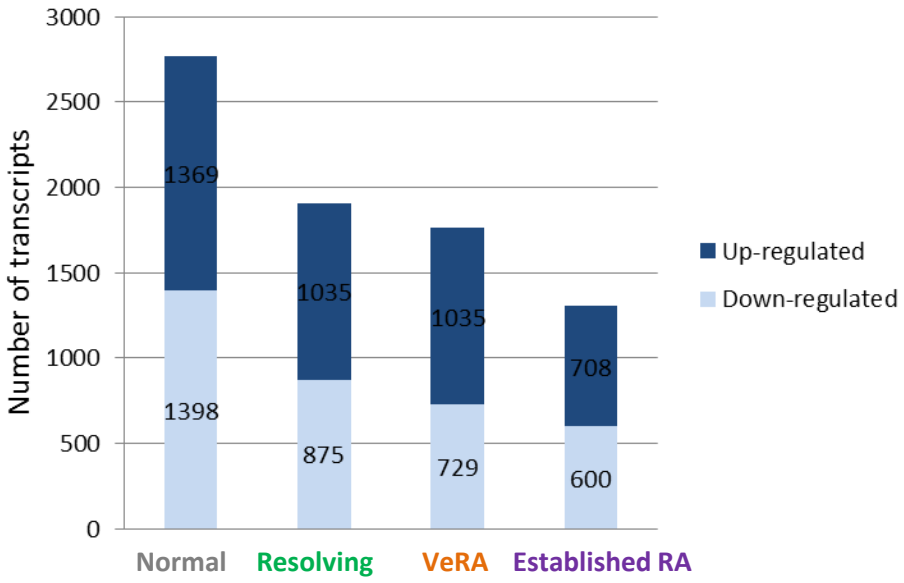

Figure 6.22 Number of transcripts up- or down- regulated by TNF stimulation in each outcome group.

To determine whether these transcripts were in common or unique to each of the groups a cord diagram was created (Figure 6.23). A total of 649 transcripts were in common between all 4 groups, 521 transcripts were in common between 3 groups, 531 between 2 groups and 1275 unique to a given group. Out of these 1275 transcripts unique to each outcome group, 806 were in the Normal group, 207 in Resolving, 135 in the VeRA and 127 in the Established RA group.

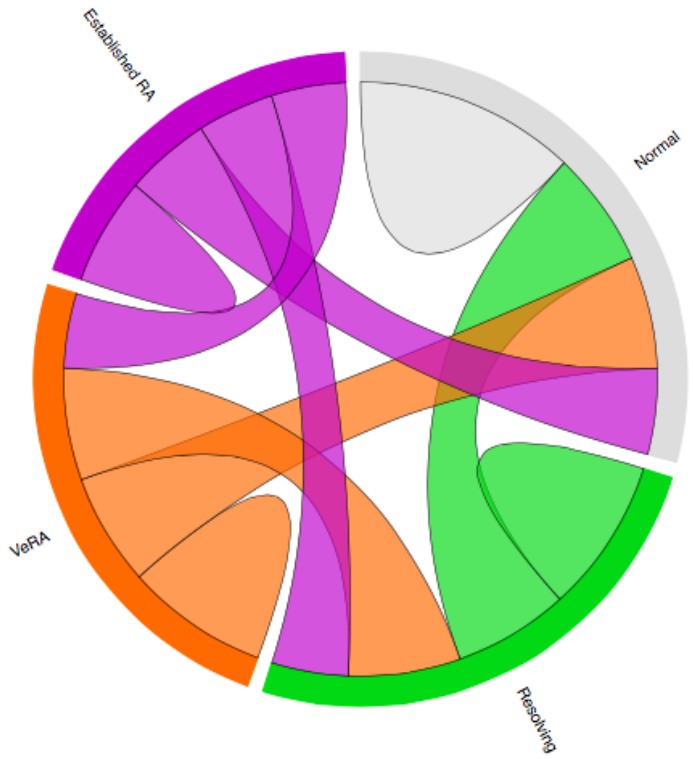

Figure 6.23 Cord diagram of TNF responses. *Graphical representation of transcripts whose expression levels changed in response to TNF stimulation. Some genes were unique to each of the outcome groups whilst others were in common between two, three or all four of the outcome groups.*

Examples of genes in common between all four groups included tumour necrosis factor alpha induced protein 3 (TNFAIP3), TNFAIP3-interacting protein 1 (TNIP1), nuclear factor of kappa light polypeptide gene enhancer in B-cells inhibitor epsilon (NFKBIE), intercellular adhesion molecule 1 (ICAM1), interferon alpha beta receptor beta chain (IFNAR2), solute carrier family 39 member 14 (SLC39A14) and GTP cyclohydrolase 1 (GCH1). The patterns of expression for these genes in the microarray experiment are shown in Figure 6.24. This group includes genes known to be rapidly induced by TNF and involved in the NF-κB signalling pathway and negative regulators of TNF signalling. Genes in common between the four outcome groups could be interpreted as a

generic synovial fibroblast response to inflammation whilst those unique to a given group may represent specific responses and their further study is warranted.

The top 50 uniquely changed transcripts in response to TNF stimulation in each group are shown in Tables 6.8 to 6.11. Amongst these transcripts, there was a selection of protein coding genes as well as long non-coding RNAs, small nucleolar RNAs, microRNAs and uncharacterised sequences. Out of the top 50 transcripts in the Normal group, TNF stimulation resulted in up-regulation of 24 and down-regulation of 26 transcripts. In the Resolving group 34 transcripts were down-regulated following TNF stimulation whilst 18 were down-regulated in the VeRA group. TNF stimulation resulted in down-regulation of 30 out of these 50 transcripts in the Established RA group.

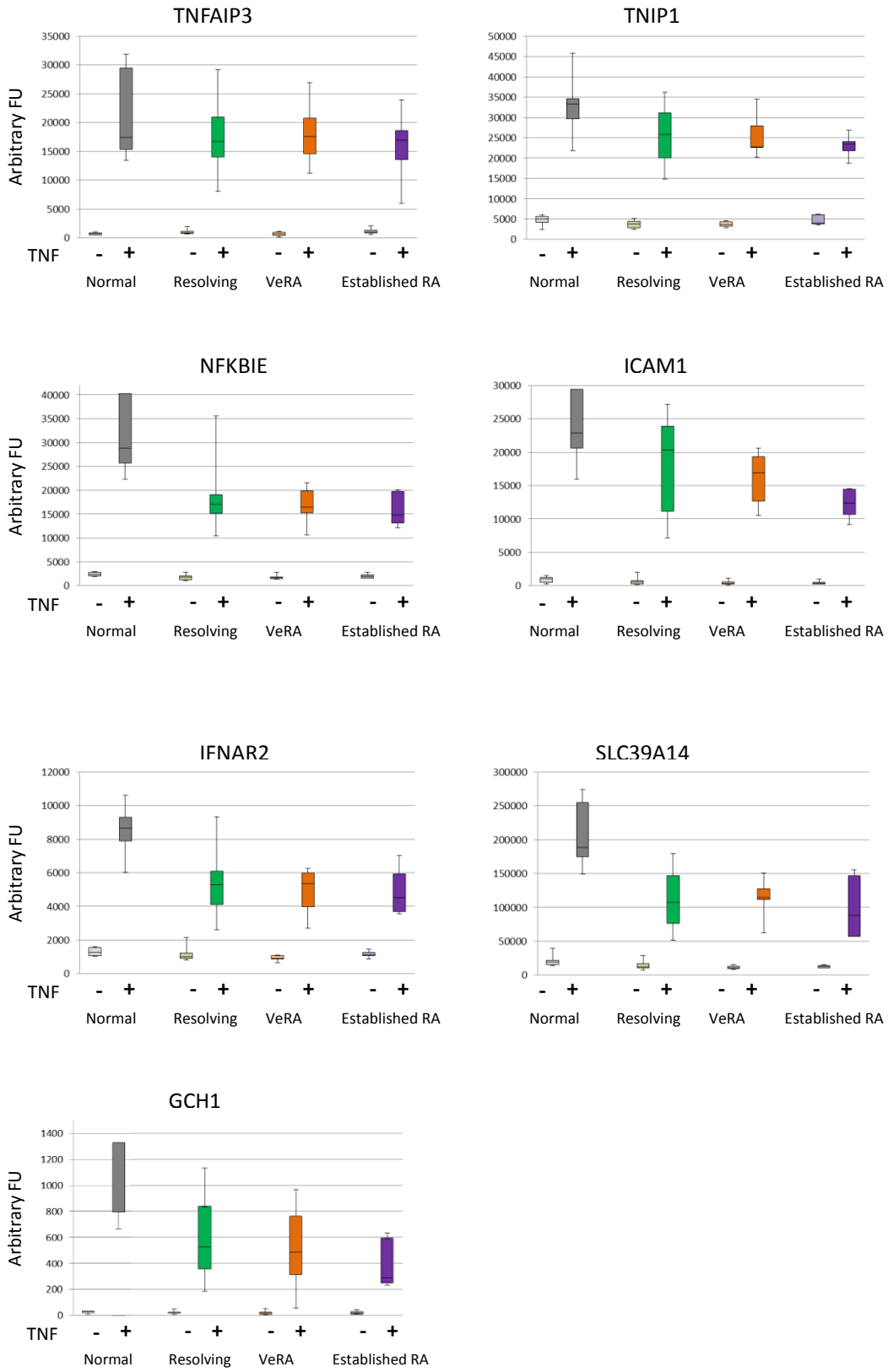

Figure 6.24 Examples of genes up-regulated by TNF stimulation in all outcome groups. *Graphs showing microarray expression data for genes that are up-regulated following TNF stimulation in all outcome groups. Unstimulated and TNF stimulated data are shown for each outcome group. Expression levels expressed as arbitrary fluorescence units (FU).*

Table 6.8 Top 50 differentially expressed transcripts in response to TNF stimulation unique to Normal samples at a fold difference of 2 and FDR<0.05.

Gene symbol	Gene name	Fold change	p value
LOC728705	Uncharacterised LOC72805	-2.2	5.94E-10
LOC93622	Morf4 family associated lncRNA	-2.1	2.43E-09
TMEM189	Transmembrane protein 189	2.0	3.19E-09
COX17	Cytochrome oxydase copper chaperone	2.5	4.84E-09
CLIP4	CAP-GLY domain containing linker protein family 4	-2.3	1E-08
ASAP2	Development and differentiation enhancing factor 2	-2.6	1.14E-08
PRMT1	Protein arginine N methyl transferase 1	2.3	1.56E-08
CCDC6	Coiled coil domain containing 6	-2.1	2.12E-08
WARS	Tryptophanyl-tRNA synthetase	3.2	2.17E-08
HSCB	HscB mitochondrial iron-sulfur cluster co-chaperone	2.1	2.35E-08
ITGAE	Integrin alpha E	-2.1	2.5E-08
SNX30	Sorting nexin family member 30	-2.0	3.72E-08
PPTC7	T cell activation protein phosphatase 2	2.0	4.86E-08
OSMR	Oncostatin M receptor	3.0	5.35E-08
ZFYVE21	Zinc finger FYVE domain containing 21	-2.5	5.69E-08
LYPLAL1	Lysophospholipase-like 1	-2.2	6.44E-08
HECTD1	HECT domain containing E3 ubiquitin protein ligase 1	-2.1	8.29E-08
SETDB2	SET domain, bifurcated 2	-2.2	1.01E-07
THC2520792	CTD-2301A4.5 (non-coding)	2.1	1.12E-07
PPCS	Phosphopantothenoylcysteine synthetase	2.1	1.19E-07
ZNF177	Zinc finger protein 177	-2.4	1.24E-07
XBP1	X-box binding protein 1	2.6	1.35E-07
CREB3	Basic leucine zipper protein	2.4	1.37E-07
XLOC_004626	Uncharacterised X LOC004626	2.3	1.52E-07
LGI1	Leucine-rich glioma inactivated -1	-19.4	1.61E-07
RHOG	Ras homolog family member G	2.0	1.65E-07
SNHG7	Small nucleolar RNA host gene 7	-2.3	1.66E-07
LOC100507100	Uncharacterised LOC100507100	-2.6	2.29E-07
XLOC_007607	Uncharacterised X LOC007607	2.1	2.33E-07
OSBPL7	Oxysterol binding protein-like 7	-2.2	2.36E-07
SMS	Spermine synthase	2.0	2.37E-07
XLOC_006513	Uncharacterised X LOC006513	-2.2	2.6E-07
ELOVL5	ELOVL fatty acid elongase 5	2.1	2.61E-07
GYS1	Glycogen synthase 1	2.4	2.68E-07
C9orf46	Plasminogen receptor C terminal lysine transmembrane protein	2.4	3.01E-07
PSMD9	Proteasome 26S subunit non-ATPase 9	2.1	3.06E-07
PDDC1	Parkinson disease 7 domain containing 1	-2.0	3.31E-07
MBLAC2	Metallo beta lactamase domain containing 2	-2.2	3.35E-07
LOC100506870	Uncharacterised LOC100506870	-2.5	3.78E-07
FAS	FAS cell surface death receptor	2.2	3.84E-07
TBC1D9	TBC1 domain family member 9	2.4	4.01E-07
SLC11A2	Solute carrier family 11 member 2	2.0	4.02E-07
SH3BP4	Transferrin receptor trafficking protein	-2.4	4.16E-07
MANF	Mesencephalic astrocyte derived neurotrophic factor	2.7	4.56E-07
XLOC_003870	Uncharacterised X LOC003870	-2.1	4.92E-07
MRPS25	Mitochondrial ribosomal protein S25	-2.1	5.07E-07
ZDHHC7	Zinc finger DHHC type containing 7	-2.3	5.09E-07
HSPA13	Heat shock protein 70kDa family member 13	2.0	5.11E-07
ALAD	Aminolevulinate dehydratase	-2.1	5.23E-07
ACOT13	Acyl-CoA thioesterase 13	-2.0	5.26E-07

Table 6.9 Top 50 differentially expressed transcripts in response to TNF stimulation unique to Resolving samples at a fold difference of 2 and FDR<0.05.

Gene symbol	Gene name	Fold change	p value
PTPRJ	Protein tyrosine phosphatase receptor type J	2.11362	1.03E-10
SASH1	SAM and SH3 domain containing 1	-2.09532	5.21E-08
AK091302	Phosphodiesterase 5A	-4.49662	1.76E-06
A_33_P3296348	Uncharacterised mRNA	2.96171	2.56E-06
SHROOM3	Protein shroom 3	-2.13088	3.25E-06
XLOC_009813	Uncharacterised X locus 009813	-2.62791	4.87E-06
TNS3	Tensin 3	2.20952	6.44E-06
ZAR1L	Zygote arrest 1 like	2.34863	7.05E-06
MGC16121	MIR503 miRNA	-2.15621	8.6E-06
SDC2	Syndecan 2	-3.51871	9.02E-06
XLOC_004072	Uncharacterised X locus 004072	-5.93241	9.23E-06
LOC285419	Uncharacterised lncRNA	-2.99693	1.05E-05
LOC100506012	PPP5 TPR Repeat domain containing Protein	-2.29491	1.53E-05
CCDC85A	Coiled coil domain containing 85A	-3.25485	1.61E-05
XLOC_l2_008031	Uncharacterised X LOC008031	2.05424	1.85E-05
KRT24	Keratin 24	-3.97843	1.96E-05
XLOC_002078	Uncharacterised XLOC002078	-2.4614	2.6E-05
SPTLC3	Serine palmitoyltransferase long chain base subunit 3	-2.0087	2.9E-05
XLOC_008005	Uncharacterised X LOC008005	2.17022	3.09E-05
LOC100129518	Uncharacterised lncRNA	-2.21534	3.44E-05
FLJ35024	Uncharacterised lncRNA	-2.13125	3.85E-05
MOK	MOK protein kinase	-2.73359	4.04E-05
XLOC_000939	Uncharacterised X LOC000939	-2.02395	4.08E-05
XLOC_008380	Uncharacterised XLOC008380	2.35173	4.54E-05
FAM201B	Family with sequence similarity 201 member B lncRNA	-2.28476	4.55E-05
XLOC_l2_015336	Uncharacterised X LOC015336	-2.24234	4.77E-05
LOC349196	Uncharacterised LOC349196	-2.20997	4.8E-05
SESN3	Sestrin 3	-2.01093	5.42E-05
ZNF474	Zinc finger protein 474	-3.08044	5.73E-05
KY	Kyphoscoliosis peptidase	2.88235	5.99E-05
XLOC_l2_000910	Uncharacterised X LOC000910	2.4936	7.04E-05
THC2620859	Uncharacterised protein THC2620859	2.25279	7.12E-05
CHD5	Chromodomain helicase DNA binding protein 5	-2.28212	7.97E-05
BCO23640	RP11-43505 lncRNA	-2.67536	9.16E-05
UBE2Q2P2	Ubiquitin conjugating enzyme E2Q family member 2 lncRNA	-2.26122	9.4E-05
AF461896	DNA damage regulated autophagy modulator 1	2.30362	9.46E-05
ANGPTL4	Angiopoietin like 4	-2.14536	0.0001
NLGN4Y	Neuroligin 4 Y linked	2.297	0.000114
IL6R	IL6 receptor	-2.1495	0.000115
A_33_P3312187	Uncharacterised mRNA	2.78986	0.00012
C6orf164	C6orf164 lncRNA	-2.26356	0.000126
THC2772049	RP11-358M11 lncRNA	-2.47335	0.000145
SYT1	Synaptotagmin-1	-2.71172	0.000148
SHISA9	Shisa family member 9	3.28885	0.000154
LOC100132057	Phosphodiesterase 4D lncRNA	-2.24219	0.000158
CAPZB	Capping protein (actin filament) muscle Z line beta	2.51007	0.000163
LOC729175	Uncharacterised LOC729175	2.17269	0.000174
XLOC_008390	Uncharacterised X LOC008390	-2.0173	0.000182
XLOC_006174	Uncharacterised X LOC006174	-2.44379	0.000185
XLOC_005808	Uncharacterised X LOC005808	-2.41793	0.000188

Table 6.10 Top 50 differentially expressed transcripts in response to TNF stimulation unique to VeRA samples at a fold difference of 2 and FDR<0.05.

Gene symbol	Gene name	Fold change	p value
STAT4	Signal transducer and activator of transcription 4	2.23957	5.5E-08
H2AFY2	H2A histone family member Y2	2.02283	6.95E-08
ATL2	Atlastin GTPase 2	2.32867	1.57E-07
FTH1P16	Ferritin heavy popypeptide 1 pseudogene 16 (non-coding)	2.10018	2.52E-07
LOC100507139	Uncharacterised LOC100507139	-3.35589	1.09E-06
EIF4E3	Eukaryotic translation initiation factor 4E family member 3	-2.0007	1.23E-06
TRIM47	Tripartite motif containing 47	2.18239	2.2E-06
PDE4DIP	Phosphodiesterase 4D interacting protein	2.02616	3.59E-06
LOC100507492	Uncharacterised LOC100507492	2.46682	5.3E-06
NEDD4L	Neural cell expressed developmentally down-regulated 4 like	2.06896	8.62E-06
XLOC_013812	Uncharacterised X LOC_013812	3.74262	9.65E-06
AK130724	Uncharacterised AK130724	2.36981	1.02E-05
AC093668.2	AC093668.2 (non-coding)	-2.24355	1.36E-05
RABEPK	Rab9 effector protein with kelch motifs	2.02678	1.38E-05
FAM66E	Family with sequence similarity 66 member E lncRNA	-2.42283	1.65E-05
YPEL2	Yippee like 2	2.0532	1.9E-05
CACHD1	Cache domain containing 1	2.18833	3.12E-05
SIRPG	Signal regulatory protein gamma	2.11617	3.49E-05
CCDC113	Coiled coil domain containing 113	-2.0549	4.16E-05
SOX12	SOX12 transcription factor	-2.23007	4.54E-05
MCM3AP-AS1	MCM3AP antisense RNA	-2.21962	5.9E-05
XLOC_004366	Uncharacterised X LOC004366	-2.20628	6.47E-05
XLOC_013898	Uncharacterised X LOC013898	2.72977	7.34E-05
EMCN	Endomucin	-2.85231	7.45E-05
AHR	Aryl hydrocarbon receptor	2.2445	0.000104
ANKLE1	Ankyrin repeat and LEM domain containing 1	2.60215	0.000128
SPINT1	Serine peptidase inhibitor	2.26922	0.00013
IL24	Interleukin 24	7.28097	0.000144
RIMS3	Regulating synaptic membrane exocytosis 3	-2.19637	0.000148
XLOC_l2_015565	Uncharacterised X LOCl2015565	-2.81286	0.000158
FTH1P27	Ferritin heavy popypeptide 1 pseudogene 27 (non-coding)	2.11174	0.000166
TAC4	Tachykinin 4	2.62731	0.000182
XLOC_009895	Uncharacterised X LOC009895	-2.17766	0.000239
EPS8L1	Epidermal growth factor receptor 8 related protein 1	2.66009	0.000243
SLC2A13	Solute carrier family 2 member 13	2.42306	0.000244
C9orf47	C9orf47 protein	3.16618	0.000267
CBLN2	Cerebellin 2 precursor	4.20478	0.000281
LOC100505841	Zinc finger protein 474 like	-2.16491	0.000294
HDAC2	Histone deacetylase 2	2.02141	0.000321
CTD-2210P24.4	Uncharacterised (protein coding)	-2.32628	0.000325
XLOC_l2_006152	Uncharacterised LOCl2006152	-2.0085	0.000335
LINC00314	Long intergenic non protein coding RNA 314	2.00459	0.000375
CMBL	Carboxymethylenebutenolidase homolog	-2.43618	0.00039
ATOH7	Atonal homolog 7	2.39881	0.000398
LOC644242	Uncharacterised LOC644242	2.59678	0.000405
XLOC_l2_008434	Uncharacterised XLOCl2008434	-2.37384	0.000474
RASGRP3	RAS guanyl releasing protein 3	2.74654	0.000503
DLGAP1-AS2	DLGAP1 antisense RNA 2 lncRNA	2.07843	0.000533
RPTN	Repetin	-3.02305	0.000541
LOC100128905	Uncharacterised LOC100128905	3.38463	0.000569

Table 6.11 Top 50 differentially expressed transcripts in response to TNF stimulation unique to Established RA samples at a fold difference of 2 and FDR<0.05.

Gene symbol	Gene name	Fold change	p value
PICALM	Phosphatidylinositol binding clathrin assembly protein	2.00067	3.21E-07
BAZ1A	Bromodomain adjacent to zinc finger domain 1A	2.06722	2.12E-06
C16orf57	C16orf57 protein	2.52146	1.35E-05
TYSND1	Trypsin domain containing 1	-2.1195	1.49E-05
FRMD4B	FERM domain containing 4B	-4.26581	1.62E-05
LOC100506775	Uncharacterised LOC100506775	-3.67598	3.33E-05
SOCS3	Suppressor of cytokine signalling 3	-2.1503	6.26E-05
RBPJ	Recombination signal binding protein for Ig kappa J region	-2.12403	6.62E-05
RGS11	Regulator of G protein signalling 11	-2.13328	9.82E-05
ENST00000419668	Uncharacterised antisense RNA (lncRNA)	2.39408	0.000112
PTCH1	Protein patched homolog 1	3.10862	0.00012
TRNP1	TMF1 regulated nuclear protein 1	-2.03988	0.000214
CAMK2N2	Calcium/calmodulin dependent protein kinase II inhibitor 2	2.48083	0.000215
EPS8L2	Epidermal growth factor receptor 8 related protein 2	-2.12781	0.000222
SEMA3A	Sema domain	2.02347	0.000226
FLOT1	Flotillin 1	-2.09533	0.000253
DIRAS3	DIRAS family GTP binding Ras like 3	2.19735	0.000254
ABCC2	ATP-binding cassette sub-family C member 2	-2.50083	0.00026
GADD45B	Growth arrest and DNA damage inducible beta	-2.21493	0.000265
PITX1	Paired like homeodomain 1	-2.72665	0.000288
ROGDI	Rogdi homolog	-2.09194	0.000291
CALD1	Caldesmon 1	-2.08523	0.000291
SIX1	SIX homeobox 1	-2.06961	0.000308
ANP32E	Acidic nuclear phosphoprotein 32 family member E	2.09761	0.000316
TGFB2	transforming growth factor beta 2	2.95298	0.000348
XLOC_010743	Uncharacterised X LOC010743	-2.17223	0.00036
TP53I11	Tumor protein p53 inducible protein 11	-2.00228	0.000383
ADARB1	Adenosine deaminase	-2.73162	0.000384
PPFIA4	Protein tyrosine phosphatase receptor type F polypeptide	-2.10584	0.000398
SYTL4	Synaptotagmin like 4	2.0833	0.000418
SLC10A7	Solute carrier family 10 member 7	2.0037	0.000421
CEP68	Centrosomal protein 68kDa	-2.00998	0.000433
ATXN1L	Ataxin 1 like	-2.23874	0.000434
UPK3B	Uroplakin 3B	-2.52761	0.000455
HGF	Hepatocyte growth factor	2.38923	0.000513
BANK1	B cell scaffold protein with ankyrin repeats 1	-2.57534	0.000525
XLOC_l2_015849	Uncharacterised X LOCl2015849	-2.61968	0.000546
PPP4R1L	Protein phosphatase 4 regulatory subunit 1 like	2.13661	0.000586
LOC100505783	Uncharacterised LOC100505783	-2.77272	0.000601
DHRS9	Dehydrogenase reductase member 9	9.77488	0.000663
LOC100130417	Uncharacterised LOC100130417	-2.45918	0.000674
HOXD3	Homeobox D3	-2.53443	0.000676
GALNTL1	Galactosamine N-acetylgalactosaminyltransferase like 1	-2.01615	0.000716
ZEB1-AS1	ZEB1 antisense RNA 1	-2.02723	0.000718
SHISA2	Shisa family member 2	5.55278	0.000724
AK126423	PDZ domain containing ring finger 3	3.06186	0.000763
DNAI2	Dynein, axonemal intermediate chain 2	2.50696	0.000786
SSR4P1	Signal sequence receptor delta 1 long non coding RNA	-2.2062	0.000792
AF085654	Immunoglobulin heavy variable 5-78	2.29593	0.000826
ENST00000354995	Uncharacterised protein	2.40941	0.000863

6.8 Microarray experiments: Discussion

This is the first body of work to systematically characterise the transcriptomic profile of cultured synovial fibroblasts in four distinct clinical outcome groups: Normal, Resolving, very early RA (VeRA) and Established RA.

Published work in this field includes the transcriptomic profiling of Established RA and Normal synovial fibroblasts analysed using RNA sequencing technologies (Heruth et al. 2012). Unstimulated cultured synovial fibroblasts (n=2 in each group) were expanded to passage 2 before RNA extraction and sequencing. A total of 277 genes were identified as differentially expressed between both groups. The majority of these genes had not been previously described in this context. Although informative, the small sample size in that study raises questions about the validity of these data and whether findings could be generalised. Del Rey and colleagues studied the transcriptomic profile of Normal and Established RA synovial fibroblasts (n=6 in each group) using microarray expression profiling (Del Rey et al. 2010). This group compared gene expression patterns of unstimulated synovial fibroblasts cultured under normoxic and hypoxic conditions. They demonstrated significant changes in gene expression patterns in both groups induced by hypoxia. When they compared transcriptomic profiles between both groups under normoxic conditions, they identified 223 differentially expressed transcripts. However, in their publication, these genes were not analysed further.

In a study of similar design to ours, Kasperkowitz and colleagues analysed the transcriptional profile of 19 cultured synovial fibroblast lines from patients with Established RA. Using unsupervised hierarchical clustering, they identified two distinct

synovial fibroblasts groups (I and II, with group II being further subdivided into IIa and IIb) based on differential expression of 484 genes. Group I was characterised by high expression of genes such as insulin like growth factor binding protein 5 (GFBP5) and insulin growth factor 2 (IGF2), genes involved in complement activation and oncogenes (MYB , TEM8 and RAB31). Group II fibroblasts were characterised by high expression of transforming growth factor beta (TGFβ) which was particularly pronounced in the IIb subgroup where cells also showed increased expression of TGFβ response genes such as collagen type 4 alpha 2 (COL4A2) and alpha smooth muscle actin (αSMA). Indeed, expression of αSMA (a myofibroblast marker) was confirmed in independent samples at mRNA and protein levels and localised to the lining layer of the synovium. These results provide strong evidence for heterogeneity within RA synovial fibroblast cultures which may relate to differing clinical phenotypes (including for example the degree of erosiveness of the arthritis) and levels of inflammation (Kasperkovitz et al. 2005). This paper followed previous work from the same group where study of synovial tissue from Established RA patients using microarrays had shown heterogeneity of gene expression patterns allowing identification of different pathogenic RA subsets (van der Pouw Kraan et al. 2003). More recently other groups have independently confirmed observations of heterogeneity within RA tissues. Dennis and colleagues identified 4 different RA subsets (which they termed myeloid, lymphoid, low inflammatory and fibroid), based on gene expression signatures of 49 Established RA synovial tissues. They subsequently tested the ability of these differing phenotypes to predict response to anti TNF treatment by applying these pre-defined gene sets to a separate patient cohort from the Gene Expression Omnibus (GEO) data repository. In doing this, they identified that expression of the myeloid phenotype at baseline was significantly higher in patients with a good EULAR treatment response at 16 weeks

(Dennis et al. 2014). Another group analysed microarray data from the GEO repository corresponding to synovial tissue samples from osteoarthritis (OA), RA and Normal joints (5 samples in each group). A statistical model was created to identify groups of genes that were differentially co-expressed in two group comparisons (RA vs. OA, RA vs. Normal and OA vs. Normal). A weighting system was developed to identify the transcription factors that most significantly contributed to differentiating RA from Normal and OA groups (Li et al. 2013). One of the identified transcription factors is in common with one identified by us, as discussed later in this chapter.

In addition to the above mentioned studies, data from candidate gene studies provide further information about the gene expression profile of Established RA synovial fibroblasts. Broadly, their expression phenotype is characterised by up-regulation of oncogenes and proto-oncogenes, adhesion molecules and MMPs and down-regulation of tumour suppressor genes.

The aim of my study was to add to the existing knowledge in two ways: (1) to unravel molecular mechanisms differentiating the resolution of early inflammatory arthritis from its persistence as RA; (2) to gain insights into RA pathogenesis, in particular progression from early RA to established, destructive disease.

We hypothesised that by comparing Resolving and VeRA samples we would identify key genes responsible for the resolution of early inflammatory arthritis. However, no differences in gene expression signatures between these two outcome groups were found in either the unstimulated or the TNF stimulated samples. There are a number of reasons that might explain why differential expression was not observed between these

outcome groups. It is possible that differences in expression between these groups exist at the time of biopsy but these are lost during synovial fibroblast culture. Evidence supporting a stable fibroblast phenotype is provided by studies demonstrating different gene expression profiles in fibroblasts from different organs that have been cultured for multiple passages (Chang et al. 2002). The stability of the Established RA synovial fibroblast phenotype *in vitro* has been previously studied. One of the most compelling pieces of evidence in favour of its stability comes from the demonstration that RA synovial fibroblasts that have been cultured for multiple passages *in vitro* display an invasive phenotype when co-implanted with normal human cartilage in the SCID mouse model in the absence of T cells and any other human cells (Muller-Ladner et al. 1996). Additionally, a study designed to address this issue supports stability of expression profile during early passages. Established RA synovial fibroblasts were cultured from passages 1 to 8 and their gene expression profile analysed using cDNA arrays at each passage. Expression profiles remained constant between passages 1 to 5 (defined as <10% differentially expressed genes between passages) but diverged significantly from passages 5 to 8 (>10% of differentially expressed genes with each passage) (Neumann et al. 2010). Based on this evidence, we designed our microarray experiments so that we would study cells at an early passage (passage 3) to minimise the effect of culture. Nevertheless, the possibility that some or all of the phenotype may have been lost in culture should still be acknowledged, particularly when considering cells in the Resolving and VeRA groups as it is not known how stable the synovial fibroblast phenotype is at such an early stage of disease.

In this respect, it is also worth noting that a major assumption of our hypothesis is that the fate of patients (resolution of inflammatory arthritis versus progression to RA) is

already decided at the time of biopsy (within 3 months of symptom onset). However, it is entirely possible that critical decision points between these two paths occur at a later stage or that there is not a single decision point but rather a gradual accumulation of changes over a longer time period. As discussed in the introductory pages of this thesis, the debate regarding the timing of the window of opportunity still continues. Whilst we chose to define this window as disease of less than 3 months duration, other researchers use definitions of 6, 12 and even 24 months. As we did not analyse samples from patients with disease duration other than less than 3 months, we are not able to draw any conclusions regarding other time periods.

A way of overcoming these limitations would be to undertake *ex vivo* study of gene expression profiles at the time of biopsy to abolish any potential culture bias in gene expression. If this was combined with the study of samples at different time points from symptom onset, this might become a powerful approach to unravelling disease mechanisms in early disease. Whilst this approach would have been technically challenging at the time these experiments were designed, it would now be possible, albeit costly, to do so. Such an approach might encompass *ex vivo* isolation and sorting of synovial fibroblasts and storage until a diagnosis could be assigned followed by analysis of transcriptomic profiles. An alternative *ex vivo* approach would be the study of synovial tissue although the disadvantage of this approach is the inability to study a cell type in isolation.

Assuming that the phenotype of synovial fibroblasts is indeed imprinted and stable in culture, our inability to identify differentially expressed genes between Resolving and VeRA patients may be, at least partly, explained by one of the well described

limitations of microarray data analysis. During differential expression analysis of microarray data, as comparisons are made across large numbers of genes, the likelihood of finding differentially expressed genes by chance increases with increasing number of genes. Hence, a statistical approach is used to control the number of false positives identified this way: the false discovery rate. However, controlling for false positives can result in increased false negatives, especially for genes where the difference between groups is small. Hence by using FDR, one decreases false positive rates but at the cost of increasing false negatives (Park et al. 2010). So, it could be that differences of small magnitude exist between both groups but we are unable to identify them in our analysis.

Taken together the results of the differential expression analysis between Resolving and VeRA samples may be considered to mean that no differences of large magnitude exist in the gene expression signatures between these groups. This may be because synovial fibroblasts do not have a key role early in disease, and that such a role only becomes apparent later in disease after continued exposure to a pro-inflammatory environment. Another possibility is that such differences only become apparent in fibroblasts from the early stages of disease when these cells are exposed to certain conditions such as during migration or when co-cultured with other cell types.

In order to investigate the question of whether significant transcriptomic changes occur between the earliest and later stages of disease, we compared VeRA and Established RA synovial fibroblasts, identifying different transcriptomic signatures. In this case, and despite the caveats outlined above, differences were of adequate magnitude to be identified. When considering the significance of these results it may be postulated that differences in gene expression are related to disease chronology (i.e. early disease

versus late disease). Under this assumption, further in depth study of differentially expressed genes may provide clues to molecular mechanisms involved in progression to chronicity.

However, varying disease severity between groups may also be responsible for the observed differences. Disease course in RA can range from mild, waxing and waning, non-destructive to aggressive, rapidly progressive and destructive disease. Traditionally the study of synovial fibroblasts has focused on analysis of samples originating from the latter patient subset. This is replicated in our Established RA group where samples from patients with aggressive disease course undergoing joint replacement surgery have been studied. Although every effort was made to match the groups as closely as possible, it is undeniable that differences between groups exist and are evidenced by differing DAS28 ESR scores at baseline (mean 4.8 in VeRA vs. mean 5.9 in Established RA) and the presence of erosions at baseline (1 out of 9 patients in which these data were available in the VeRA groups vs. 6 out of 6 patients in which these data were available in Established RA group). In this context, the effect of treatment on gene expression profiles must also be considered. Although patients in the Established RA group were receiving a relatively small number of therapies at the time of sample collection by today's standards (most patients were on DMARD monotherapy with one patient not on treatment), both concurrent and previous treatment would inevitably have affected synovial fibroblasts and their microenvironment. This is in stark contrast to patients in the VeRA group who were DMARD naïve. From a pragmatic point of view, one should recognise that it may be difficult to unravel the relative contributions of disease chronology, disease severity and treatment as in practice they tend to be inextricably

linked. For example, patients with longer disease duration would almost inevitably have had more treatment than those with shorter disease duration.

Acknowledging the considerations thus far outlined, detailed study of identified targets is warranted. Proposed targets for further study include CD300A, CSRNP1, EGR1, EN1, FOS, HAS3, HES1, KMT2E, LIMS3L and MME that have already been independently validated by PCR. Table 6.12 shows these genes with a short description of the functions associated with their proteins and their disease associations. For the benefit of the reader the patterns of expression of these genes in the microarray experiments are illustrated in Figure 6.25.

Some of the proteins encoded by these genes have not been previously described in the RA literature. Of relevance, CD300A is a protein involved in immune regulation and CSRNP1 has been associated with carcinomas (Borrego et al. 2013; Ishiguro et al. 2001). Others have been studied in the context of RA. Of particular interest are EGR1 and MME. EGR1 is a transcription factor that activates target genes involved in cell differentiation and mitosis. Li and colleagues identified EGR1 as a key transcription factor differentiating RA from OA and Normal synovial tissue samples (Li et al. 2013). In another study, EGR1 was shown to be expressed by synovial fibroblasts in RA synovial tissues. Cultured RA synovial fibroblasts expressed higher levels of EGR1 mRNA compared to OA synovial fibroblasts. As EGR1 is involved in cell proliferation, proliferation rates were assessed but no increased proliferation was observed (Aicher et al. 1994). Instead overexpression of EGR1 in immortalised human fibroblasts has been associated with activation of type I and type II collagen genes and of tissue inhibitor of metalloproteinases (TIMP 1, 2 and 3) (Aicher et al. 2003;Alexander et al. 2002). Interestingly, EGR1 has also been shown to act as a negative regulator of inflammatory

responses in cultured RA synovial fibroblasts (Faour et al. 2005). Putting this together it is tempting to speculate that reduction of EGR1 expression over the course of disease (from VeRA to Established RA) may result in increased MMP production and enhanced inflammatory responses.

MME is a zinc dependent enzyme that inactivates peptides by cleaving the amino side of hydrophobic residues. It is expressed by common myeloid progenitors but also by lymphoblasts in acute lymphoblastic leukaemia where surface expression of MME is used as diagnostic marker. This enzyme can be released to the extracellular space and increased levels have been found in the plasma and synovial fluid of RA patients compared to OA patients and healthy controls (Matucci-Cerinic et al. 1993) as well as in RA synovial tissue where it was postulated to be produced by synovial fibroblasts (Sreedharan et al. 1990). More recently, another MME family member, MMEL1 has been associated together with CTLA4 with increased RA susceptibility in the Han Chinese population (Danoy et al. 2011). Although it is not clear what precise role this gene may play in RA, its further study would be very informative.

Excess production of hyaluronic acid has been proposed as a contributor to RA progression. Whilst usually involved in maintaining joint homeostasis, excess production of this acid occurs during inflammation and has been associated with a series of pro-inflammatory roles such as acting as a chemoattractant, inducing neoangiogenesis and inducing expression of pro-inflammatory molecules by endothelial cells and leucocytes (reviewed in Stuhlmeier 2005). Hyaluronic acid is produced by three enzymes; hyaluronan synthases 1, 2 and 3 (HAS1, HAS2 and HAS3). HAS2 and HAS3 are constitutively expressed by cultured RA synovial fibroblasts and HAS1

expression can be induced by stimulation of cultures with TGFβ. Glucocorticoid treatment results in suppression of HAS1, HAS2 and HAS3 mRNA expression through MAP kinase dependent mechanisms whilst leflunomide suppresses hyaluronic acid production by cultured RA synovial fibroblasts in a dose dependent manner by blocking HAS1 induction (Stuhlmeier et al. 2004;Stuhlmeier 2005). Our finding of increased HAS3 expression by Established RA synovial fibroblasts is in keeping with these data and may indicate that increased hyaluronic acid production is an important feature in the progression to chronicity in RA.

Comparing gene expression profiles between unstimulated and TNF stimulated samples in each outcome group allowed us to address a third research question: is the effect of TNF stimulation on transcriptional signatures generic or are there outcome group-specific responses to TNF?

The results of these analyses revealed clear changes in gene expression signatures in response to TNF. Several pathways were involved in TNF responses. Whilst many of them were in common between all groups, others were unique to some groups or in common only between early inflammatory arthritis groups with a few unique to a given outcome group. Thus, similarities in TNF response between groups were identified that we propose represent a generic synovial fibroblast response to pro-inflammatory stimuli. These include genes rapidly induced by TNF and involved in the NF-κB signalling pathway and negative regulators of TNF signalling.

TNF responses that appeared unique to individual outcome groups were also identified. The in depth study of these unique signatures may provide new exciting data in this

area. To take this work forward, the next step should be to validate microarray results at mRNA and protein levels. Of note, within the top 50 uniquely changed transcripts in response to TNF in the Resolving group there was a very high proportion of uncharacterised and non-protein coding regulatory genes. Whilst in itself this makes the further study of these transcripts significantly more challenging, this may also be an indicator of the higher degree of regulation that these cells are subjected to or able to exert which may be associated with a role in the resolution of inflammatory arthritis.

Amongst these non-protein coding regulatory genes there are several lncRNAs. The study of lncRNAs is an exciting new field in synovial fibroblast research that is in its infancy as demonstrated by the fact the available publications are only in abstract format. Thus careful consideration and further work in this direction would significantly add to this area. Work undertaken by Steffen Gay's group demonstrated differential lncRNA expression between resting, unstimulated OA and RA synovial fibroblasts (Bertoncelj et al. 2013). Subsequent analysis of lncRNA expression patterns in response to 24 hour TNFα and IL1β stimulation revealed no differences in response between these groups. LncRNAs whose expression varied in response to TNFα included metastasis associated lung adenocarcinoma transcript 1 (MALAT1) and growth arrest specific 5 (GAS5) both down-regulated following stimulation and antisense long non-coding RNA in the INK4 locus (ANRIL) whose expression was up-regulated upon stimulation (Bertoncelj et al. 2014). To compare these results with ours, I assessed whether expression levels of these lncRNAs had changed in response to TNF in our dataset. Whilst expression of ANRIL was not modified by TNF in any of the groups, expression of MALAT1 and GAS5 were down-regulated in all four groups studied. Whilst no conclusive interpretations can be made from these findings and reproduction

of these results at PCR level would be required for their validation, it is nevertheless interesting to find similar responses to TNF stimulation in the different outcome groups assessed in both studies which may indicate that down-regulation of these transcripts is a generic synovial fibroblast response to TNF stimulation.

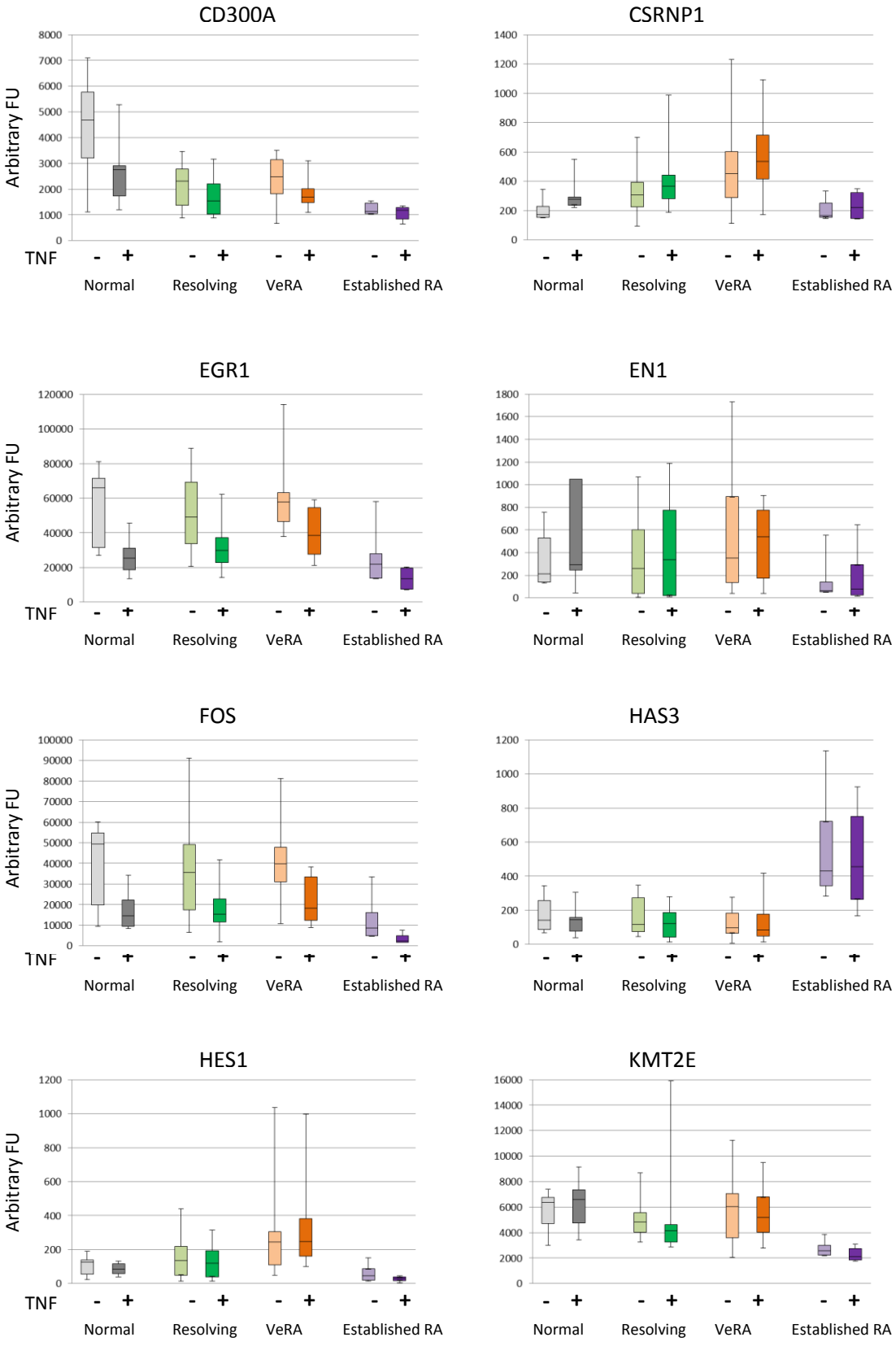
CD300A
CSRNP1
EGR1
EN1
FOS
HAS3
HES1
KMT2E
Arbitrary FU
TNF
- + - + - + - +
Normal
Resolving
VeRA
Established RA

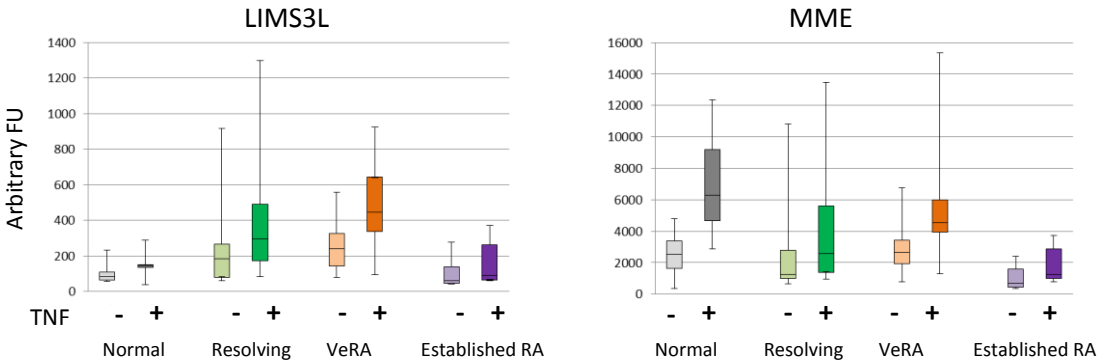

Figure 6.25 Expression levels of validated genes in unstimulated and TNF stimulated samples in all outcome groups. *Graphs showing microarray expression data for genes that were validated by PCR. Unstimulated and TNF stimulated data are shown for each outcome group. Expression levels expressed as arbitrary fluorescence units (FU).*

Table 6.12 Differentially expressed genes between VeRA and Established RA validated by PCR.

Symbol	Name & Description	Disease associations
CD300A	• Cluster of differentiation 300A. • Cell surface protein in leukocytes, monocytes & neutrophils.	Involved in immune response signalling (Borrego 2013).
CSRNP1	• Cysteine serine rich nuclear protein 1. • Proposed as tumour suppressor gene.	Decreased expression in lung, liver, colon and kidney carcinomas (Ishiguro et al. 2001).
EGR1	• Early growth response 1. • Transcriptional regulator involved in cell differentiation & mitosis.	Associated with prostate and breast cancer where it promotes progression & glioblastoma where it inhibits tumour growth (Yang et al. 2003). EGR1 has been identified as a key differentially expressed transcription factor that distinguishes RA from OA and Normal synovial tissue (Li et al. 2013). EGR1 is constitutively expressed by Established RA synovial fibroblasts. Its expression has been associated with induction of type I and type II collagen genes and activation of tissue inhibitors of metalloproteinases (TIMP 1, 2 and 3) (Aicher et al. 1994;Aicher et al. 2003;Alexander et al. 2002).
EN1	• Homeobox protein engrailed 1 • Role in controlling pattern formation during development.	Associated with congenital central hypoventilation syndrome (Weese-Mayer et al. 2003).
FOS	• FBJ murine osteosarcoma viral homolog (also known as cFOS). • Transcription factor: component of the AP-1 complex.	AP-1 regulates gene expression in response to pro-inflammatory stimuli and has been involved in up-regulation of MMP expression by synovial fibroblasts. Study of adherent cell extracts from RA synovial tissues demonstrated high AP-1 binding activity compared to OA tissues. AP-1 binding correlated with c-fos and c-jun expression and disease activity (Asahara et al. 1997).
HAS3	• Hyaluronan synthase 3. • Enzyme involved in synthesis of hyaluronic acid: degradation product readily produced at inflammation sites that facilitates cell migration.	HAS3 (together with HAS2) is constitutively expressed by cultured RA synovial fibroblasts. Expression is suppressed by glucocorticoid treatment. In contrast HAS1 is not constitutively expressed but expression can be induced by TGFβ (Stuhlmeier et al. 2004). Leflunomide suppresses hyaluronic acid production by cultured RA synovial fibroblasts in a dose dependent manner by blocking HAS1 induction (Stuhlmeier 2005).
HES1	• Hairy and enhancer of split-1. • Key gene of the Notch signalling cascade. The target genes of this pathway remain poorly defined.	Abnormal expression of members of the Notch pathway has been shown in T cells from RA patients (Ng et al. 2001). Identified as IL1β target gene in chondrocytes where it influences cartilage matrix remodelling genes (Ottaviani et al. 2010).
KMT2E	• Lysine specific methyltransferase 2E. • Histone methyltransferase that specifically mono- and dimethylates lysine at position 4 of histone H3	Involved in haematopoiesis regulation. RA synovial fibroblasts cultured under hypoxic conditions display higher protein levels of another histone

	(K4H3). • Specific tag for epigenetic transcriptional activation.	mark: methylation of lysine at position 27 of histone H3 (K27H3) (Heron et al. 2014).
LIMS3L	• LIM and senescent cell antigen like domains 3 like. • Member of the LIM family of proteins: involved in cytoskeletal organisation.	The function of this protein remains undefined in the literature. Other members of the LIM family of proteins have been implicated in regulation of lamellipodia production and adhesion in mouse embryonic fibroblasts (Feng et al. 2005).
MME	• Membrane metalloendopeptidase. Also known as cluster of differentiation 10 or neprylisin. • Inactivates peptides by cleaving their amino side. • Examples of targeted peptides: glucagon, substance P, neurotensin.	Cell surface marker used for the diagnosis of acute lymphocytic leukaemia. Also associated with Burkitt's lymphoma, hairy cell leukaemia, myeloma and Alzheimer's disease. Increased MME levels in plasma and synovial fluid of RA patients compared to OA patients and healthy controls (Matucci-Cerinic et al. 1993). Increased MME levels in RA synovial tissue (postulated to be produced by synovial fibroblasts) (Sreedharan et al. 1990). MME family member, MMEL1 has been associated together with CTLA4 with increased RA susceptibility in the Han Chinese population (Danoy et al. 2011).

6.9 Further considerations and future work

Gene expression is a dynamic process that changes in response to environmental stimuli. In an attempt to study the response of synovial fibroblasts in different outcome groups to a pro-inflammatory microenvironment we stimulated cells with TNFα for 24 hours. Although informative, this approach is merely an *in vitro* model that does not fully replicate all environmental cues synovial fibroblasts encounter in the joint. Obvious limitations of this approach are the arbitrary definition of TNFα stimulation time and the lack of other environmental factors such as hypoxia, interactions with other cells and cartilage and other factors that may be critical but are yet to be defined. For these reasons, more complex *in vitro* and *in vivo* models should be used to complement this work. A good starting point would be the study of gene expression profiles of synovial fibroblasts from different outcome groups when co-implanted with normal cartilage under the kidney capsule of SCID mice.

In an attempt to relate gene expression to synovial fibroblast biology, we used differential expression analysis. This type of analysis allows characterisation of molecular differences associated with specific biological effects. This type of analysis can be seen as hypothesis generating and allows description of putative targets for further study. However, other approaches to the analysis of microarray data exist and would provide additional information from the microarray experiments performed in this thesis. Class prediction analyses could be undertaken in order to aid biomarker detection. Such analyses may provide clues to group of genes that would predict progression to persistent RA in early inflammatory arthritis. This would be of great clinical relevance as knowing which patients are more likely to develop RA from

disease onset would promote early and aggressive treatment of this patient group and prevent aggressive treatment of those patients in whom such predictive factors are absent. Unsupervised classification analysis may also prove very informative. So far, we have described hypothesis based approaches to data analysis in which assumptions are made regarding the expected results. By undertaking unsupervised analysis this limitation would be overcome.

Following differential expression analyses, attempts were made to take this work further into validation steps. Thus, microarray expression data were validated by real time quantitative PCR. Nevertheless, it should be acknowledged that by using this approach, potentially very interesting targets may have been overlooked. During data filtering for gene target selection non-protein coding genes were excluded. Whilst this is a commonly used approach that has the major advantage of selecting targets for which reagents are readily available (Jaluria et al. 2007), it would have invariable resulted in loss of key information. Amongst those genes not selected for PCR there were long non-coding RNAs, small nucleolar RNAs and small nuclear RNAs. Additionally, microRNAs were identified during differential analysis in response to TNF stimulation. In the light of the available literature regarding microRNAs and the emerging literature regarding long non-coding RNAs, it is very likely that the analysis of these sequences will be crucial in providing new key disease targets.

7 General discussion

The central hypothesis of my thesis was that synovial fibroblasts from patients in different clinical outcome groups would display differing functional and transcriptional characteristics.

This hypothesis was based on the knowledge that synovial fibroblasts from patients with Established RA are involved in disease pathogenesis at two fundamental levels: by perpetuating inflammation and by causing bone and cartilage destruction (Bottini et al. 2013). It was also based on data indicating that treatment of RA during the early window of opportunity results in significantly better outcomes (van der Linden et al. 2010) and that at molecular and histological levels, RA of symptom duration of 3 months or less may be a distinct entity (Raza et al. 2005; Schumacher Jr. et al. 1994).

Three comparisons were of particular interest:

(1) By comparing synovial fibroblasts in the Resolving and VeRA groups I aimed to identify key differences between resolution and persistence of early inflammatory arthritis.

(2) By comparing VeRA and Established RA fibroblasts I intended to gain insights into the progression from early RA to established, destructive disease.

(3) By comparing the transcriptional response to TNF stimulation of fibroblasts in different outcome groups I aimed to determine generic as well as outcome group-specific responses to a pro-inflammatory environment.

With this approach a number of assumptions were made. The main one being that synovial fibroblasts are implicated in the early stages of inflammatory arthritis. This hypothesis suggested that synovial fibroblasts might help decide the fate of these patients by determining whether their arthritis would resolve spontaneously or persist as RA. Further assumptions included that any of these suggested functional or transcriptional differences would be of biological relevance and that we would be able to find such differences by using the experimental methods of our choice.

As I have described, when I assessed the functional characteristics of synovial fibroblasts in the different outcome groups, I failed to find differences between groups using some experimental methods (scratch test and invasion assay) but found differences with another (cell exclusion zone assay). Additionally, the characterisation of the transcriptomic profile of these cells using SAGE technology was fraught with problems but promising hypothesis-generating results were obtained with microarray experiments.

The potential differences between techniques and the potential significance of these differing results have already been discussed and will not be repeated here. Instead, I will focus this discussion on the relevance of these findings and how they may provide a basis for further discoveries in this field. It is important to remember at this point that the study of Resolving, very early (VeRA) and Early RA synovial fibroblasts has never been approached before. It is thus the more remarkable that we did indeed find differences in the characteristics of cells in these groups.

One of the main findings to come out of this work is the observation of differential migration between synovial fibroblasts in different outcome groups. Through the novel application of a cell exclusion zone assay to the study of synovial fibroblast migration, I found that cells from patients with VeRA and Established RA displayed comparable and much slower migration rates than those from Normal joints. It is remarkable that fibroblasts that were obtained from patients and subsequently cultured for 4 to 6 passages displayed such strong migratory phenotypes. This suggests that this is an important characteristic and that it may be an early feature of RA. Based on these findings further study of fibroblast migration is warranted to ascertain its role in disease pathogenesis. To this end, a number of experiments could be performed. Small molecule inhibitors or small interfering RNAs could be used to selectively inhibit the function of different proteins involved in cell migration including Rho, Rac and PI3K. Assessment of the effects of this inhibition on cell migration in different groups might help define important targets causing differential cell migration. Complementary experiments where overexpression of these proteins is induced prior to assessment of cell migration could also be performed. At the same time, data obtained from microarray experiments should be further analysed to identify genes involved in cell migration that are differentially expressed between groups of interest. It is however possible that, such genes may only be found when gene expression is studied in the context of migration. Thus, assessment of transcriptomic profiles of cells in different outcome groups during migration should strongly be considered.

Another finding of interest to come out of this work is the identification of differentially expressed genes between very early and Established RA. These genes may provide keys to molecular mechanisms involved in progression to chronicity and/or severe disease.

Some validation work has already been started and microarray expression results have been replicated at PCR level for some of these genes. Determining whether the protein products of these genes are present and differentially expressed on synovial tissue samples from these patients should be the next step. This approach would enable confirmation that differential gene transcription leads to differential protein production for these genes (two processes that are not always associated owing to post-transcriptional regulation of gene expression) and that the differences in expression are present *ex vivo*, indicating that these observations are not an artefact of *in vitro* culture.

To fully capitalise on these microarray data, non-protein coding genes that were overlooked in the initial validation should be considered as they may provide key information to differential gene regulation between these groups. The study of epigenetic mechanisms that may be involved in the regulation of expression levels of those genes differentially expressed between groups has already begun. This work is being carried out through our collaboration with Professor Steffen Gay and his group, leading experts on the study of DNA methylation and miRNA expression in RA synovial fibroblasts. The methylation status of promoters of differentially expressed genes between these groups is being assessed to determine whether differential DNA methylation may account for the observed differences in gene expression. Furthermore, study of miRNA expression by cells in these outcome groups is also under way. If successful, this approach would provide mechanistic insight into how these differences are generated and maintained and, more importantly, may provide a tool to modify transcriptional phenotypes.

Although the type of analysis I performed did not identify statistically significant differentially expressed genes between the Resolving and VeRA groups, further work should be performed to conclusively prove a lack of difference. The simplest initial approach would be to make use of the existing microarray data and perform class prediction analysis. Even if no differences in gene expression were found with the parameters established during differential analysis, class prediction analysis may lead to identification of groups of expressed and co-expressed genes that would allow prediction of diagnostic category. This work has already been started through a collaboration with the Professor of computing sciences at the University of Groningen, Michael Biehl. Preliminary analysis of expression data suggests that discrimination of patients with resolving inflammatory arthritis and very early RA is feasible. By applying a linear classification scheme he found that data from TNF stimulated samples was predictive of disease outcome with an area under the curve value (AUC) of 0.69. Interestingly, data from unstimulated samples only yielded a random classification performance (AUC=0.49) (Figure 7.1). The same method was applied to data from Normal and Established RA samples, obtaining nearly perfect receiver operating characteristic curves with AUC close to 1.

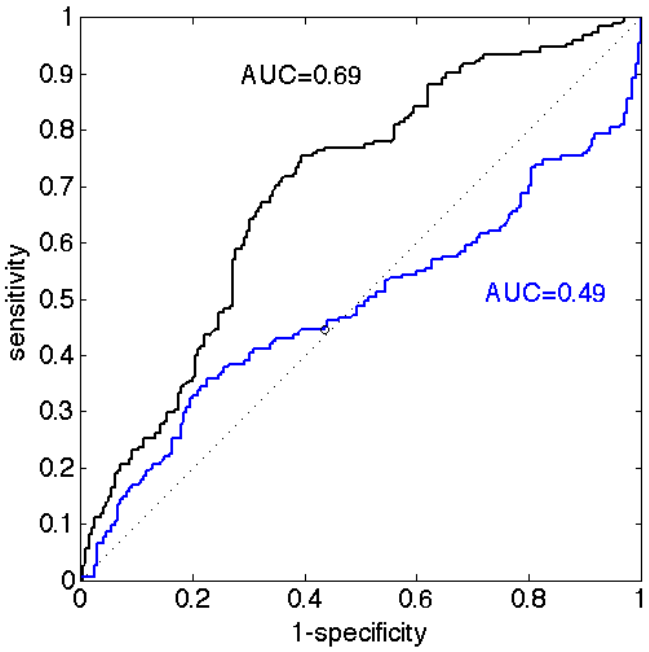

Figure 7.1 Receiver operating characteristic curves indicating the performance of a binary classifier system applied to unstimulated and TNF stimulated microarray data from Resolving and VeRA samples. *A class prediction model was created based on raw microarray data from unstimulated and TNF stimulated samples in the Resolving (n=15) and VeRA (n=13) groups. The classifier system was able to predict outcome for the TNF stimulated (AUC=0.69) but not for the unstimulated samples (AUC=0.49). Black line: TNF stimulated samples data, Blue line: unstimulated samples data.*

This observation is important for two reasons. It gives an indication that synovial fibroblasts may indeed be implicated in both the resolution of inflammatory arthritis and in RA during the very early (≤3 months) window of opportunity and that is thus important to continue work in this field. Furthermore, it also emphasises that in order to identify significant functional differences between these groups, characterisation should not be performed under resting conditions but rather through dynamic *in vitro* approaches such as after TNF stimulation (as described) or during migration.

Additionally, the *ex vivo* study of gene expression of synovial fibroblasts isolated at the time of biopsy should be considered. Although these experiments were not possible at the time of initiation of this thesis, the development of a reliable technique for *ex vivo*

synovial fibroblast isolation in our group together with advances in microarray technologies where ever smaller RNA quantities are required for accurate transcriptomic analysis make it a feasible option. This approach would bypass any potential effects of *in vitro* culture on cellular phenotypes.

Another area of promise that warrants further analysis and verification of results is the comparison between unstimulated and TNF stimulated samples. The study of the different ways in which synovial fibroblasts respond to pro-inflammatory stimuli may prove key to unravel pathogenic mechanisms. This observation is further strengthened by the preliminary results of the class prediction analysis. To take this work forward, filtering of microarray data should be performed to identify target genes for further validation. In this instance, it may be that the study of genes that are uniquely modified by TNF stimulation in each group may prove more useful so that outcome-group specific responses can be determined. As stated earlier, this filtering strategy should also include non-protein coding genes, especially given the observation that such regulatory genes are particularly prevalent in the Resolving group, suggesting that post-transcriptional regulation of gene expression is crucial in the resolution of inflammatory arthritis. Interestingly, our data on lncRNAs may indeed prove complementary to that already discussed of Bertoncelj and colleagues (Bertoncelj et al. 2013; Bertoncelj et al. 2014).

Additionally, unsupervised hierarchical clustering of microarray data sets should be performed. This approach would provide completely unbiased information regarding relationships between these cells. We can speculate about what such analysis might

show. It is likely that TNF stimulated cells would cluster together and separately from unstimulated cells. Given our observations regarding HOX genes, it is also likely that cells will cluster according to joint of origin.

8 Future work

In this body of work I have comprehensively functionally and transcriptionally characterised synovial fibroblasts in five different clinical outcome groups. In doing so, I have produced an extensive amount of data. The potential significance of these findings and possible areas of further work have been detailed in Chapter 7. However, given the wide-ranging possibilities for future study, I will in this chapter map out the most relevant approaches that should be taken as next steps in the mining of these data. Much of this work is currently being carried out through collaborations with experts in the molecular biology and computational biology fields.

The focus of this continued effort is currently placed on further analysis and validation of data looking at the effect of TNF stimulation on gene expression signatures in different clinical outcome groups. This work is being undertaken at different levels simultaneously:

1. Validation of differentially expressed transcripts in response to TNF stimulation: using the same techniques that I have described for the validation of differentially expressed genes between Early and Late RA samples, independent validation of results at PCR level is being undertaken. Making use of the lists of top 50 uniquely changed transcripts in response to TNF stimulation in each group (Tables 6.8 to 6.11), further filtering is being performed to select five protein coding genes in each list. This work involves literature search looking at transcript function and researcher guided selection of relevant genes. It also involves selection of genes for which reagents are available for validation at protein level. Once a decision has been made on candidates, primers will

be designed and real time quantitative PCR undertaken for validation of expression data. In parallel, staining of synovial tissue sections looking for *ex vivo* expression of the protein products of these genes will also be undertaken. This body of work has been conceived as necessary validation of the response to TNF stimulation data analysis. The microarray data together with its validation at PCR and protein levels will hopefully be publishable as a paper describing outcome group specific signatures to TNF stimulation.

To complement this work, further research into the kinetics of synovial fibroblast responses to TNF is being planned. This is because TNF induced genes can respond rapidly (within an hour of stimulation) and may have returned to baseline by 24 hours. Current efforts are directed to securing funding to investigate time-courses of genome wide transcriptional responses to TNF in synovial fibroblasts of different outcome groups. Independently of this, the patterns of expression of genes of interest identified in this section will be investigated over a 24 hour time-course using real time quantitative PCR. This is important in order to understand whether the identified differentially induced genes in response to TNF between outcome groups are really TNF-induced or not in one outcome group or another, or whether the snap-shot analysis has captured subtle differences of kinetics between groups.

2. Gene co-expression analysis. Computational analysis of data looking at co-expressed genes and their links across the different outcome groups. This body of work is designed to take the differential expression analysis that has already been performed a step further. During differential expression analysis, individual genes that are differentially induced in response to TNF stimulation between different clinical outcome groups have been identified. However, the individual identification of these

genes does not provide information about relationships between them. From a systems biology perspective, co-expression analysis is important as co-expressed genes are usually functionally related, often controlled by the same transcriptional regulatory programmes or members of the same pathway or protein complex. This type of analysis should help narrow down candidates for further in depth study as the description of genes that are part of a co-expressed gene network would be of higher biological relevance than that of isolated genes whose expression is modified in response to TNF stimulation. A two-step co-expression analysis will be performed. In the first step a co-expression measure will be selected and a similarity score will be calculated for each pair of genes using this measure. In the second step a significance threshold for this measure will be determined and gene pairs that have a similarity score higher than the threshold will be considered to have a significant co-expression relationship. This work will be performed using the Differentially co-expressed Genes and Links (DCGL) package in the R software environment (Liu et al. 2010).

3. Regulatory network analysis. Co-expression analysis establishes relationships between pairs of genes but does not determine the direction and type of this relationship. In order to identify the regulators that contribute to differential co-expression, regulatory analysis will be performed. This will allow identification of co-expressed genes that are regulated by a given transcription factor. Additionally, a regulatory impact factor will be calculated by applying a metric to each transcription factor that combines the change in co-expression between the transcription factor and the differentially co-expressed target genes. This will enable ranking of transcription factors from most to least significant. The work outlined in points 2 and 3 will be

performed by specialists at the School of Computer Sciences of Birmingham University (Professor Peter Tino and Dr Shan He).

4. Further computational analysis of data looking at relationships between protein coding and non-protein coding, regulatory, transcripts. In the analysis that has already been performed I identified several thousand transcripts that changed in response to TNF stimulation. Amongst these transcripts there are protein coding genes as well as non-protein coding, regulatory, sequences (long non-coding RNAs, micro-RNAs, small nucleolar RNAs and small nuclear RNAs). In an attempt to unravel the epigenetic mechanisms regulating expression of protein coding genes in response to TNF, the relationships between these and regulatory sequences will be analysed using computational algorithms. This work will be performed by specialists at the School of Computer Sciences of Birmingham University. Once these relationships are established and key regulatory sequences identified, molecular biology experiments will be performed to validate computational analysis and dissect molecular mechanisms.

For illustrative purposes I will imagine that a given micro-RNA is identified as having a key regulatory role on the response to TNF stimulation. Further experiments for the study of this target will be designed that might include enforced expression of this micro-RNA (using transfection techniques) in synovial fibroblasts and analysis of the effect of this enforced expression on its target genes (by PCR). In parallel, complementary experiments involving target gene silencing using micro-RNA mimics and inhibition of target gene binding to micro-RNA using antagomirs could be used to demonstrate that target gene expression is being modified by that specific micro-RNA. Such experiments will be designed and performed in collaboration with Professor

Steffen Gay and his group at the University of Zurich. If successful, this approach would provide mechanistic insight into how differences in gene expression in response to TNF stimulation are generated and maintained and, may provide a tool to modify transcriptional phenotypes.

5. The metabolic profiling of parallel unstimulated and TNF stimulated samples to those used in these project have been the subject of analysis in work performed by other researchers within our group. To ensure that target gene selection remains firmly in the context of biologically meaningful observations, these metabolic data will be combined with the microarray expression data described in this thesis. This work will enable identification of pathways common to both datasets and will be performed using the Stemformatics platform. This platform combines bioinformatics and biostatistics tools for integration of transcriptional and metabolic data (Wells et al. 2013). This work is being performed in collaboration with Dr Christine Wells at the School of Life Sciences of the University of Glasgow.

6. Class prediction analysis. In the context of the TNF stimulated dataset and specifically in relation to the Resolving and VeRA groups, class prediction analysis is being performed. This work has already been started by Professor Michael Biehl (Professor of computing sciences at the University of Groningen). Preliminary results obtained using linear classification methods suggest that discrimination of patients with resolving inflammatory arthritis and very early RA is feasible at the time of onset of inflammatory arthritis. Through the application of a linear classification scheme, data from TNF stimulated samples was predictive of disease outcome with an area under the curve value (AUC) of 0.69. Interestingly, data from unstimulated samples only yielded

a random classification performance (AUC=0.49). The same method was applied to data from Normal and Established RA samples, obtaining nearly perfect receiver operating characteristic curves with AUC close to 1. This preliminary analysis is being followed up by further in depth analysis using matrix relevance learning vector quantization (RLVQ). This type of analysis makes use of an algorithm that allows introduction of a full matrix of relevance factors in the distance measure so that correlations between features and their relative importance for the classification scheme can be determined and automated (Schneider et al. 2009). Thus the algorithm is used to identify sets of transcripts that most effectively discriminate between sets of biological samples, in this case, synovial fibroblasts belonging to different outcome groups (Resolving vs. VeRA). Initial application of this analysis to the dataset has resulted on identification of a set of transcripts that strongly discriminate between both outcome groups. On further inspection, the majority of these transcripts have been found to be sex-linked. Given this observation, analysis is currently being repeated paying particular attention to hidden gender biases and results are awaited with interest.

9 APPENDIX

Table 9.1Custom gene sets used in real time PCR assay in microfluidic cards.

Assay ID	Symbol	Protein encoded by gene	Function/Relevance
Hs99999905_m1	GAPDH	Glyceraldehyde 3 phosphate dehydrogenase	Housekeeping gene.
Hs00187842_m1	B2M	Beta 2 microglobulin	Housekeeping gene.
Hs01003372_m1	VCAM1	Vascular cell adhesion protein 1	Cell adhesion molecule expressed by human RA synovial fibroblasts. Marker of activated lining layer synovial fibroblasts (Bottini et al. 2013).
Hs00535586_s1	CD248	Endosialin	Cell surface marker expressed human RA fibroblasts in the sublining layer (Filer 2013). Associated with synovial hyperplasia and leukocyte accumulation in animal models of arthritis (Maia et al. 2010).
Hs00366766_m1	PDPN	Podoplanin	Cell surface marker expressed by RA fibroblasts in the lining layer and associated with expression of αSMA (Ekwall et al. 2011;Filer 2013).
Hs00355202_m1	LGALS1	Galectin 1	Galectin family member with immunosuppressive and anti-inflammatory role. Expressed by cultured RA synovial fibroblasts and in the sublining layer of RA synovial tissues (Dasuri et al. 2004;Ohshima et al. 2003).
Hs00371321_m1	LGALS9	Galectin 9	Galectin family member associated with anti-inflammatory properties. Induces apoptosis of cultured RA synovial fibroblasts (Seki et al. 2007).
Hs00173587_m1	LGALS3	Galectin 3	Galectin family member associated with pro-inflammatory roles. Expressed in RA synovial tissues and by cultured RA synovial fibroblasts where it is particularly expressed at sites of attachment to cartilage and induces pro-inflammatory cytokine secretion (Neidhart et al. 2005;Ohshima et al. 2003).

Hs00263821_m1	LGALS12	Galectin 12	Galectin family member involved in cell cycle regulation and apoptosis. Expressed by cultured RA synovial fibroblasts (Dr Magdalena A Bik thesis).
Hs00222859_m1	CXCL16	Chemokine ligand 16	CXC chemokine family member. Produced by RA synovial fibroblasts. Mediates T cell recruitment to the synovium (Muller-Ladner et al. 2007;Ruth et al. 2006).
Hs00899658_m1	MMP1	Matrix metalloproteinase 1	Matrix metalloproteinase secreted by RA synovial fibroblasts. Involved in cartilage destruction (Bottini et al. 2013).
Hs01548727_m1	MMP2	Matrix metalloproteinase 2	Matrix metalloproteinase secreted by RA synovial fibroblasts. Involved in cartilage destruction (Bottini et al. 2013).
Hs00968308_m1	MMP3	Matrix metalloproteinase 3	Matrix metalloproteinase secreted by RA synovial fibroblasts. Involved in cartilage destruction (Bottini et al. 2013;Okada et al. 1989).
Hs00234579_m1	MMP9	Matrix metalloproteinase 9	Matrix metalloproteinase secreted by RA synovial fibroblasts (Tolboom et al. 2002).
Hs00233992_m1	MMP13	Matrix metalloproteinase 13	Matrix metalloproteinase secreted by RA synovial fibroblasts. Involved in cartilage destruction (Bottini et al. 2013;Lindy et al. 1997).
Hs00377632_m1	CTSL1	Cathepsin L1	Protease involved in cartilage destruction. Expressed in the RA synovium at sites of invasion (Muller-Ladner et al. 1996;Pap et al. 2000b).
Hs00947433_m1	CTSB	Cathepsin B	Protease involved in cartilage destruction. Expressed in RA synovium at sites of invasion (Pap et al. 2000b).
Hs02339312_g1	SUMO1	Small ubiquitin like modifier 1	Overexpressed by RA synovial fibroblasts conferring protection from Fas and TNF mediated apoptosis (Oslejskova et al. 2009;Senolt et al. 2006).
Hs00243201_m1	S100A4	Metastasin	Calcium binding protein involved in diverse biological regulatory activities. Expressed in RA synovium and cultured synovial fibroblasts where it induces MMP (Senolt et al. 2006).
Hs00183740_m1	DKK1	Dickkopf related protein	Negative regulator of the Wnt signalling pathway that promotes bone destruction and is expressed on RA synovial tissue (Diarra et al. 2007;Goldring et al. 2007).
Hs00237184_m1	NAMPT	Nicotinamide phosphoribosyltransferase/visfatin	Adipokine that promotes pro-inflammatory cytokine production

			and motility of RA synovial fibroblasts (Meier et al. 2012).
Hs00237119_m1	MMP14	Matrix metalloproteinase 14	Membrane type MMP that regulates MMP2 activity Expressed in RA synovium together with MMP2 (Goldbach-Mansky et al. 2000).
Hs00166156_m1	CTSK	Cathepsin K	Protease involved in cartilage destruction. Expressed by RA synovial fibroblasts and macrophages (Pap et al. 2000b).
Hs99999901_s1	18S	18S ribosomal RNA	Housekeeping gene.
Hs00171254_m1	IGF2	Insulin like growth factor 2	Hormone protein with similar structure to insulin. Increased expression in cultured RA synovial fibroblasts (Kasperkovitz et al. 2005).
Hs00909449_m1	ACTA2	Alpha smooth muscle actin	Marker of secretory pro-fibrotic myofibroblasts. Expressed by a subset of fibroblasts in the RA synovium localising to the lining layer (Ekwall et al. 2011;Kasperkovitz et al. 2005).
Hs01014511_m1	TLR2	Toll like receptor 2	Toll like receptor expressed by cultured RA synovial fibroblasts and RA synovial tissue of patients with disease of less than 12 months duration (Ospelt et al. 2008).
Hs00152933_m1	TLR3	Toll like receptor 3	Together with TLR4, the most abundantly expressed TLR by cultured RA synovial fibroblasts and RA synovial tissue of patients with disease of less than 12 months duration. Stimulation of TLR3 in these cells leads to increased expression ofIL-6, MMP3 and MMP13 (Bombardieri et al. 2011;Ospelt et al. 2008).
Hs00152939_m1	TLR4	Toll like receptor 4	Together with TLR3, the most abundantly expressed TLR by cultured RA synovial fibroblasts and RA synovial tissue of patients with disease of less than 12 months duration (Ospelt et al. 2008).
Hs00243522_m1	TNFSF11	Receptor activator of nuclear factor kappa B ligand	RANKL is expressed by RA synovial fibroblasts and promotes monocyte to osteoclast differentiation in co-culture models (Takayanagi et al. 2000).
Hs00174774_m1	LGALS3BP	Galectin 3 binding protein	Galectin family member with a role in tumour invasion and host. Expressed on the lining layer of RA synovial tissue particularly at sites of invasion (Ohshima et al. 2003).
Hs00171524_m1	SLIT3	Slit homolog 3	Member of the repellent factor family. Has repulsive functions in nervous system development when bound to its receptor ROBO3.

			This receptor is expressed by cultured RA synovial fibroblast and treatment of cells with its ligand, Slit3, results in inhibition of fibroblast migration *in vitro* (Denk et al. 2010).
Hs00363301_m1	TRERF1	Transcriptional regulating factor 1	Identified as differentially expressed between RA and OA synovial fibroblasts in previous microarray work from our group (Filer A, unpublished).
Hs00230846_m1	SHOX	Short statue homeobox	Identified as differentially expressed between RA and OA synovial fibroblasts in previous microarray work from our group (Filer A, unpublished).
Hs00184008_m1	PIAS1	Protein inhibitor of STAT1	Represses transcription of inflammatory gene promoters (Liu et al. 2008). Identified as differentially expressed between RA and OA synovial fibroblasts in previous microarray work from our group (Filer A, unpublished).
Hs01099999_m1	EGF	Epidermal growth factor	Its receptor is expressed by cultured RA synovial fibroblasts. Stimulation of this receptor results in production of pro-inflammatory cytokines such as IL8 and VEGF (Yamane et al. 2008).
Hs00266645_m1	FGF2	Fibroblast growth factor 2	Member of the fibroblast growth factor family involved in endothelial cell proliferation. Induces RANKL expression by cultured RA synovial fibroblasts and osteoclast maturation (Nakano et al. 2004).
Hs00610488_m1	TP53BP2	Tumour suppressor p53 binding protein 2	Apoptosis regulator. Expression of mutants of the tumour suppressor protein p53 by RA synovial tissue and cultured has been associated to fibroblasts survival via apoptosis regulation (Firestein et al. 1996).
Hs00167241_m1	HTR2A	Serotonin receptor 2A	Expressed by cultured RA synovial fibroblasts. Precise function unknown but thought to have a protective role in disease pathogenesis (Seddighzadeh et al. 2010).
Hs00224228_m1	TNS3	Tensin 3	Involved in actin remodelling and cell migration (Katz et al. 2007) Identified as differentially expressed between RA and OA synovial fibroblasts in previous microarray work from our group

			(Filer A, unpublished).
Hs01026149_m1	EPAS1	Endothelial PAS domain containing protein 1 Encodes Hypoxia inducible factor 2α	Encodes part of a transcription factor involved in up-regulation of gene expression in response to hypoxia (Brahimi-Horn et al. 2005). Identified as differentially expressed between RA and OA synovial fibroblasts in previous microarray work from our group (Filer A, unpublished).
Hs00153153_m1	HIF1A	Hypoxia inducible factor 1α	Transcription factor activated by hypoxia and during inflammation. Expression is up-regulated in in RA lining layer and in cultured RA synovial fibroblasts exposed to pro-inflammatory stimuli (Westra et al. 2007).
Hs00202612_m1	PADI4	Peptidyl arginine deaminase 4	Enzyme that catalyses deamination of arginine residues to citrulline. Associated with susceptibility to RA. Expressed in synovial tissue and fluid (Arend et al. 2012).
Hs00153408_m1	MYC	MYC	Proto-oncogene expressed by RA synovial fibroblasts thought to be involved in fibroblast activation and in tissue invasion and destruction (Huber et al. 2006).
Hs00234119_m1	RAF1	RAF proto-oncogene	Expressed by cultured RA synovial fibroblasts associated with aggressive behaviour (Pap et al. 2000b).
Hs00381211_m1	SYVN1	Synoviolin 1	Pro-proliferative and antiapoptotic protein secreted by cultured RA synovial fibroblasts (Mor et al. 2005).
Hs00170103_m1	INHBA	Inhibin beta A	Subunit of activin A. Activin A is expressed in RA synovial tissue and cultured synovial fibroblasts and associates with proliferation (Ota et al. 2003).
Hs00171022_m1	CXCL12	Chemokine ligand 12	Constitutive chemokine produced by RA synovial fibroblasts involved in inappropriate leucocyte retention (Burger et al. 2001).

Table 9.2 List of primer pair sequences of target genes analysed by PCR identified in SAGE experiments. The sequences of all housekeeper genes tested are also shown here.

Gene symbol	Forward primer	Reverse primer
CAMLG	AACTCGGAACAGCGCATCAA	CACCCAGCACTACTCGCTTT
Chordin	GCGCATCAGTGGACACATTG	*GGTCACAGATCACCGTTCGT*
CHP	ATTTCCGCCCCATTGAGGAT	TTGTTGCTTCGGCTGTTGAG
COMP	TGCGTTCTTCTGCTCACCCTG	*TCCATCACCGTGTTTTTCAGGA*
DFFB	AAGGCTTGGAGTCCCGATTT	TGTCGAAGTAGCTGCCATTGT
E2F2	GCCCAGCTACTGCTACCTACTA	AATCCCCTCCAGATCCAGCTT
F11R	*CGTGCCTTCAGCAACTCTTC*	*GTCAAAGTGGCCTCGGCTAT*
FGF5	CCCGGATGGCAAAGTCAATG	GAAAACGCTCCCTGAACTTGC
MDM2	CCATGCCTGCCCACTTTAGA	CAGGCTGCCATGTGACCTAA
cMET	TGACTTAGCCAACCGAGAGA	TTGAGAGGTTCTTTCCACCAAGT
PAK2	TTGATGGTGCTGCCAAGTCT	*CCAGAAGCCCCTTGTCCAAT*
PDPK1	GCCCACAGTGTTGCAGATTG	GTGAAGCAGCACTGAACACG
SNX1	GAGGGCCGCTTTAGAAAGGT	TGCTGCAGCTTATCAGGCTT
SOCS3	GACGGAGACTTCGATTCGGG	AACTTGCTGTGGGTGACCAT
TGFbR1	ACAACCGCACTGTCATTCAC	TCTCCAAATCGACCTTTGCCA
TRAIL-R4	GTGCACAGAGGGTGTGGATT	TTCTACACGTCCGGCACATC
VAMP A	TGGAAGCTGTGTGGAAAGAGG	TGACAGTCGGAGCATTCCCT
XIAP	CGGAGTTGGCATTTCCAGATT	TGATGTCTGCAGGTACACAAG
PRKCI	CCAAGCCAAGCGTTTCAACA	TCCATGGGCATCACTGGTTC
PTK2	TTGATGGTGCTGCCAAGTCT	CCAGAAGCCCCTTGTCCAAT
RAB3B	TCACGAGAAGCGGGTGAAAC	TAGCCCAGTCTTGGACAGCA
GAPDH	GTCAGCCGCATCTTCTTTTGC	AATCCGTTGACTCCGACCTTCC
18S	AACCCGTTGAACCCCATT	CCATCCAATCGGTAGCG
UBC	CGGGATTTGGGTCGCAGTTCTTG	CGATGGTGTCACTGGGCTCAAC
HMBS	AGGAGTTCAGTGCCATCATC	GCAGCGAAGCAGAGTCTC
RPL13a	AAGGTCGTGCGTCTGAAG	GAGTCCGTGGGTCTTGAG
B2M	GTATGCCTGCCGTGTGAAC	AAAGCAAGCAAGCAGAATTTGG
Bactin	CGGCATCGTCACCAACTG	AACATGATCTGGGTCATCTTCTC
HPRT1	TGACACTGGCAAAACAATGA	GGTCCTTTTCACCGCAAGCT
SDHA	TGGGAACAAGAGGGCATCTG	CCACCACTGCATCAAATTCATG

Table 9.3 List of primer pair sequences of target genes analysed by PCR identified in microarray experiments.

Gene symbol	Forward primer	Reverse primer
ALX1	ATGGAGACGCTGGACAATGAG	CTTTCACGGGAGACATTCGGA
CD300A	TCAAAGCTGGTGACCATTCA	GGAGGCCACAGTGCTGTATT
DFNB31	GCTACGTCACCAACCACATC	TTCTCATCCCCTCCTTGC
EGR1	CAACTACCCTAAGCTGGAGGAGA	CTCGTTGTTCAGAGAGATGTCAG
FMN1	TATTTGGCGGGTGGAGA	CAAGCTCCCTGTGATTCTCTG
FOSB	TCTTCCTCCCCTCAACAGTG	CCTCCTGGAGAGGATGTGA
HAS3	TTTGGCTGTTTTCCCTCTGC	ACATTTGGAGGGCAAGCAAG
HLX	CCCTATGCTGTGCTCACGAA	CTGCTTTCGGTCCGGCTT
ISLR2	GGTTTGTCTCACGTGTTGCAG	GAACATCGCGGCTCCCAATA
ISM2	TCATCAGCACCGACTTCTCA	GAAAGTTCTCCCGTGCAACA
KMT2E	TGGGGATTGATAGGCAGCAT	ACAGGAACCTCATCACCACT
LRIG1	GTAAAGGCTGCTGGTGTTGG	TTCCAGTCCCAGCTCAGTTT
MIA2	ACAAAACTGCTGGCAGACCT	CCTGCCCACAAATCTTCCCT
MME	GTCAGGTTGGCTCTTCAGGTT	TTCTGACTTGCCCATCACCT
MPPED2	GCCTGCTTCCATCTTTTGCT	TGTTGTAGTGCGTGAATGCC
OLFM1	CCAGGCAGTTTAAGGGCTAA	CTACAGTCGCATGCAAAGAGA
OR2H1	TGAGGGCCTGCTTTCTGATT	TGAGGCATGGGGCCTTTTGGG
PABPC1L	ACAAAGGCCGTGACAGAGAT	ATGGCAGGCAGGAAGTAGC
SKAP1	CTTCCCTCTCTCCTGCCTTT	TGCCTCTTCCCACTTGTCTT
TTC9C	GAGACCAGCCTGACCAA	CCCGAGTAGCTGGGTTTACA
CSRNP1	CTGGATGAGAATGCCAACCT	ATCTGGCAGAGCCTGGAGTA
EN1	GCAACCCGGCTATCCTACTT	ATGTAGCGGTTTGCCTGGAA
ETV3	AGGAGGTGGAGGGTATCAGT	GCCACCTCATCTGGATCCTT
FOS	AAGGAGAATCCGAAGGGAAA	CCTTCTCCTTCAGCAGGTTG
HES1	GGCCAGTTTGCTTTCCTCAT	GAGGTGGGTTGGGGAGTTTA
HLX	GACACGTTTCCAGGTCCCTA	GGCTTGTTTCCAGGTCCCTA
LIMS3L	CCCTGCATTATCCCAGAGAA	GCTCCCCATTACTGTTCACG
PER3	AGCTACCTGCACCCTGAAGA	CGAACTTTATGCCGACCAAT
PLEKHG4	CAGGCCCAAGGCTCTTTTCA	TGGGCCAAAGCCCTAGAGAA
RUNX1	CTACCGCAGCCATGAAGAAC	GCTCGGAAAAGGACAAGCTC

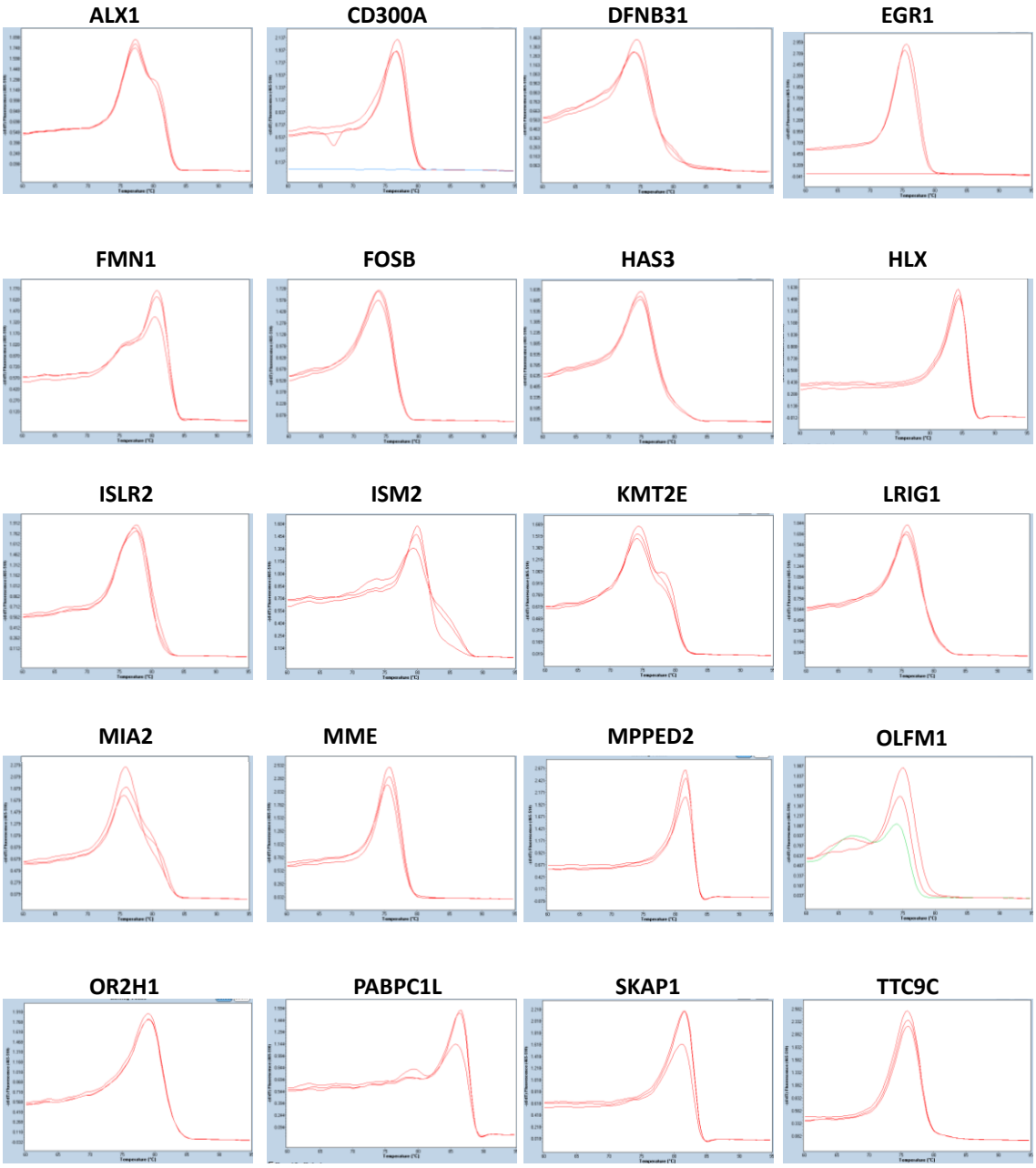

Figure 9.1 Melting curve analysis graphs of primer pairs used in validation of microarray data (unstimulated VeRA vs. Established RA comparison).

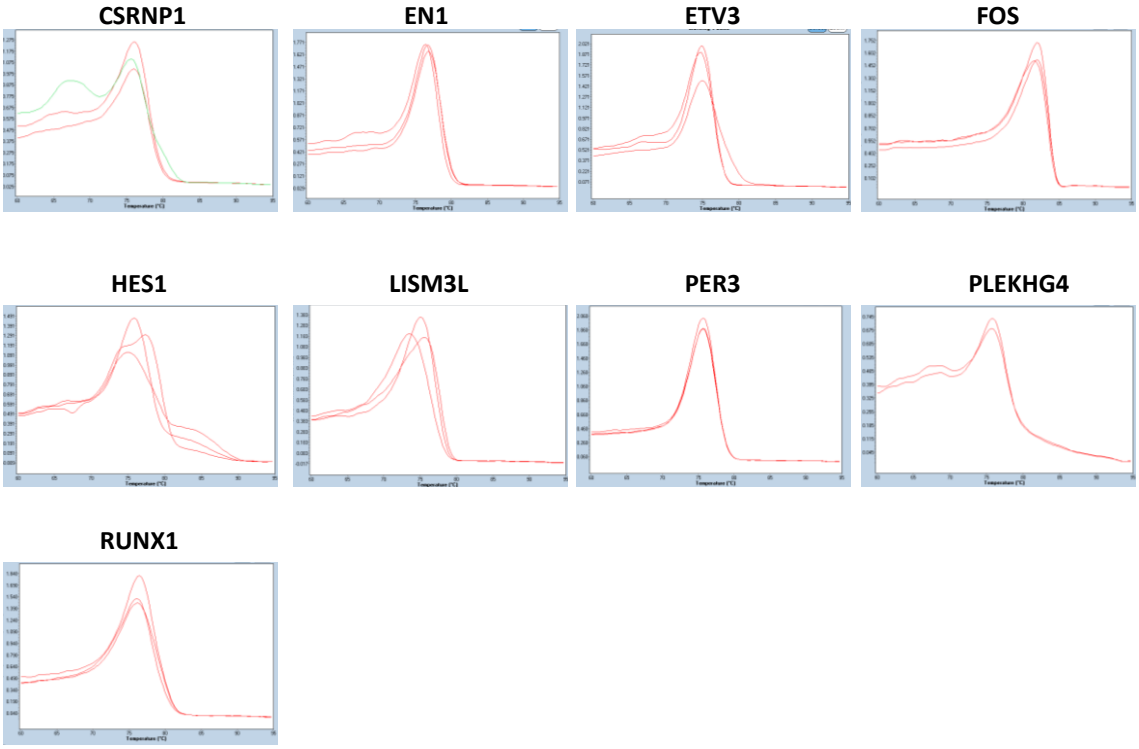

Figure 9.2 Melting curve analysis graphs for primer pairs used in validation of microarray data (TNF stimulated VeRA vs. Established RA comparison). *The melting curves of primer pairs for genes in common with unstimulated samples are represented in Figure 8.1.*

Table 9.4 RNA quantity and quality of samples used in SAGE experiments. *Measured RNA quantity for each sample is represented (mean of triplicate measurement) together with RIN values indicating RNA quality (optimal 8-10).*

Sample SOLID ID	Sample ID	Total RNA (ng/µl)	RIN value
A1	BX081	207.0	9.00
A2	BX016	186.6	9.10
A3	BX022	77.8	8.80
A4	BX003	379.6	9.10
A5	BX063	403.4	9.00
A6	BX038	272.3	8.90
A7	BX010	317.1	8.90
A8	BX082	518.9	9.00
B1	BX055	632.4	9.00
B2	BX066	630.1	9.00
B3	BX031	579.0	9.00
B4	BX014	305.6	8.70
B5	BX004	272.1	9.10
B6	BX064	453.1	9.10
B7	BX070	654.4	8.90
B8	BX083	312.9	9.00
C1	BX077	304.8	9.10
C2	BX018	621.8	9.10
C3	BX015	225.3	9.10
C4	BX048	185.6	8.80
C5	BX069	543.4	8.00
C6	BX076	148.5	9.10
C7	BX088	214.3	9.00
C8	BX033	341.7	8.90
D1	BX075	655.1	8.00
D2	BX093	595.4	8.00
D3	BX042	522.2	8.00
D4	BX013	557.1	7.80
D5	BX005	803.3	7.90
D6	BX095	463.4	8.00
D7	BX089	474.3	7.80
D8	BX008	213.8	8.00
E1	RA06SY	221.9	9.20
E2	RA15SY	101.3	9.60
E3	RA20SY	124.6	9.80
E4	RA23SY	159.4	9.20
E5	RA25SY	93.1	9.80
E6	RA28SY	59.9	9.40
E7	RA29SY	51.4	9.70
E8	RA37SY	112.1	9.80

Table 9.5 Measured RNA concentration and 260/280 and 260/230 ratios of synovial fibroblast samples used in microarray experiments.

Sample Number	Sample ID	Total RNA Concentration (ng/µl)	260/280 ratio	260/230 ratio
Sample 1	Bx003	128.6	2.04	2.03
Sample 2	Bx003	138.5	2.04	1.73
Sample 3	Bx004	158.2	2.05	2.22
Sample 4	Bx004	152.7	2.08	2.04
Sample 5	Bx005	176.5	2.01	1.91
Sample 6	Bx005	175.6	2.03	1.56
Sample 7	BX008	187.9	2.02	2.07
Sample 8	BX008	193.5	2.04	2.07
Sample 9	BX010	175.8	2.03	2.11
Sample 10	BX010	178.8	2.01	1.83
Sample 11	BX011	180.1	1.97	1.82
Sample 12	BX011	184.0	2.02	2.06
Sample 13	BX013	180.6	2.01	1.74
Sample 14	BX013	184.8	2.03	2.01
Sample 15	BX015	178.4	2.03	2.09
Sample 16	BX015	178.2	1.98	1.76
Sample 17	BX020	169.3	2.02	1.87
Sample 18	BX020	164.8	2.03	1.91
Sample 19	BX024	177.4	2.02	2.06
Sample 20	BX024	174.4	2.04	2.17
Sample 21	BX028	180.6	2.01	1.96
Sample 22	BX028	174.2	2.01	1.94
Sample 23	BX030	181.2	1.98	1.93
Sample 24	BX030	181.4	2.03	2.08
Sample 25	BX031	171.4	2.01	1.98
Sample 26	BX031	189.6	2.01	2.11
Sample 27	BX033	192.4	2.04	2.09
Sample 28	BX033	191.6	2.02	2.01
Sample 29	BX038	184.2	2.03	1.94
Sample 30	BX038	184.5	1.97	1.88
Sample 31	BX040	182.9	2.02	2.05
Sample 32	BX040	194.8	2.02	1.96
Sample 33	BX042	149.1	2.04	2.11
Sample 34	BX042	175.0	2.03	2.08
Sample 35	BX045	172.1	2.01	2.03
Sample 36	BX045	168.0	2.02	1.91
Sample 37	BX048	196.9	2.05	2.11
Sample 38	BX048	162.9	2.02	1.94
Sample 39	BX049	185.6	2.04	2.03
Sample 40	BX049	173.0	2.03	2.01
Sample 41	BX054	110.7	2.01	1.75
Sample 42	BX054	170.0	2.04	1.94
Sample 43	BX063	179.8	2.04	2.11
Sample 44	BX063	186.7	2.01	1.77
Sample 45	BX064	171.7	2.04	2.02
Sample 46	BX064	75.5	1.90	1.53
Sample 47	BX065	184.2	2.04	1.51

Sample 48	BX065	181.8	2.07	1.51
Sample 49	BX070	174.1	2.03	1.90
Sample 50	BX070	161.9	2.02	1.81
Sample 51	BX071	171.3	2.01	1.83
Sample 52	BX071	163.8	2.09	1.54
Sample 53	BX072	160.8	2.08	1.51
Sample 54	BX072	176.7	2.05	1.97
Sample 55	BX076	101.5	1.88	1.51
Sample 56	BX076	167.3	1.93	1.52
Sample 57	BX081	190.4	2.03	2.01
Sample 58	BX081	176.6	2.02	1.98
Sample 59	BX082	184.6	2.01	1.92
Sample 60	BX082	183.1	2.05	1.88
Sample 61	BX083	161.3	2.02	2.01
Sample 62	BX083	119.9	1.98	1.69
Sample 63	BX084	148.1	2.01	1.92
Sample 64	BX084	173.9	1.98	2.03
Sample 65	BX085	159.6	2.03	2.01
Sample 66	BX085	190.8	1.91	1.51
Sample 67	BX087	195.4	2.02	1.88
Sample 68	BX087	136.5	2.04	2.05
Sample 69	BX088	182.5	2.03	2.07
Sample 70	BX088	120.4	2.01	1.91
Sample 71	BX089	173.8	2.01	1.81
Sample 72	BX089	114.5	1.98	1.92
Sample 73	BX092	182.3	2.01	1.82
Sample 74	BX092	132.1	1.78	1.57
Sample 75	BX094	162.0	1.95	1.54
Sample 76	BX094	148.6	1.99	1.83
Sample 77	RA06SY	174.7	1.98	1.89
Sample 78	RA06SY	185.3	2.01	1.89
Sample 79	RA15SY	167.5	2.05	2.26
Sample 80	RA15SY	179.9	2.01	1.85
Sample 81	RA20SY	197.3	2.01	2.03
Sample 82	RA20SY	180.9	2.04	2.14
Sample 83	RA23SY	202.1	2.04	1.94
Sample 84	RA23SY	185.1	2.04	1.97
Sample 85	RA25SY	186.7	2.02	1.83
Sample 86	RA25SY	187.9	2.01	1.79
Sample 87	RA28SY	190.6	2.02	2.09
Sample 88	RA28SY	187.0	2.04	2.05
Sample 89	RA29SY	170.8	2.03	2.06
Sample 90	RA29SY	183.8	2.01	1.88
Sample 91	RA37SY	132.0	1.96	1.52
Sample 92	RA37SY	173.7	1.96	1.80

Table 9.6 List of differentially expressed transcripts identified by microarray between unstimulated VeRA and Established RA samples at a fold difference of 2 and FDR<0.05.

Agilent probe ID	Gene symbol	p value
A_21_P0000502	RNU11 (small nuclear RNA)	2.93E-08
A_23_P83798	ALX1	3.15E-05
A_33_P3279708	RNU2-2 (small nuclear RNA)	2.16E-06
A_33_P3267263	RNU1-5 (small nuclear RNA)	1.63E-07
A_23_P100730	SKAP1	2.16E-05
A_33_P3413808	PABPC1L	2.43E-06
A_33_P3423285	SETD5-antisense RNA (lncRNA)	1.61E-06
A_21_P0005609	LOC100216545	4.50E-06
A_33_P3388636	FLJ40606	5.65E-06
A_21_P0004515	XLOC_004452	1.31E-06
A_23_P344125	ISM2	3.26E-06
A_33_P3399693	Protein LOC100128374	8.34E-05
A_21_P0000385	SNORD88C	2.94E-05
A_32_P105825	MPPED2	8.79E-05
A_33_P3370094	MME	1.12E-05
A_19_P00316370	LOC100506178	1.56E-05
A_32_P379467	ISLR2	3.89E-05
A_21_P0010269	XLOC_014003	5.94E-06
A_21_P0014898	LOC100652951	1.40E-05
A_33_P3248354	OLFM1	5.16E-05
A_24_P940897	OR2H1	2.99E-05
A_33_P3355371	TTC9C	4.14E-06
A_33_P3290707	MME	3.96E-05
A_23_P117387	MIA2	6.41E-05
A_23_P126266	HLX	1.82E-05
A_21_P0000269	SNORA52 (small nucleolar)	2.15E-05
A_33_P3371204	BX098631	2.29E-05
A_33_P3324505	KMT2E	1.01E-05
A_33_P3379881	FMN1	3.44E-05
A_24_P376129	DFNB31	2.83E-05
A_23_P429998	FOSB	3.89E-05
A_21_P0010386	LOC100271722	3.18E-05
A_23_P214080	EGR1	2.58E-05
A_21_P0004839	XLOC_005176	2.72E-05
A_21_P0004050	XLOC_004524	5.74E-05
A_33_P3348001	LOC100130458	4.74E-05
A_23_P109636	LRIG1	3.90E-05
A_23_P207037	CD300A	6.90E-05
A_23_P393034	HAS3	4.03E-05
A_33_P3346067	LOC388813	6.48E-05

Table 9.7 List of differentially expressed transcripts identified by microarray between TNF stimulated VeRA and Established RA samples at a fold difference of 2 and FDR<0.05.

Agilent probe ID	Gene symbol	p value
A_32_P113812	ENST00000425161	1.30E-07
A_33_P3423285	SETD5-antisense RNA (lncRNA)	1.93E-07
A_23_P429998	FOSB	2.92E-07
A_21_P0014532	LOC100287415	6.72E-07
A_33_P3388636	FLJ40606	7.66E-07
A_23_P6596	HES1	1.64E-06
A_33_P3343452	ANKRD30B	2.05E-06
A_33_P3267263	RNU1-5 (small nuclear RNA)	3.82E-06
A_23_P106194	FOS	3.96E-06
A_21_P0005609	LOC100216545	4.28E-06
A_33_P3282205	AK026419	4.82E-06
A_21_P0000502	RNU11 (small nuclear RNA)	5.22E-06
A_33_P3295173	HSPB11	6.31E-06
A_24_P34155	RUNX1	7.05E-06
A_33_P3392405	C10orf99	8.70E-06
A_21_P0014498	LOC100506978	8.82E-06
A_23_P83798	ALX1	9.91E-06
A_23_P345460	PLEKHG4	1.31E-05
A_21_P0008322	XLOC_010804	1.33E-05
A_23_P117387	MIA2	1.45E-05
A_21_P0008666	XLOC_011338	1.86E-05
A_21_P0004691	XLOC_005480	2.05E-05
A_23_P214080	EGR1	2.14E-05
A_21_P0003803	XLOC_004182	2.23E-05
A_33_P3370094	MME	2.33E-05
A_23_P43337	FREM1	2.61E-05
A_23_P126266	HLX	2.78E-05
A_33_P3279708	RNU2-2 (small nuclear RNA)	2.83E-05
A_33_P3324505	KMT2E	2.90E-05
A_21_P0010386	LOC100271722	3.00E-05
A_21_P0001232	XLOC_001230	3.23E-05
A_33_P3385161	EFCAB9	3.40E-05
A_19_P00321096	XLOC_001394	4.09E-05
A_33_P3237050	OR4K14	4.13E-05
A_33_P3314468	IMMT	4.39E-05
A_33_P3268310	LIMS3L	4.66E-05
A_23_P400945	ETV3	4.68E-05
A_21_P0014451	LOC100287506	4.91E-05
A_23_P254688	TMEM108	4.95E-05
A_23_P157333	EPHA1	5.08E-05
A_21_P0010510	LOC100133612	5.21E-05
A_24_P927325	C2CD3	5.43E-05
A_24_P732099	HBBP1	5.74E-05
A_23_P139635	DAO	5.88E-05
A_21_P0012315	XLOC_l2_009302	6.09E-05
A_23_P121011	CSRNP1	6.52E-05
A_23_P89981	CYP2F1	6.69E-05
A_21_P0009749	XLOC_013275	7.05E-05

A_33_P3282305	ADARB2	7.10E-05
A_33_P3285799	AKD1	7.17E-05
A_21_P0008263	XLOC_010693	7.21E-05
A_21_P0007249	XLOC_009233	7.43E-05
A_33_P3332414	ABCB1	7.58E-05
A_21_P0014359	LOC100506418	8.05E-05
A_21_P0014657	LOC100506502	8.52E-05
A_21_P0010481	XLOC_014404	8.58E-05
A_33_P3248610	ASXL2	8.65E-05
A_33_P3409337	C14orf45	8.68E-05
A_21_P0014898	LOC100652951	9.35E-05
A_33_P3290707	MME	9.60E-05
A_24_P230948	PER3	9.70E-05
A_19_P00316897	ENST00000514376	0.000101
A_33_P3839897	RNU4ATAC (small nuclear RNA)	0.000103
A_33_P3245238	SULT1C2	0.00011
A_23_P66682	HOXB6	0.000111
A_33_P3224070	CSRNP1	0.000123
A_23_P41599	PCDHB8	0.00013
A_33_P3269109	GUCY1A3	0.000133
A_24_P260101	MME	0.000133
A_21_P0011683	ZNF729	0.000144
A_33_P3298440	LOC729324	0.000155
A_23_P5679	CFC1	0.000155
A_23_P56404	EN1	0.000165
A_21_P0000269	SNORA52 (small nucleolar RNA)	0.000194
A_33_P3407746	PPM1B	0.000213
A_33_P3892710	SNORA22 (small nucleolar RNA)	0.000214
A_23_P393034	HAS3	0.000216
A_33_P3385002	ELK1	0.000232
A_21_P0005421	XLOC_006223	0.000248

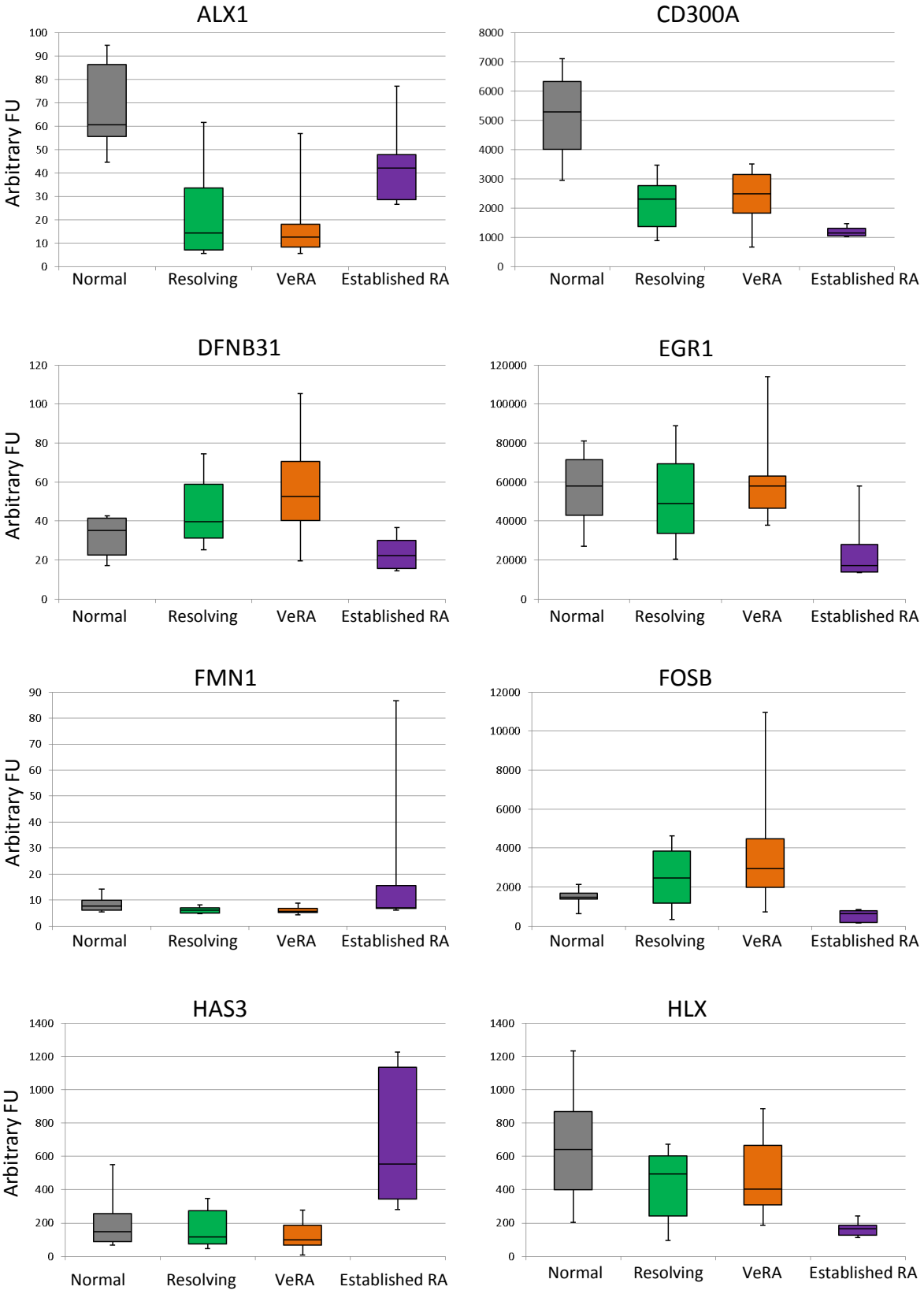
ALX1
CD300A
DFNB31
EGR1
FMN1
FOSB
HAS3
HLX
Arbitrary FU
Normal
Resolving
VeRA
Established RA

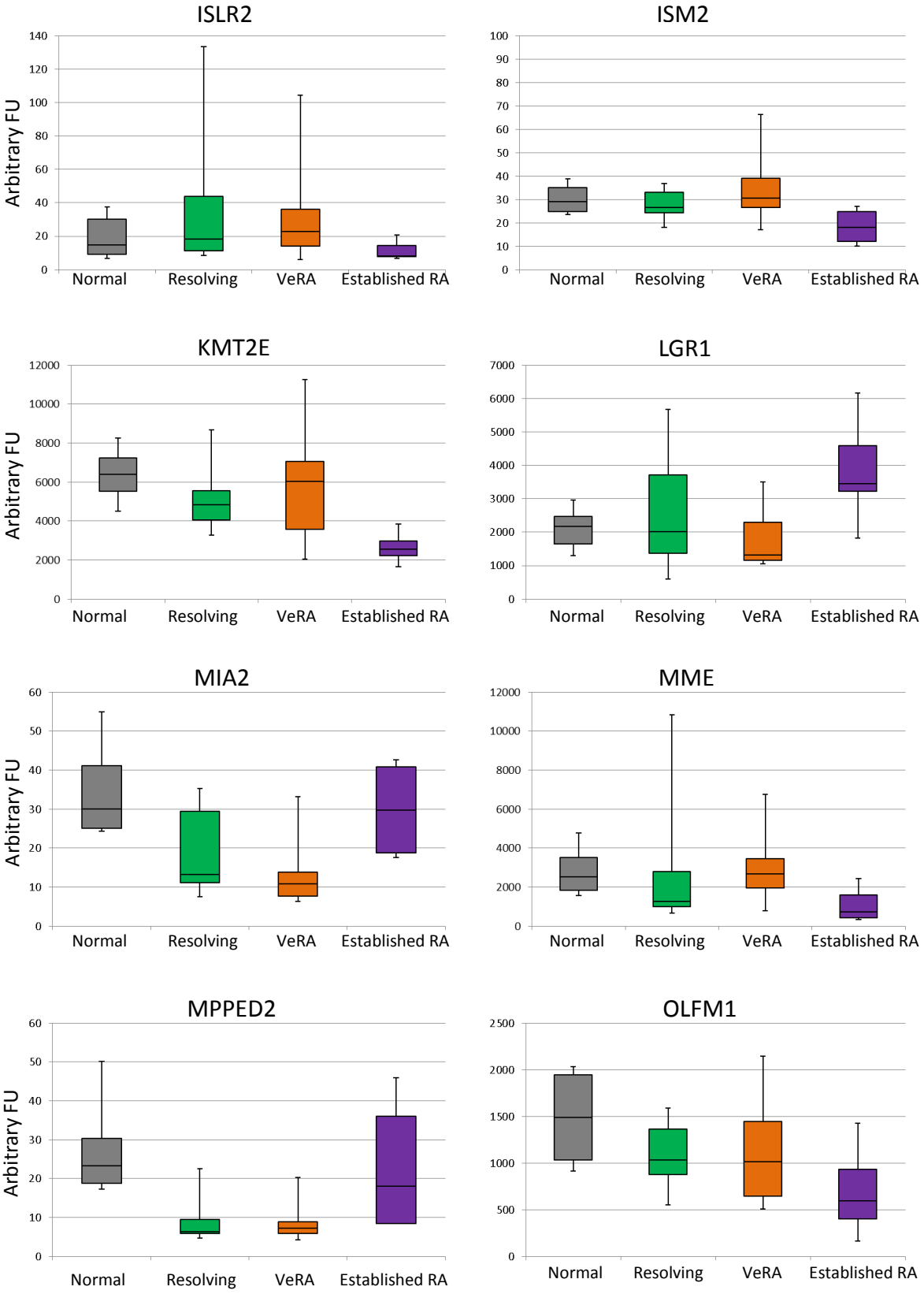
ISLR2
Arbitrary FU
0
20
40
60
80
100
120
140
Normal
Resolving
VeRA
Established RA
ISM2
0
10
20
30
40
50
60
70
80
90
100
KMT2E
0
2000
4000
6000
8000
10000
12000
LGR1
0
1000
2000
3000
4000
5000
6000
7000
MIA2
0
10
20
30
40
50
60
MME
0
2000
4000
6000
8000
10000
12000
MPPED2
OLFM1
0
500
1000
1500
2000
2500

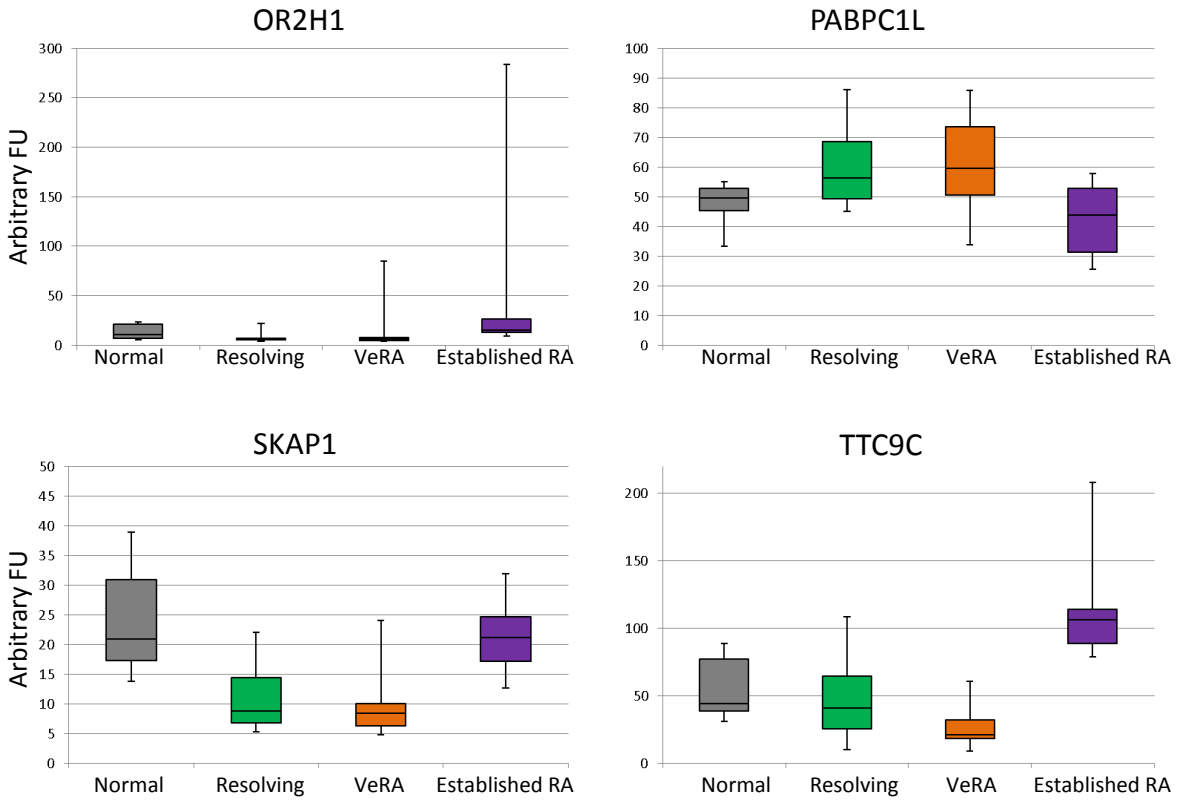

Figure 9.3 Expression levels of selected target genes assessed by microarray in unstimulated samples. *Raw microarray data representing expression levels of 20 target genes in unstimulated Normal (n=8), Resolving (n=15), VeRA (n=13) and Established RA (n=7) samples are represented. Expression levels expressed as arbitrary fluorescence units (FU).*

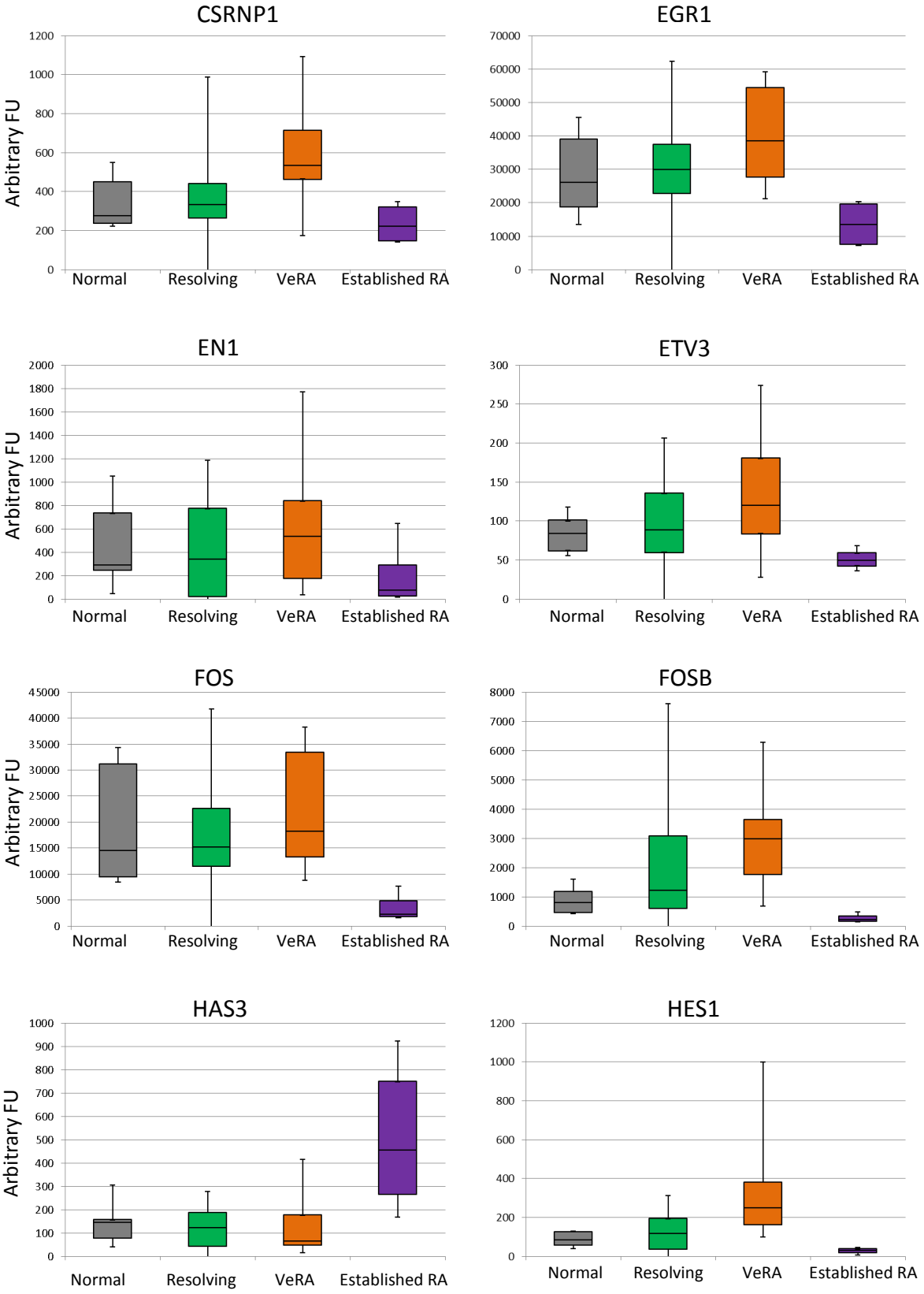
CSRNP1
Arbitrary FU
0
200
400
600
800
1000
1200
Normal
Resolving
VeRA
Established RA
EGR1
0
10000
20000
30000
40000
50000
60000
70000
EN1
0
200
400
600
800
1000
1200
1400
1600
1800
2000
ETV3
0
50
100
150
200
250
300
FOS
0
5000
10000
15000
20000
25000
30000
35000
40000
45000
FOSB
0
1000
2000
3000
4000
5000
6000
7000
8000
HAS3
0
100
200
300
400
500
600
700
800
900
1000
HES1
0
200
400
600
800
1000
1200

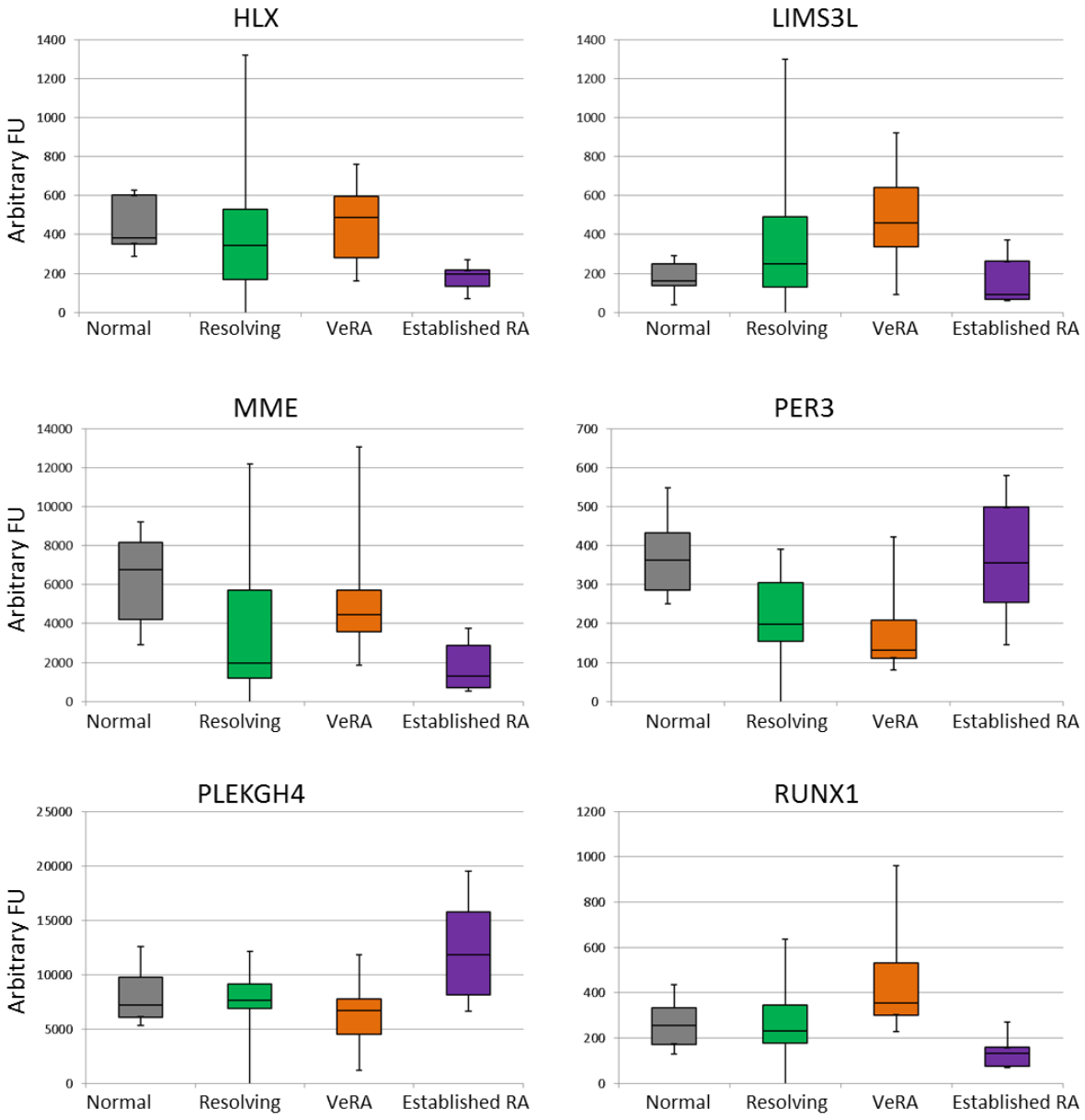

Figure 9.4 Expression levels of selected target genes assessed by microarray in TNF stimulated samples. *Raw microarray data representing expression levels of 14 target genes in TNF stimulated Normal (n=8), Resolving (n=15), VeRA (n=13) and Established RA (n=7) samples are represented. Expression levels expressed as arbitrary fluorescence units (FU).*

References

Aicher, W. K., Alexander, D., Haas, C., Kuchen, S., Pagenstecher, A., Gay, S., Peter, H. H., & Eibel, H. 2003, "Transcription factor early growth response 1 activity up-regulates expression of tissue inhibitor of metalloproteinases 1 in human synovial fibroblasts", *Arthritis Rheum.*, vol. 48, no. 2, pp. 348-359.

Aicher, W. K., Heer, A. H., Trabandt, A., Bridges, S. L., Jr., Schroeder, H. W., Jr., Stransky, G., Gay, R. E., Eibel, H., Peter, H. H., Siebenlist, U., & . 1994, "Overexpression of zinc-finger transcription factor Z-225/Egr-1 in synoviocytes from rheumatoid arthritis patients", *J.Immunol.*, vol. 152, no. 12, pp. 5940-5948.

Aletaha, D., Eberl, G., Nell, V. P., Machold, K. P., & Smolen, J. S. 2004, "Attitudes to early rheumatoid arthritis: changing patterns. Results of a survey", *Ann.Rheum.Dis.*, vol. 63, no. 10, pp. 1269-1275.

Aletaha, D., Neogi, T., Silman, A. J., Funovits, J., Felson, D. T., Bingham, C. O., III, Birnbaum, N. S., Burmester, G. R., Bykerk, V. P., Cohen, M. D., Combe, B., Costenbader, K. H., Dougados, M., Emery, P., Ferraccioli, G., Hazes, J. M., Hobbs, K., Huizinga, T. W., Kavanaugh, A., Kay, J., Kvien, T. K., Laing, T., Mease, P., Menard, H. A., Moreland, L. W., Naden, R. L., Pincus, T., Smolen, J. S., Stanislawska-Biernat, E., Symmons, D., Tak, P. P., Upchurch, K. S., Vencovsky, J., Wolfe, F., & Hawker, G. 2010, "2010 rheumatoid arthritis classification criteria: an American College of Rheumatology/European League Against Rheumatism collaborative initiative", *Ann.Rheum.Dis.*, vol. 69, no. 9, pp. 1580-1588.

Alexander, D., Judex, M., Meyringer, R., Weis-Klemm, M., Gay, S., Muller-Ladner, U., & Aicher, W. K. 2002, "Transcription factor Egr-1 activates collagen expression in immortalized fibroblasts or fibrosarcoma cells", *Biol.Chem.*, vol. 383, no. 12, pp. 1845-1853.

Arend, W. P. & Firestein, G. S. 2012, "Pre-rheumatoid arthritis: predisposition and transition to clinical synovitis", *Nat.Rev.Rheumatol.*, vol. 8, no. 10, pp. 573-586.

Arnett, F. C., Edworthy, S. M., Bloch, D. A., McShane, D. J., Fries, J. F., Cooper, N. S., Healey, L. A., Kaplan, S. R., Liang, M. H., Luthra, H. S., & . 1988, "The American Rheumatism Association 1987 revised criteria for the classification of rheumatoid arthritis", *Arthritis Rheum.*, vol. 31, no. 3, pp. 315-324.

Asahara, H., Fujisawa, K., Kobata, T., Hasunuma, T., Maeda, T., Asanuma, M., Ogawa, N., Inoue, H., Sumida, T., & Nishioka, K. 1997, "Direct evidence of high DNA binding activity of transcription factor AP-1 in rheumatoid arthritis synovium", *Arthritis Rheum.*, vol. 40, no. 5, pp. 912-918.

Baecher-Allan, C., Viglietta, V., & Hafler, D. A. 2002, "Inhibition of human CD4(+)CD25(+high) regulatory T cell function", *J.Immunol.*, vol. 169, no. 11, pp. 6210-6217.
Boers, M. 2003, "Understanding the window of opportunity concept in early rheumatoid arthritis", *Arthritis Rheum.*, vol. 48, no. 7, pp. 1771-1774.

Boers, M., Verhoeven, A. C., Markusse, H. M., van de Laar, M. A., Westhovens, R., van Denderen, J. C., van, Z. D., Dijkmans, B. A., Peeters, A. J., Jacobs, P., van den Brink, H. R., Schouten, H. J., van der Heijde, D. M., Boonen, A., & van der Linden, S. 1997, "Randomised comparison of combined step-down prednisolone, methotrexate and sulphasalazine with sulphasalazine alone in early rheumatoid arthritis", *Lancet*, vol. 350, no. 9074, pp. 309-318.

Bombardieri, M., Kam, N. W., Brentano, F., Choi, K., Filer, A., Kyburz, D., McInnes, I. B., Gay, S., Buckley, C., & Pitzalis, C. 2011, "A BAFF/APRIL-dependent TLR3-stimulated pathway enhances the capacity of rheumatoid synovial fibroblasts to induce AID expression and Ig class-switching in B cells", *Ann.Rheum.Dis.*, vol. 70, no. 10, pp. 1857-1865.

Borrego, F. 2013, "The CD300 molecules: an emerging family of regulators of the immune system", *Blood*, vol. 121, no. 11, pp. 1951-1960.

Bottini, N. & Firestein, G. S. 2013, "Duality of fibroblast-like synoviocytes in RA: passive responders and imprinted aggressors", *Nat.Rev.Rheumatol.*, vol. 9, no. 1, pp. 24-33.

Bradley, K., Scatizzi, J. C., Fiore, S., Shamiyeh, E., Koch, A. E., Firestein, G. S., Gorges, L. L., Kuntsman, K., Pope, R. M., Moore, T. L., Han, J., & Perlman, H. 2004, "Retinoblastoma suppression of matrix metalloproteinase 1, but not interleukin-6, through a p38-dependent pathway in rheumatoid arthritis synovial fibroblasts", *Arthritis Rheum*, vol. 50, no. 1, pp. 78-87.

Brahimi-Horn, M. C. & Pouyssegur, J. 2005, "The hypoxia-inducible factor and tumor progression along the angiogenic pathway", *Int.Rev.Cytol.*, vol. 242, pp. 157-213.

Broere, F., Apasov, S. G., Sitkovsky, M. V., & van Edem, W. 1999, "T cell subsets and T-cell mediated immunity," in *Principles of Immunopharmacology*, 1 edn, F. P. Nijkamp & M. J. Parnham, eds., Springer, Basel, pp. 15-27.

Buckley, C. D., Amft, N., Bradfield, P. F., Pilling, D., Ross, E., Arenzana-Seisdedos, F., Amara, A., Curnow, S. J., Lord, J. M., Scheel-Toellner, D., & Salmon, M. 2000, "Persistent induction of the chemokine receptor CXCR4 by TGF-beta 1 on synovial T cells contributes to their accumulation within the rheumatoid synovium", *J.Immunol.*, vol. 165, no. 6, pp. 3423-3429.

Buckley, C. D., Pilling, D., Lord, J. M., Akbar, A. N., Scheel-Toellner, D., & Salmon, M. 2001, "Fibroblasts regulate the switch from acute resolving to chronic persistent inflammation", *Trends Immunol.*, vol. 22, no. 4, pp. 199-204.

Burger, J. A., Zvaifler, N. J., Tsukada, N., Firestein, G. S., & Kipps, T. J. 2001, "Fibroblast-like synoviocytes support B-cell pseudoemperipolesis via a stromal cell-derived factor-1- and CD106 (VCAM-1)-dependent mechanism", *J.Clin.Invest*, vol. 107, no. 3, pp. 305-315.

Cader, M. Z., Filer, A., Hazlehurst, J., de, P. P., Buckley, C. D., & Raza, K. 2011, "Performance of the 2010 ACR/EULAR criteria for rheumatoid arthritis: comparison with 1987 ACR criteria in a very early synovitis cohort", *Ann Rheum Dis*, vol. 70, no. 6, pp. 949-955.

Cascao, R., Rosario, H. S., Souto-Carneiro, M. M., & Fonseca, J. E. 2010, "Neutrophils in rheumatoid arthritis: More than simple final effectors", *Autoimmun.Rev.*, vol. 9, no. 8, pp. 531-535.

Ceribelli, A., Yao, B., Dominguez-Gutierrez, P. R., Nahid, M. A., Satoh, M., & Chan, E. K. 2011, "MicroRNAs in systemic rheumatic diseases", *Arthritis Res.Ther.*, vol. 13, no. 4, p. 229.

Chabaud, M., Durand, J. M., Buchs, N., Fossiez, F., Page, G., Frappart, L., & Miossec, P. 1999, "Human interleukin-17: A T cell-derived proinflammatory cytokine produced by the rheumatoid synovium", *Arthritis Rheum.*, vol. 42, no. 5, pp. 963-970.

Chan, A., Akhtar, M., Brenner, M., Zheng, Y., Gulko, P. S., & Symons, M. 2007, "The GTPase Rac regulates the proliferation and invasion of fibroblast-like synoviocytes from rheumatoid arthritis patients", *Mol.Med.*, vol. 13, no. 5-6, pp. 297-304.

Chan, A., Filer, A., Parsonage, G., Kollnberger, S., Gundle, R., Buckley, C. D., & Bowness, P. 2008, "Mediation of the proinflammatory cytokine response in rheumatoid arthritis and spondylarthritis by interactions between fibroblast-like synoviocytes and natural killer cells", *Arthritis Rheum.*, vol. 58, no. 3, pp. 707-717.

Chang, H. Y., Chi, J. T., Dudoit, S., Bondre, C., van de Rijn, M., Botstein, D., & Brown, P. O. 2002, "Diversity, topographic differentiation, and positional memory in human fibroblasts", *Proc.Natl.Acad.Sci.U.S.A*, vol. 99, no. 20, pp. 12877-12882.

Cho, M. L., Yoon, C. H., Hwang, S. Y., Park, M. K., Min, S. Y., Lee, S. H., Park, S. H., & Kim, H. Y. 2004, "Effector function of type II collagen-stimulated T cells from rheumatoid arthritis patients: cross-talk between T cells and synovial fibroblasts", *Arthritis Rheum.*, vol. 50, no. 3, pp. 776-784.

Chu, C. Q., Field, M., Allard, S., Abney, E., Feldmann, M., & Maini, R. N. 1992, "Detection of cytokines at the cartilage/pannus junction in patients with rheumatoid arthritis: implications for the role of cytokines in cartilage destruction and repair", *Br.J.Rheumatol.*, vol. 31, no. 10, pp. 653-661.

Chu, C. Q., Field, M., Feldmann, M., & Maini, R. N. 1991, "Localization of tumor necrosis factor alpha in synovial tissues and at the cartilage-pannus junction in patients with rheumatoid arthritis", *Arthritis Rheum.*, vol. 34, no. 9, pp. 1125-1132.

Chuang, L. Y., Cheng, Y. H., & Yang, C. H. 2013, "Specific primer design for the polymerase chain reaction", *Biotechnol.Lett.*, vol. 35, no. 10, pp. 1541-1549.

Cortessis, V. K., Thomas, D. C., Levine, A. J., Breton, C. V., Mack, T. M., Siegmund, K. D., Haile, R. W., & Laird, P. W. 2012, "Environmental epigenetics: prospects for studying epigenetic mediation of exposure-response relationships", *Hum.Genet.*, vol. 131, no. 10, pp. 1565-1589.

Cush, J. J. 2007, "Early rheumatoid arthritis -- is there a window of opportunity?", *J.Rheumatol.Suppl*, vol. 80, pp. 1-7.

Danoy, P., Wei, M., Johanna, H., Jiang, L., He, D., Sun, L., Zeng, X., Visscher, P. M., Brown, M. A., & Xu, H. 2011, "Association of variants in MMEL1 and CTLA4 with rheumatoid arthritis in the Han Chinese population", *Ann.Rheum.Dis.*, vol. 70, no. 10, pp. 1793-1797.

Dasuri, K., Antonovici, M., Chen, K., Wong, K., Standing, K., Ens, W., El-Gabalawy, H., & Wilkins, J. A. 2004, "The synovial proteome: analysis of fibroblast-like synoviocytes", *Arthritis Res.Ther.*, vol. 6, no. 2, p. R161-R168.

de Pablo, P., Chapple, I. L., Buckley, C. D., & Dietrich, T. 2009, "Periodontitis in systemic rheumatic diseases", *Nat.Rev.Rheumatol.*, vol. 5, no. 4, pp. 218-224.

de Rooy, D. 2012, "Genetic studies on components of the Wnt signalling pathway and the severity of joint destruction in rheumatoid arthritis", *Ann.Rheum.Dis.*, doi:10.1136.

Degli-Esposti, M. A., Dougall, W. C., Smolak, P. J., Waugh, J. Y., Smith, C. A., & Goodwin, R. G. 1997, "The novel receptor TRAIL-R4 induces NF-kappaB and protects against TRAIL-mediated apoptosis, yet retains an incomplete death domain", *Immunity.*, vol. 7, no. 6, pp. 813-820.

Del Rey, M. J., Izquierdo, E., Usategui, A., Gonzalo, E., Blanco, F. J., Acquadro, F., & Pablos, J. L. 2010, "The transcriptional response of normal and rheumatoid arthritis synovial fibroblasts to hypoxia", *Arthritis Rheum.*, vol. 62, no. 12, pp. 3584-3594.

Denk, A. E., Kaufmann, S., Stark, K., Schedel, J., Lowin, T., Schubert, T., & Bosserhoff, A. K. 2010, "Slit3 inhibits Robo3-induced invasion of synovial fibroblasts in rheumatoid arthritis", *Arthritis Res.Ther.*, vol. 12, no. 2, p. R45.

Dennis, G., Holweg, C. T. J., Kummerfeld, S. K., Choy, D. F., Setiadi, A. F., Hackney, J. A., Haverty P.M., & Gilbert, H. 2014, "Synovial phenotypes in rheumatoid arthritis correlate with response to biologic therapeutics", *Arthritis Res.Ther.* p. R90.

Dheda, K., Huggett, J. F., Bustin, S. A., Johnson, M. A., Rook, G., & Zumla, A. 2004, "Validation of housekeeping genes for normalizing RNA expression in real-time PCR", *Biotechniques*, vol. 37, no. 1, pp. 112-119.

Diarra, D., Stolina, M., Polzer, K., Zwerina, J., Ominsky, M. S., Dwyer, D., Korb, A., Smolen, J., Hoffmann, M., Scheinecker, C., van der Heide, D., Landewe, R., Lacey, D., Richards, W. G., & Schett, G. 2007, "Dickkopf-1 is a master regulator of joint remodeling", *Nat.Med.*, vol. 13, no. 2, pp. 156-163.

Dillies, M. A., Rau, A., Aubert, J., Hennequet-Antier, C., Jeanmougin, M., Servant, N., Keime, C., Marot, G., Castel, D., Estelle, J., Guernec, G., Jagla, B., Jouneau, L., Laloe, D., Le, G. C., Schaeffer, B., Le, C. S., Guedj, M., & Jaffrezic, F. 2013, "A comprehensive evaluation of normalization methods for Illumina high-throughput RNA sequencing data analysis", *Brief.Bioinform.*, vol. 14, no. 6, pp. 671-683.

Edwards, J. C., Szczepanski, L., Szechinski, J., Filipowicz-Sosnowska, A., Emery, P., Close, D. R., Stevens, R. M., & Shaw, T. 2004, "Efficacy of B-cell-targeted therapy with rituximab in patients with rheumatoid arthritis", *N.Engl.J.Med.*, vol. 350, no. 25, pp. 2572-2581.

Ehrenstein, M. R., Evans, J. G., Singh, A., Moore, S., Warnes, G., Isenberg, D. A., & Mauri, C. 2004, "Compromised function of regulatory T cells in rheumatoid arthritis and reversal by anti-TNFalpha therapy", *J.Exp.Med.*, vol. 200, no. 3, pp. 277-285.

Ekwall, A. K., Eisler, T., Anderberg, C., Jin, C., Karlsson, N., Brisslert, M., & Bokarewa, M. I. 2011, "The tumour-associated glycoprotein podoplanin is expressed in fibroblast-like synoviocytes of the hyperplastic synovial lining layer in rheumatoid arthritis", *Arthritis Res.Ther.*, vol. 13, no. 2, p. R40.

Etienne-Manneville, S. & Hall, A. 2002, "Rho GTPases in cell biology", *Nature*, vol. 420, no. 6916, pp. 629-635.

Eyre, S., Bowes, J., Diogo, D., Lee, A., Barton, A., Martin, P., Zhernakova, A., Stahl, E., Viatte, S., McAllister, K., Amos, C. I., Padyukov, L., Toes, R. E., Huizinga, T. W., Wijmenga, C., Trynka, G., Franke, L., Westra, H. J., Alfredsson, L., Hu, X., Sandor, C., de Bakker, P. I., Davila, S., Khor, C. C., Heng, K. K., Andrews, R., Edkins, S., Hunt, S. E., Langford, C., Symmons, D., Concannon, P., Onengut-Gumuscu, S., Rich, S. S., Deloukas, P., Gonzalez-Gay, M. A., Rodriguez-Rodriguez, L., Arlsetig, L., Martin, J., Rantapaa-Dahlqvist, S., Plenge, R. M., Raychaudhuri, S., Klareskog, L., Gregersen, P. K., & Worthington, J. 2012, "High-density genetic mapping identifies new susceptibility loci for rheumatoid arthritis", *Nat.Genet.*, vol. 44, no. 12, pp. 1336-1340.

Faour, W. H., Alaaeddine, N., Mancini, A., He, Q. W., Jovanovic, D., & Di Battista, J. A. 2005, "Early growth response factor-1 mediates prostaglandin E2-dependent transcriptional suppression of cytokine-induced tumor necrosis factor-alpha gene expression in human macrophages and rheumatoid arthritis-affected synovial fibroblasts", *J Biol.Chem.*, vol. 280, no. 10, pp. 9536-9546.

Feng, Y. & Longmore, G. D. 2005, "The LIM protein Ajuba influences interleukin-1-induced NF-kappaB activation by affecting the assembly and activity of the protein kinase Czeta/p62/TRAF6 signaling complex", *Mol.Cell Biol.*, vol. 25, no. 10, pp. 4010-4022.

Filer, A. 2013, "The fibroblast as a therapeutic target in rheumatoid arthritis", *Curr.Opin.Pharmacol.*, vol. 13, no. 3, pp. 413-419.

Filer, A., Parsonage, G., Smith, E., Osborne, C., Thomas, A. M., Curnow, S. J., Rainger, G. E., Raza, K., Nash, G. B., Lord, J., Salmon, M., & Buckley, C. D. 2006, "Differential survival of leukocyte subsets mediated by synovial, bone marrow, and skin fibroblasts: site-specific versus activation-dependent survival of T cells and neutrophils", *Arthritis Rheum.*, vol. 54, no. 7, pp. 2096-2108.

Firestein, G. S., Nguyen, K., Aupperle, K. R., Yeo, M., Boyle, D. L., & Zvaifler, N. J. 1996, "Apoptosis in rheumatoid arthritis: p53 overexpression in rheumatoid arthritis synovium", *Am.J.Pathol.*, vol. 149, no. 6, pp. 2143-2151.

Flores-Borja, F., Jury, E. C., Mauri, C., & Ehrenstein, M. R. 2008, "Defects in CTLA-4 are associated with abnormal regulatory T cell function in rheumatoid arthritis", *Proc.Natl.Acad.Sci.U.S.A*, vol. 105, no. 49, pp. 19396-19401.

Friedl, P., Sahai, E., Weiss, S., & Yamada, K. M. 2012, "New dimensions in cell migration", *Nat.Rev.Mol.Cell Biol.*, vol. 13, no. 11, pp. 743-747.

Frye, C. A., Yocum, D. E., Tuan, R., Suyana, E., Seftor, E. A., Seftor, R. E., Khalkhali-Ellis, Z., Moore, T. L., & Hendrix, M. J. 1996, "An in vitro Model for Studying Mechanisms Underlying Synoviocyte-Mediated Cartilage Invasion in Rheumatoid Arthritis", *Pathol.Oncol.Res.*, vol. 2, no. 3, pp. 157-166.

Fujikawa, Y., Sabokbar, A., Neale, S., & Athanasou, N. A. 1996, "Human osteoclast formation and bone resorption by monocytes and synovial macrophages in rheumatoid arthritis", *Ann.Rheum.Dis.*, vol. 55, no. 11, pp. 816-822.

Gerlag, D. M., Raza, K., van Baarsen, L. G., Brouwer, E., Buckley, C. D., Burmester, G. R., Gabay, C., Catrina, A. I., Cope, A. P., Cornelis, F., Dahlqvist, S. R., Emery, P., Eyre, S., Finckh, A., Gay, S., Hazes, J. M., van der Helm-van Mil, Huizinga, T. W., Klareskog, L., Kvien, T. K., Lewis, C., Machold, K. P., Ronnelid, J., van, S. D., Schett, G., Smolen, J. S., Thomas, S., Worthington, J., & Tak, P. P. 2012, "EULAR recommendations for terminology and research in individuals at risk of rheumatoid arthritis: report from the Study Group for Risk Factors for Rheumatoid Arthritis", *Ann.Rheum.Dis.*, vol. 71, no. 5, pp. 638-641.

Germann, T., Szeliga, J., Hess, H., Storkel, S., Podlaski, F. J., Gately, M. K., Schmitt, E., & Rude, E. 1995, "Administration of interleukin 12 in combination with type II collagen induces severe arthritis in DBA/1 mice", *Proc.Natl.Acad.Sci.U.S.A*, vol. 92, no. 11, pp. 4823-4827.

Goekoop-Ruiterman, Y. P., de Vries-Bouwstra, J. K., Allaart, C. F., van, Z. D., Kerstens, P. J., Hazes, J. M., Zwinderman, A. H., Ronday, H. K., Han, K. H., Westedt, M. L., Gerards, A. H., van Groenendael, J. H., Lems, W. F., van Krugten, M. V., Breedveld, F. C., & Dijkmans, B. A. 2005, "Clinical and radiographic outcomes of four different treatment strategies in patients with early rheumatoid arthritis (the BeSt study): a randomized, controlled trial", *Arthritis Rheum.*, vol. 52, no. 11, pp. 3381-3390.

Goldbach-Mansky, R., Lee, J. M., Hoxworth, J. M., Smith, D., Duray, P., Schumacher, R. H., Jr., Yarboro, C. H., Klippel, J., Kleiner, D., & El-Gabalawy, H. S. 2000, "Active synovial matrix metalloproteinase-2 is associated with radiographic erosions in patients with early synovitis", *Arthritis Res.*, vol. 2, no. 2, pp. 145-153.

Goldring, S. R. & Goldring, M. B. 2007, "Eating bone or adding it: the Wnt pathway decides", *Nat.Med.*, vol. 13, no. 2, pp. 133-134.

Gregersen, P. K., Silver, J., & Winchester, R. J. 1987, "The shared epitope hypothesis. An approach to understanding the molecular genetics of susceptibility to rheumatoid arthritis", *Arthritis Rheum.*, vol. 30, no. 11, pp. 1205-1213.

Han, Z., Boyle, D. L., Aupperle, K. R., Bennett, B., Manning, A. M., & Firestein, G. S. 1999, "Jun N-terminal kinase in rheumatoid arthritis", *J.Pharmacol.Exp.Ther.*, vol. 291, no. 1, pp. 124-130.

Hardy, R., Juarez, M., Naylor, A., Tu, J., Rabbitt, E. H., Filer, A., Stewart, P. M., Buckley, C. D., Raza, K., & Cooper, M. S. 2012, "Synovial DKK1 expression is regulated by local glucocorticoid metabolism in inflammatory arthritis", *Arthritis Res.Ther.*, vol. 14, no. 5, p. R226.

Haringman, J. J., Gerlag, D. M., Zwinderman, A. H., Smeets, T. J., Kraan, M. C., Baeten, D., McInnes, I. B., Bresnihan, B., & Tak, P. P. 2005, "Synovial tissue macrophages: a sensitive biomarker for response to treatment in patients with rheumatoid arthritis", *Ann.Rheum.Dis.*, vol. 64, no. 6, pp. 834-838.

Heron, K., Turner, J. D., Hardie, D., Adams, H., Raza, K., Buckley, C. D., Tennant, D., & Filer, A. Hypoxic regulation of epigenetic modifications during disease progression in rheumatoid arthritis. Rheumatology 53 (Suppl 1), i36. 30-4-2014. Ref Type: Abstract.

Heruth, D. P., Gibson, M., Grigoryev, D. N., Zhang, L. Q., & Ye, S. Q. 2012, "RNA-seq analysis of synovial fibroblasts brings new insights into rheumatoid arthritis", *Cell Biosci.*, vol. 2, no. 1, p. 43.

Horai, R., Saijo, S., Tanioka, H., Nakae, S., Sudo, K., Okahara, A., Ikuse, T., Asano, M., & Iwakura, Y. 2000, "Development of chronic inflammatory arthropathy resembling rheumatoid arthritis in interleukin 1 receptor antagonist-deficient mice", *J.Exp.Med.*, vol. 191, no. 2, pp. 313-320.

Horwitz, R. & Webb, D. 2003, "Cell migration", *Curr.Biol.*, vol. 13, no. 19, p. R756-R759.

Hosaka, S., Akahoshi, T., Wada, C., & Kondo, H. 1994, "Expression of the chemokine superfamily in rheumatoid arthritis", *Clin.Exp.Immunol.*, vol. 97, no. 3, pp. 451-457.

Huber, L. C., Distler, O., Tarner, I., Gay, R. E., Gay, S., & Pap, T. 2006, "Synovial fibroblasts: key players in rheumatoid arthritis", *Rheumatology.(Oxford)*, vol. 45, no. 6, pp. 669-675.

Hulkower, K. I. 2011, "Cell Migration and Invasion Assays as Tools for Drug Discovery", *Pharmaceutics*, doi: 10.3390.

Ichikawa, K., Liu, W., Fleck, M., Zhang, H., Zhao, L., Ohtsuka, T., Wang, Z., Liu, D., Mountz, J. D., Ohtsuki, M., Koopman, W. J., Kimberly, R., & Zhou, T. 2003, "TRAIL-R2 (DR5) mediates apoptosis of synovial fibroblasts in rheumatoid arthritis", *J.Immunol.*, vol. 171, no. 2, pp. 1061-1069.

Ishiguro, H., Tsunoda, T., Tanaka, T., Fujii, Y., Nakamura, Y., & Furukawa, Y. 2001, "Identification of AXUD1, a novel human gene induced by AXIN1 and its reduced expression in human carcinomas of the lung, liver, colon and kidney", *Oncogene*, vol. 20, no. 36, pp. 5062-5066.

Ishikawa, H., Hirata, S., Andoh, Y., Kubo, H., Nakagawa, N., Nishibayashi, Y., & Mizuno, K. 1996, "An immunohistochemical and immunoelectron microscopic study of adhesion molecules in synovial pannus formation in rheumatoid arthritis", *Rheumatol.Int.*, vol. 16, no. 2, pp. 53-60.

Jacobs, R. A., Perrett, D., Axon, J. M., Herbert, K. E., & Scott, D. L. 1995, "Rheumatoid synovial cell proliferation, transformation and fibronectin secretion in culture", *Clin.Exp.Rheumatol.*, vol. 13, no. 6, pp. 717-723.

Jaluria, P., Konstantopoulos, K., Betenbaugh, M., & Shiloach, J. 2007, "A perspective on microarrays: current applications, pitfalls, and potential uses", *Microb.Cell Fact.*, vol. 6, p. 4.

Jungel, A., Baresova, V., Ospelt, C., Simmen, B. R., Michel, B. A., Gay, R. E., Gay, S., Seemayer, C. A., & Neidhart, M. 2006, "Trichostatin A sensitises rheumatoid arthritis synovial fibroblasts for TRAIL-induced apoptosis", *Ann.Rheum.Dis.*, vol. 65, no. 7, pp. 910-912.

Kallberg, H., Padyukov, L., Plenge, R. M., Ronnelid, J., Gregersen, P. K., van der Helm-Van Mil AH, Toes, R. E., Huizinga, T. W., Klareskog, L., & Alfredsson, L. 2007, "Gene-gene and gene-environment interactions involving HLA-DRB1, PTPN22, and smoking in two subsets of rheumatoid arthritis", *Am.J.Hum.Genet.*, vol. 80, no. 5, pp. 867-875.

Karouzakis, E., Gay, R. E., Michel, B. A., Gay, S., & Neidhart, M. 2009, "DNA hypomethylation in rheumatoid arthritis synovial fibroblasts", *Arthritis Rheum.*, vol. 60, no. 12, pp. 3613-3622.

Kasperkovitz, P. V., Timmer, T. C., Smeets, T. J., Verbeet, N. L., Tak, P. P., van Baarsen, L. G., Baltus, B., Huizinga, T. W., Pieterman, E., Fero, M., Firestein, G. S., van der Pouw Kraan TC, & Verweij, C. L. 2005, "Fibroblast-like synoviocytes derived from patients with rheumatoid arthritis show the imprint of synovial tissue heterogeneity: evidence of a link between an increased myofibroblast-like phenotype and high-inflammation synovitis", *Arthritis Rheum.*, vol. 52, no. 2, pp. 430-441.

Katz, M., Amit, I., Citri, A., Shay, T., Carvalho, S., Lavi, S., Milanezi, F., Lyass, L., Amariglio, N., Jacob-Hirsch, J., Ben-Chetrit, N., Tarcic, G., Lindzen, M., Avraham, R., Liao, Y. C., Trusk, P., Lyass, A., Rechavi, G., Spector, N. L., Lo, S. H., Schmitt, F., Bacus, S. S., & Yarden, Y. 2007, "A reciprocal tensin-3-cten switch mediates EGF-driven mammary cell migration", *Nat.Cell Biol.*, vol. 9, no. 8, pp. 961-969.

Kellner, H. 2013, "Targeting interleukin-17 in patients with active rheumatoid arthritis: rationale and clinical potential", *Ther.Adv.Musculoskelet.Dis*, vol. 5, no. 3, pp. 141-152.

Khandpur, R., Carmona-Rivera, C., Vivekanandan-Giri, A., Gizinski, A., Yalavarthi, S., Knight, J. S., Friday, S., Li, S., Patel, R. M., Subramanian, V., Thompson, P., Chen, P., Fox, D. A., Pennathur, S., & Kaplan, M. J. 2013, "NETs are a source of citrullinated autoantigens and stimulate inflammatory responses in rheumatoid arthritis", *Sci.Transl.Med.*, vol. 5, no. 178, p. 178ra40.

Kiener, H. P., Niederreiter, B., Lee, D. M., Jimenez-Boj, E., Smolen, J. S., & Brenner, M. B. 2009, "Cadherin 11 promotes invasive behavior of fibroblast-like synoviocytes", *Arthritis Rheum.*, vol. 60, no. 5, pp. 1305-1310.

Kinloch, A., Lundberg, K., Wait, R., Wegner, N., Lim, N. H., Zendman, A. J., Saxne, T., Malmstrom, V., & Venables, P. J. 2008, "Synovial fluid is a site of citrullination of autoantigens in inflammatory arthritis", *Arthritis Rheum.*, vol. 58, no. 8, pp. 2287-2295.

Kinne, R. W., Brauer, R., Stuhlmuller, B., Palombo-Kinne, E., & Burmester, G. R. 2000, "Macrophages in rheumatoid arthritis", *Arthritis Res.*, vol. 2, no. 3, pp. 189-202.

Klareskog, L., Stolt, P., Lundberg, K., Kallberg, H., Bengtsson, C., Grunewald, J., Ronnelid, J., Harris, H. E., Ulfgren, A. K., Rantapaa-Dahlqvist, S., Eklund, A., Padyukov, L., & Alfredsson, L. 2006, "A new model for an etiology of rheumatoid arthritis: smoking may trigger HLA-DR (shared epitope)-restricted immune reactions to autoantigens modified by citrullination", *Arthritis Rheum.*, vol. 54, no. 1, pp. 38-46.

Koch, A. E., Kunkel, S. L., Burrows, J. C., Evanoff, H. L., Haines, G. K., Pope, R. M., & Strieter, R. M. 1991, "Synovial tissue macrophage as a source of the chemotactic cytokine IL-8", *J.Immunol.*, vol. 147, no. 7, pp. 2187-2195.

Koch, A. E., Kunkel, S. L., Harlow, L. A., Mazarakis, D. D., Haines, G. K., Burdick, M. D., Pope, R. M., Walz, A., & Strieter, R. M. 1994, "Epithelial neutrophil activating peptide-78: a novel chemotactic cytokine for neutrophils in arthritis", *J.Clin.Invest*, vol. 94, no. 3, pp. 1012-1018.

Koch, A. E., Kunkel, S. L., Shah, M. R., Hosaka, S., Halloran, M. M., Haines, G. K., Burdick, M. D., Pope, R. M., & Strieter, R. M. 1995, "Growth-related gene product alpha. A chemotactic cytokine for neutrophils in rheumatoid arthritis", *J.Immunol.*, vol. 155, no. 7, pp. 3660-3666.

Kraan, M. C., Versendaal, H., Jonker, M., Bresnihan, B., Post, W. J., Hart, B. A., Breedveld, F. C., & Tak, P. P. 1998, "Asymptomatic synovitis precedes clinically manifest arthritis", *Arthritis Rheum.*, vol. 41, no. 8, pp. 1481-1488.

Krumlauf, R. 1994, "Hox genes in vertebrate development", *Cell*, vol. 78, no. 2, pp. 191-201.

Kurosaka, M. & Ziff, M. 1983, "Immunoelectron microscopic study of the distribution of T cell subsets in rheumatoid synovium", *J.Exp.Med.*, vol. 158, no. 4, pp. 1191-1210.

Laragione, T., Brenner, M., Mello, A., Symons, M., & Gulko, P. S. 2008, "The arthritis severity locus Cia5d is a novel genetic regulator of the invasive properties of synovial fibroblasts", *Arthritis Rheum.*, vol. 58, no. 8, pp. 2296-2306.

Laragione, T. & Gulko, P. S. 2010, "mTOR regulates the invasive properties of synovial fibroblasts in rheumatoid arthritis", *Mol.Med.*, vol. 16, no. 9-10, pp. 352-358.

Lee, D. M., Kiener, H. P., Agarwal, S. K., Noss, E. H., Watts, G. F., Chisaka, O., Takeichi, M., & Brenner, M. B. 2007, "Cadherin-11 in synovial lining formation and pathology in arthritis", *Science*, vol. 315, no. 5814, pp. 1006-1010.

Lefevre, S., Knedla, A., Tennie, C., Kampmann, A., Wunrau, C., Dinser, R., Korb, A., Schnaker, E. M., Tarner, I. H., Robbins, P. D., Evans, C. H., Sturz, H., Steinmeyer, J., Gay, S., Scholmerich, J., Pap, T., Muller-Ladner, U., & Neumann, E. 2009, "Synovial fibroblasts spread rheumatoid arthritis to unaffected joints", *Nat.Med.*, vol. 15, no. 12, pp. 1414-1420.

Li, G., Han, N., Li, Z., & Lu, Q. 2013, "Identification of transcription regulatory relationships in rheumatoid arthritis and osteoarthritis", *Clin.Rheumatol.*, vol. 32, no. 5, pp. 609-615.

Lindy, O., Konttinen, Y. T., Sorsa, T., Ding, Y., Santavirta, S., Ceponis, A., & Lopez-Otin, C. 1997, "Matrix metalloproteinase 13 (collagenase 3) in human rheumatoid synovium", *Arthritis Rheum.*, vol. 40, no. 8, pp. 1391-1399.

Linn-Rasker, S. P., van der Helm-Van Mil AH, van Gaalen, F. A., Kloppenburg, M., de Vries, R. R., le, C. S., Breedveld, F. C., Toes, R. E., & Huizinga, T. W. 2006, "Smoking is a risk factor for anti-CCP antibodies only in rheumatoid arthritis patients who carry HLA-DRB1 shared epitope alleles", *Ann.Rheum.Dis.*, vol. 65, no. 3, pp. 366-371.

Liu, B. & Shuai, K. 2008, "Targeting the PIAS1 SUMO ligase pathway to control inflammation", *Trends Pharmacol.Sci.*, vol. 29, no. 10, pp. 505-509.

Liu, B. H., Yu, H., Tu, K., Li, C., Li, Y. X., & Li, Y. Y. 2010, "DCGL: an R package for identifying differentially coexpressed genes and links from gene expression microarray data", *Bioinformatics.*, vol. 26, no. 20, pp. 2637-2638.

Lubberts, E. 2008, "IL-17/Th17 targeting: on the road to prevent chronic destructive arthritis?", *Cytokine*, vol. 41, no. 2, pp. 84-91.

MacGregor, A. J., Snieder, H., Rigby, A. S., Koskenvuo, M., Kaprio, J., Aho, K., & Silman, A. J. 2000, "Characterizing the quantitative genetic contribution to rheumatoid arthritis using data from twins", *Arthritis Rheum.*, vol. 43, no. 1, pp. 30-37.

Maia, M., de, V. A., Janssens, T., Moons, M., van, L. K., Tavernier, J., Lories, R. J., & Conway, E. M. 2010, "CD248 and its cytoplasmic domain: a therapeutic target for arthritis", *Arthritis Rheum.*, vol. 62, no. 12, pp. 3595-3606.

Marok, R., Winyard, P. G., Coumbe, A., Kus, M. L., Gaffney, K., Blades, S., Mapp, P. I., Morris, C. J., Blake, D. R., Kaltschmidt, C., & Baeuerle, P. A. 1996, "Activation of the transcription factor nuclear factor-kappaB in human inflamed synovial tissue", *Arthritis Rheum.*, vol. 39, no. 4, pp. 583-591.

Matsumura, H., Ito, A., Saitoh, H., Winter, P., Kahl, G., Reuter, M., Kruger, D. H., & Terauchi, R. 2005, "SuperSAGE", *Cell Microbiol.*, vol. 7, no. 1, pp. 11-18.

Matucci-Cerinic, M., Lombardi, A., Leoncini, G., Pignone, A., Sacerdoti, L., Spillantini, M. G., & Partsch, G. 1993, "Neutral endopeptidase (3.4.24.11) in plasma and synovial fluid of patients with rheumatoid arthritis. A marker of disease activity or a regulator of pain and inflammation?", *Rheumatol.Int.*, vol. 13, no. 1, pp. 1-4.

McCoy, K. D. & Le, G. G. 1999, "The role of CTLA-4 in the regulation of T cell immune responses", *Immunol.Cell Biol.*, vol. 77, no. 1, pp. 1-10.

McGettrick, H. M., Smith, E., Filer, A., Kissane, S., Salmon, M., Buckley, C. D., Rainger, G. E., & Nash, G. B. 2009, "Fibroblasts from different sites may promote or inhibit recruitment of flowing lymphocytes by endothelial cells", *Eur.J.Immunol.*, vol. 39, no. 1, pp. 113-125.

McInnes, I. B. & Schett, G. 2011, "The pathogenesis of rheumatoid arthritis", *N.Engl.J.Med.*, vol. 365, no. 23, pp. 2205-2219.

Meier, F. M., Frommer, K. W., Peters, M. A., Brentano, F., Lefevre, S., Schroder, D., Kyburz, D., Steinmeyer, J., Rehart, S., Gay, S., Muller-Ladner, U., & Neumann, E. 2012, "Visfatin/pre-B-cell colony-enhancing factor (PBEF), a proinflammatory and cell motility-changing factor in rheumatoid arthritis", *J.Biol.Chem.*, vol. 287, no. 34, pp. 28378-28385.

Melnyk, V. O., Shipley, G. D., Sternfeld, M. D., Sherman, L., & Rosenbaum, J. T. 1990, "Synoviocytes synthesize, bind, and respond to basic fibroblast growth factor", *Arthritis Rheum.*, vol. 33, no. 4, pp. 493-500.

Miagkov, A. V., Kovalenko, D. V., Brown, C. E., Didsbury, J. R., Cogswell, J. P., Stimpson, S. A., Baldwin, A. S., & Makarov, S. S. 1998, "NF-kappaB activation provides the potential link between inflammation and hyperplasia in the arthritic joint", *Proc.Natl.Acad.Sci.U.S.A*, vol. 95, no. 23, pp. 13859-13864.

Micke, P. & Ostman, A. 2004, "Tumour-stroma interaction: cancer-associated fibroblasts as novel targets in anti-cancer therapy?", *Lung Cancer*, vol. 45 Suppl 2, p. S163-S175.

Mor, A., Abramson, S. B., & Pillinger, M. H. 2005, "The fibroblast-like synovial cell in rheumatoid arthritis: a key player in inflammation and joint destruction", *Clin.Immunol.*, vol. 115, no. 2, pp. 118-128.

Morel, J., Audo, R., Hahne, M., & Combe, B. 2005, "Tumor necrosis factor-related apoptosis-inducing ligand (TRAIL) induces rheumatoid arthritis synovial fibroblast proliferation through mitogen-activated protein kinases and phosphatidylinositol 3-kinase/Akt", *J.Biol.Chem.*, vol. 280, no. 16, pp. 15709-15718.

Mottonen, T., Hannonen, P., Leirisalo-Repo, M., Nissila, M., Kautiainen, H., Korpela, M., Laasonen, L., Julkunen, H., Luukkainen, R., Vuori, K., Paimela, L., Blafield, H., Hakala, M., Ilva, K., Yli-Kerttula, U., Puolakka, K., Jarvinen, P., Hakola, M., Piirainen, H., Ahonen, J., Palvimaki, I., Forsberg, S., Koota, K., & Friman, C. 1999, "Comparison of combination therapy with single-drug therapy in early rheumatoid arthritis: a randomised trial. FIN-RACo trial group", *Lancet*, vol. 353, no. 9164, pp. 1568-1573.

Muller-Ladner, U., Kriegsmann, J., Franklin, B. N., Matsumoto, S., Geiler, T., Gay, R. E., & Gay, S. 1996, "Synovial fibroblasts of patients with rheumatoid arthritis attach to and invade normal human cartilage when engrafted into SCID mice", *Am.J.Pathol.*, vol. 149, no. 5, pp. 1607-1615.

Muller-Ladner, U., Ospelt, C., Gay, S., Distler, O., & Pap, T. 2007, "Cells of the synovium in rheumatoid arthritis. Synovial fibroblasts", *Arthritis Res.Ther.*, vol. 9, no. 6, p. 223.

Murphy, C. A., Langrish, C. L., Chen, Y., Blumenschein, W., McClanahan, T., Kastelein, R. A., Sedgwick, J. D., & Cua, D. J. 2003, "Divergent pro- and antiinflammatory roles for IL-23 and IL-12 in joint autoimmune inflammation", *J.Exp.Med.*, vol. 198, no. 12, pp. 1951-1957.

Nakano, K., Okada, Y., Saito, K., & Tanaka, Y. 2004, "Induction of RANKL expression and osteoclast maturation by the binding of fibroblast growth factor 2 to heparan sulfate proteoglycan on rheumatoid synovial fibroblasts", *Arthritis Rheum.*, vol. 50, no. 8, pp. 2450-2458.

Nakano, K., Whitaker, J. W., Boyle, D. L., Wang, W., & Firestein, G. S. 2013, "DNA methylome signature in rheumatoid arthritis", *Ann.Rheum.Dis.*, vol. 72, no. 1, pp. 110-117.

Nakasa, T., Shibuya, H., Nagata, Y., Niimoto, T., & Ochi, M. 2011, "The inhibitory effect of microRNA-146a expression on bone destruction in collagen-induced arthritis", *Arthritis Rheum*, vol. 63, no. 6, pp. 1582-1590.

Nanki, T., Shimaoka, T., Hayashida, K., Taniguchi, K., Yonehara, S., & Miyasaka, N. 2005, "Pathogenic role of the CXCL16-CXCR6 pathway in rheumatoid arthritis", *Arthritis Rheum.*, vol. 52, no. 10, pp. 3004-3014.

Neidhart, M., Seemayer, C. A., Hummel, K. M., Michel, B. A., Gay, R. E., & Gay, S. 2003, "Functional characterization of adherent synovial fluid cells in rheumatoid arthritis: destructive potential in vitro and in vivo", *Arthritis Rheum.*, vol. 48, no. 7, pp. 1873-1880.

Neidhart, M., Zaucke, F., von, K. R., Jungel, A., Michel, B. A., Gay, R. E., & Gay, S. 2005, "Galectin-3 is induced in rheumatoid arthritis synovial fibroblasts after adhesion to cartilage oligomeric matrix protein", *Ann.Rheum.Dis.*, vol. 64, no. 3, pp. 419-424.

Nell, V. P., Machold, K. P., Eberl, G., Stamm, T. A., Uffmann, M., & Smolen, J. S. 2004, "Benefit of very early referral and very early therapy with disease-modifying anti-rheumatic drugs in patients with early rheumatoid arthritis", *Rheumatology.(Oxford)*, vol. 43, no. 7, pp. 906-914.

Neumann, E., Riepl, B., Knedla, A., Lefevre, S., Tarner, I. H., Grifka, J., Steinmeyer, J., Scholmerich, J., Gay, S., & Muller-Ladner, U. 2010, "Cell culture and passaging alters gene expression pattern and proliferation rate in rheumatoid arthritis synovial fibroblasts", *Arthritis Res.Ther.*, vol. 12, no. 3, p. R83.

Ng, C. T., Biniecka, M., Kennedy, A., McCormick, J., Fitzgerald, O., Bresnihan, B., Buggy, D., Taylor, C. T., O'Sullivan, J., Fearon, U., & Veale, D. J. 2010, "Synovial tissue hypoxia and inflammation in vivo", *Ann.Rheum.Dis.*, vol. 69, no. 7, pp. 1389-1395.

Ng, W. F., Duggan, P. J., Ponchel, F., Matarese, G., Lombardi, G., Edwards, A. D., Isaacs, J. D., & Lechler, R. I. 2001, "Human CD4(+)CD25(+) cells: a naturally occurring population of regulatory T cells", *Blood*, vol. 98, no. 9, pp. 2736-2744.

Nykanen, P., Helve, T., Kankaanpaa, U., & Larsen, A. 1978, "Characterization of the DNA-synthesizing cells in rheumatoid synovial tissue", *Scand.J.Rheumatol.*, vol. 7, no. 2, pp. 118-122.

Ohshima, S., Kuchen, S., Seemayer, C. A., Kyburz, D., Hirt, A., Klinzing, S., Michel, B. A., Gay, R. E., Liu, F. T., Gay, S., & Neidhart, M. 2003, "Galectin 3 and its binding protein in rheumatoid arthritis", *Arthritis Rheum.*, vol. 48, no. 10, pp. 2788-2795.

Okada, Y., Takeuchi, N., Tomita, K., Nakanishi, I., & Nagase, H. 1989, "Immunolocalization of matrix metalloproteinase 3 (stromelysin) in rheumatoid synovioblasts (B cells): correlation with rheumatoid arthritis", *Ann.Rheum.Dis.*, vol. 48, no. 8, pp. 645-653.

Oslejskova, L., Grigorian, M., Hulejova, H., Vencovsky, J., Pavelka, K., Klingelhofer, J., Gay, S., Neidhart, M., Brabcova, H., Suchy, D., & Senolt, L. 2009, "Metastasis-inducing S100A4 protein is associated with the disease activity of rheumatoid arthritis", *Rheumatology.(Oxford)*, vol. 48, no. 12, pp. 1590-1594.

Ospelt, C., Brentano, F., Rengel, Y., Stanczyk, J., Kolling, C., Tak, P. P., Gay, R. E., Gay, S., & Kyburz, D. 2008, "Overexpression of toll-like receptors 3 and 4 in synovial tissue from patients with early rheumatoid arthritis: toll-like receptor expression in early and longstanding arthritis", *Arthritis Rheum.*, vol. 58, no. 12, pp. 3684-3692.

Ota, F., Maeshima, A., Yamashita, S., Ikeuchi, H., Kaneko, Y., Kuroiwa, T., Hiromura, K., Ueki, K., Kojima, I., & Nojima, Y. 2003, "Activin A induces cell proliferation of fibroblast-like synoviocytes in rheumatoid arthritis", *Arthritis Rheum.*, vol. 48, no. 9, pp. 2442-2449.

Ottaviani, S., Tahiri, K., Frazier, A., Hassaine, Z. N., Dumontier, M. F., Baschong, W., Rannou, F., Corvol, M. T., Savouret, J. F., & Richette, P. 2010, "Hes1, a new target for interleukin 1beta in chondrocytes", *Ann Rheum Dis*, vol. 69, no. 8, pp. 1488-1494.

adyukov, L., Silva, C., Stolt, P., Alfredsson, L., & Klareskog, L. 2004, "A gene-environment interaction between smoking and shared epitope genes in HLA-DR provides a high risk of seropositive rheumatoid arthritis", *Arthritis Rheum.*, vol. 50, no. 10, pp. 3085-3092.

Palao, G., Santiago, B., Galindo, M., Paya, M., Ramirez, J. C., & Pablos, J. L. 2004, "Down-regulation of FLIP sensitizes rheumatoid synovial fibroblasts to Fas-mediated apoptosis", *Arthritis Rheum.*, vol. 50, no. 9, pp. 2803-2810.

Pap, T., Aupperle, K. R., Gay, S., Firestein, G. S., & Gay, R. E. 2001, "Invasiveness of synovial fibroblasts is regulated by p53 in the SCID mouse in vivo model of cartilage invasion", *Arthritis Rheum*, vol. 44, no. 3, pp. 676-681.

Pap, T., Franz, J. K., Hummel, K. M., Jeisy, E., Gay, R., & Gay, S. 2000a, "Activation of synovial fibroblasts in rheumatoid arthritis: lack of Expression of the tumour suppressor PTEN at sites of invasive growth and destruction", *Arthritis Res.*, vol. 2, no. 1, pp. 59-64.

Pap, T., Muller-Ladner, U., Gay, R. E., & Gay, S. 2000b, "Fibroblast biology. Role of synovial fibroblasts in the pathogenesis of rheumatoid arthritis", *Arthritis Res.*, vol. 2, no. 5, pp. 361-367.

Park, B. S. & Mori, M. 2010, "Balancing false discovery and false negative rates in selection of differentially expressed genes in microarrays", *Open.Access.Bioinformatics.*, vol. 2010, no. 2, pp. 1-9.

Patel, D. D., Zachariah, J. P., & Whichard, L. P. 2001, "CXCR3 and CCR5 ligands in rheumatoid arthritis synovium", *Clin.Immunol.*, vol. 98, no. 1, pp. 39-45.

Pavlidis, P., Li, Q., & Noble, W. S. 2003, "The effect of replication on gene expression microarray experiments", *Bioinformatics.*, vol. 19, no. 13, pp. 1620-1627.

Perkins, D. O., Jeffries, C., & Sullivan, P. 2005, "Expanding the 'central dogma': the regulatory role of nonprotein coding genes and implications for the genetic liability to schizophrenia", *Mol.Psychiatry*, vol. 10, no. 1, pp. 69-78.

Perlman, H., Georganas, C., Pagliari, L. J., Koch, A. E., Haines, K., III, & Pope, R. M. 2000, "Bcl-2 expression in synovial fibroblasts is essential for maintaining mitochondrial homeostasis and cell viability", *J.Immunol.*, vol. 164, no. 10, pp. 5227-5235.

Perlman, H., Nguyen, N., Liu, H., Eslick, J., Esser, S., Walsh, K., Moore, T. L., & Pope, R. M. 2003, "Rheumatoid arthritis synovial fluid macrophages express decreased tumor necrosis factor-related apoptosis-inducing ligand R2 and increased decoy receptor tumor necrosis factor-related apoptosis-inducing ligand R3", *Arthritis Rheum.*, vol. 48, no. 11, pp. 3096-3101.

Persson, G. R. 2012, "RA and periodontitis inflammatory and infectious connections a review of the literature", *J Oral Microbiol*, vol. 4, p. 11829.

Pilling, D., Akbar, A. N., Girdlestone, J., Orteu, C. H., Borthwick, N. J., Amft, N., Scheel-Toellner, D., Buckley, C. D., & Salmon, M. 1999, "Interferon-beta mediates stromal cell rescue of T cells from apoptosis", *Eur.J.Immunol.*, vol. 29, no. 3, pp. 1041-1050.

Pillinger, M. H., Rosenthal, P. B., Tolani, S. N., Apsel, B., Dinsell, V., Greenberg, J., Chan, E. S., Gomez, P. F., & Abramson, S. B. 2003, "Cyclooxygenase-2-derived E prostaglandins down-regulate matrix metalloproteinase-1 expression in fibroblast-like synoviocytes via inhibition of extracellular signal-regulated kinase activation", *J.Immunol.*, vol. 171, no. 11, pp. 6080-6089.

Pistoia, V. 1997, "Production of cytokines by human B cells in health and disease", *Immunol.Today*, vol. 18, no. 7, pp. 343-350.

Plenge, R. M., Padyukov, L., Remmers, E. F., Purcell, S., Lee, A. T., Karlson, E. W., Wolfe, F., Kastner, D. L., Alfredsson, L., Altshuler, D., Gregersen, P. K., Klareskog, L., & Rioux, J. D. 2005, "Replication of putative candidate-gene associations with rheumatoid arthritis in >4,000 samples from North America and Sweden: association of susceptibility with PTPN22, CTLA4, and PADI4", *Am.J.Hum.Genet.*, vol. 77, no. 6, pp. 1044-1060.

Pretzel, D., Pohlers, D., Weinert, S., & Kinne, R. W. 2009, "In vitro model for the analysis of synovial fibroblast-mediated degradation of intact cartilage", *Arthritis Res.Ther.*, vol. 11, no. 1, p. R25.

Qu, Z., Garcia, C. H., O'Rourke, L. M., Planck, S. R., Kohli, M., & Rosenbaum, J. T. 1994, "Local proliferation of fibroblast-like synoviocytes contributes to synovial hyperplasia. Results of proliferating cell nuclear antigen/cyclin, c-myc, and nucleolar organizer region staining", *Arthritis Rheum.*, vol. 37, no. 2, pp. 212-220.

Rajeevan, M. S., Ranamukhaarachchi, D. G., Vernon, S. D., & Unger, E. R. 2001, "Use of real-time quantitative PCR to validate the results of cDNA array and differential display PCR technologies", *Methods*, vol. 25, no. 4, pp. 443-451.

Rath, H. C., Herfarth, H. H., Ikeda, J. S., Grenther, W. B., Hamm, T. E., Jr., Balish, E., Taurog, J. D., Hammer, R. E., Wilson, K. H., & Sartor, R. B. 1996, "Normal luminal bacteria, especially Bacteroides species, mediate chronic colitis, gastritis, and arthritis in HLA-B27/human beta2 microglobulin transgenic rats", *J.Clin.Invest*, vol. 98, no. 4, pp. 945-953.

Ray, N. B., Nieva, D. R., Seftor, E. A., Khalkhali-Ellis, Z., & Naides, S. J. 2001, "Induction of an invasive phenotype by human parvovirus B19 in normal human synovial fibroblasts", *Arthritis Rheum.*, vol. 44, no. 7, pp. 1582-1586.

Raza, K., Buckley, C. E., Salmon, M., & Buckley, C. D. 2006, "Treating very early rheumatoid arthritis", *Best.Pract.Res.Clin.Rheumatol.*, vol. 20, no. 5, pp. 849-863.

Raza, K., Falciani, F., Curnow, S. J., Ross, E. J., Lee, C. Y., Akbar, A. N., Lord, J. M., Gordon, C., Buckley, C. D., & Salmon, M. 2005, "Early rheumatoid arthritis is characterized by a distinct and transient synovial fluid cytokine profile of T cell and stromal cell origin", *Arthritis Res.Ther.*, vol. 7, no. 4, p. R784-R795.

Raza, K., Saber, T. P., Kvien, T. K., Tak, P. P., & Gerlag, D. M. 2012, "Timing the therapeutic window of opportunity in early rheumatoid arthritis: proposal for definitions of disease duration in clinical trials", *Ann Rheum Dis*, vol. 71, no. 12, pp. 1921-1923.

Raza, K., Stack, R., Kumar, K., Filer, A., Detert, J., Bastian, H., Burmester, G. R., Sidiropoulos, P., Kteniadaki, E., Repa, A., Saxne, T., Turesson, C., Mann, H., Vencovsky, J., Catrina, A., Chatzidionysiou, A., Hensvold, A., Rantapaa-Dahlqvist, S., Binder, A., Machold, K., Kwiakowska, B., Ciurea, A., Tamborrini, G., Kyburz, D., & Buckley, C. D. 2011, "Delays

in assessment of patients with rheumatoid arthritis: variations across Europe", *Ann.Rheum.Dis.*, vol. 70, no. 10, pp. 1822-1825.

Reedquist, K. A., Ludikhuize, J., & Tak, P. P. 2006, "Phosphoinositide 3-kinase signalling and FoxO transcription factors in rheumatoid arthritis", *Biochem.Soc.Trans.*, vol. 34, no. Pt 5, pp. 727-730.

Rinn, J. L., Bondre, C., Gladstone, H. B., Brown, P. O., & Chang, H. Y. 2006, "Anatomic demarcation by positional variation in fibroblast gene expression programs", *PLoS.Genet.*, vol. 2, no. 7, p. e119.

Ruth, J. H., Haas, C. S., Park, C. C., Amin, M. A., Martinez, R. J., Haines, G. K., III, Shahrara, S., Campbell, P. L., & Koch, A. E. 2006, "CXCL16-mediated cell recruitment to rheumatoid arthritis synovial tissue and murine lymph nodes is dependent upon the MAPK pathway", *Arthritis Rheum.*, vol. 54, no. 3, pp. 765-778.

Salmon, M., Pilling, D., Borthwick, N. J., Viner, N., Janossy, G., Bacon, P. A., & Akbar, A. N. 1994, "The progressive differentiation of primed T cells is associated with an increasing susceptibility to apoptosis", *Eur.J.Immunol.*, vol. 24, no. 4, pp. 892-899.

Sanger, F. & Coulson, A. R. 1975, "A rapid method for determining sequences in DNA by primed synthesis with DNA polymerase", *J.Mol.Biol.*, vol. 94, no. 3, pp. 441-448.

Sanger, F., Nicklen, S., & Coulson, A. R. 1977, "DNA sequencing with chain-terminating inhibitors", *Proc.Natl.Acad.Sci.U.S.A*, vol. 74, no. 12, pp. 5463-5467.

Scher, J. U., Sczesnak, A., Longman, R. S., Segata, N., Ubeda, C., Bielski, C., Rostron, T., Cerundolo, V., Pamer, E. G., Abramson, S. B., Huttenhower, C., & Littman, D. R. 2013, "Expansion of intestinal Prevotella copri correlates with enhanced susceptibility to arthritis", *Elife.*, vol. 2, p. e01202.

Schett, G., Tohidast-Akrad, M., Smolen, J. S., Schmid, B. J., Steiner, C. W., Bitzan, P., Zenz, P., Redlich, K., Xu, Q., & Steiner, G. 2000, "Activation, differential localization, and regulation of the stress-activated protein kinases, extracellular signal-regulated kinase, c-JUN N-terminal kinase, and p38 mitogen-activated protein kinase, in synovial tissue and cells in rheumatoid arthritis", *Arthritis Rheum.*, vol. 43, no. 11, pp. 2501-2512.

Schneider, P., Biehl, M., & Hammer, B. 2009, "Adaptive relevance matrices in learning vector quantization", *Neural Comput.*, vol. 21, no. 12, pp. 3532-3561.

Schumacher, H. R., Jr., Bautista, B. B., Krauser, R. E., Mathur, A. K., & Gall, E. P. 1994, "Histological appearance of the synovium in early rheumatoid arthritis", *Semin.Arthritis Rheum.*, vol. 23, no. 6 Suppl 2, pp. 3-10.

Scott, D. L. 2000, "Prognostic factors in early rheumatoid arthritis", *Rheumatology.(Oxford)*, vol. 39 Suppl 1, pp. 24-29.

Scott, M. P. 1992, "Vertebrate homeobox gene nomenclature", *Cell*, vol. 71, no. 4, pp. 551-553.

Seddighzadeh, M., Korotkova, M., Kallberg, H., Ding, B., Daha, N., Kurreeman, F. A., Toes, R. E., Huizinga, T. W., Catrina, A. I., Alfredsson, L., Klareskog, L., & Padyukov, L. 2010, "Evidence for interaction between 5-hydroxytryptamine (serotonin) receptor 2A and MHC type II molecules in the development of rheumatoid arthritis", *Eur.J.Hum.Genet.*, vol. 18, no. 7, pp. 821-826.

Seki, M., Sakata, K. M., Oomizu, S., Arikawa, T., Sakata, A., Ueno, M., Nobumoto, A., Niki, T., Saita, N., Ito, K., Dai, S. Y., Katoh, S., Nishi, N., Tsukano, M., Ishikawa, K., Yamauchi, A., Kuchroo, V., & Hirashima, M. 2007, "Beneficial effect of galectin 9 on rheumatoid arthritis by induction of apoptosis of synovial fibroblasts", *Arthritis Rheum.*, vol. 56, no. 12, pp. 3968-3976.

Senolt, L., Grigorian, M., Lukanidin, E., Simmen, B., Michel, B. A., Pavelka, K., Gay, R. E., Gay, S., & Neidhart, M. 2006, "S100A4 is expressed at site of invasion in rheumatoid arthritis synovium and modulates production of matrix metalloproteinases", *Ann.Rheum.Dis.*, vol. 65, no. 12, pp. 1645-1648.

Shi, J., Knevel, R., Suwannalai, P., van der Linden, M. P., Janssen, G. M., van Veelen, P. A., Levarht, N. E., van der Helm-Van Mil AH, Cerami, A., Huizinga, T. W., Toes, R. E., & Trouw, L. A. 2011, "Autoantibodies recognizing carbamylated proteins are present in sera of patients with rheumatoid arthritis and predict joint damage", *Proc.Natl.Acad.Sci.U.S.A*, vol. 108, no. 42, pp. 17372-17377.

Shigeyama, Y., Pap, T., Kunzler, P., Simmen, B. R., Gay, R. E., & Gay, S. 2000, "Expression of osteoclast differentiation factor in rheumatoid arthritis", *Arthritis Rheum.*, vol. 43, no. 11, pp. 2523-2530.

Sreedharan, S. P., Goetzl, E. J., & Malfroy, B. 1990, "Elevated synovial tissue concentration of the common acute lymphoblastic leukaemia antigen (CALLA)-associated neutral endopeptidase (3.4.24.11) in human chronic arthritis", *Immunology*, vol. 71, no. 1, pp. 142-144.

Stanczyk, J., Ospelt, C., Karouzakis, E., Filer, A., Raza, K., Kolling, C., Gay, R., Buckley, C. D., Tak, P. P., Gay, S., & Kyburz, D. 2011, "Altered expression of microRNA-203 in rheumatoid arthritis synovial fibroblasts and its role in fibroblast activation", *Arthritis Rheum.*, vol. 63, no. 2, pp. 373-381.

Stanczyk, J., Pedrioli, D. M., Brentano, F., Sanchez-Pernaute, O., Kolling, C., Gay, R. E., Detmar, M., Gay, S., & Kyburz, D. 2008, "Altered expression of MicroRNA in synovial fibroblasts and synovial tissue in rheumatoid arthritis", *Arthritis Rheum.*, vol. 58, no. 4, pp. 1001-1009.

Staton, C. A., Reed, M. W., & Brown, N. J. 2009, "A critical analysis of current in vitro and in vivo angiogenesis assays", *Int.J.Exp.Pathol.*, vol. 90, no. 3, pp. 195-221.

Stockinger, B. & Veldhoen, M. 2007, "Differentiation and function of Th17 T cells", *Curr.Opin.Immunol.*, vol. 19, no. 3, pp. 281-286.

Strietholt, S., Maurer, B., Peters, M. A., Pap, T., & Gay, S. 2008, "Epigenetic modifications in rheumatoid arthritis", *Arthritis Res.Ther.*, vol. 10, no. 5, p. 219.

Stuhlmeier, K. M. 2005, "Effects of leflunomide on hyaluronan synthases (HAS): NF-kappa B-independent suppression of IL-1-induced HAS1 transcription by leflunomide", *J Immunol.*, vol. 174, no. 11, pp. 7376-7382.

Stuhlmeier, K. M. & Pollaschek, C. 2004, "Glucocorticoids inhibit induced and non-induced mRNA accumulation of genes encoding hyaluronan synthases (HAS): hydrocortisone inhibits HAS1 activation by blocking the p38 mitogen-activated protein kinase signalling pathway", *Rheumatology.(Oxford)*, vol. 43, no. 2, pp. 164-169.

Sundarrajan, M., Boyle, D. L., Chabaud-Riou, M., Hammaker, D., & Firestein, G. S. 2003, "Expression of the MAPK kinases MKK-4 and MKK-7 in rheumatoid arthritis and their role as key regulators of JNK", *Arthritis Rheum*, vol. 48, no. 9, pp. 2450-2460.

Takayanagi, H., Iizuka, H., Juji, T., Nakagawa, T., Yamamoto, A., Miyazaki, T., Koshihara, Y., Oda, H., Nakamura, K., & Tanaka, S. 2000, "Involvement of receptor activator of nuclear factor kappaB ligand/osteoclast differentiation factor in osteoclastogenesis from synoviocytes in rheumatoid arthritis", *Arthritis Rheum.*, vol. 43, no. 2, pp. 259-269.

Takemura, S., Braun, A., Crowson, C., Kurtin, P. J., Cofield, R. H., O'Fallon, W. M., Goronzy, J. J., & Weyand, C. M. 2001, "Lymphoid neogenesis in rheumatoid synovitis", *J.Immunol.*, vol. 167, no. 2, pp. 1072-1080.

Tarca, A. L., Romero, R., & Draghici, S. 2006, "Analysis of microarray experiments of gene expression profiling", *Am.J.Obstet.Gynecol.*, vol. 195, no. 2, pp. 373-388.

Taylor, P. C. & Sivakumar, B. 2005, "Hypoxia and angiogenesis in rheumatoid arthritis", *Curr.Opin.Rheumatol.*, vol. 17, no. 3, pp. 293-298.

Tolboom, T. C., Pieterman, E., van der Laan, W. H., Toes, R. E., Huidekoper, A. L., Nelissen, R. G., Breedveld, F. C., & Huizinga, T. W. 2002, "Invasive properties of fibroblast-like synoviocytes: correlation with growth characteristics and expression of MMP-1, MMP-3, and MMP-10", *Ann.Rheum.Dis.*, vol. 61, no. 11, pp. 975-980.

Tolboom, T. C., van der Helm-Van Mil AH, Nelissen, R. G., Breedveld, F. C., Toes, R. E., & Huizinga, T. W. 2005, "Invasiveness of fibroblast-like synoviocytes is an individual patient characteristic associated with the rate of joint destruction in patients with rheumatoid arthritis", *Arthritis Rheum.*, vol. 52, no. 7, pp. 1999-2002.

Trevino, V., Falciani, F., & Barrera-Saldana, H. A. 2007, "DNA microarrays: a powerful genomic tool for biomedical and clinical research", *Mol.Med.*, vol. 13, no. 9-10, pp. 527-541.

Umekita, K., Trenkmann, M., Kolling, C., Michel, B. A., Gay, R., Gay, S., & Bertoncelj, F. M. The feedback loop between long noncoding rna nron and nfat5 regulates the inflammatory response of rheumatoid arthritis synovial fibroblasts. Ann Rheum Dis 73 (Suppl 2). 2014.
Ref Type: Abstract.

van Amelsfort, J. M., Jacobs, K. M., Bijlsma, J. W., Lafeber, F. P., & Taams, L. S. 2004, "CD4(+)CD25(+) regulatory T cells in rheumatoid arthritis: differences in the presence, phenotype, and function between peripheral blood and synovial fluid", *Arthritis Rheum.*, vol. 50, no. 9, pp. 2775-2785.

van der Linden, M. P., le, C. S., Raza, K., van der Woude, D., Knevel, R., Huizinga, T. W., & van der Helm-Van Mil AH 2010, "Long-term impact of delay in assessment of patients with early arthritis", *Arthritis Rheum.*, vol. 62, no. 12, pp. 3537-3546.

van der Pouw Kraan, van Gaalen, F. A., asperkovitz, P. V., Verbeet, N. L., Smeets, T. J. M., Kraan, M. C., Fero, M., Tak, P. P., Huizinga, T. W. J., Pieterman, E., Breedveld, F. C., Alizadeh, A. A., & Verveij, C. L. 2003a, "Rheumatoid arthritis is a heterogeneus disease: evidence for differences in the activation of the STAT-1 pathway between rheumatoid tissues", *Arthritis and Rheumatism*. vol. 48, no. 8, pp. 2131-2145.

van der Pouw Kraan, van Gaalen, F. A., Huizinga, T. W., Pieterman, E., Breedveld, F. C., & Verweij, C. L. 2003b, "Discovery of distinctive gene expression profiles in rheumatoid synovium using cDNA microarray technology: evidence for the existence of multiple pathways of tissue destruction and repair", *Genes Immun.*, vol. 4, no. 3, pp. 187-196.

van Steenbergen, H. W., Huizinga, T. W., & van der Helm-Van Mil AH 2013, "The preclinical phase of Rheumatoid Arthritis, what is acknowledged and what needs to be assessed?", *Arthritis Rheum.*, doi: 10.1002.

Velculescu, V. E., Zhang, L., Vogelstein, B., & Kinzler, K. W. 1995, "Serial analysis of gene expression", *Science*, vol. 270, no. 5235, pp. 484-487.

Verpoort, K. N., van Gaalen, F. A., van der Helm-Van Mil AH, Schreuder, G. M., Breedveld, F. C., Huizinga, T. W., de Vries, R. R., & Toes, R. E. 2005, "Association of HLA-DR3 with anti-cyclic citrullinated peptide antibody-negative rheumatoid arthritis", *Arthritis Rheum*, vol. 52, no. 10, pp. 3058-3062.

Villiger, P. M., Terkeltaub, R., & Lotz, M. 1992, "Production of monocyte chemoattractant protein-1 by inflamed synovial tissue and cultured synoviocytes", *J.Immunol.*, vol. 149, no. 2, pp. 722-727.

Vincenti, M. P., Coon, C. I., & Brinckerhoff, C. E. 1998, "Nuclear factor kappaB/p50 activates an element in the distal matrix metalloproteinase 1 promoter in interleukin-1beta-stimulated synovial fibroblasts", *Arthritis Rheum.*, vol. 41, no. 11, pp. 1987-1994.

Wang, S. Y., Liu, Y. Y., Ye, H., Guo, J. P., Li, R., Liu, X., & Li, Z. G. 2011, "Circulating Dickkopf-1 is correlated with bone erosion and inflammation in rheumatoid arthritis", *J.Rheumatol.*, vol. 38, no. 5, pp. 821-827.

Weese-Mayer, D. E., Berry-Kravis, E. M., Zhou, L., Maher, B. S., Silvestri, J. M., Curran, M. E., & Marazita, M. L. 2003, "Idiopathic congenital central hypoventilation syndrome: analysis of genes pertinent to early autonomic nervous system embryologic development and identification of mutations in PHOX2b", *Am.J.Med.Genet.A*, vol. 123A, no. 3, pp. 267-278.

Wegner, N., Wait, R., Sroka, A., Eick, S., Nguyen, K. A., Lundberg, K., Kinloch, A., Culshaw, S., Potempa, J., & Venables, P. J. 2010, "Peptidylarginine deiminase from Porphyromonas gingivalis citrullinates human fibrinogen and alpha-enolase: implications for autoimmunity in rheumatoid arthritis", *Arthritis Rheum.*, vol. 62, no. 9, pp. 2662-2672.

Wells, C. A., Mosbergen, R., Korn, O., Choi, J., Seidenman, N., Matigian, N. A., Vitale, A. M., & Shepherd, J. 2013, "Stemformatics: visualisation and sharing of stem cell gene expression", *Stem Cell Res.*, vol. 10, no. 3, pp. 387-395.

Westra, J., Brouwer, E., Bos, R., Posthumus, M. D., Doornbos-van der Meer, B., Kallenberg, C. G., & Limburg, P. C. 2007, "Regulation of cytokine-induced HIF-1alpha expression in rheumatoid synovial fibroblasts", *Ann.N.Y.Acad.Sci.*, vol. 1108, pp. 340-348.

Wilkinson, L. S., Pitsillides, A. A., Worrall, J. G., & Edwards, J. C. 1992, "Light microscopic characterization of the fibroblast-like synovial intimal cell (synoviocyte)", *Arthritis Rheum.*, vol. 35, no. 10, pp. 1179-1184.

Willemze, A., Trouw, L. A., Toes, R. E., & Huizinga, T. W. 2012, "The influence of ACPA status and characteristics on the course of RA", *Nat.Rev.Rheumatol.*, vol. 8, no. 3, pp. 144-152.

Wilske, K. R. & Healey, L. A. 1989, "Remodeling the pyramid--a concept whose time has come", *J.Rheumatol.*, vol. 16, no. 5, pp. 565-567.

Woodman, I. 2013, "Rheumatoid arthritis: unravelling the roles of NETs in RA", *Nat.Rev.Rheumatol.*, vol. 9, no. 5, p. 258.

Yamane, S., Ishida, S., Hanamoto, Y., Kumagai, K., Masuda, R., Tanaka, K., Shiobara, N., Yamane, N., Mori, T., Juji, T., Fukui, N., Itoh, T., Ochi, T., & Suzuki, R. 2008, "Proinflammatory role of amphiregulin, an epidermal growth factor family member whose expression is augmented in rheumatoid arthritis patients", *J.Inflamm.(Lond)*, vol. 5, p. 5.

Yamanishi, Y., Boyle, D. L., Green, D. R., Keystone, E. C., Connor, A., Zollman, S., & Firestein, G. S. 2005, "p53 tumor suppressor gene mutations in fibroblast-like synoviocytes from erosion synovium and non-erosion synovium in rheumatoid arthritis", *Arthritis Res.Ther.*, vol. 7, no. 1, p. R12-R18.

Yamanishi, Y., Boyle, D. L., Rosengren, S., Green, D. R., Zvaifler, N. J., & Firestein, G. S. 2002, "Regional analysis of p53 mutations in rheumatoid arthritis synovium", *Proc.Natl.Acad.Sci.U.S.A*, vol. 99, no. 15, pp. 10025-10030.

Yamasaki, K., Nakasa, T., Miyaki, S., Ishikawa, M., Deie, M., Adachi, N., Yasunaga, Y., Asahara, H., & Ochi, M. 2009, "Expression of MicroRNA-146a in osteoarthritis cartilage", *Arthritis Rheum*, vol. 60, no. 4, pp. 1035-1041.

Yamazaki, D., Kurisu, S., & Takenawa, T. 2005, "Regulation of cancer cell motility through actin reorganization", *Cancer Sci.*, vol. 96, no. 7, pp. 379-386.

Yang, S. Z. & Abdulkadir, S. A. 2003, "Early growth response gene 1 modulates androgen receptor signaling in prostate carcinoma cells", *J.Biol.Chem.*, vol. 278, no. 41, pp. 39906-39911.

Zhao, C., Fernandes, M. J., Prestwich, G. D., Turgeon, M., Di, B. J., Clair, T., Poubelle, P. E., & Bourgoin, S. G. 2008, "Regulation of lysophosphatidic acid receptor expression and function in human synoviocytes: implications for rheumatoid arthritis?", *Mol.Pharmacol.*, vol. 73, no. 2, pp. 587-600.

Zhu, W., Meng, L., Jiang, C., He, X., Hou, W., Xu, P., Du, H., Holmdahl, R., & Lu, S. 2011, "Arthritis is associated with T-cell-induced upregulation of Toll-like receptor 3 on synovial fibroblasts", *Arthritis Res.Ther.*, vol. 13, no. 3, p. R103.

Zimmermann, T., Kunisch, E., Pfeiffer, R., Hirth, A., Stahl, H. D., Sack, U., Laube, A., Liesaus, E., Roth, A., Palombo-Kinne, E., Emmrich, F., & Kinne, R. W. 2001, "Isolation and characterization of rheumatoid arthritis synovial fibroblasts from primary culture--primary culture cells markedly differ from fourth-passage cells", *Arthritis Res.*, vol. 3, no. 1, pp. 72-76.